SEDIMENTOLOGY AND HYDROCARBON POTENTIAL OF THE PAPAROA COAL MEASURES LACUSTRINE MUDSTONES

A thesis submitted in partial fulfilment

of the requirements for the Degree of

MASTER OF SCIENCE IN GEOLOGY

at the University of Canterbury

by

Emma-Nell Olivia Cody

University of Canterbury

2015

Frontispiece

Faulted and folded Rewanui Formation coals and sandstone beds at Roa Mine

Abstract

Potential lacustrine source rocks have been recognised in several Cretaceous syn-rift basins including the producing Taranaki Basin, but have not been officially recognised from drill core and seismic data. The late-Cretaceous Paparoa Coal Measures contain three lacustrine mudstone formations which outcrop in several localities and have been extensively drilled for coal mining. These formations are considered to be an easily accessible analogue for late-Cretaceous lacustrine source rocks in New Zealand and also provide valuable information regarding syn-depositional tectonics and basin formation during the late-Cretaceous.

Stratigraphic columns and isopach maps were constructed from field work and drill hole descriptions and results showed variations in lithofacies across the basin. The western side of the basin is characterised by sandy lithofacies, abundant proximal turbidites and debris flows. The transition to a sub-aerial environment is marked by thick conglomerate and meter wide rip-up clasts. The central and eastern sections of the basin show massive mudstone, distal turbidites, low energy fluvial sandstones and thin, discontinuous coal. Isopach maps constructed from drill hole data identified three NNE – SSW oriented lakes with lacustrine sediment of up to 180m thick truncated by the eastern Roa – Mt Buckley Fault Zone. It was determined fault control during deposition was to the west and the basin extended further than its current location. Revisions to isopach models highlighted a lack of change in basin orientation during deposition of the Paparoa sediments. Plate reconstructions combined with direct evidence from the basin indicate formation of the Paparoa Coal Measures could have occurred in either a rift or transtensional basin.

The mudstones were geochemically assessed for hydrocarbon potential using a Source Rock Analyser (SRA). Preliminary analysis of the three mudstones has shown TOC values ranging from 1.0 to 4.5 wt.%, HI values ranging from 68 to 552 mHC/gTOC and Tmax results show the mudstones to range in maturity from immature to late – mature. A sample from the Waiomo Formation has excellent potential for oil generation and the low maturity results for the Goldlight Formation make it a potential shale gas resource.

These results have shown the potential for hydrocarbon bearing lacustrine source rocks to exist in the Greymouth Coalfield. In addition, revisions have been made to basin formation which should be considered. Due to the availability of data from the Paparoa lacustrine source rocks, they should be used as an accessible analogue for Taranaki and other Late Cretaceous basins.

Table of contents

List of tables and figures

Tables

Figures

Graphs

Chapter 1 Introduction

1.1 Introduction

The Late Cretaceous sediments that make up the Paparoa Coal Measures have long been known as coal bearing and have been economically important since the late 1800's. The Paparoa Coal Measures are found in the Greymouth Coalfield on the West Coast of New Zealand's South Island (Figure 1.1) and are the only coal-bearing sequence within the coalfield.

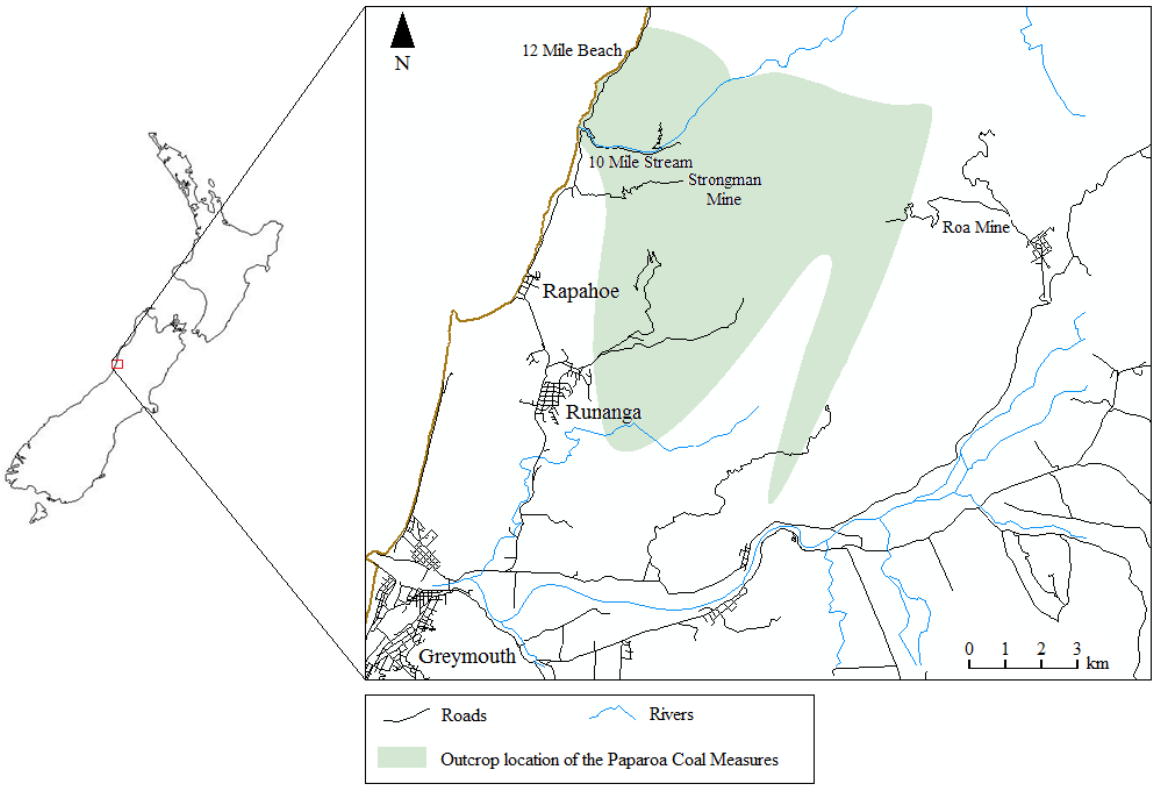

Figure 1.1 Location map of the Greymouth Coalfield and outcrop of the Paparoa Coal Measures. Coal mining is ongoing at Strongman and Roa Mines while underground mining at Spring Creek, just east of Runanga has been suspended.

There are three lacustrine mudstone formations within the Paparoa Coal Measures which will be the subject of this thesis and are known as the Ford, Waiomo and Goldlight Mudstone Members (Figure 1.2). These mudstones outcrop in several areas throughout the coalfield

with the northwest section around 10 Mile Creek and 12 Mile Beach being the main focus for field studies. Drill cores from around the coalfield were also looked at, particularly where outcrop was not accessible or available.

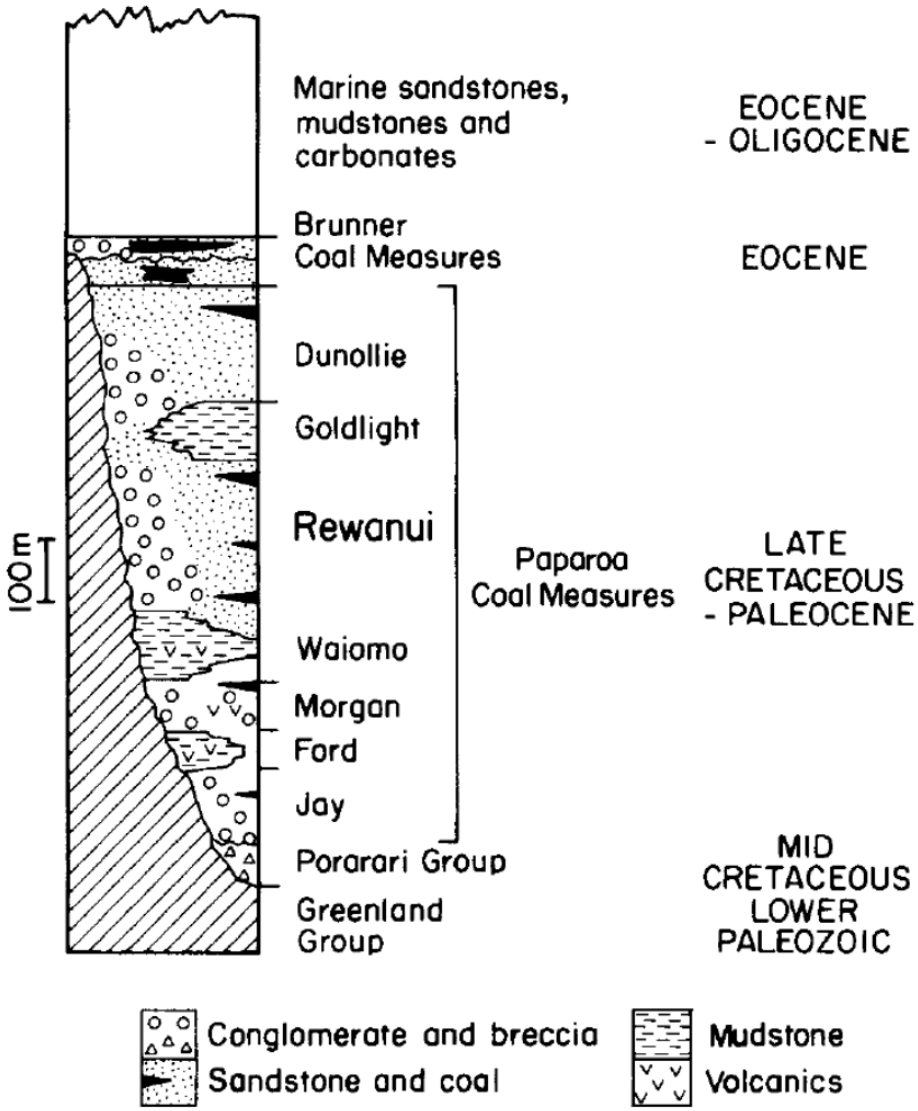

Figure 1.2. Summary table of the Greymouth Coalfield Stratigraphy, taken from Boyd & Lewis 1995.

Numerous studies have been undertaken on the basin over the last century to gain an understanding on the coal measures with most of that work focusing on the coal bearing strata. The earliest description of the "Paparoa Beds" was presented by Morgan (1911) however the first major investigation into the Greymouth coalfield was undertaken by Maxwell Gage (1952). Over time, this information has been refined and altered with

revisions to nomenclature made but the major results and conclusions outlined by Gage are still the basis for our understanding of the coalfield.

The basement rocks which underlie the Paparoa Coal Measures are the Ordovician age Greenland Group turbidites which are found along the majority of the West Coast of the South Island (Mortimer et al. 2013). In some locations within the Greymouth Coalfield, basement is defined by the Mid-Cretaceous Pororari Group which is related to the rifting of New Zealand from Gondwana (Nathan et al. 2002; Laird 1994; Laird & Bradshaw 2004). These older sediments are then overlain by the Late Cretaceous Paparoa Coal Measures, the Eocene Brunner Coal Measures and the transgressive Island Sandstone, Kaiata Formation and regressive Oligocene Cobden Limestone (Gage 1952; Ward 1997; Nathan et al. 2002).

Due to the focus on coal and economic development, the lacustrine mudstones of the Paparoa Coal Measures have never been studied in great detail and are only used as "marker beds" by the coal companies. Gage (1952) admitted this himself and due to mapping conventions only classified the thick Goldlight Formation as a massive mudstone without accounting for any other sub-aqueous lake facie. Since the publication of The Greymouth Coalfield (Gage 1952) revisions have been made, resulting in several stratigraphic problems, particularly in the northwest corner of the coalfield. As well as these stratigraphic problems, further work needs to be undertaken on the economic potential and sedimentology of the mudstones to gain a better understanding on basin history, depositional environment and New Zealand source rocks.

1.2 Economic geology

Coal was first identified in the Greymouth Coalfield by Thomas Brunner in 1847 (Morgan 1911) along the Grey River and mining began in this area 20 years later (McNee 1997). Over the last 150 years, numerous mining operations have been undertaken around the Greymouth Coalfield, expanding northwards from the initial mining operation at Brunnerton. The Greymouth Coalfield contains the best low ash, low sulphur bituminous coals within New Zealand (Ward 1997).

Currently there are 3 active mine sites within the Greymouth Coalfield, mining Rewanui and Morgan coals; Spring Creek (currently not mining due to the coal downturn), Strongman Mine at 9 Mile Stream and Roa Mine to the east. Spring Creek and Strongman Mine are both run by Solid Energy which is a state owned coal company within New Zealand. Roa Mine is

owned by NZ Coal and Carbon a privately owned coal company. In conjunction with these larger mines are smaller privately owned permit areas owned by local residents.

Analysis of the coals within the Greymouth Coalfield show mainly bituminous type coals with low ash yields, low moisture and high swelling properties (Suggate 1959; Sara 1963; Suggate 2012; Newman 1985; Zhongsheng 2002). Studies have shown that moisture and swelling are directly related to the volatility and rank of the coals, with rank increasing from west to east (Suggate 1959, Sara 1963, Gage 1959) across the coalfield.

Early drilling and coal exploration around Kotuku and Lake Brunner unearthed evidence of petroleum shows within seeps and drill holes (Morgan 1911; Nathan et al. 2002). Further work has shown the occurrence of oil and gas shows within other mine workings including Liverpool Mine (Gage 1952). Identification of terrestrial biomarkers within the oil seeps indicates they are derived from a similar source to those in Taranaki i.e. Cretaceous aged coals from the Paparoa Coal Measures (Hirner & Lyon 1989; Frankenberger et al. 1994).

As of yet, no commercial quantities of hydrocarbons have been discovered within the Greymouth Coalfield and surrounding areas but drilling programmes by Mosman Oil and Gas are currently being undertaken near the Kotuku anticline with early results showing minor oil and gas shows. No work has yet been done on analysing the lacustrine mudstones as a potential source rock.

1.3 Geological history

Formation of the Paparoa Basin is directly associated with the mid to Late Cretaceous breakup of the Gondwana continent and separation of New Zealand from Australia (Laird & Bradshaw 2004; Laird 1994). Up until 105 Ma, the eastern margin of Gondwana was dominated by a convergent plate boundary system which at this time, abruptly changed to an extensional regime. The cause for this change is thought to have occurred due to the failure of the subduction system and allowed for proto New Zealand to be captured by the western edge of the eastward moving Pacific Plate (Laird & Bradshaw 2003). The opening of the Tasman Sea began just before 80ma and continued until 52ma (Gaina et al. 1998). During this time, numerous extensional features such as grabens and half grabens began to form and were infilled with terrestrial sediment (Laird & Bradshaw 2003). Initially Paparoa Basin fill took the form of alluvial fan conglomerates known as the Hawks Crag Breccia within the Pororari

Group. These conglomerates were deposited in the earliest stages of rifting with pollen dating indicating an approximate age of 112 – 99 Ma (Nathan 1978).

Within the Paparoa Coal Measures, faulting is said to have been controlled from the eastern margin, in a similar area to the modern day Roa – Mt Buckley fault zone (Gage 1952). This formed an asymmetrical basin with fluctuations in subsidence rate accounting for the alternation of fluvial and lacustrine formations within the basin (Saneyoshi et al. 2006). Isopach models (Gage 1952; Newman 1985; Ward 1997) show the lower Jay and Ford Formations (Figure 1.2) are oriented to the NW-SE compared to the younger isopachs which show a basin orientation of NNE – SSW. This change in basin orientation is inferred to have been due to a change in dominant extension direction. Another theory for the formation of the Paparoa Coal Measures involves no dramatic change in extension direction. Instead, the NNE - SSW bounding faults were oriented parallel to transform faults which formed during the early stages of the Gondwana extensional regime (Laird 1994). The reactivation of these transform faults would have resulted in a transtensional regime that controlled basin formation along the entire West coast of New Zealand (Laird 1994; Bishop 2010). Local faults within the Paparoa Basin are oriented in a NNE-SSW direction and have now been reactivated as reverse faults due to the current compressional tectonic regime which controls faulting in New Zealand (Stahl 2014).

1.4 Lithostratigraphy

The stratigraphy of the Paparoa Coal Measures has been redefined numerous times over the past 100 years, leading to a complex amalgamation of members and formations (Table 1.1) Currently there are 5 formations and 3 members which break down into the Jay, Ford, Rewanui, Goldlight and Dunollie Formations and the Morgan, Waiomo and Rewanui Members of the Rewanui Formation (Gage 1952; Newman 1985; Ward 1997; Nathan 1978).

For the purposes of this thesis, naming will be simplified with all members elevated to Formation status. By doing this, naming reverts back to what was originally published (Gage1952). The official change from formations to members occurred during publication of the QMaps (Nathan 1978) with the reason being the Paparoa Coal Measures are not found outside of the Greymouth Coalfield. Based on the definition of a formation as a body of rock that is identified by lithology and is mapable at the surface and subsurface (Boggs 2006), the downgrade to member for some or all of the units was unnecessary.

<table>
<tr><th colspan="5">Nomenclature of the Paparoa Coal Measures</th></tr>
<tr><th>Gage 1952</th><th colspan="2">Nathan 1978</th><th colspan="2">Ward 1997</th></tr>
<tr><td>Jay Formation</td><td rowspan="8">Paparoa Formation</td><td>Jay Coal Measures Member</td><td>Jay Formation</td><td></td></tr>
<tr><td rowspan="2">Ford Formation</td><td rowspan="2">Ford Mudstone Member</td><td rowspan="2">Ford Formation</td><td>Ford Formation</td></tr>
<tr><td>Ford Transitional Member</td></tr>
<tr><td>Morgan Formation</td><td>Morgan Coal Measures Member</td><td rowspan="3">Rewanui Formation</td><td>Morgan Coal Measures Member</td></tr>
<tr><td>Waiomo Formation</td><td>Waiomo Mudstone Member</td><td>Waiomo Mudstone Member</td></tr>
<tr><td>Rewanui Formation</td><td>Rewanui Coal Measures Member</td><td>Rewanui Coal Measures Member</td></tr>
<tr><td rowspan="2">Goldlight Formation</td><td rowspan="2">Goldlight Mudstone Member</td><td rowspan="2">Goldlight Formation</td><td>Goldlight Formation</td></tr>
<tr><td>Goldlight Transitional Member</td></tr>
<tr><td>Dunollie Formation</td><td>Dunollie Coal Measures Member</td><td>Dunollie Formation</td><td></td></tr>
</table>

Table 1.1. Summary table of Paparoa Coal Measures nomenclature and revisions. The last published and official terminology is presented by Nathan (1978). The last revisions were made by Ward in 1997. Within this thesis, terminology will refer back to origin naming as outlined by Gage (1952).

1.4.1 Jay Formation

The Jay Formation is the oldest formation within the Paparoa Coal Measures and is mainly composed of sandstones, conglomerates and thin coal seams. The Formation is subdivided into two units based on over all composition (Gage 1952).

The lower Jay (ii) is described as predominantly Greenland Group derived conglomerate with occasional vein quartz, hornfels and quartzose sandstone. This conglomerate is usually sub-rounded to sub-angular and clast supported with clast sizes of up to 25cm in the far west of the coalfield. There is no apparent evidence of granite clasts within the Jay (ii) which are common in the younger Rewanui and Dunollie Formations, (Gage 1952; Newman 1985).

The upper Jay (iii) contains much finer sandstones and siltstones with numerous thin, discontinuous coal seams and other carbonaceous horizons. Coal seams within the Jay (iii) are often dirty and not considered to be economically viable (Newman 1985).

The conglomeratic Jay (ii) is primarily found throughout the western half of the coalfield while the Jay (iii) is found on top of this horizon in the west and is the time equivalent to Jay (ii) in the east (Gage 1952). Due to a general lack of deep drill holes in the coalfield, it is hard to determine the lateral relationship between the two.

The conglomerates of the Jay (ii) are considered to be fluvial, while the upper Jay (iii) sandstones and coal formed in a lower energy flood plain/ meandering river environment. Dating of the Jay Formation gave an age of deposition of around 71 Ma (Laird 1994) which coincides with the beginning of Tasman Sea Floor spreading (Gaina et al. 1998). It should also be noted that the Jay (ii) is often hard to distinguish from the underlying Pororari Group conglomerates which is found in the more northern areas of the coalfield (Newman 1985).

1.4.2 Ford Formation

The first mudstone within the Paparoa Group is the Ford Mudstone, originally described as a dark grey to brown grey siltstone with thin sandy laminations, with an overall thickness of <60 m (Newman 1985; Ward 1997). In some areas, the siltstone also contains conglomerate lenses with a similar composition to the Jay (ii), dominated by Greenland Group sandstone and quartz clasts (Gage 1952). The abundance of laminations within the Ford Formation distinguishes it from the other more massive mudstones within the Paparoa Group. Fossils from within the Ford Formation include numerous leaf impressions and plant debris. Well preserved freshwater mollusc and land snail fossils can also be found (Gage 1952).

Outcrop and drill hole data shows that the Ford Formation is mainly confined to the east from Roa Mine down to Spring Creek Mine (Gage 1952). Recent unpublished revisions to drill hole data made by Ward (1997) place the Ford Formation at 12 Mile Beach, replacing the mapped Waiomo Formation. However, in published maps, the 12 Mile Beach section is still known as Waiomo Formation (Nathan 1978).

The presence of freshwater molluscs and high organic material are all evidence that the Ford Formation formed from a lake environment as opposed to being a marine mudstone (Gage 1952). Lake inundation in-filled paleotopography during deposition of the Jay Formation which resulted in a small lake that was influenced by faulting (Gage 1952; Ward 1997). The

inter bedding of sandstone and siltstone is from turbidites which travelled into the lake (Chang & Chun 2012). There is also evidence for fluvial systems entering the lake and forming the conglomerate lenses near the top and bottom of the formation. This smattering of conglomerate within the siltstone is an indication of gradual lake formation and also marks the time where lake shallowing occurred and the transition back to a fluvial system began (Ward 1997; Gage 1952).

1.4.3 Morgan Formation

The Morgan Formation is made up of two quite distinct facies: 1) igneous clast conglomerates and 2) conglomerates, sandstones and coal. The igneous clast conglomerate is confined to a small area to the east around Roa Mine and also includes basaltic lava flows and pillow lavas (Gage 1952). This section is much thicker than in other areas of the coalfield with over 400m of volcanic rock (Gage 1952; Newman 1985). Correlation between the Morgan Volcanics and basalts at Mt Camelback and the Ahahura-1 drill hole gives an approximate age of 68 Ma for the Morgan Formation (Laird 1994).

The remaining Morgan is composed of Greenland Group derived conglomerates almost indistinguishable from Jay (ii), brown to grey sandstones with faint bedding and quartz pebbles and fine carbonaceous mudstone and shale in the finer sections of sediment. Coal within the Morgan but very thick (>5m), low ash and sulphur and high swell (Andrew Holley, personal communication 2015). There is also no evidence of granite clasts within the conglomerate (Gage 1952).

The volcanic conglomerates of the Morgan Formation are confined to the eastern side of the Greymouth Coalfield around Roa Mine while non-volcanic conglomeratic facies are found in the east and northwest. South-eastward towards Spring Creek, the Morgan Formation becomes finer grained with more sandstone and carbonaceous horizons (Gage 1952). The carbonaceous mudstone can also be seen at 12 Mile Beach as the Morgan Formation transitions to the overlying mudstone.

The inclusion of coarsening conglomerates to the east is an indication of faulting in this area which began to infill the Ford Lake from this side. Gage (1952) estimates that a volcano arose in this area advancing to the west and formed pillow lavas when it reached the Ford lake system. In other areas of the coalfield, the formation of conglomerates is thought to have been from erosion of Greenland Group basement and possible re-working of Jay

conglomerates that were unconsolidated. All other fine grained material is likely a result of advancing fans and deltas that eventually in-filled the Ford lake system until it was a low lying plain with small raised mires and peat bogs (Gage 1952).

1.4.4 Waiomo Formation

The majority of the Waiomo Formation is described as a dark grey/brown, massive mudstone and siltstone (Gage 1952; Newman 1985; Ward 1997). There is occasional evidence of thin, normally graded bedding and the contacts with the underlying Morgan and overlying Rewanui Formations are gradational over several meters. The Waiomo Formation is thickest in the north of the coalfield and thins out gradually towards the south where the upper contact with the Rewanui is highly gradational with an inclusion of abundant, fragmented plant fossils (Newman 1985; Gage 1952). Rare freshwater molluscs and occasional snail fossils were found within the Waiomo Formation and are identical to those seen within the Ford Formation (Ward 1997).

Original mapping had the Waiomo Formation extending from the western side of the coalfield at 12 Mile Beach across to Roa Mine where it is now truncated by the Roa – Mt Buckley Fault zone (Gage 1952). The formation also appears to thin out gradually towards the south around Spring Creek and Rewanui Mines (Figure 1). In the northern section of the coalfield the Waiomo is up to 60m thick while in other areas including Spring Creek and Rewanui, the average thickness is 30 – 50m. Due to the resemblance of the Waiomo Formation to the Ford Formation at 12 Mile Beach, Ward (1997) suggested revisions be made to the last published maps and the Ford Formation should instead be recognised. The last published map (Nathan 1978) still shows the Waiomo Formation to be located at 12 Mile Beach.

The Waiomo Formation is also interpreted to have formed in a lake environment, marked by the massive mudstone facies, fresh water fossils and terrestrial snails found in drill core (Gage 1952).

1.4.5 Rewanui Formation

The Rewanui Formation is the thickest coal bearing unit within the Greymouth Coalfield and is divided into two compositional suites based on lithology and source area (Ward 1997).

The Eastern Compositional Suite is comprised of mostly sandstone made up of quartz and mica and rare granule conglomerates (Gage 1952; Ward 1997). Associated coal seams are thick and numerous and there are also several carbonaceous mudstone horizons (Ward 1997; Gage 1952). Sandstones are commonly yellow and can contain cross bedding, ripples and channelization (Ward 1997).

The Western Compositional contains very thick and extensive conglomerates that become finer towards the centre of the basin (Ward 1997). The conglomerates include large granite and hornfel clasts as well as the usual Greenland Group and vein quartz clasts. Clasts can get up to boulder size in the northwest and are always rounded to sub rounded with slight imbrication showing flow direction to the south/south-east (Ward 1997; Gage 1952; Newman 1985). In several areas dark, massive mudstone rip up clasts can also be found (Ward 1997).

Palynology work by Ward (1997) has placed the Cretaceous -Tertiary boundary near the top of the Rewanui Formation at 7 Mile Stream giving the formation an approximate age of 65 Ma. In this area, the boundary is commonly known to occur just below the last coal horizon within the formation.

The Eastern Compositional Suite sedimentary rocks are mainly confined to the Roa Mine area where the Rewanui coal seams are currently mined. The actual contact between the Western and Eastern Compositional Suites is arbitrary and hasn't been truly identified (Ward 1997).The Western Compositional Suite has its thickest sediments to the northwest where the Rewanui is several hundred meters thick (Gage 1952). These conglomerates gradually fine out into the basin with the finer grained facies of the Western Compositional suite seen around Spring Creek and 7 Mile Stream (Ward 1997).

Coal seams within the Rewanui are found throughout most of the coalfield with current mining of the Rewanui occurring at Strongman and Roa Mines. Seams can be up to 10m thick with most coal found near the top and bottom of the formation (Newman 1985; Suggate 2012; Ward 1997).

The Eastern Compositional Suite with its quartzo-feldspathic sandstone and current indicators (cross bedding, channels, ripples) is characteristic of a fluvial environment, while the coal seams are known to have formed from raised mires in a very low energy swamp environment. This eastern area would have been low lying with meandering rivers and oxbow lakes, (Ward 1997; Newman 1985; Gage 1952).

The Western Compositional Suite was deposited in higher energy, low-angle alluvial fan environment as seen by the very thick succession of boulder and cobble clast conglomerate at 12 Mile Beach (Ward 1997). Imbrication indicating flow to the south and the addition of granite clasts within the Rewanui indicates a source area to the north/ northwest (Gage 1952).

1.4.6 Goldlight Formation

Original mapping of the Goldlight Formation described it as a massive grey to dark grey mudstone (Gage 1952). In some areas of the coalfield, centimetre thick sideritic concretions can be found which are stained orange and are highly indurated. Most recently, non-massive mudstone facies has been included in the classification of the Goldlight Formation with fine sandstone and minor conglomerates to the northwest added as a Goldlight Transitional Member (Ward 1997). In some areas, leaf and plant fossils can be found as well as mica flakes but these only occur in the south of the coalfield (Gage 1952).

The Goldlight Formation is present across the entire Greymouth Coalfield except in the northwest region where it laterally transitions to time equivalent conglomerates of the Rewanui and Dunollie Formations. In most other areas, the Goldlight Formation is over 100m thick apart from in the northeast where it has been eroded from the surface and to the southwest where it thins out to 50 meters thick (Newman 1985; Ward 1952).

The very fine grain size, lack of marine fossils and inclusion of siderite bands are all evidence that the Goldlight Formation was deposited in a lake environment (Gage 1952). The massive, very fine siltstone to mudstone seen particularly around Spring Creek is likely formed from hemipelagic sedimentation with little influence from sediment transport processes. (Ward 1997; Gage 1952).

1.4.7 Dunollie Formation

The Dunollie Formation is mainly composed of yellow sandstone with siltstone and carbonaceous mudstone bedding (Nunweek 2001; Ward 1997; Gage 1952). Coal within the Formation is not particularly extensive and is often split. In the northwest, the Dunollie quickly transitions to thick conglomerates indistinguishable from the Rewanui conglomerates at the same location. Near the river mouth of 10 Mile Stream, the conglomerates are highly leached and white in colour (Gage 1952; Nunweek 2001).

The Dunollie Formation is mostly eroded in the northeast corner of the coalfield but crops out in the central area around Sewell Peak, Spring Creek and 9 Mile Stream and in the western area at 10 Mile Creek and 12 Mile Beach (Figure 1). In these locations thickness varies from 10's of meters to over 100m just east of Strongman Mine (Gage 1952; Nunweek 2001; Newman 1985). From 9 Mile Stream north, the Dunollie is dominated by conglomerate facies. In this area it is hard to determine the thickness of the unit due to the inability to clearly differentiate between the Rewanui and Dunollie Formations but a thickness of over 200m is assumed (Gage 1952).

As with the other coal bearing formations, the Dunollie Formation is interpreted as being deposited in a fluvial environment due to the presence of channelised conglomerates and sandstones (Ward 1997; Gage 1952). Imbrication seen at 12 Mile Beach indicates flow direction towards the south with a possible source area to the north and northwest (Ward 1997; Gage 1952).

1.3.8 Brunner P

At the top of Spring Creek road, the Dunollie transitions to a polymict conglomerate and up section, a quartzose sandstone similar in appearance to the Eocene Brunner "grit" seen further north. This gravel and conglomerate in the Greymouth Coalfield is termed Palaeocene Brunner Formation (Nunweek 2001). This formation was proposed to try and better define the change between the Dunollie Formation and Palaeocene aged Brunner Coal Measures only recognised within the Greymouth Coalfield

The Palaeocene Brunner Formation marks an increase in tectonic uplift and subsequent erosion (Newman 1985; Nunweek 2001) forming coarser sedimentary rocks with a different composition to the granite and Greenland group conglomerate at the beach.

1.5 Scope and study objectives

Past research on the Paparoa Coal Measures has predominantly focused on the coal bearing formations and coal geology with little work done on the three lacustrine formations. Sedimentology of the mudstones provides information on deposition and can add insight into the history of the basin. In addition, the interest in New Zealand petroleum basins has increased in the last few decades, particularly for the Greymouth Coalfield due to similarities

in age and basin history between the two localities. The Paparoa Coal Measures are known to contain oil shows indicating the presence of a working petroleum system (Gage 1952; Nathan et al 2002). By focusing on non-marine and non-coaly source rocks, new insight can be added to what we know about New Zealand petroleum basins and this information can also be applied to other similar basins around the country.

The main objectives of this study are:

- Describe and redefine the lacustrine mudstones with a focus on revisions to nomenclature and isopach maps.
- Perform source rock analysis on the lacustrine mudstones to determine their overall source rock potential.
- Determine whether the mudstones would be a suitable reservoir for gas and could be considered as a shale gas.
- Use updated descriptions and definitions of the mudstone to redefine basin history and tectonic setting during formation of the Paparoa Coal Measures.
- Compare Greymouth coalfield with other New Zealand Late-Cretaceous basins

To answer these questions I will be combining field work and lab analysis. Field work will be focused around the northwest and Spring Creek Mine (Figure 1) due to access. Limited field work was completed in the east. To account for this, drill core was used to account for lack of out crop data. Source Rock analysis will be undertaken in Wellington at GNS Laboratories in Lower Hutt using core obtained from the MBIE core store in Featherston. From this analysis, I will be able to determine how mature the mudstones are and if they could generate oil or gas, how much organic content is in the mudstones and whether the mudstones could be a source for shale gas.

Chapter 2 Sedimentology

2.1 Introduction

For economic reasons, previous work on the Paparoa Coal Measures has focused predominantly on the four coal bearing formations. The earliest work identified several horizons of basal conglomerate, shale, sandstone and coal which were eventually organised into the current 7 formations of the Paparoa Coal Measures (Gage 1952). At the same time, fossil evidence was discovered that showed freshwater molluscs and land snails were present in a number of horizons across all 3 mudstone formations. This suggests the thick, massive mudstones were deposited in a lacustrine environment (Gage 1952).

The focus of this chapter is to look at and analyse the sedimentology of the mudstones in detail and to recognize their importance not just as marker beds for the four coal bearing formations but as valuable tools for assessing the tectonic controls and paleo-environment during this time. By describing the sedimentology in detail, new lithofacies associations can be created and applied to the three mudstone formations in order to determine depositional environments and define the distribution of these facies across the coalfield. The size and shape of the ancient lakes will also be used to gain a better understanding of the tectonic processes which shaped the basin and influenced deposition during this time.

2.2 Previous work and controversies

The nature of outcrop and terrain in the Greymouth Coalfield has always resulted in problems with stratigraphy for all 7 Formations. Combined with the high number of faults and similarities between the formations, accurate identification of formations has always proven difficult. Over the years, this has resulted in several stratigraphic issues evolving with most focused in the 12 Mile Beach to 10 Mile Creek area (Figure 2.1).

2.2.1 12 Mile Beach

One of the main controversies associated with the Paparoa Coal Measures has been around the identification of the mudstones at 12 Mile Beach and the general similarities between the Ford and Waiomo Formations in this north-western area.

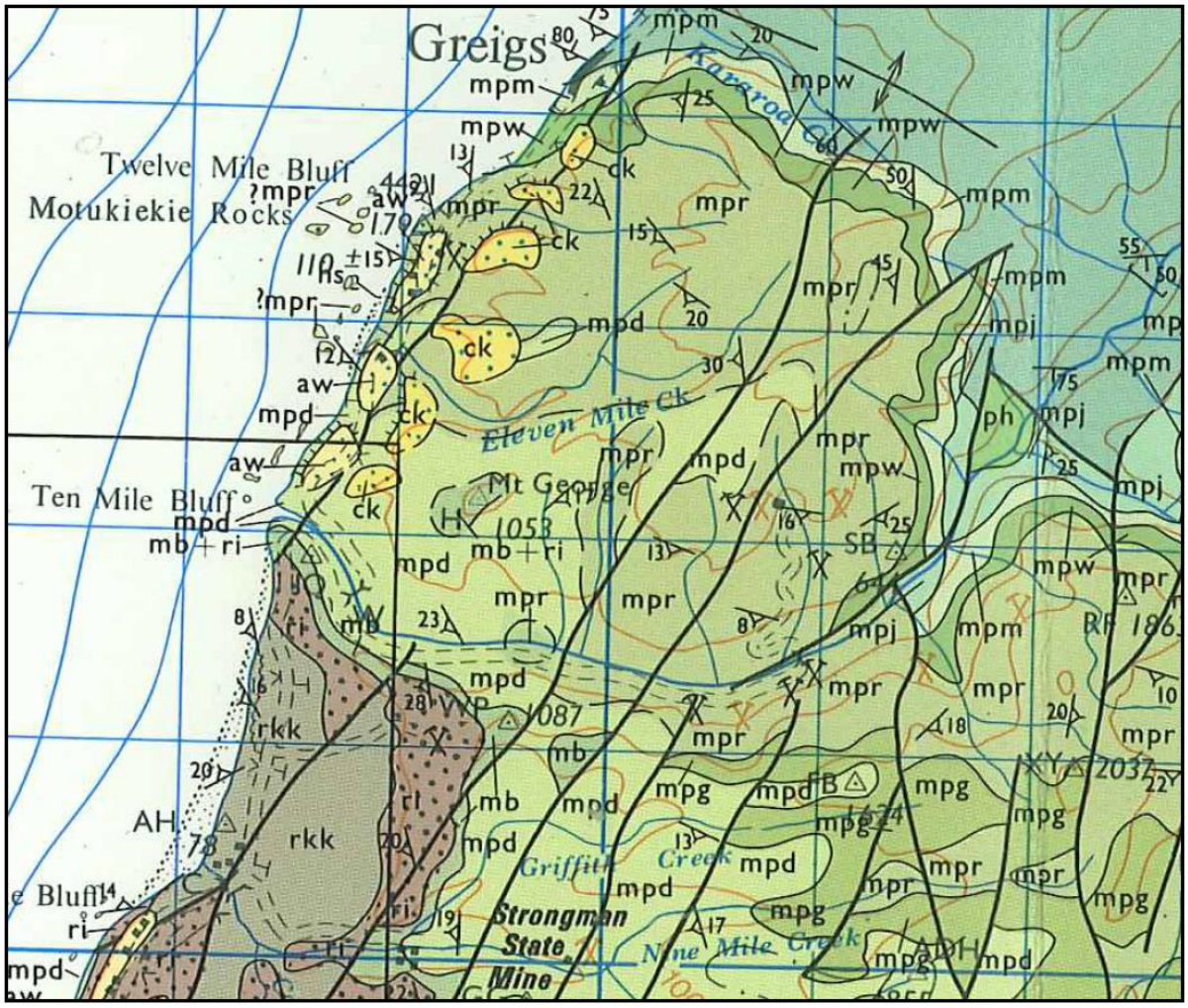

Figure 2.1. Simplified map of the Greymouth Coalfield northwest corner (Nathan 1978). Complicated faulting and similarities in appearance between the mudstones often results in stratigraphic problems across the coalfield.

The original mapping by Gage labelled the 12 Mile Beach mudstone as Waiomo Formation however the well laminated section bears more resemblance to the Ford Formation than to the more massive, darker Waiomo Formation (Gage 1952). This was further confirmed in 1978 with the publication of a by Simon Nathan (Nathan 1978) who also labelled the 12 Mile Beach section as Waiomo Formation. In recent years, Simon Ward (1997) has revised the 12 Mile Beach section by relabeling the mudstone as Ford Formation due to the similarities in sedimentology between the two.

2.2.2 Revision of the Goldlight Formation

During the original mapping of the coalfield by Gage (1952), the Goldlight Formation was classified as only massive mudstone due to the naming requirements set out by Gage (1952). Due to this, all other shallow lake facies that should be included in the Goldlight Formation are grouped together with either the Rewanui or Dunollie Formations. In his thesis, Ward partially acknowledges this by adding a Goldlight Transitional Member to the Goldlight Formation (Table 1.1) however this member only covers the lake edge sediments found in the northwest corner. These changes will be further developed within this thesis to include non-massive mudstone within the Goldlight Formation across other areas of the coalfield.

2.2.3 Previous isopach modelling

Isopach modelling of the formations to date has highlighted what appears to be a change in basin orientation during the deposition of the coal measures. Isopachs created by Gage (1952), Newman (1985) and Ward (1997) all indicated a changed in orientation. Both Newman (1985) and Ward (1997) have built on the first isopachs created by Gage (1952) as new drill hole data has become available. The most recent isopachs show two very deep lakes (the Ford and Goldlight lakes) while the Waiomo Formation is thin and found mainly to the east of the coalfield. Naming of the mudstone at 12 Mile Beach has a substantial impact on isopach distribution. The isopachs shown below obtained from Ward (1997) show the Ford Formation (Figure 2.2) extending to the western edge of the basin while the Waiomo Formation stops well west of the Strongman Mine area and is quite constrained to a small area (Figure 2.3). This doesn't conform with current accepted mapping practice but they are the most recent isopachs.

The Ford Formation isopach (Figure 2.2) shows a NW – SE oriented lake with very thick sediment around the Strongman Mine – Roa area (Ward 1997). The Ford Formation is also shown to extend into 12 Mile Beach and the north-western corner of the coalfield contrary to what was mapped by Gage (1952) and Nathan (1978). The orientation of the Ford Formation (and the underlying Jay Formation) has been the primary evidence supporting a change in basin orientation during deposition of the Paparoa Coal Measures.

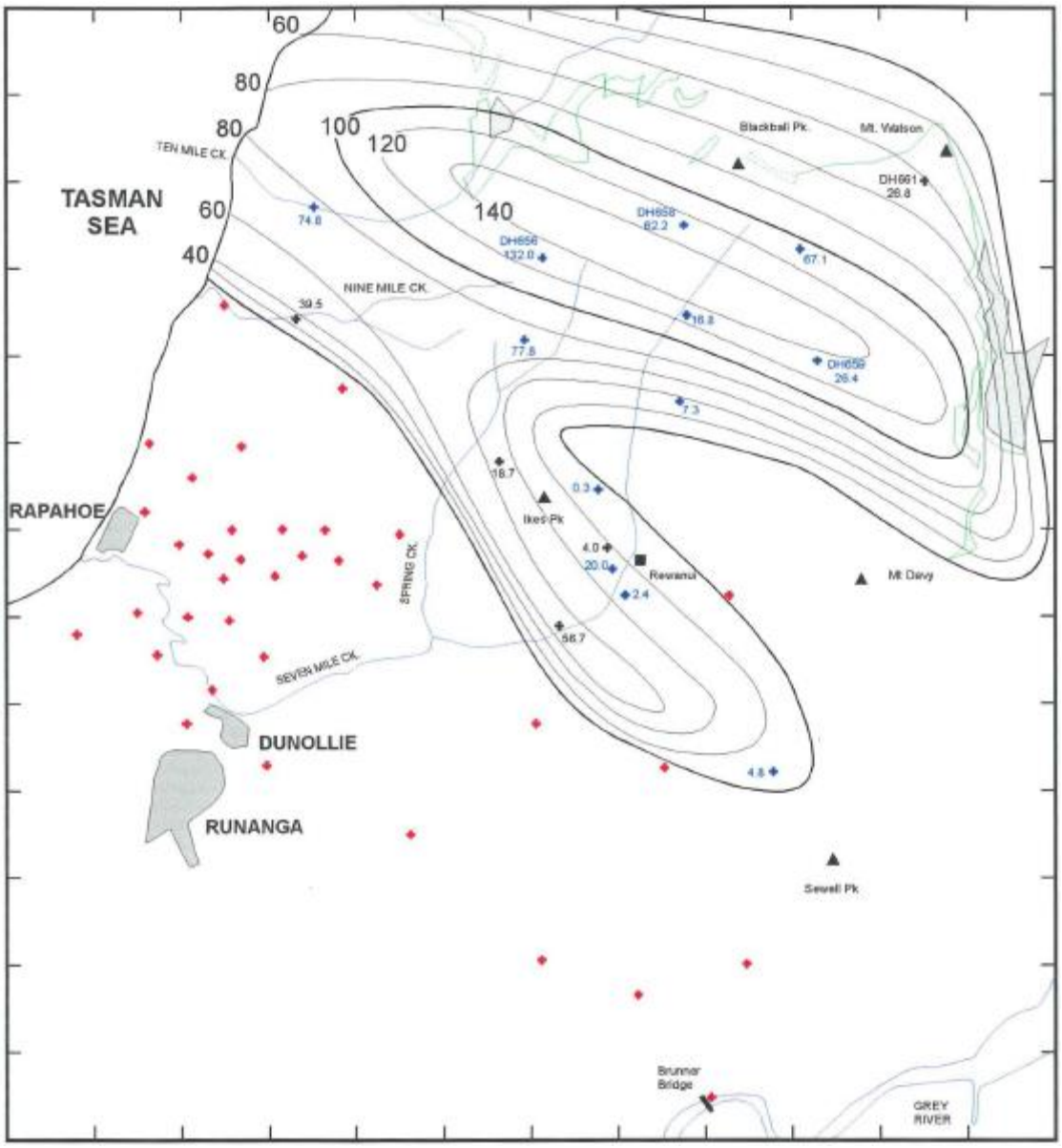

Figure 2.2. Ford Formation isopach adapted from Ward (1997). The Ford Formation appears to be thick and extensive across the northern half of the coalfield and shows a NW – SE orientation.

The Waiomo Formation isopach (Figure 2.3) shows a lake located quite far to the east which doesn't extend towards the northwest past Strongman Mine (Ward 1997). The shape of the isopach is also quite round and doesn't show a clear orientation compared to the earlier Ford Formation isopach. A small, isolated depocentre to the south is also shown which isn't connected to the main lake. The overall thickness of the Waiomo Formation is less than 60m in comparison to the Ford and Goldlight lakes which appear to be over 100m thick in many places.

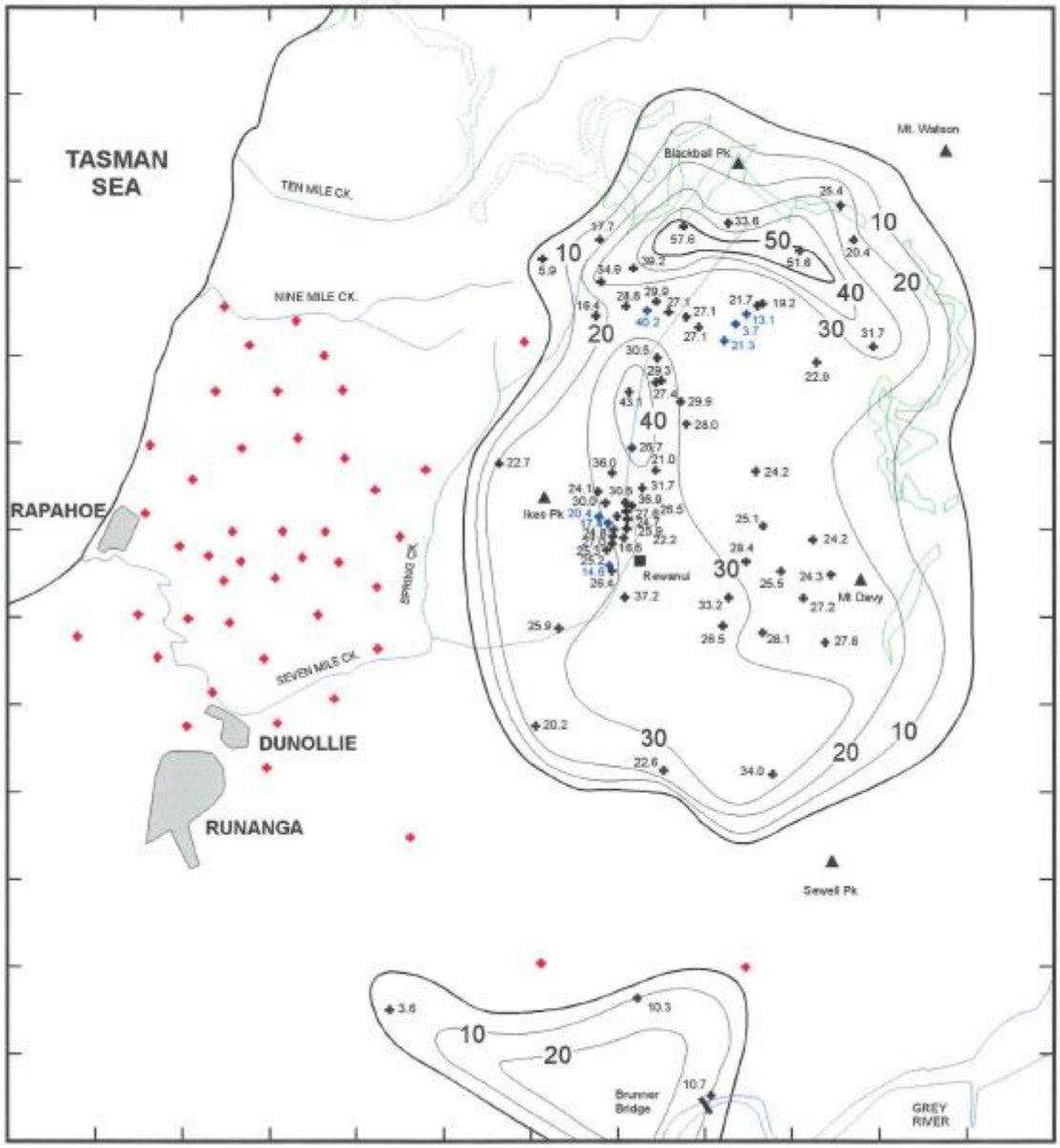

Figure 2.3. The Waiomo Formation isopach adapted from Ward (1997) showing two separate depocentres. The Waiomo Formation doesn't extend west of Strongman Mine. The basement high which separates the two depocentres also appears to be oriented in a E – W direction, almost parallel to the Ford Formation isopach.

The Goldlight Formation isopach (Figure 2.4) shows a substantially larger lake in comparison to the other lacustrine isopachs (Ward 1997). The Goldlight isopach is oriented in a NNE – SSW direction, perpendicular to the orientation of the Ford Formation and is the primary evidence for the change in basin orientation. The extent of the Goldlight Formation is much greater than the older Ford and Waiomo Formations reaching to past the northern and southern edges of the Greymouth Coalfield.

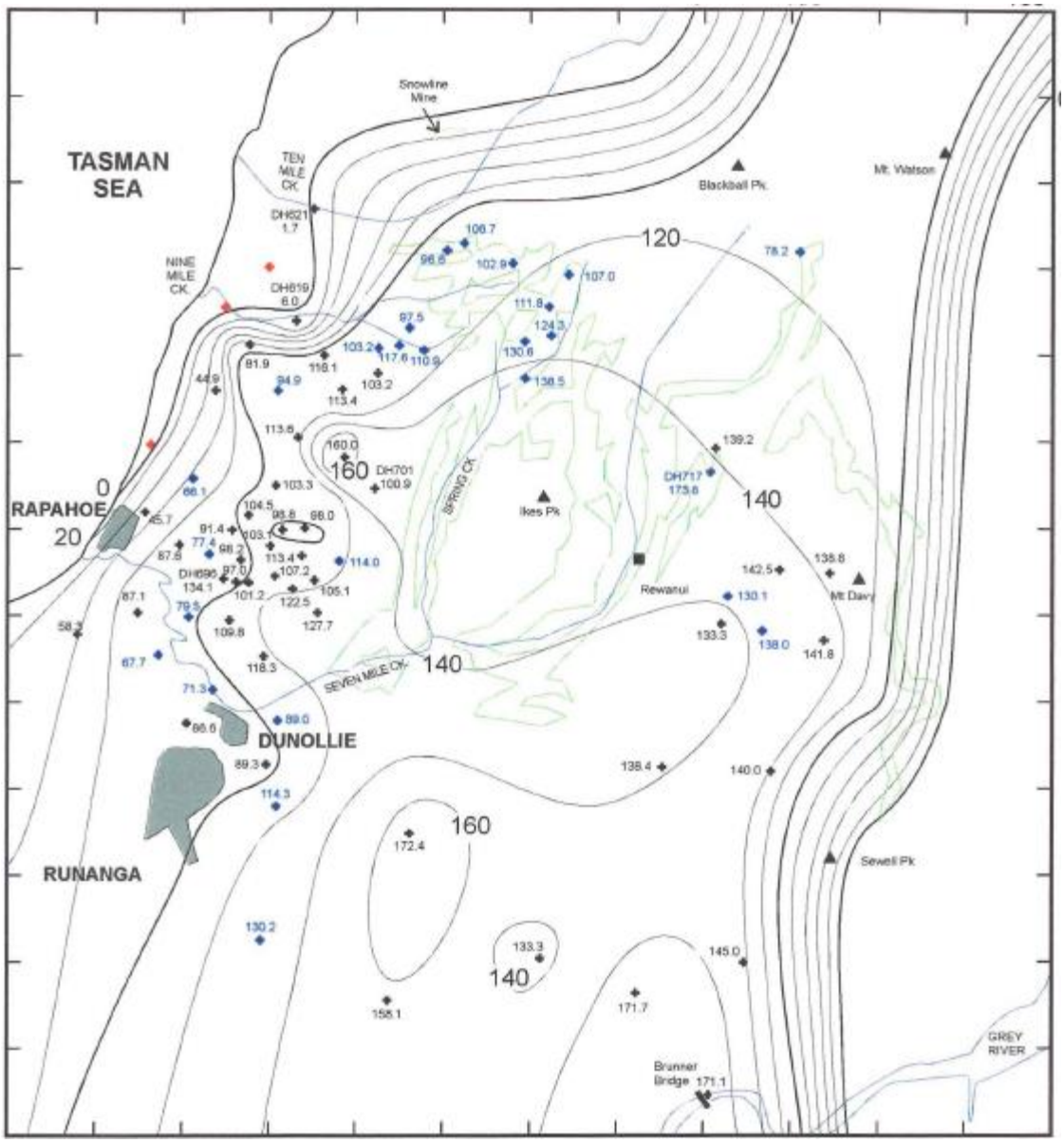

Figure 2.4. Goldlight Formation isopach map showing the great extent of the Goldlight Lake north and south of the coalfield. It should be noted the lack of Goldlight Formation in the Northwest corner of the coalfield. Adapted from Ward (1997).

2.3 Methods

2.3.1 Field measurements and techniques

A number of key field techniques and observations were undertaken to allow for the construction of stratigraphic columns and collection of samples. From this data collection and analysis, decisions could then be made regarding revisions to nomenclature, isopach maps

and basin history. To complete these objectives field work and analysis was undertaken on outcrop and drill core. Updated drill hole information was also supplied than contained information on over 1000 holes across the coalfield.

Due to the dangerous terrain and dense vegetation, access to outcrop within the coalfield is extremely limited. Mine roads and mine sites offer the best outcrop but due to current operations, access was intermittent. Access to the eastern side of the coalfield via Roa Mine Road was unavailable and the closest drill holes to this area were used instead. Streams also provide some access to outcrop but are prone to flash floods due to the West Coast's high rainfall. Although outcrop is poor, there are a high number of drill holes available from across the basin. Over 1000 drill hole details were made available through Solid Energy for analysis.

Field descriptions and stratigraphic sections

Field descriptions and measurements were made in as much detail as possible given the conditions and quality of outcrop. At poor and isolated outcrops, only lithologic descriptions were possible. At continuous and accessible outcrop, stratigraphic columns were measured to 5 - 10cm. From this the majority of stratigraphic columns were constructed on a 1:50 scale with some stratigraphic columns containing more or less detail depending on the quality of outcrop and facies identified. Measurements and descriptions were taken in the normal fashion using standard measurement devices. Measured sections continued into the under and overlying formations to fully include the contacts and to gain a full understanding of the depositional environment during the times of lake level rise and fall.

Drill core descriptions

Drill core descriptions were conducted using the same methods as for field descriptions resulting in the construction of several stratigraphic columns. The selection of core was dependant on availability at the core store, the quality of core and the location. Descriptions were made in the same manner as when conducting investigations in the field and drill core stratigraphic columns are drawn at the same scale as outcrop stratigraphic columns. Several very thick Goldlight Formation stratigraphic columns were drawn to fit on one page as they only consisted of massive mudstone.

Conglomerate clasts counts

Clasts counts were undertaken to help distinguish between the different conglomerate formations in several locations. A 1m ruler was used with clast identification taken every 1cm for a total of 300 counts. This was carried out at 12 Mile Beach to aid in the classification of the mudstone in this location.

Siltstone point counts

Point counting was carried out on several thin sections taken from 12 Mile Beach to determine the origin of rip-up clasts at the base of the Rewanui Formation. 300 counts were done on each thin section by identifying minerals under the microscope at random.

2.3.2 Localities

Field work was undertaken over a period of several months between February and May 2014 and was focused around the northwest section of the coalfield. Overall outcrop within the Greymouth coalfield is limited due to dense vegetation and steep slopes and rivers are often subject to flash flooding. Two good locations for outcrop access where 12 Mile Beach and 10 Mile Creek but other localities visited were Strongman Mine, Spring Creek Mine and Roa Mine.

12 Mile Beach has an almost 60m section of continuous mudstone with a small section that is blocked by a landslide. This allowed for a thorough investigation of the mudstone and surrounding conglomerates but was dependant on tides and the inclement weather. To the south is 10 Mile Creek which contains several key outcrop localities. Along the main access road to 10 Mile Creek is a section of sandy Goldlight, accessed by crossing 10 Mile Creek while further up at the base of Docherty Creek is the Waiomo Formation. This Waiomo Formation is hard to access and limited in outcrop. At the top of 10 Mile Creek overlooking the valley, is a recently cut road that allows access to more Goldlight Formation which bears resemblance to the Goldlight in 10 Mile Creek. Strongman Mine, Spring Creek Mine and Seven Mile all showed thick sequences of massive Goldlight mudstone while Roa Mine to the east showed highly faulted Ford and Waiomo Formation outcrop.

Drill core localities were based on the availability of core at the New Zealand Petroleum and Minerals (NZP&M) core store in Featherston. The decision was made to use this library of

core samples as many of the cores from newer drill holes aren't retained. This decision meant that while the drill holes studied are older they are evenly distributed across the coalfield.

When describing stratigraphic columns, the Greymouth Coalfield was subdivided into four blocks based on location (Figure 2.5). These differ slightly to the blocks commonly associated with coal mining.

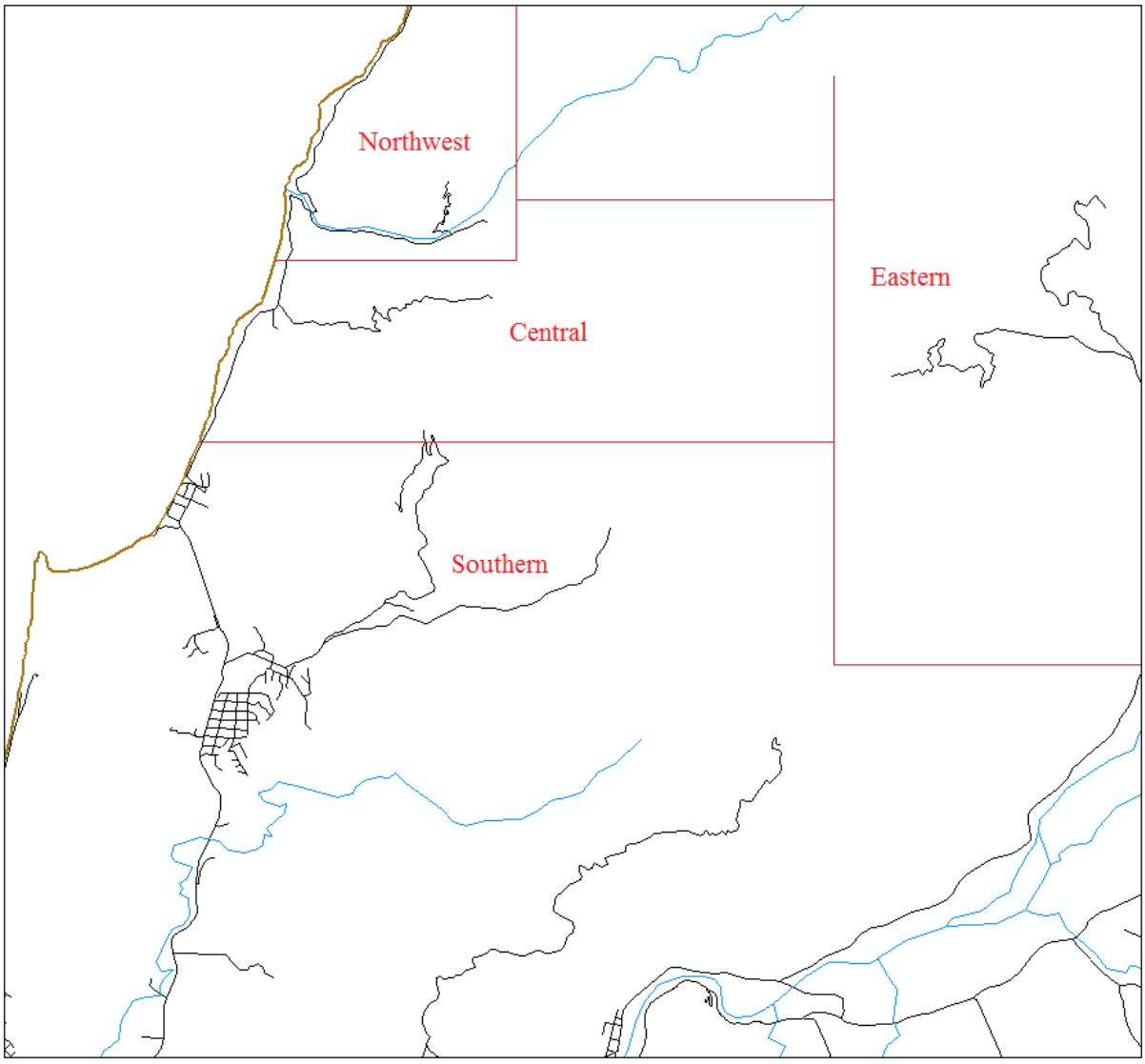

Figure 2.5. Location map for block division used within the Greymouth Coalfield.

2.3.3 Isopach maps

Isopach maps were created using drill hole data supplied by Solid Energy and supplemented by outcrop data and drill hole data available on the NZP&M website. Several isopach maps

have been created in the past by Gage (1952), Newman (1987) and Ward (1997) but a surge in drilling over the last 2 decades has resulted in 600 new drill holes across the coalfield. By including these new drill holes, adding in the transitional shoreline lithologies and new sedimentological data a more inclusive and accurate isopach model could be created for each lacustrine formation.

Initially, all drill holes which intersected the lacustrine deposits were selected with 146 holes intersecting the Ford Formation, 362 intersecting the Waiomo Formation and 473 intersecting the Goldlight Formation. These numbers were then narrowed down by eliminating drill holes which showed major discrepancies in thickness from faulting, and drill holes which were very similar to others surrounding them. The latter was done due to the sheer number of drill holes which often overlapped and made it difficult to read. Additional outcrop information and several other drill holes were added which allowed for more complete isopach maps to be created.

2.4 Lithofacies associations

Using core and outcrop descriptions, the lacustrine mudstones and accompanying transitional sedimentary rocks have been divided into facies associations and outlined in Table 2.1. Due to the similarities between the mudstones in terms of distribution and sedimentology, facies associations encompass all three lacustrine formations. Associated depositional environments are also outlined.

2.4.1 Facies association 1a: Deep lake

Massive grey to black mudstone with occasional purple or brown colouring (Figure 2.6). Fossils identified by Gage (1952) and Ward (1997) may be locally abundant and include small leaves, freshwater snails and molluscs (*Hyridella sp.*) and pollen (*Nothofagus sp.*). Other information on fossils within the coalfield can be found on FRED (Fossil Record Database). Facies 1a can be found throughout the coalfield.

Facies Number				
1a	Massive mudstone with occasional well defined leaf fossils.	Deep lake		Deep lake
1b	Inter-bedded siltstone to fine sandstone. Basal contact is often sharp, wavy over mm. Normal grading.	Distal turbidites		
2a	Normally graded very coarse to medium sandstone. Occasional basal conglomerate. Channelised or lenticular beds.	Proximal turbidites		Slope
2b	Matrix supported coarse sandstone to pebble conglomerate. Massive to reverse grading, angular to sub rounded.	Debris flows		
3a	Reversly graded sandstone, usually channelised (10 - 15m). Occasional laminations and normal grading. Micaceous.	Mouth bar/ delta		River/ river mouth
3b	Granule to boulder, clast supported conglomerate. Rounded to sub- angular, sometimes imbricated,moderate to poor sorting. Occasional thin sandstone lenses.	Braided river/ low angle alluvial fan		
3c	Medium to coarse sandstone, distorted laminations, bioturbated, ripples and small cross bedding.	Meandering river delta		
4a	Laminated medium sandstone to mudstone with plant material.	Lake margin, low energy		Lake edge
4b	Siltstone/ fine sandstone with abundant fragmented fossilised plant material. Micaceous, faintly laminated.	Shallow marshy lake/ isolated pond		
5a	Carbonaceous claystone	Developing or flooded peat bog/ marsh		Coal mire
5b	Coal	Peat bog		

Table 2.1. Summary diagram of facies associations and interpreted depositional environments identified in this study.

Figure 2.6. Goldlight Formation massive mudstone at Spring Creek Mine, (7 Mile Stream).

The presence of massive mudstone indicates deposition beyond the direct influence of any shoreline or slope processes (Renaut & Gierlowski-Kordesch 2010). Primary deposition would have been from hemipelagic sedimentation (Henrich & Hudecki 2011) due to the lack of evidence of bed load transport. The presence of very rare leaf material and pollen such as *Nothofagus* (southern beech) obtained from the Fossil Record Database (FRED) indicate an environment quite similar to what we see today.

2.4.2 Facies association 1b: Distal turbidites

Grey to dark grey siltstone (occasional light grey, purple and brown) with thin beds (<3cm) of lighter grey, brown or purple fine sandstone (Figure 2.7). The abundance of bedding within the siltstone varies with some locations showing stacked beds while others are separated by thick sequences of massive mudstone and siltstone on a metre scale. Basal contacts are erosional and wavy while upper contacts are slightly gradational. Beds are

normal graded and often wavy with little variation in thickness. Facies 1b can be found throughout the coalfield.

Figure 2.7. Thin, faintly laminated mudstone and fine sandstone within the Waiomo Formation, 10 Mile Creek.

The sharp basal contact of many of the beds indicate erosion and scouring before deposition of the overlying material. This is indicative of downslope flow transport mechanisms such as turbidity currents or debris flow (Boggs 2006). Normal grading and the lack of coarse sediment is evidence of fine grained lacustrine turbidite deposits (Chang & Chun 2012).

The formation of lacustrine turbidites can occur in several ways depending on the angle of the slope. Turbidites which flow down low angle slopes occur where sediment laden rivers enter the lake. In areas with steeper slopes, turbidites can begin as sub-aerial debris flows which transform into low concentration flows as sediment is transported into a sub-aqueous setting (Stow 1996). Turbidites can also form as underwater slumps in soft unconsolidated sediment at the top of steep slopes. The fine grain size, as seen in facies association 1b, can also be an indication of the distance travelled by the turbidity current (Shanmugan 2002).

2.4.3 Facies association 2a: Proximal turbidites

Massive, grey siltstone to medium sandstone inter-bedded with normally graded, very coarse to fine sandstone at the top (Figure 2.8), commonly separated by other facies. Beds are up to 1m thick and often channelized, incising into underlying siltstone / sandstone on a cm scale. The basal coarse and often massive sandstone can contain angular to sub rounded pebble clasts which are dominantly quartz in composition. In some locations iron staining can occur from weathering and the beds are brown instead of grey. As the beds fine upwards the sandstone can show wavy laminations and ripples of dark grey mudstone. These laminations occur only in the finer sandstone of the turbidite sequence and bear resemblance to the distal turbidites of Facies 1b. Facies 2a can be found in most areas of the coalfield but is most common to the north-west.

Figure 2.8. Proximal turbidites within the Waiomo Formation, 12 Mile Beach.

The presence of normally graded sandstone beds with occasional conglomerate clasts cut into underlying finer sedimentary rocks are interpreted to be deposited from high energy turbidity currents. The lower basal sandstone with occasional pebble clasts matches with the Ta

division of the turbidite model created by Bouma (Arnott 2010). The upper laminated sandstone resembles the Tc division of the Bouma sequence, which is characterised by wavy or convolute lamina. The gradational top contact of the beds represents the gradual settling of sediment that has been entrained and transported by these turbidity currents.

Turbidity currents often scour out underlying strata resulting in a mixing of sediments as they travel down slope (Boggs 2006). When deposition occurs, the larger heavier clasts are deposited first along with coarse sand in a structure-less but gradational overall unit. The medium to fine sand and sparse laminations are deposited during the middle stage of the turbidity current with the laminations and occasional ripples indicating the existence of a current. The upper contact of the current grades back to siltstone, indicating a gradual settling out of the sediment left as the turbidity current moves through (Chang & Chun 2012). The siltstone between turbidites results from settling of finer sediment out of suspension once the turbidity current has moved through (Stow et al 1996).

2.4.4 Facies association 2b: Debris flows

Lithofacies 2b comprises brown, massive, poorly sorted, angular to sub-rounded matrix supported, granule to cobble conglomerate (Figure 2.9). Beds are channelized and up to 1.5m thick and exhibit faint reverse grading. Basal contacts are erosional and undulating with relief of up to 15cm while the upper contacts are gradational over several cm's to 10's of cm's. Clast compositions are mostly Greenland Group siltstone and vein quartz with rare dark grey mudstone. The matrix is brown medium to coarse sandstone. Facies 2b is found in the north-west of the field area around the 12 Mile Beach and 10 Mile Creek areas.

The presence of matrix supported mostly angular conglomerate with scarce reverse grading and channelised bedding is an indication of debris flow deposits. Debris flows are more concentrated than turbidites with higher sediment yield leading to the lack of grading and general disorganisation of the deposit during deposition (Blair 1999). Flows may start sub-aerially and be transported down fluvial channels out into the lacustrine slope edge (Miall 2010). Debris flows may also occur in sub-aqueous environments due to sediment loading on steep sub-aqueous slumps leading to slope failure (Boggs 2006).

Figure 2.9. Matrix supported debris flows within the Goldlight Formation shoreline, 10 Mile Creek.

2.4.5 Facies association 3a: Mouth bar/delta

Facies 3a consists of brown, micaceous, reversely graded very fine to coarse sandstone. Beds are usually channelised and can be up to 15m wide (Figure 2.10). Faint laminations can often be seen in the finer sandstone and in rare occasions, normal grading is also present. In some locations, reversely graded sandstone can transition conformably into the proximal turbidites of lithofacies 2a. Facies 3a is mainly found in the north-western corner of the coalfield.

Reverse grading within sandstone beds combined with thickening of these beds up sequence is indicative of a prograding mouth bar environment (Bhattacharya 2010). The coarser sediment is indicative of a higher energy delta front / mouth bar environment which sits directly in front of the outgoing river mouth. This creates a higher energy environment hence the large dominant grain size. The fine grained sediment between these reversely graded mouth bar channels indicates the time when these mouth bars are abandoned by channel avulsion. Delta succession and progradation is easily identified through the thickening of

beds. As deltas prograde out into the lake, coarser sediment is transported further out and lies on top of the finer grained sediment which was transported earlier through channel avulsion (Jones & Hajek 2007, Makaske et al. 2002).

Figure 2.10. Reversely graded sandstones and occasional conglomerate within the Goldlight Formation, 10 Mile Creek.

2.4.6 Facies association 3b: Delta plain/ River channel (braided)

Lithofacies 3b is a clast supported, granule to boulder conglomerate (Figure 2.11). Clast composition is predominantly Greenland Group siltstone with vein quartz. The Rewanui and Dunollie Formation conglomerates also contain granite and dark grey mudstone rip-up clasts. Clasts are rounded to sub angular and show faint imbrication with moderate to poor sorting. Within the conglomerates there can sometimes be carbonaceous lenses of light grey, faintly laminated, fine sandstone. Facies 3b is found in the west and north-west of the coalfield.

Figure 2.11. Rewanui conglomerates at 10 Mile Creek.

The rounded, clast supported and imbricated conglomerates seen in several areas of the Greymouth Coalfield are all evidence of coarse grained braided rivers (Turkmen et al. 2007). The size of the conglomerates is a good indication of the distance travelled as is the rounding of the individual casts. Larger clast size indicates that clasts haven't travelled very far from a source area due to the energy required to move larger and heavier rocks. Similarly, angular clasts usually correspond to less distance travelled as rounding occurs during transport. The conglomerates of lithofacies 3a are large in size but also rounded. It appears that the conglomerate was sourced from a large catchment area resulting in the large clasts size which also allowed for the roundness of the conglomerates without reducing their clast size. From this it appears the source area to the north/west was in close proximity to the beach and this source area was also large which allowed for rounding to occur before the river exited the catchment area (Miall 2010).

The sandstone lenses seen within the conglomerates are sandy bedforms and bar top channels which form as the main river channel migrates away (Collinson 1996). The proximity to underlying lacustrine mudstones also indicates that these conglomerates were deposited in a delta plain environment.

2.4.7 Facies association 3c: Meandering river delta

Lithofacies 3c comprised red, fine to medium sandstone with usually distorted, discontinuous laminations (Figure 2.12). Laminations are heavily bioturbated but when they haven't been distorted they can show small scale ripples and cross bedding. This facies is mainly found in the central section of the coalfield. In some locations, vertical root fossils can also be found.

Figure 2.12. Distorted laminations within the Goldlight Formation / Rewanui Formation gradational contact. The orange nodules contain pyrite.

Although this facies exhibits many similarities to the other sandier laminated facies described, the distortions of the laminations and the red colour of the sandstone lends itself to a sub-aerial environment where deposition is marked by intermittent overtopping of the river banks and formation of red soils. This is further enforced by the presence of root fossils which are always found in sub-aerial or shallow water environments (Bhattacharya et al. 2010).

The low energy laminations found within this facies are often distorted and bioturbated, indicating the sediment was exposed to surface processes shortly after deposition.

Bioturbation is common in sub-aqueous environments but the nature of the bioturbation differs (MacEachern et al. 2010). Meandering river deltas commonly form defined and are separated by lowland floodplains with levees and crevasse splays common (Bhattacharya et al. 2010). The presence of red soils represents the abandoning of the channel through river avulsion while thin lacustrine deposits represent lake level transgression and episodic flooding (Bhattacharya 2010).

2.4.8 Facies association 4a: Lake shore

Facies 4a is made up of laminated but occasionally massive, medium brown to grey, fine to coarse sandstone and siltstone (Figure 2.13). Plant remains including leaves and twigs can be found and are usually whole and well preserved. Laminations are usually well developed and wavy, with the finer grain sizes sometimes containing faint carbonaceous material. Sandstones are usually micaceous and quartzo-feldspathic. Grading, if seen, is normal. This facies is found in the northwest margin of the coalfield.

Figure 2.13. Sandy and silty lake edge deposits within the Goldlight Formation, 10 Mile Creek.

These laminated sandier sediments are interpreted as being proximal to pro-grading deltas and are found in the northwest corner of the coalfield. The sandstones of Facies 4a don't commonly show grading but if they do it is normal and they are slightly finer grained. This facies is likely to have formed as a beach or shallow lake margin due to the presence of semi-sorted sandstones and siltstones (Renault & Gierlowski-Kordesch 2010).

2.4.9 Facies association 4b: Marshy lake edge

Lithofacies 4b is made up of grey / brown very fine sandstone with abundant fragmented plant fossils (Figure 2.14). The sandstone is micaceous and shows very faint evidence of laminations and bioturbation with rare vertical fossilised rootlets. Plant remains include broken leaves and twigs and other debris. Occasional land snail fossils can also be seen which measure approximately 1.5 – 2cm across. Facies 4b is found in the central, eastern and south-western sections of the coalfield.

Figure 2.14. Carbonaceous mudstone and quartzose sandstone within the Rewanui Formation.

The combination of fine grain size and numerous broken plant remains is an indication of a low energy environment with the preservation of plant material during deposition. The combination of fine grain size and abundance of plant material indicates the environment of deposition low energy and marshy. Sediment supply to this area was likely from meandering rivers with sediment fed into the lack from meandering river deltas. A lack of turbidites within the facies is also an indication of a low angle slope environment (Renaut & Gierlowski-Kordesch 2010).

2.4.10 Facies association 5a: Developing/ dying peat bog

Lithofacies 5a consists of carbonaceous dark grey to black siltstone to claystone (Figure 2.15). The appearance is greasy and soft and it's hard to discern individual leaf fossils. This facies is found in most central and eastern sections of the coalfield as the mudstones transition to coal. The lack of discernible plant material within this facies separates it from facies 4b.

Figure 2.15. Coal transitioning to carbonaceous mudstone within the Rewanui Formation at Roa Mine. This is topped with indurated quarto-feldspathic medium to coarse sandstone.

The inclusion of more carbonaceous material in this facies is an indication of a developing peat bog in a sub-aerial environment (Collinson 1996). Some organic material may still be

discernible but the overall impression is of a fine grained environment with limited drainage caused by plant growth at the surface.

2.4.11 Facies association 5b: Peat bog

Facies 5b is made up of black, hard, often fragmented coal (Figure 2.16). It is often "dirty" with sandy laminations and clear individual sand grains seen within the coal. Coal seams are found throughout the coalfield with thin, split, sediment laden seams in the north-west and thick (~20m), high quality coal seams in the centre and the eastern sections of the coalfield.

Figure 2.16. Coal seam bounded by conglomerates within the Morgan Formation at Roa Mine.

Coal as described above commonly forms in peat bogs and raised mires (Diessel 1992). As vegetation inhibits drainage, peat mires form which over time transform into coal. The coal seen during this study was often quite "dirty" with obvious siltstone and sandstone sediment included in with the organic material. This indicates that the peat bogs were still being influenced by small amounts of sediment supplied by small streams.

2.4.12 Distribution of lithofacies

Lithofacies variations can be seen across the coalfield. In the north-west are higher energy deposits including clast and matrix supported conglomerates that have been interpreted as being from braided rivers and debris flows (lithofacies 3b and 2b respectively). This area also contains the thickest proximal turbidite deposits (lithofacies 2a), thinnest coal seams (lithofacies 5b) and coarse grained sandstone lake shore line facies (4a).

In the central and eastern sections of the coalfield are the thickest massive mudstone deposits and distal turbidites (lithofacies 1a and 1b) interpreted as deep water lacustrine deposits. These become thinner towards the edges of the coalfield where they transition to sub – aerial environments as marked by shallow marshy lake sediments and crevasse splay deposits (lithofacies 4b and 3c). In many locations these become carbonaceous mudstone and coal (lithofacies 5a and 5c) interpreted as developing peat bogs in a sub-aerial environment.

2.4 Goldlight Lake

Although the Goldlight Formation is the youngest lacustrine mudstone within the Paparoa Coal Measures, it is described first due to the abundance of information from outcrop and drill core. The Goldlight Mudstone was originally described by Maxwell Gage (1952) as massive dark brown to dark grey mudstone with occasional siderite bands and concretions that outcropped in various areas across the coalfield. It was noted that only the massive mudstone facies would be classified as Goldlight due to mapping convention and all other time equivalent non-massive mudstone facies would be classified as either Rewanui or Dunollie. This has applied to all mapping and consequent interpretation of the Goldlight Mudstone since. In recent years “transitional” Goldlight, the sandy, shallow lake facies, have been included in core logs and stratigraphy (Ward 1997) but a proper study into these facies has not been undertaken.

A focus within this thesis has been to describe and interpret the Goldlight Mudstone as a whole, not just the massive mudstone which represents only the deep lake environment. By reclassifying the “transitional” Goldlight and including these additional facies the true extent of the lake can be determined, particularly to the north-west, and a better understanding of the basin as a whole can be developed.

2.4.1 Goldlight Formation isopach map

To create a revised isopach map, data from 472 drill holes that intersected the Goldlight Formation were analysed (Appendix 3). From this, 48 drill holes were used to represent the Goldlight Formation in each area. Additionally, several revisions to the Goldlight Formation were taken into consideration when creating the new isopach model. By adding new transitional proximal to shoreline lithofacies, the thickness of the Goldlight increases and there was a small change to the extent in the north-west around 10 Mile Creek.

The Goldlight Formation isopach map (Figure 2.17) bears many similarities to the previous isopach created by Ward (1997) which showed the unit to be thick, widespread and oriented in a NNE – SSW direction. The new drill hole data and inclusion of sandier lithofacies has increased the thickness within the revised map from 140m to 180+m. The new isopach also shows the Goldlight extending further to the north-west. Instead of extrapolating the Goldlight isopach northward, the decision was made to illustrate regions where younger erosion has thinned the Goldlight by truncating the isopach contours against the edge of the coalfield rather than closing the contours. Similarly, the Goldlight stops abruptly next to the Roa – Mt Buckley Fault zone. This unconformity is more pronounced due to the greater depths of the Goldlight Formation to the east. Although previous work has stated faulting in this area controlled subsidence and deposition within the basin, the fact that all three mudstone units stop abruptly against it suggests that the edge of the coalfield has been offset or truncated by this younger fault system.

The Goldlight Formation is the largest lake in the basin as well as the thickest. Although the northern and eastern margins of the Formation have been eroded or offset, the great depths of the lake at the edges of the coalfield suggest the Goldlight Lake extended far beyond the confines of its current outcrop location. A lack of drill hole data to the south also inhibits the understanding of the lake within this area but it appears to also extend further here as well.

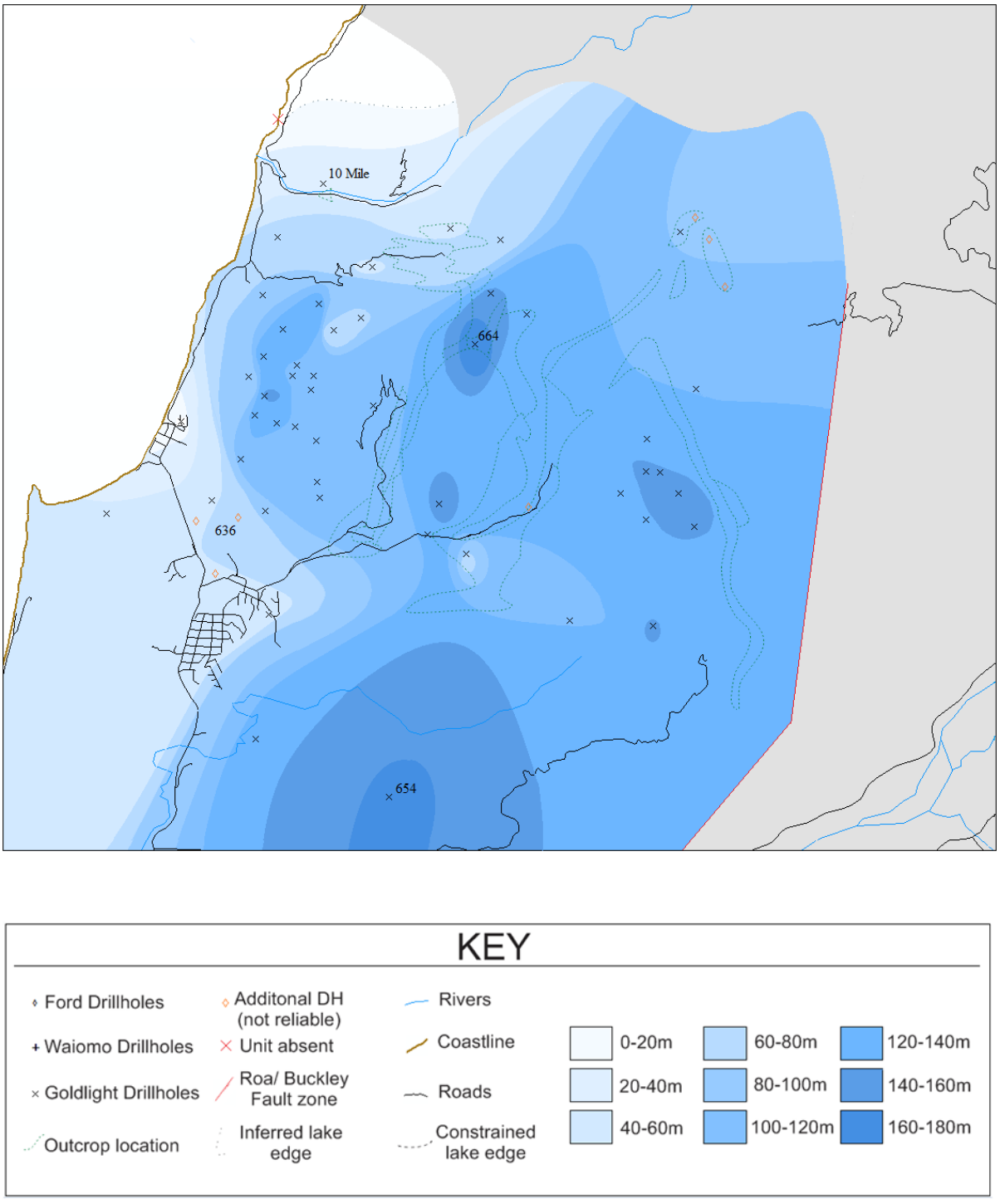

Figure 2.17. Goldlight Formation isopach map and key for all lacustrine isopachs. The orientation and extent of this revised isopach is similar in aspect to the Ward (1997) isopach except depth contours no stop at the eastern boundary instead of close.

2.4.2 Goldlight Formation sedimentology

Central block

The Goldlight Mudstone around Strongman Mine exhibits the traditional massive mudstone (Figure 2.18) facies that the Formation was originally described as having. DH 664 (Figure 2.19) is representative of the area and what can be found in multiple drill holes.

DH 664 (Figure 2.19) contains 30m s of shallow, marshy lake edge facies (facies 4b) that transitions into over 150m of massive mudstone. The gradual change from Rewanui to Goldlight shows cyclical flooding of several small peat bogs as lake level rises. The presence of coal and numerous carbonaceous mudstone zones is indicative of a low relief flood plain environment with numerous small raised mires and ox-bow lakes. This was gradually swallowed by a transgressive lake margin, with lake depths gradually deepening in this area.

The first few meters of this transition contain wavy, thinly laminated siltstones and fine sandstones with rare, poorly defined cross beds just above the Rewanui Formation. These units are slumped and heavily distorted indicating soft-sediment deformation occurred shortly after deposition. As this area is overlain by the Goldlight shoreline, deposition is expressed in the form of reversely graded mouth bar and delta deposits (Facies 3a) and low energy, laminated lake edge deposits (Facies 4a). Both show evidence of organic material throughout.

The transition to massive mudstone occurs over 2 meters and is noticeably less organic indicating that at this point the lake was large enough that the transport of organic material from the lake edge didn't reach this area. The presence of massive mudstone this thick (> 100 m) suggests deposition occurred in an area of the Goldlight Lake unaffected by sub-aqueous slope processes like turbidites. The presence of the lake margin facies can be found in 10 Mile Creek several km north of this location, thus it appears the lake deepened rapidly towards this area of the coalfield.

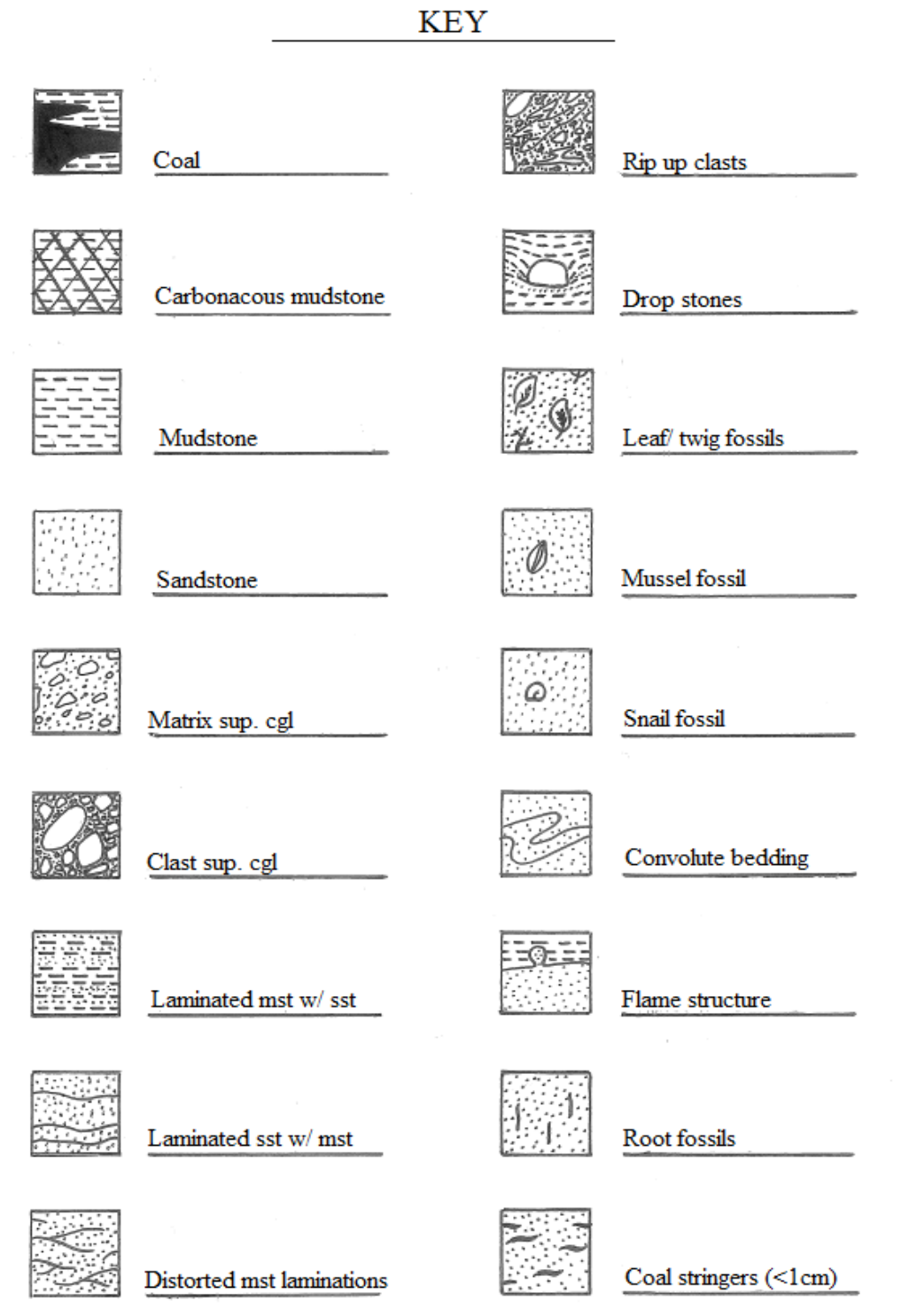

Figure 2.18. Stratigraphic column key.

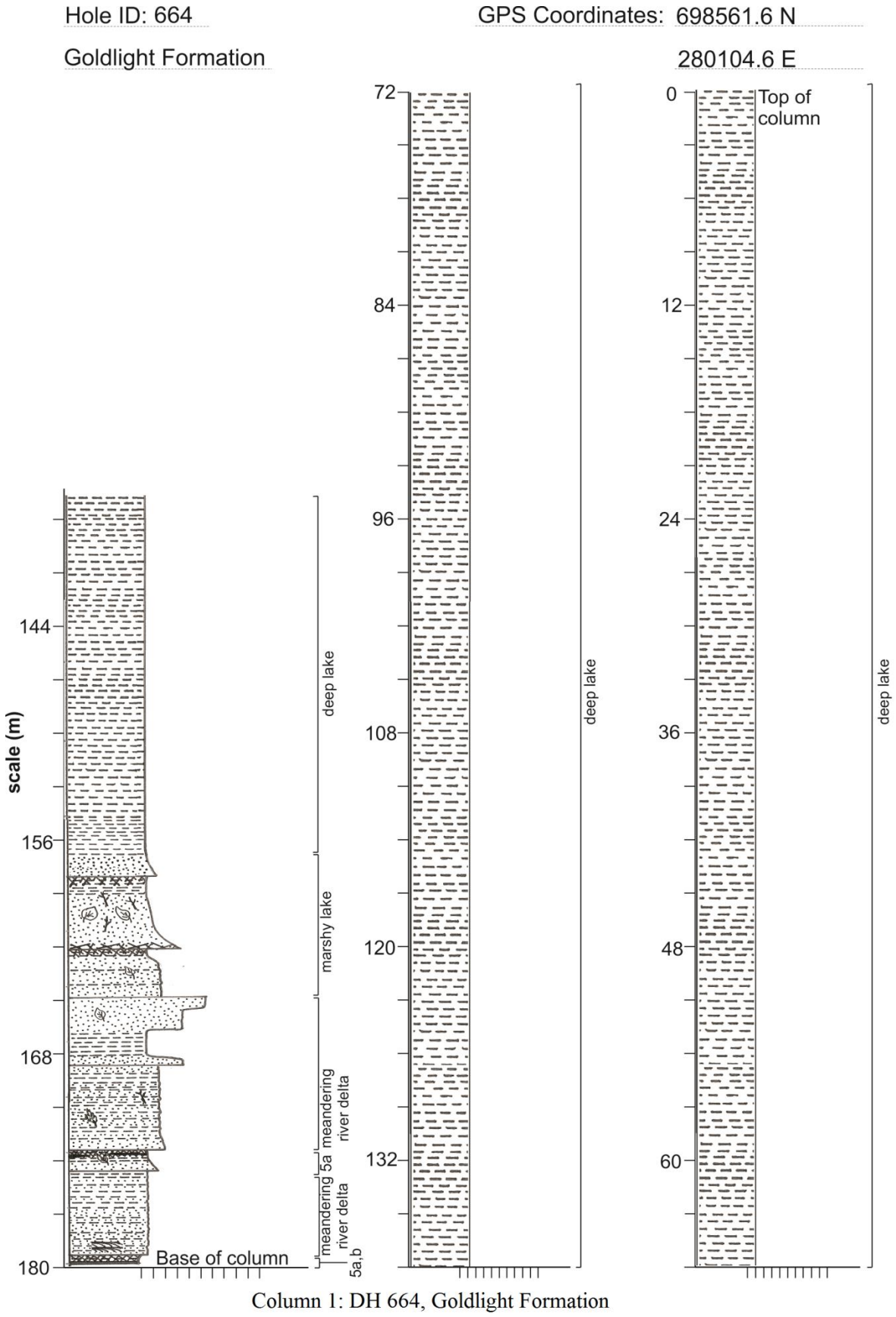

Figure 2.19. DH 664 stratigraphic column.

Eastern block

Data from the eastern side of the basin (Figure 2.5)) is limited for the Goldlight Mudstone due to the lack of available drill holes and erosion of the Goldlight Mudstone and Dunollie Coal Measures. As the Goldlight has been previously mapped in this location, it will be present as massive mudstone that is truncated by the Roa – Mt Buckley Fault Zone (Nathan 1978). Limited drill hole data shows sandstone and carbonaceous mudstone laminations beginning as the Goldlight Formation transitions to the underlying Rewanui Formation.

Southern block

The Goldlight Formation in the southern half of the Greymouth Coalfield is characterised by thick massive mudstone with gradational contacts (over 10's of m) to the under and overlying formations. Drill holes in the central southern area contain volcanic intrusions through the middle of the Goldlight Formation (DH 654 and DH 651) while DH 653 (Figure 2.20) in the west contains predominantly organic rich mudstone, sandstone and coal.

DH 653 (Figure 2.20) shows a deep lake environment affected by thin distal turbidites and organic rich sediment. The lower gradational contact between the Rewanui and Goldlight Formations begins with thin bands of carbonaceous mudstone and very fine sandstone. The lake shore is characterised by very fine to medium sandstone with fluctuating amounts of organic material found throughout the core indicating the area was shallow and marshy (facies 4b).

The gradual contact between the underlying very fine sandstone overlying massive mudstone shows the increase in water depth, with a distinct lack of the proximal turbidites as seen in other areas of the basin. Organic material was still present but not as common. The extent of massive mudstone (facies 1a) without any coarser grained sediment indicates that lake level was quite high in this location.

The contact with the overlying Dunollie Coal Measures is again gradational with the addition of thin sandstone and coal bands up to 3cm thick. Predominant grain size increases from mudstone to laminated fine to medium sandstone for several meters with several channel features, produced as rivers infilled the lake edge (facies 3c).

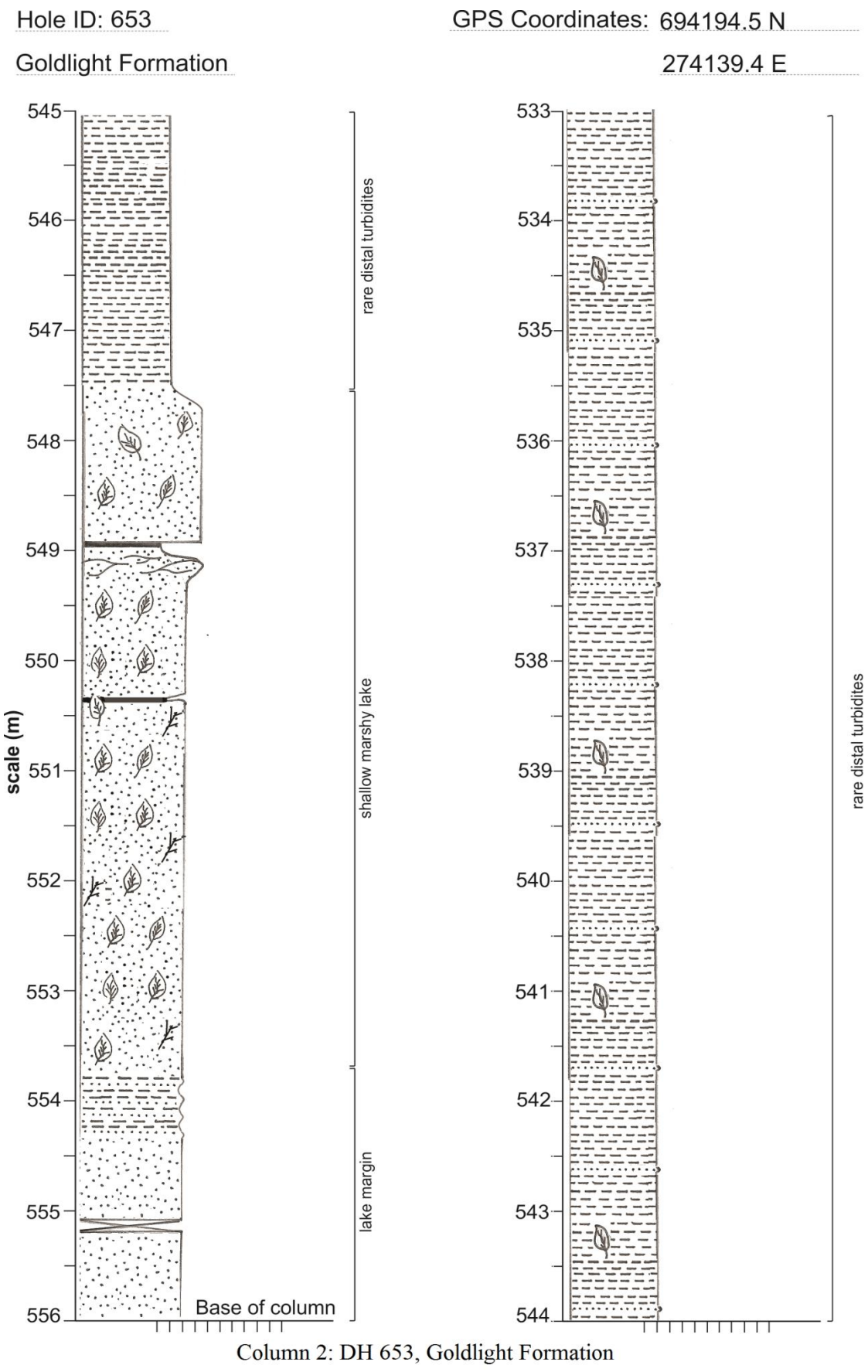

Figure 2.20. DH 653 stratigraphic column.

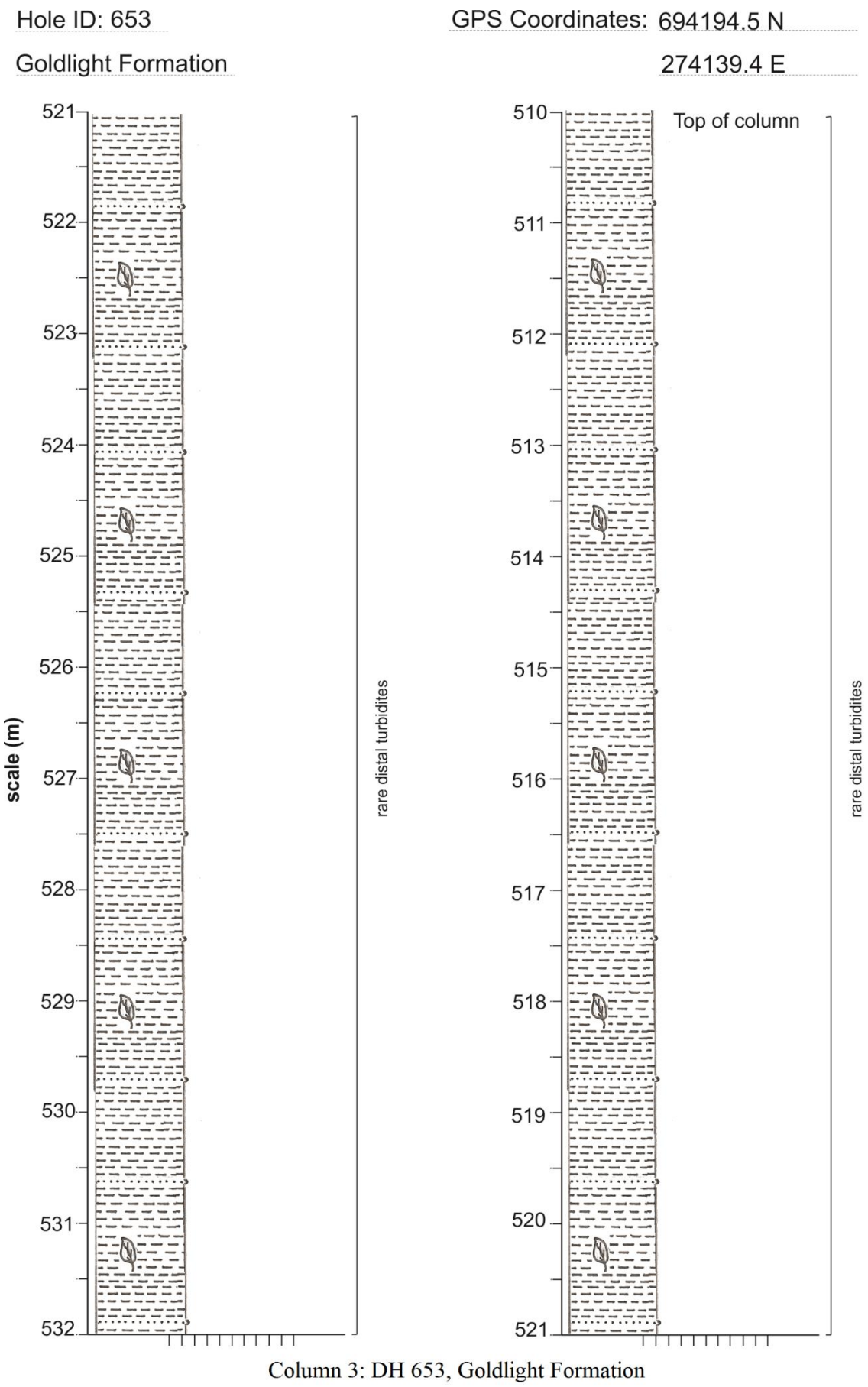

Figure 2.20. DH 653 stratigraphic column.

Moving northeast, DH 636 (Figure 2.21) bears many similarities to what is seen in DH 653. Coal lenses and carbonaceous mudstone of the Rewanui Formation transition quite abruptly into massive mudstone (facies 1a), marking the point where the low lying basin was flooded by the Goldlight Lake. The Goldlight Formation here is considerably thicker than in DH 653 with almost 90m of massive mudstone containing abundant fossilised plant material.

A basin high to the southwest has had an impact on deposition within this area of the southern block. The underlying contact between Rewanui Formation and the Goldlight Formation shows lake level transgression and inundation over several metres of carbonaceous mudstone and coal (facies 5a and 5b). This is followed by 90m of organic rich siltstone (facies 4b) before the sediment becomes less organic rich. The contact between the Goldlight Mudstone and Dunollie Coal Measures begins with the inclusion of several sections of reversely graded, micaceous sandstone, deposited from a delta pro-grading into the shallowing lake (facies 3a). The top of DH 636 shows a thick sequence of faintly laminated carbonaceous mudstone (facies 4b) and sandstone indicating a shallow lake shore environment (facies 4a).

The shallowing of the Goldlight Lake to the southwest which is seen in the Goldlight isopach map combined with the organic rich nature of the mudstone in this location indicates a basin high was present to the south-west of the coalfield. The lack of thick turbidites in this area indicates slope angle was shallow and sediment was likely source from low angle flood plain and meandering river deltas.

DH 654 (Figure 2.22) is the southernmost drill core that contains Goldlight Formation within the Greymouth Coalfield (Figure 19). Here, the transition to a deep lake environment is graduated. The overall thickness of the Goldlight Formation in this area exceeds 200m with the top and bottom of the Formation separated by a 50m thick volcanic intrusion. Drill core was not available for the top of the section however interpretations could be made from core logs available from NZP&M.

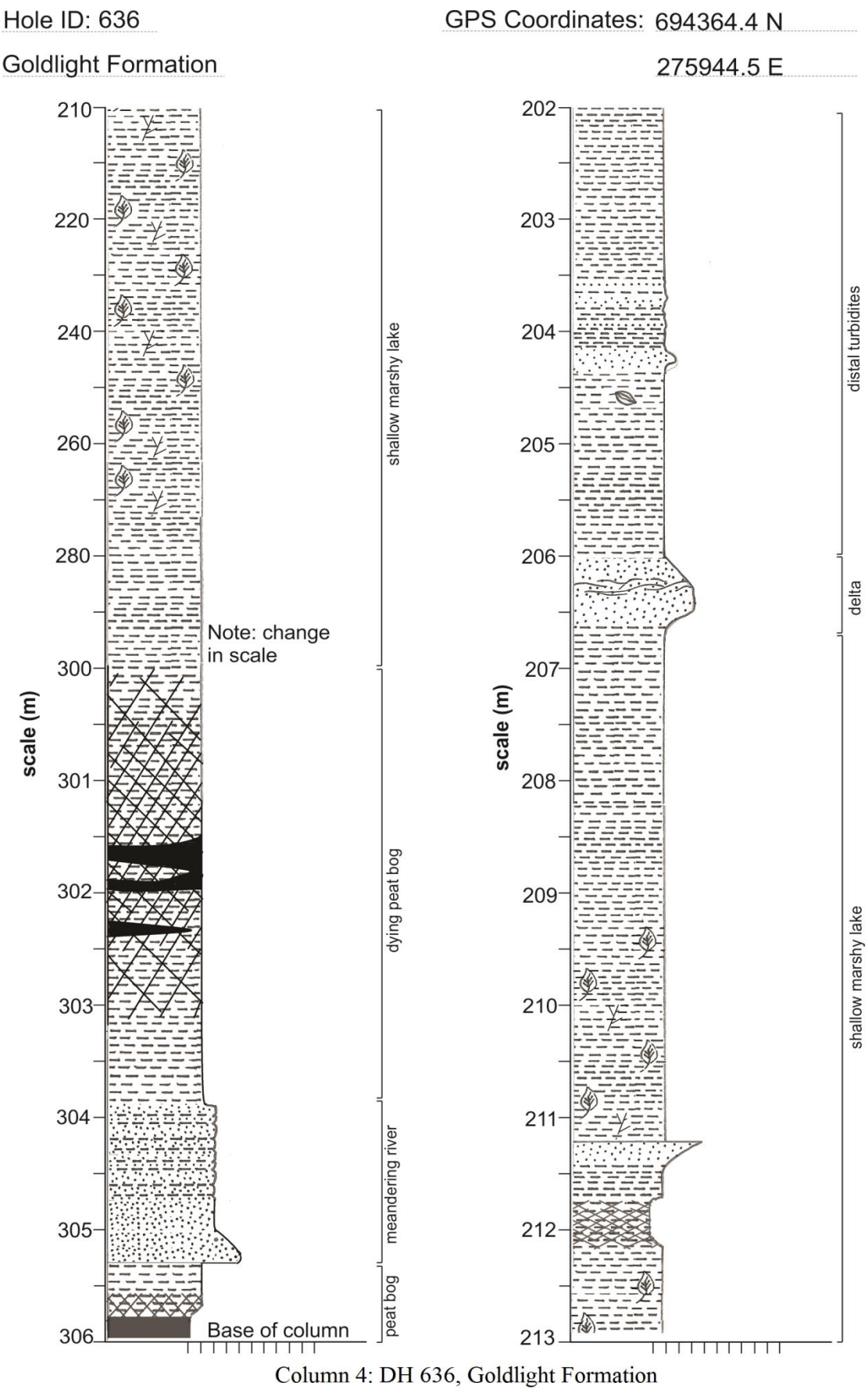

Figure 2.21. DH 636 stratigraphic column.

Hole ID: 636

GPS Coordinates: 694364.4 N

Goldlight Formation

275944.5 E

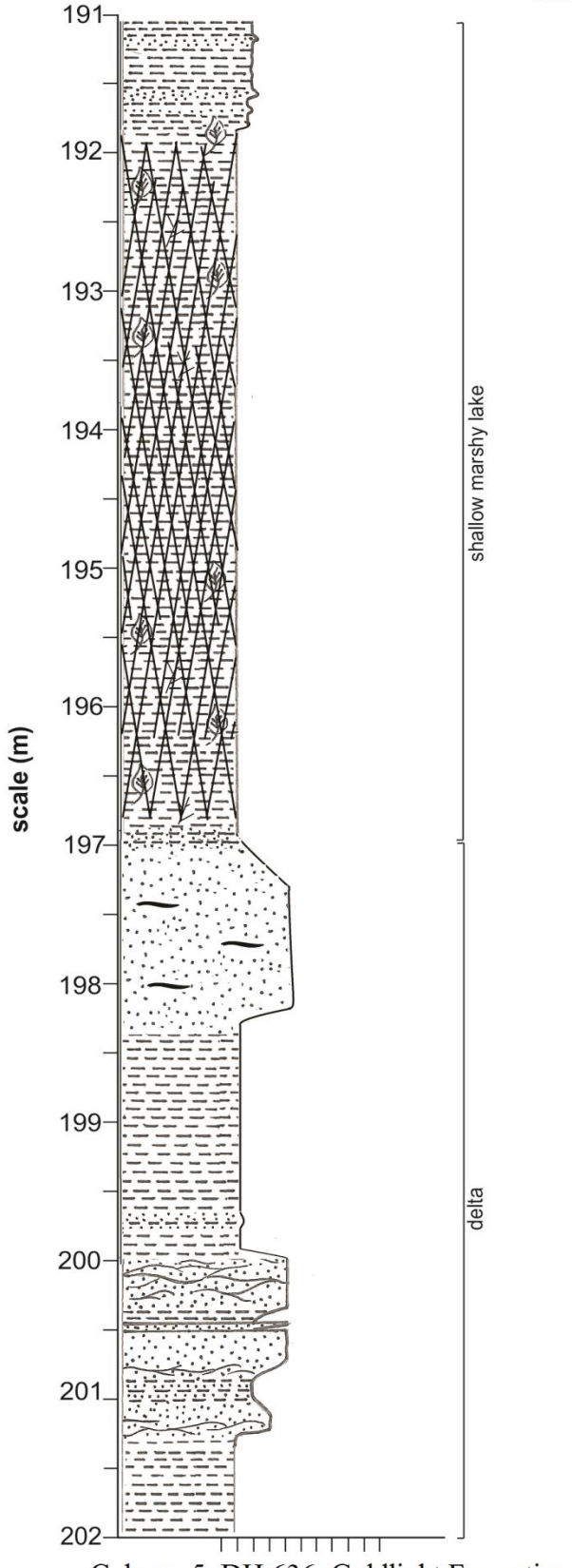

Column 5: DH 636, Goldlight Formation

Figure 2.21. DH 636 stratigraphic column.

In this area, the Rewanui Formation and Goldlight Formation contact again shows coal and carbonaceous mudstone (facies 5a, 5b) being overlain by laminated very fine sandstone as the Goldlight Lake formed. The transition from Rewanui Formation to Goldlight Formation is the same as all other Goldlight stratigraphic columns with the gradual flooding of a peat bog. This is replaced by a shallow lake shore represented by laminations of fine sandstone and siltstone (facies 4a) and influenced by river avulsion resulting in mouth bar and delta sandstones (facies 3a). The change to massive mudstone is gradual, occurring over 20m, with sparse, thin, distal turbidites being found before it becomes massive mudstone.

Approximately 20m of massive mudstone can be seen before it is truncated at 630m a volcanic dyke. This has formed a baked margin affected up to 1.5m of the mudstone. The mudstone is fractured and filled with veins of quartz that fan out from the overlying intrusion. The intrusion itself is microcrystalline with small quartz veins throughout. The upper part of the intrusion is brecciated and broken but still shows the dispersed veins described above. This indicates it was completely intruded rather than being a surface flow and that the intrusion was into shallow, wet sediments not completely lithified at the time of intrusion (Cas & Wright 1987). The Goldlight Formation logged on top of the intrusion (Figure 2.22) is entirely massive for 13m, is often faulted and in some places graphitised. Although not logged, this massive mudstone continues for another 25m before coarser grained siltstone and sandstone laminations begin to appear.

Northwest block

The Goldlight Formation in the northwest area lacks deep lake facies including both massive mudstone and distal turbidite facies (Figure 2.23). The stratigraphic column from10 Mile Stream shows a lake margin depositional environment dominated by coarsening and thickening upwards mouth bar/ delta sandstone beds (Facies 3a) punctuated by thick debris flow deposits. These transitions upwards into a slope edge environment with abundant proximal turbidites. Direct contacts between the Goldlight Formation and the Rewanui and Dunollie Formations in this location are unavailable due to faulting and poor outcrop.

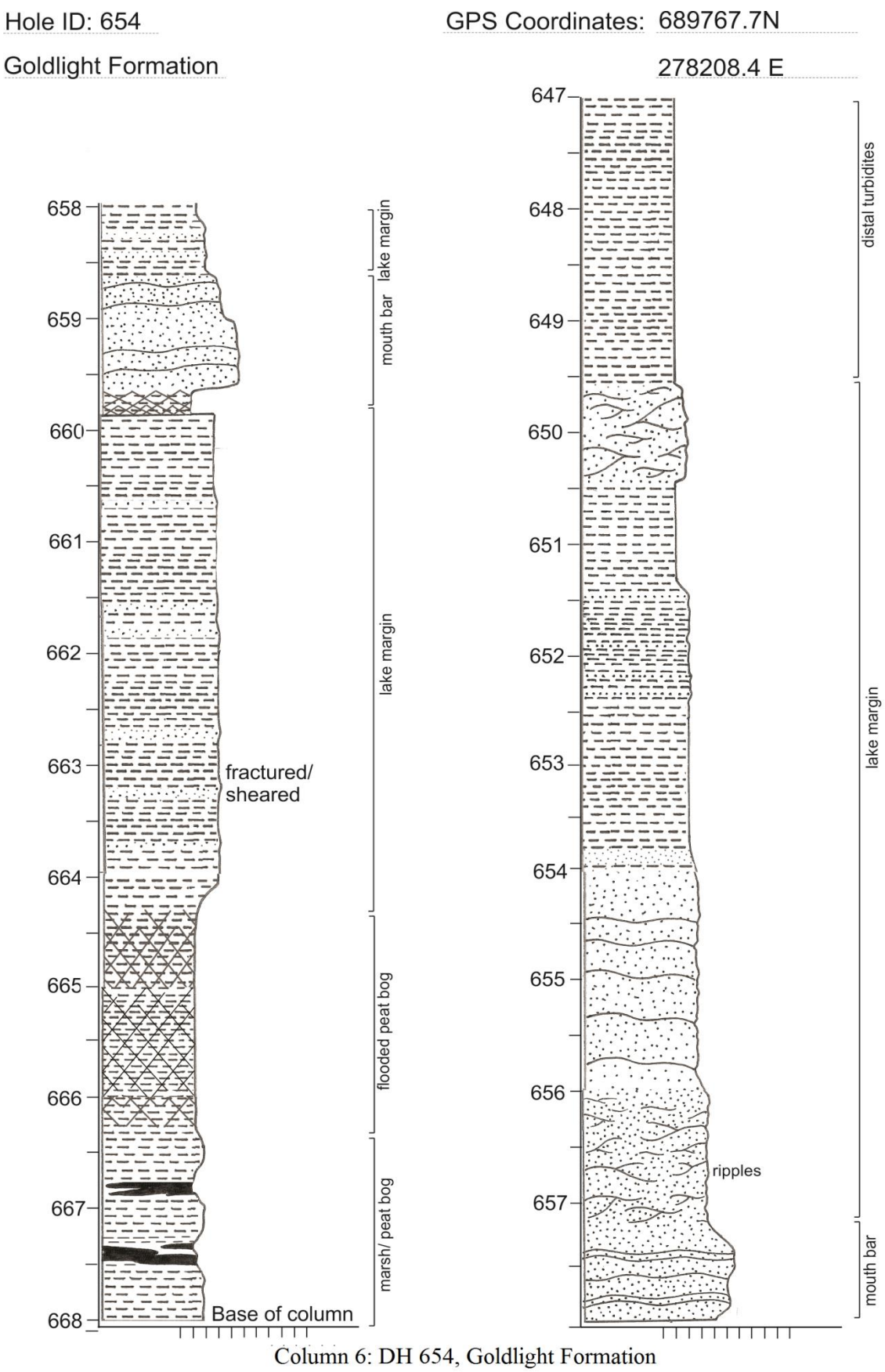

Figure 2.22. DH 654 stratigraphic column.

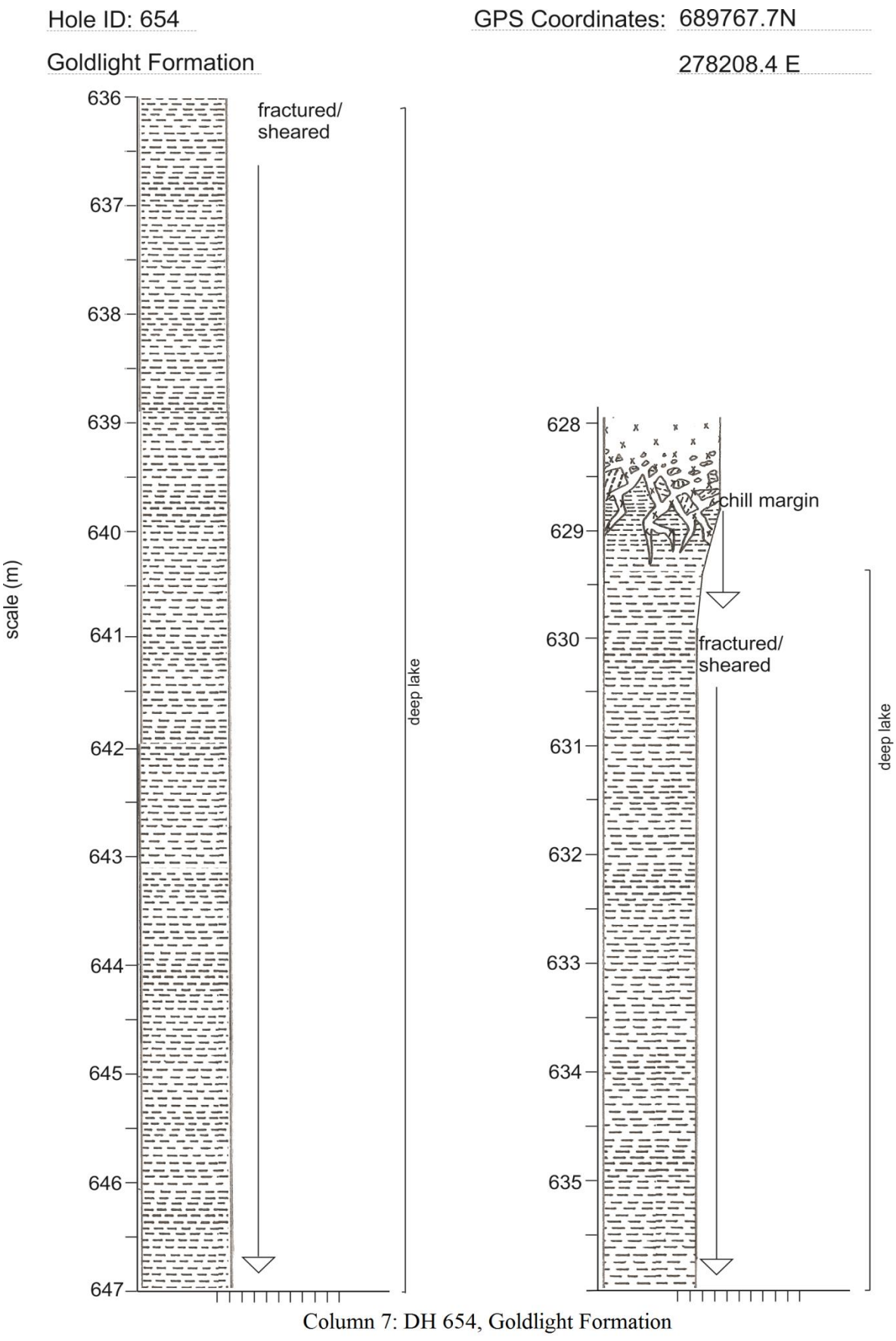

Figure 2.22. Dh 654 stratigraphic column.

Hole ID: 654

GPS Coordinates: 689767.7N

Goldlight Formation

278208.4 E

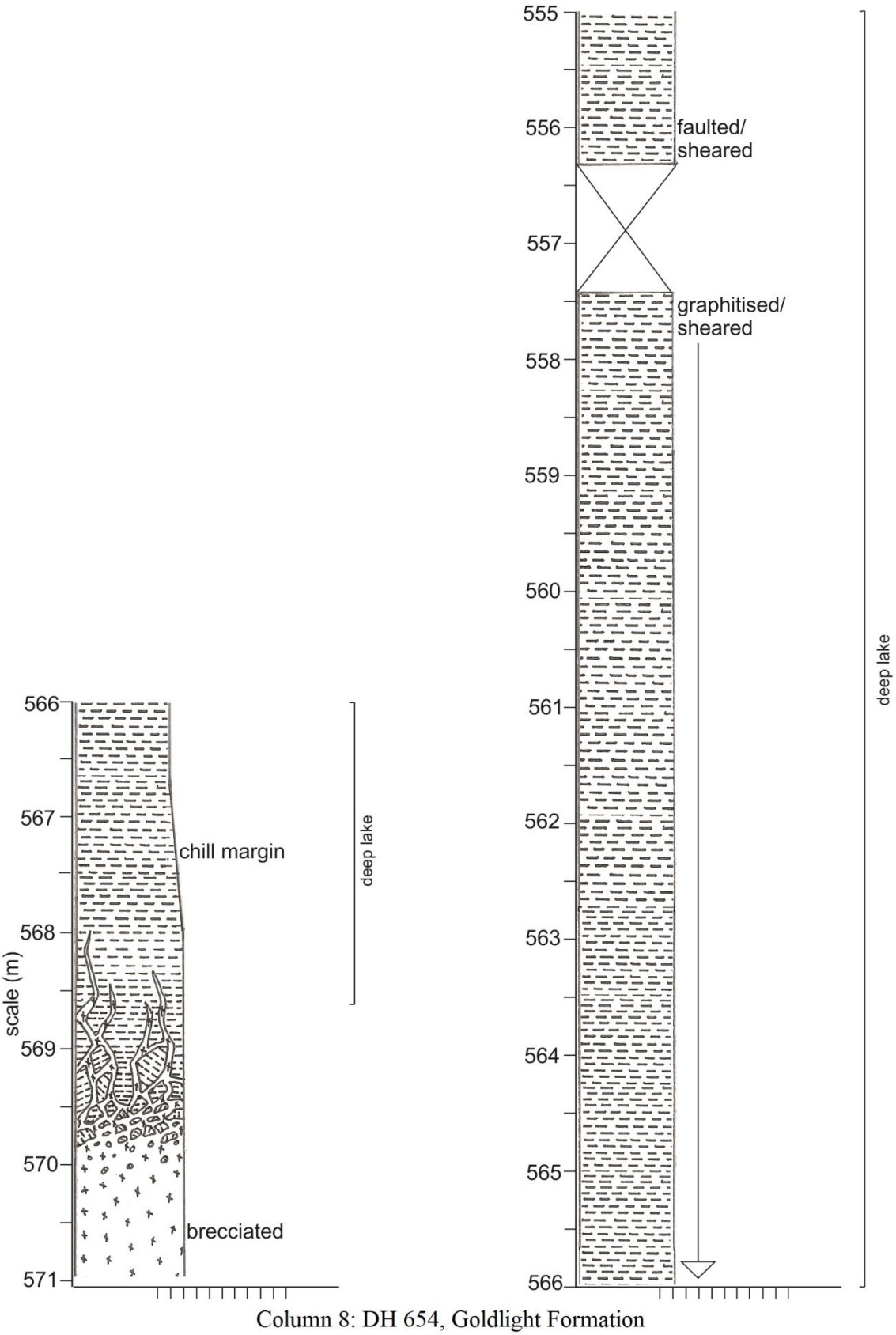

Figure 2.22. DH 654 stratigraphic column.

The base of the 10 Mile Creek stratigraphic column consists of primarily reversely graded sandstone beds with thicken up section, originating from mouth bar deposits (facies 3a) with occasional flood-derived, thin conglomerate beds. This sandstone bed is incised by a very thick debris flow (facies 2b) or series of debris flows transported by a nearby river channel. This pattern is replayed several times over the next few meters of outcrop with three clear episodes of flooding identified in the sedimentary record, suggesting channel avulsion on a delta front. Migration of the river channel is also observed through the gradual absence of mouth bar deposits from 8.5 metres. Instead the predominant depositional environment is lower energy lake margin.

The remaining overlying 6 meters contains proximal turbidites as opposed to debris flows indicating lake level rise. These proximal turbidites likely originated as debris flows, transported by nearby fluvial systems and represent slope failure in a sub-aqueous environment (Sletten et al. 2003). This implies that the sub-aqueous environment had a steep slope with rapid drop off from gravelly fan delta front into deep water. Outcrop from this point was inaccessible due to a water fall, but can be observed from the 10 Mile Road for approximately 30 meters. It appears to show finer grained sediment with no obvious evidence of conglomerates which could easily be seen from the road in the earlier part of the section. This indicates that the lake continued to deepen at this point.

The Goldlight Formation on the northern slopes of 10 Mile Creek has recently exhumed by a local coal miner. It lies at approximately 450m above sea level and is accessed by mine roads across 10 Mile Creek. It also appears to have been deposited in a shallow lake edge environment, but in one that was much lower in energy. Outcrop quality in this location is poor so no accurate stratigraphic column could be produced but outcrop appears to show medium to fine sandstone that grades over 10’s of meters into fine sandstone and siltstone with abundant meter wide concretions. These concretions contain a repeated sequence of thin (<3cm) turbidites. There is no evidence of debris flows within however the presence of close by high energy deposits in lower 10 Mile Creek suggests a steep slope environment with sandy sediment supply (Facies 4a).

Location: 10 Mile Stream: GPS Coordinates: 698165.9 N

Goldlight Formation 282151.5 E

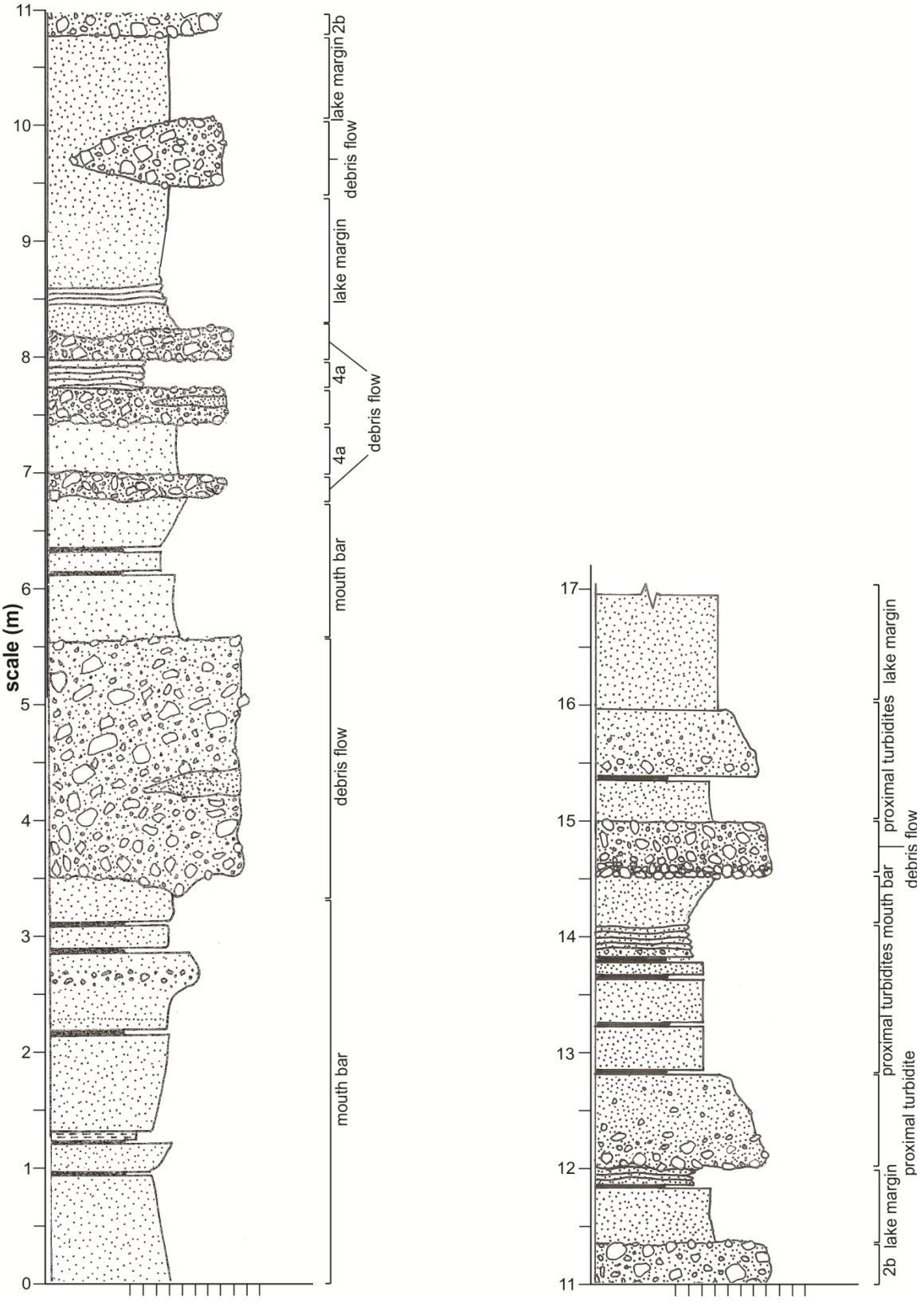

Column 9: 10 Mile Creek, Goldlight Formation

Figure 2.23. 10 Mile Creek Stratigraphic column.

Although the Goldlight Formation does not extend to 12 Mile Beach, there is evidence for a possible lake edge in close proximity to this location. Sandy interbeds (Figure 2.24) are common within the extensive Rewanui / Dunollie conglomerates and can be thick (<5m) and continuous with carbonaceous horizons. When considering the sandy interbeds, this location should be classed as the true western margin for the Goldlight Formation.

Figure 2.24. Sandy interbeds within the upper Rewanui Formation. These are considered to be time equivalent to the Goldlight Formation.

2.5 Waiomo Lake

The Waiomo Formation in the northwest section of the coalfield has often been confused with the Ford Formation due to the similarities in facies. 12 Mile Beach mudstone is well laminated and doesn't contain the dark purple grey mudstone that is often associated with the Waiomo Formation. A significant amount of time was spent during this thesis deciding whether the mudstone at 12 Mile Beach was Ford Formation or Waiomo Formation. The conclusion arrived at was based on the presence of Waiomo Formation in DH 621 from lower

10 Mile Creek, and the pinching out of the Ford Formation at the top of Strongman Mine (Section 2.5.3).

Overall, the Waiomo Formation lacks the thick, massive mudstone facies that is so common within the Goldlight Formation. Instead, significant portions are well laminated and sandier while the massive mudstone occurs as thinner beds between these laminated sections.

2.5.1 Waiomo Formation isopach map

The latest drill hole data supplied by Solid Energy included 361 drill holes that intersected the Waiomo Formation; 78 were used to develop the revised isopach map (Appendix 3). The allocation of Waiomo Formation at 12 Mile Beach was also taken into account in the creation of the isopach.

The revisions to the Waiomo isopach map (Figure 2.25) show a much smaller lake than the Goldlight Formation isopach map but larger than the previously interpreted Waiomo isopachs (Gage 1952; Newman 1985; Ward 1997). Sediment thickness is also much less with the thickest Waiomo sediments found to the northwest rather than to the east as previously interpreted (Gage 1952; Newman 1985; Ward 1997). The isopach map also shows two quite distinct depocentres; one to the northwest and one in the central and eastern section of the isopach map. It is unclear whether these are strictly coeval or whether the depocentre migrates slightly through time.

The largest depocentre covers the central and eastern side of the coalfield and is oriented in an NNE – SSW direction, perpendicular to the primary extension direction affecting the basin (Figure 2.25). This orientation also occurs in the Goldlight Formation isopach map (Section 2.4.1) Overall sediment thickness does not exceed 40m. The isopach also shows almost 20m of Waiomo Formation sitting directly next to the Roa - Mt Buckley Fault Zone.

The western depocentre is also oriented in a NNE – SSW direction with the thickest measured section of 56m outcropping at 12 Mile Beach. The Waiomo Formation in this isopach appears to extend both offshore and further to the southwest in comparison to earlier isopachs (Figure 5).

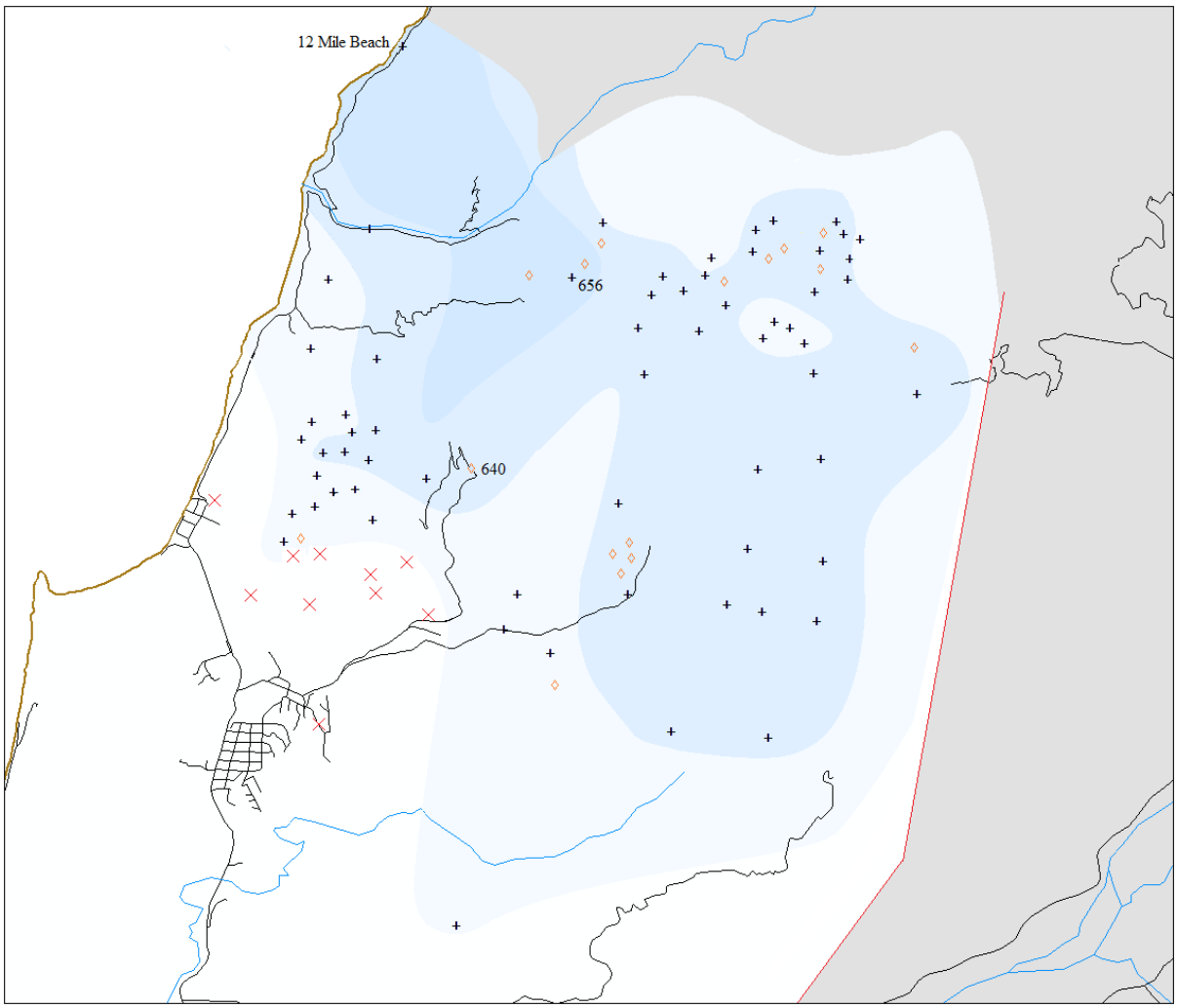

Figure 2.25. Waiomo Formation isopach map.

Although both depocentres are oriented in a NNE – SSW direction, the overall orientation of the dual depocentre lake appears to be perpendicular to this in a NW – SE direction. This could be due to several reasons and may not represent a change in basin orientation. The primary consideration is that the Waiomo Formation developed during a time when the size of the basin increased dramatically (Gage 1952). Isopachs of all 7 Paparoa Group formations show a dramatic increase in geographic context from the Morgan to the Rewanui Formation. This is also evident when comparing the Goldlight and Waiomo Formation isopach maps as the Goldlight Formation is far more extensive. It appears this change is best shown in the Waiomo Formation isopach map which shows the lake extending further to the west than earlier isopachs. The presence of two depocentres also supports the idea of deposition initiating in the central/ eastern section of the basin and as an increase in subsidence to the west occurs, deposition begins to occur in this area. This results in the two NNE – SSW

oriented depocentres that slightly interact within the centre of the coalfield and the overall NW – SE orientation of the Waiomo Formation which occurs due to the growth of the basin toward the west.

2.5.2 Waiomo Formation sedimentology

Central block

The Waiomo Formation within the central block of the Greymouth Coalfield varies in thickness but in general lacks the very thick massive mudstone that the Goldlight Formation is known for. The central block is characterised by fine grained sandstones, organic rich siltstone and coal.

DH 656 (Figure 2.28) located near Strongman Mine (Figure 2.5), begins in a sub-aerial environment with Morgan Formation coal and medium sandstone. This repeats the pattern established by the Goldlight Formation section of drowning of peat bogs as lake levels rise. In this case the Morgan Formation peat bogs became submerged and a lake margin formed in this area. The decrease in grain size up section and inclusion of several thin distal turbidites (facies 1b) can be interpreted as a continued rise in lake level allowing for the formation and transport of turbidites down slope. The increased number of turbidites up section in Column 28 is likely due to an increase in sediment supply into the lake leading to slope instability (e.g. Stow 1996).

Eastern block

Access to eastern outcrop is only available through private mine roads and outcrop available was in poor quality. The close proximity to the Roa – Mt Buckley Fault Zone has resulted in sheared and fractured outcrop and it was hard to discern detail and grain size.

Several locations at Roa Mine were used to approximate sedimentology of the Waiomo Formation on this east side. Figure 2.26 shows offset Waiomo and Rewanui Formation at the north-eastern end of the Greymouth Coalfield. 3m of mudstone was available and was silty with faint laminations (facies 1b) that quickly graded to 10cm of carbonaceous mudstones (facies 4a). This was topped by coarse, cross bedding sandstone and coal from the lower Rewanui Formation (facies 3c and facies 5b). Massive mudstone and dark grey shale can be

found in this location as it made up the majority of overburden removed from above the Morgan coal.

Figure 2.26. Downthrown Waiomo and lower Rewanui Formation (faulted to left off picture) showing laminated siltstone grading to thin carbonaceous mudstone.

Further east along the Roa – Mt Buckley Fault Zone lies what appears to be laminated mudstone (Figure 2.27). The mudstone is brown and fine grained (not as fine as the mudstone in the over burden outlined in Figure 2.26) and highly weathered. An estimated thickness in this location is 35m.

Figure 2.27. Waiomo Formation in the eastern block

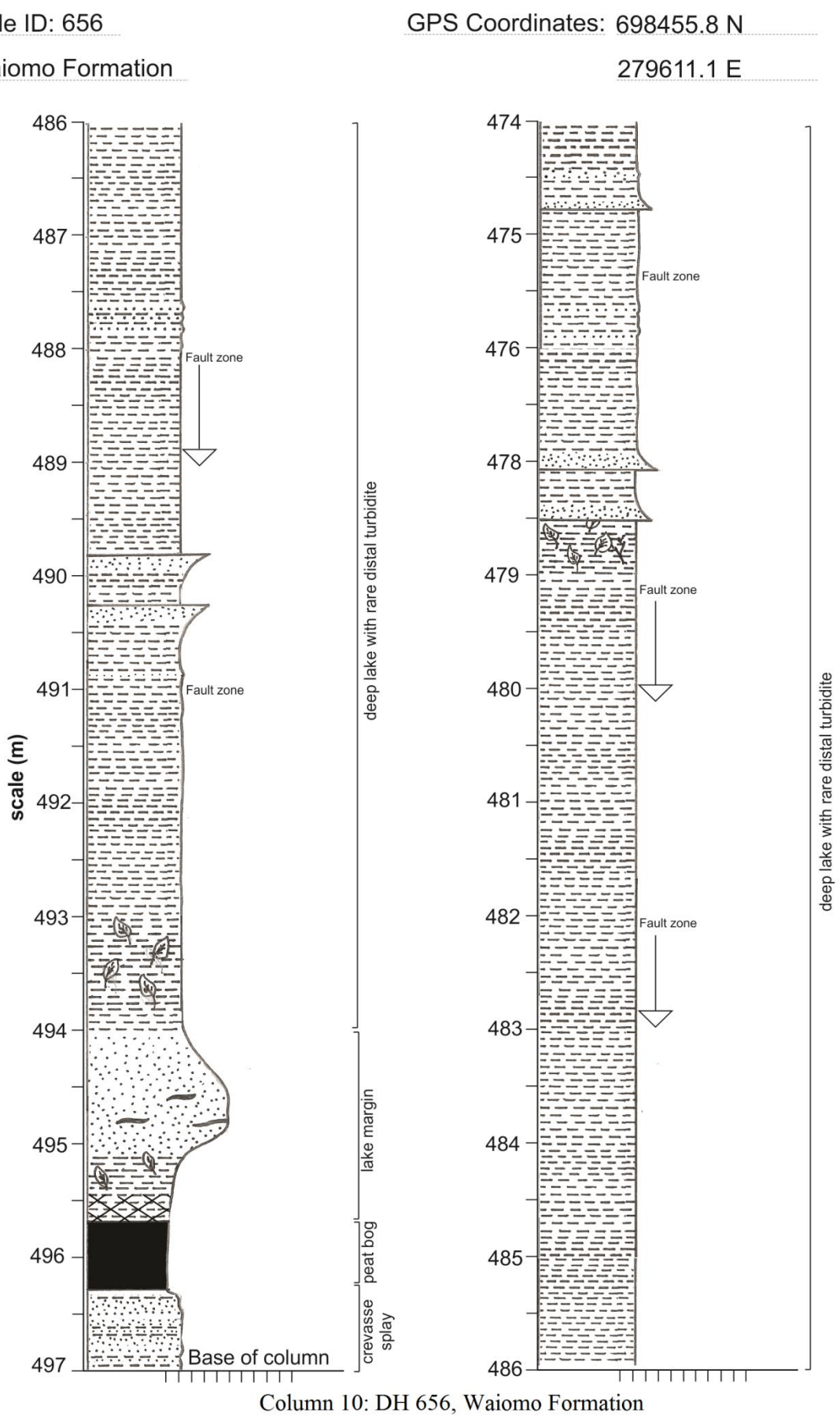

Figure 2.28. DH 656 stratigraphic column.

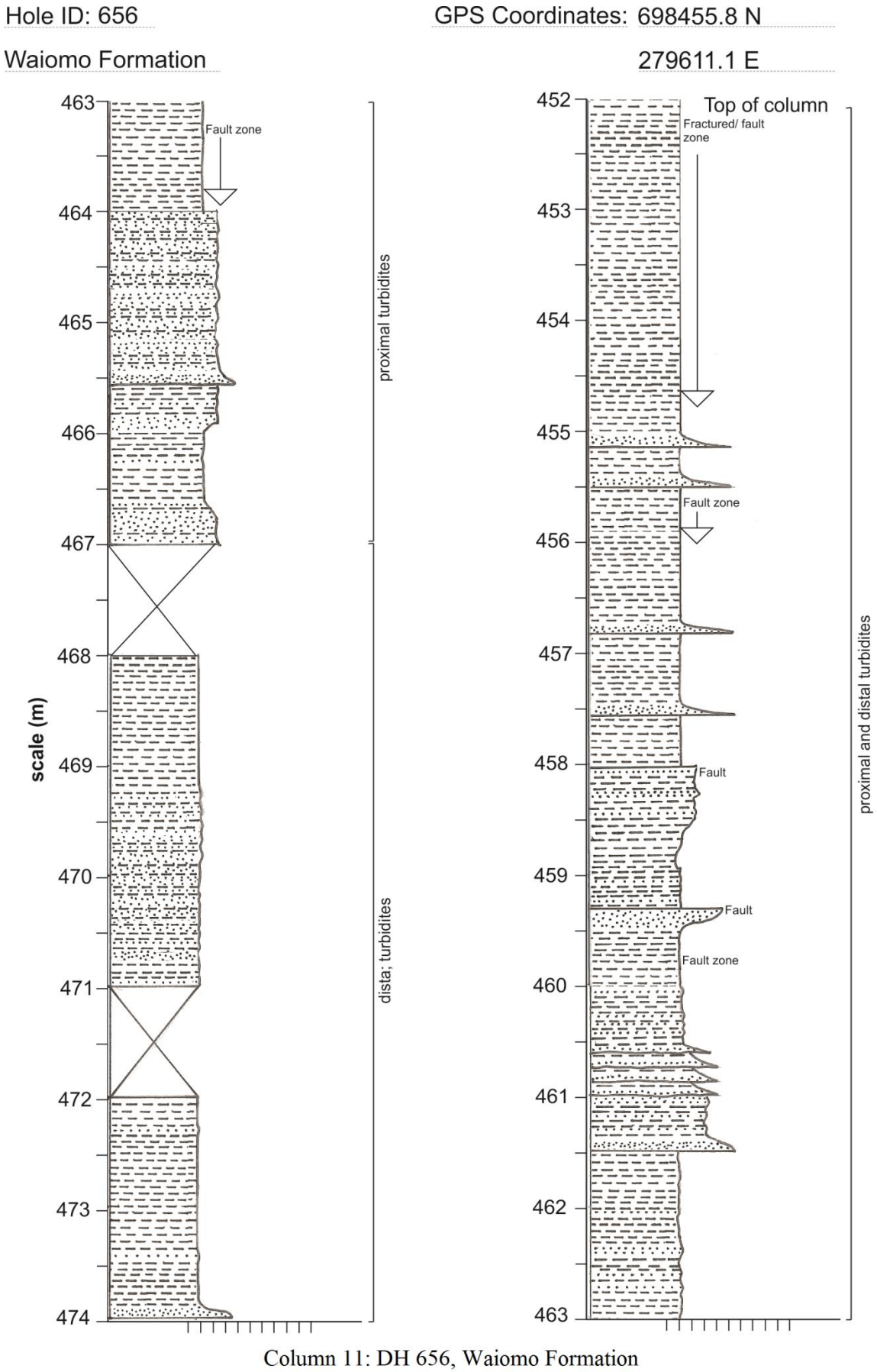

Figure 2.28. DH 656 stratigraphic column.

Southern block

The Waiomo Formation within the southern half of the coalfield is very similar to that seen within the central block (Figure 2.5). Distal turbidites are common but the southern block also contains several sections of medium sandstone and coarse grained, gravelly proximal turbidites.

The bottom lower contact of Waiomo with Morgan Formation in DH 640 (Figure 2.29) begins with thin, split coal lenses and reversely graded, laminated sandstone, deposited through flooding of a peat bog and formation of a shallow lake margin. From this point up section for 5m, shallow lake margin facies are replaced with laminated siltstone and sandstone, interrupted by three thick, proximal turbidites with basal conglomerate transported from a nearby slope (lithofacies 2a). These turbidites are overlain by several meters of faulted and occasionally carbonaceous massive mudstone, the first sign of hemipelagic sedimentation in a distal lake environment.

From 418 – 406m, numerous distal turbidites, proximal turbidites with their conglomeratic basal contacts and reversely graded sandstone beds can be seen. A thin, channelised debris flow deposit (lithofacies 2b) can also be found indicating close proximity to lake edge as debris flows deposits form from steep slope transport. The presence of a debris flow within this area of the lake indicates high relief in close proximity to DH 640 allowing for the transport and deposition of the angular, matrix supported conglomerate. The top 5m of this now shoreline lake section begins to exhibit the gradual changes associated with lake level rise as the occurrence of turbidites decreases and thicker sections of massive mudstone are found.

The second zone of massive mudstone is similar in appearance to the mudstone deposited during the initial increase in lake level. Organics can be seen in several locations as well as several snail fossils. Up section, an increase in grain size is seen resulting in reversely graded sandstone with distorted laminations and convolute bedding indicating sub-aqueous slumping. This is topped by a possible slumped or faulted feature of light grey very fine sandstone / siltstone.

The top of the Waiomo Formation in DH 640 (Figure 2.29) shows several meters of organic rich siltstone which gradually becomes more carbonaceous and finishes in one meter of slightly silty, black coal. This is interpreted as a gradual decrease in lake level allowing for the formation of a peat bog and the deposition of the Rewanui Formation.

Overall, DH 640 appears to show fluctuations in lake level, identified through the change from massive mudstone to higher energy lake edge facies and back to massive mudstone. Given the conglomeratic nature of the proximal turbidites in this location it is likely there was some form of relief nearby allowing for the transport of higher energy deposits.

Northwest block

The well laminated mudstone section at 12 Mile Beach has been assigned to the Waiomo Formation with the reasons outlined above and at the end of the Waiomo section (Section 2.5.3). The quality of outcrop in this location allowed for a detailed description of the sediments with a separate, close up stratigraphic column Waiomo – Rewanui contact available in Appendix 1. The outcrop at 12 Mile Beach is accessible in the cliff face and shore platform and allowed for an almost complete stratigraphic column to be constructed (Figure 2.31).

The basal 10m of column 13 shows alternating clasts supported, sub-rounded conglomerates belonging to the Morgan Formation and the initial sub-aqueous mouth bar and proximal turbidite deposits belonging to the Waiomo Formation. The inter-fingering of these facies is not due to fluctuations in lake levels but due to fluctuations of sediment into the lake from channel avulsion in the delta. Lake levels slowly increased, giving rise to the transition from mouth bar to proximal turbidites (facies 2a) to distal turbidites while the thick conglomerates represent periods of alluvial fan growth into the lake.

From 10m, the decrease in grain size is quite sudden and the predominant facies are light grey siltstone and laminated sandstone, formed from distal turbidites (facies 2a). These turbidite beds extend in outcrop onto the shore platform (Figure 2.30) and are occasionally interbedded with very red sandstone beds. Thin section analysis of the red beds showed iron staining and a very fine sandstone to mudstone matrix. This section of occasional laminations and red beds continues for 16m to the edge of the shore platform.

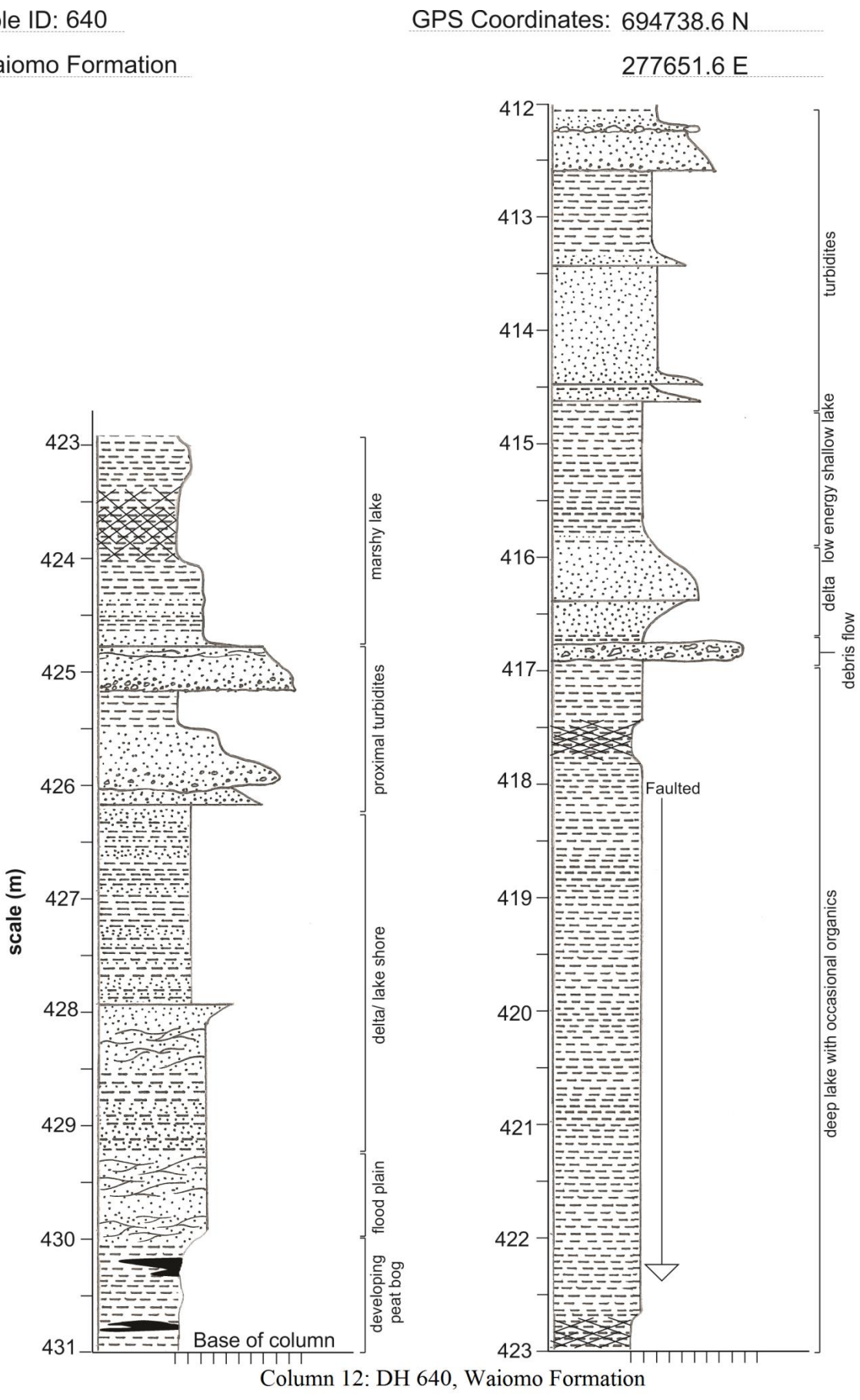

Figure 2.29. DH 640 stratigraphic column.

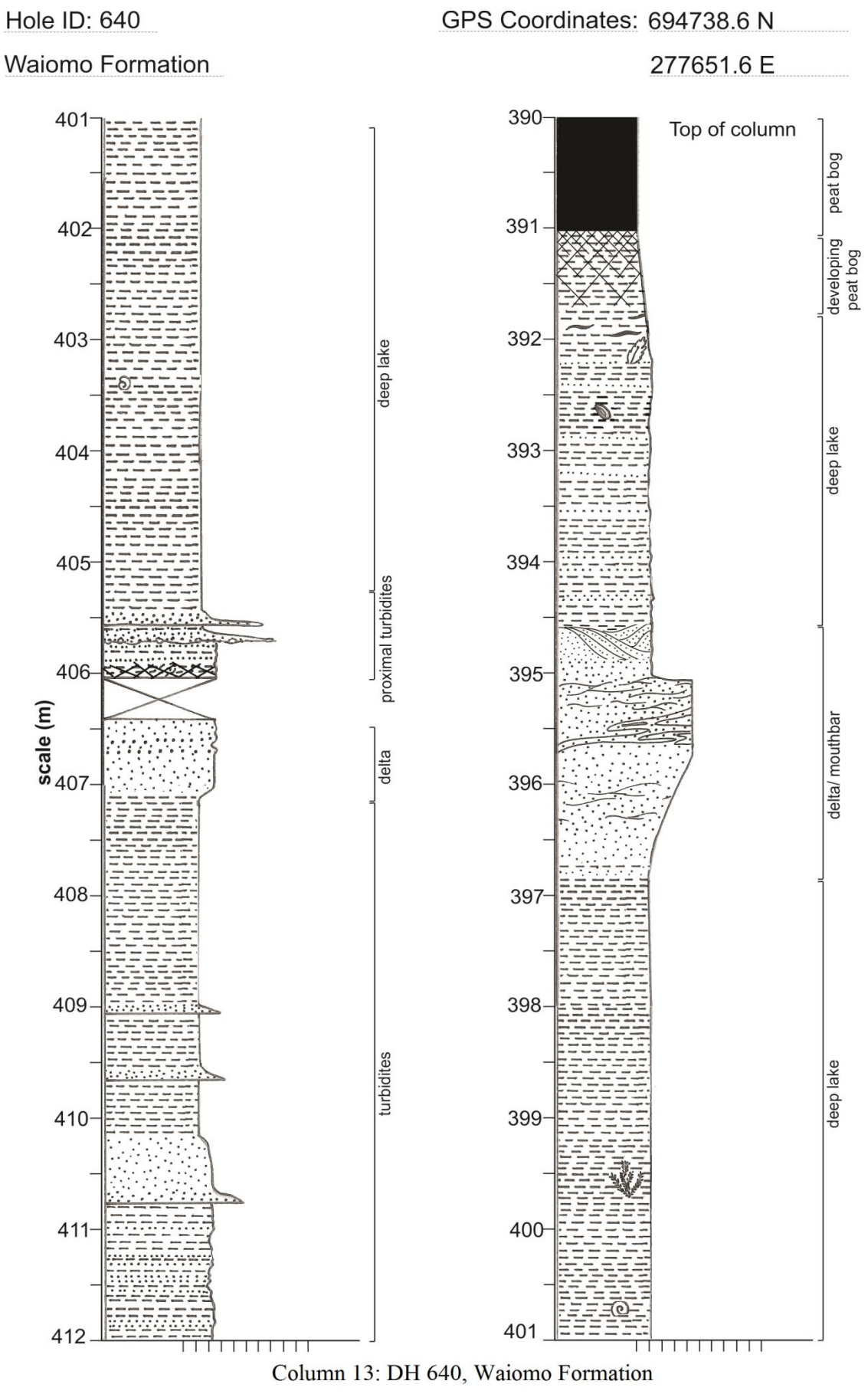

Figure 2.29. DH 640 stratigraphic column.

A cliff collapse partially obscures up to 20m of outcrop and separates the shore platform distal turbidites from the overlying section cropping out in the cliff face. In the first discernible bedding above the collapsed zone, a small debris flow can be found that contains soft sediment clasts of purple/ grey mudstone that matches the appearance of the dark mudstone beds nearby. The angularity of the colloquially termed rip up clasts indicates they are slumped derived and formed as the debris flow they are found in undercut soft, partially consolidated sediment (e.g. Knight 2009).

The first 5m above the small rip up clasts shows an overall gradual increase in grain size and interpreted decrease in lake level as siltstone changes to fine, laminated sandstone. Throughout this section, medium sandstone proximal turbidites (facies 2a) can be found with some showing evidence of ripples and laminations. This zone also contains thin clast-supported conglomerate lenses and carbonaceous mudstone drapes indication soft sediment deformation on a slope.

Figure 2.30. Folded Waiomo Formation laminated siltstones, sandstones and conglomerates at 12 Mile Beach.

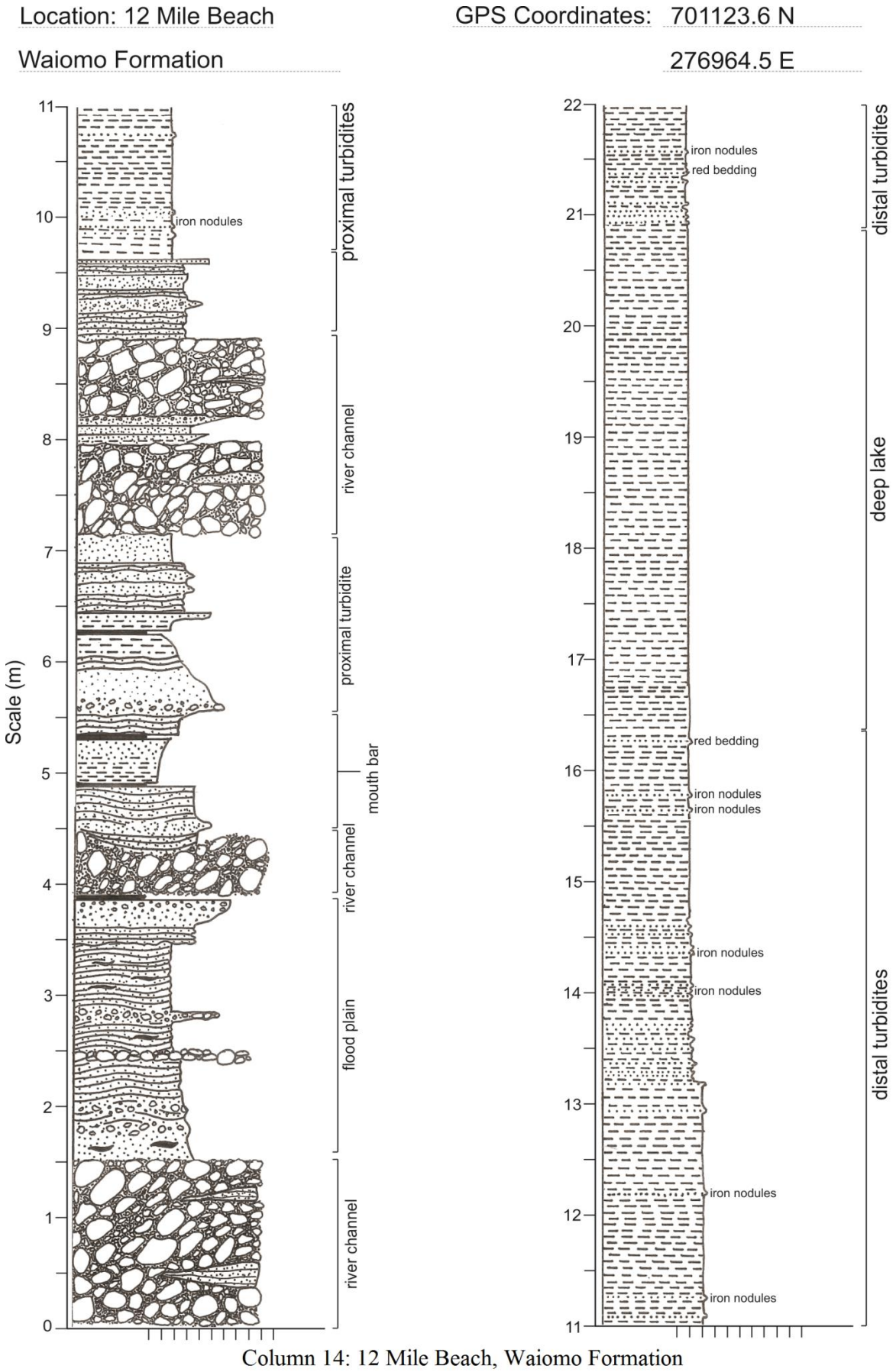

Figure 2.31. 12 Mile Beach stratigraphic column.

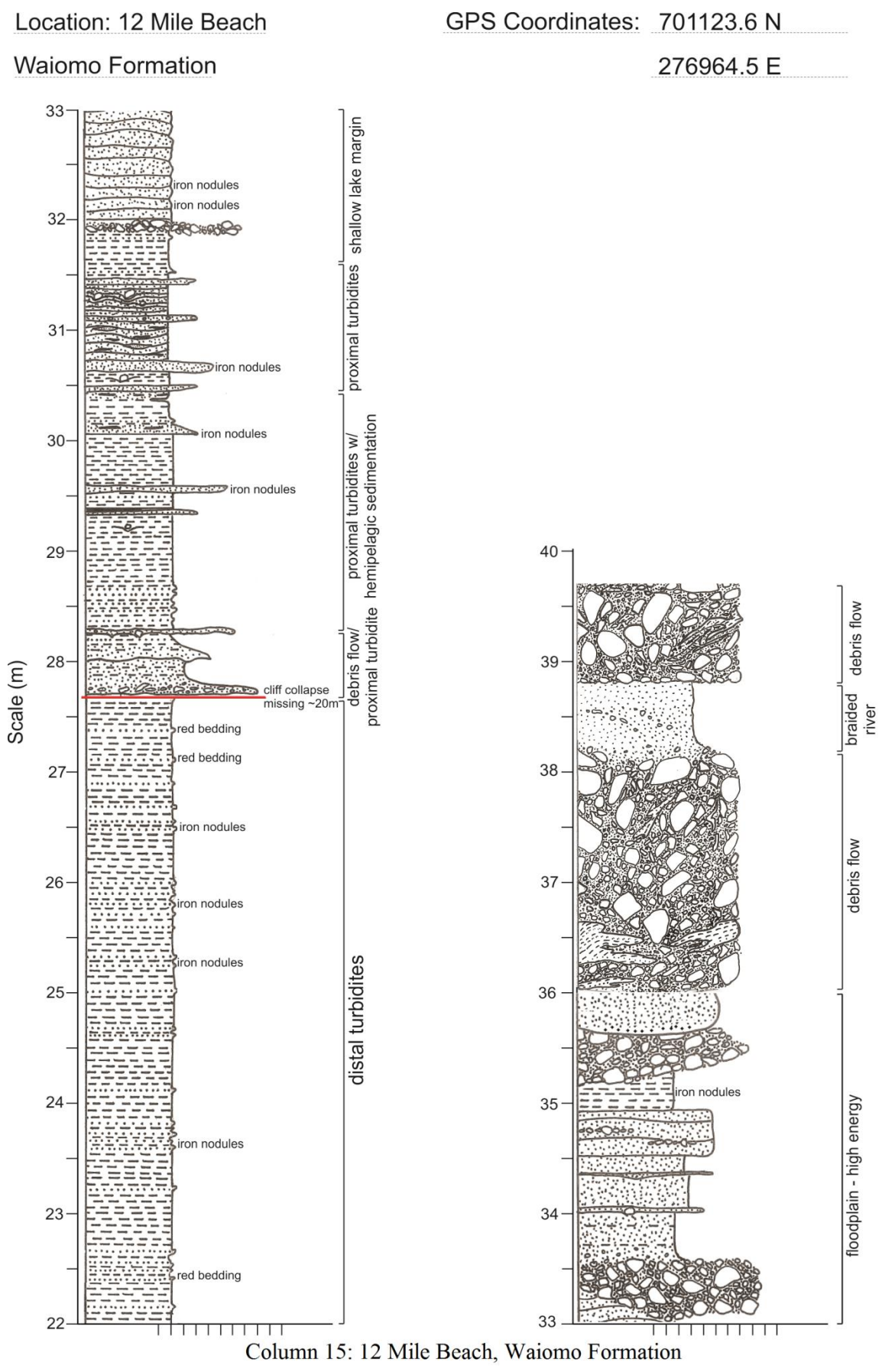

Figure 2.31. 12 Mile Beach stratigraphic column.

One of the more interesting features within this section of the 12 Mile stratigraphic column are the large, isolated conglomerate clasts which indent and disrupt the underlying laminated siltstones. These clasts are interpreted as drop stones (Figure 2.32). Drop stones form as single clasts fall vertically through the water column and land displacing underlying sediment (Bennett et al. 1996). A common mode of formation for drop stones is through the transportation of clasts on icebergs and glaciers. As these ice bodies melt, the rocks are released and land on the sea floor or lake floor below however the environment in this area at the time of deposition appears to be similar to what we find today. This is evidenced through the abundance of Beech tree pollen found in the Goldlight Formation (ward 1997) which are also found throughout the West Coast and New Zealand today. This environment was not cold enough for major bodies of ice to form and thus, an alternative mode of transport should be determined.

Figure 2.32. Drop stone within the Waiomo Formation at 12 Mile Beach. Multiple dropstones can be seen in outcrop, displacing underlying sediment.

The nature of deposition in this area lends itself to the idea of drop stones originally being transported onto vegetation found at the edge of the lake. The numerous debris flows already described, may have overtopped reeds and grass mats at the edge of the lake which were also released from the lake edge through force. These grass mats would eventually become water logged and sink, releasing any conglomerate clasts contained on them and allowing for the formation of drop stones.

The last section of deeper water facies occurs between 33 and 35m. Laminations and fine sandstone are likely to be a very shallow lake margin which is strongly impacted by river channels depositing thin debris flows and fluvial conglomerates. The top 5m show very thick, matrix supported conglomerate interpreted as a debris flow (facies 2b) which has eroded into the underling sandstone and conglomerate by almost 2m. This debris flow contains angular clasts of Greenland Group sandstone, quartz and granite which is associated with the Rewanui Formation. There are also up to one meter wide rip up clasts of laminated, dark grey mudstone (Figure 2.33). Thin section analysis was undertaken on these rip up clasts and the underlying Waiomo Formation which showed striking similarities in clasts composition indicating the rip up clasts are from the Waiomo Formation. Specific compositions of both samples appear to show 60% quartz, 12% mica, 10% matrix (very fine grained), 5% chlorite and with the remainder including organics and very rare feldspar. The mode of formation of these rip up clasts is the same as what was described earlier but on a larger scale. These formed through undercutting and consequent slumping of partially consolidated Waiomo sediment (Knight 2009).

This top five meters also contains a coarse sandstone channel which shows cross bedding and marks the beginning of the Rewanui Formation. The Rewanui Formation at this location is composed of cobble to boulder conglomerates in excess of 400m thick.

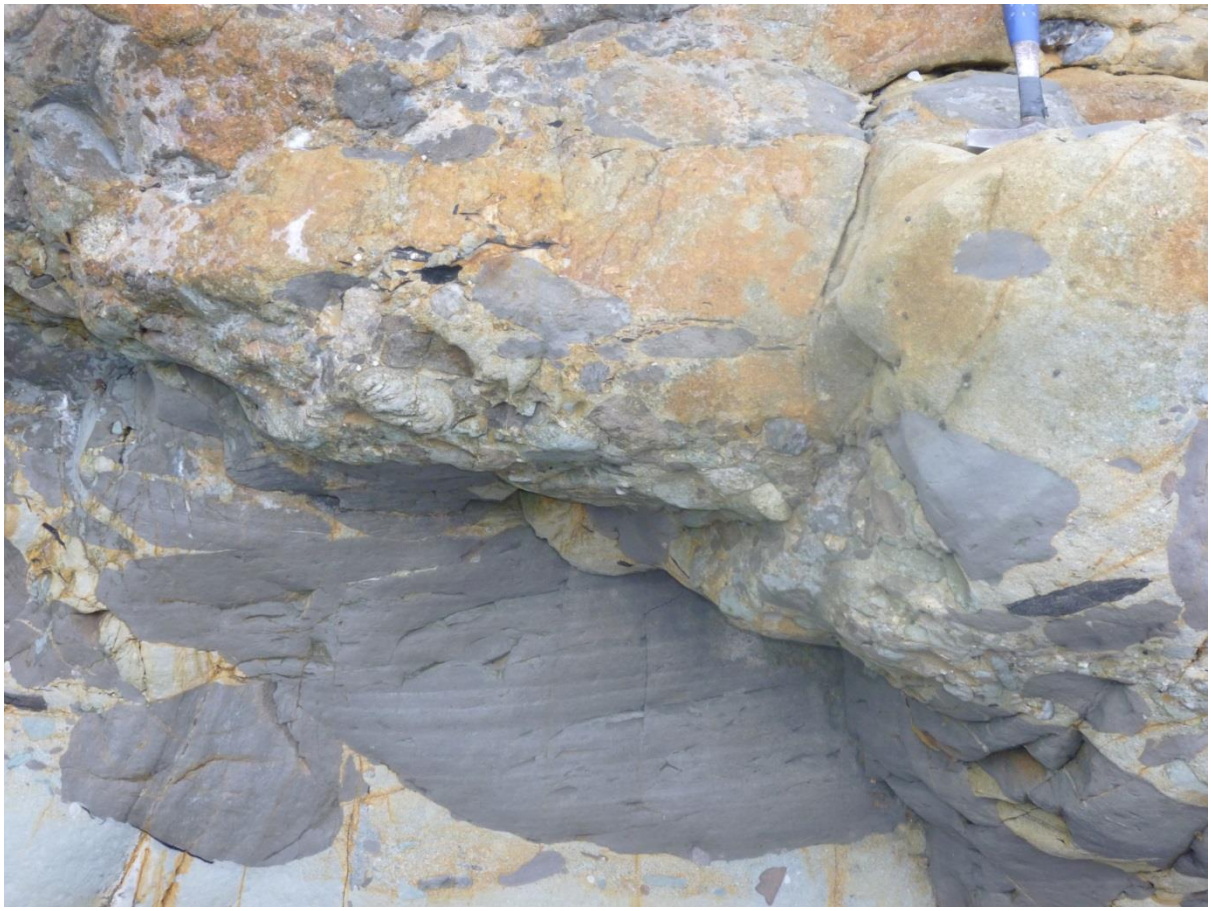

Figure 2.33. Large rip up clasts within the Rewanui debrites at 12 Mile Beach. Clast composition strongly resembles that of the underlying Waiomo Formation indication undercutting and erosion of unconsolidated Waiomo sediment at the time of deposition.

2.5.3 Revisions to 12 Mile Beach mudstone

One current area of contention between those who study the Paparoa Coal Measures is what mudstone is location at 12 Mile Beach. Initially, the section was mapped by Gage (1952) as Waiomo Formation although he noted that the well laminated lacustrine sediments strongly resembled the Ford Formation he saw further east. In 1978, Nathan produced the revised maps for Greymouth and included the 12 Mile section within the Waiomo Formation and is revised in Nathan et al. 2002.

The most recent person to address the area was Ward (1997) in his PhD and he considered the 12 Mile Beach section as Ford Formation; his evidence being that the Waiomo Formation thinned out around Spring Creek Mine and the light colour and well laminated section at 12 Mile Beach didn't resemble the Waiomo Formation in any other places.

This thesis includes the 12 Mile Beach section in the original Waiomo Formation. The reasons for including the 12 Mile Beach section are outlined below:

- Waiomo Formation was identified in DH 621 which is located 1km upstream from the head of 10 Mile Creek. This Waiomo was 36m thick. Jay Formation was also previously noted in this drill hole but no Ford Formation.
- A very thick section of Waiomo Formation can also be seen in Docherty Creek which feeds from Strongman Mine down into 10 Mile Creek. A clear stratigraphic column of this section is not available as outcrop can't be accessed but it is estimated to be roughly 40 - 50m in thickness. A stratigraphic column was drawn from the very top 10m of this section which shows a well laminated siltstone and sandstone with thin conglomerate lenses and small debris flows. This location is 2km upstream from DH 621.
- At 12 Mile Beach, the mudstone is conformable with the overlying and underlying conglomerates. Although it is possible the underlying conglomerate could be Jay due to the similarities between the Morgan and Jay conglomerates, the top conglomerate is the Rewanui Formation. The top few meters of mudstone at 12 Mile Beach are interbedded with conglomerates which indicates a gradually shallowing environment. As well as this, in 12 Mile bluff above the road and along the beach, there appears to be well laminated sedimentary rocks bearing resemblance to the mudstones sitting above the thick Rewanui channel.
- Revision of the Ford Formation isopachs show that it is not as thick as previously thought. Analysis of the drill holes around Strongman Mine also show that the very thick "Ford" may likely be repeated due to faulting in this area. From this information, and comparisons of the raw isopach data, it was decided that the Ford Formation pinched out around Strongman Mine.

From this information it can be seen that the Waiomo Formation doesn't appear to pinch out west of Strongman Mine and stratigraphically, it doesn't make sense to classify the 12 Mile Beach section as Ford Formation. The conglomerates and mudstone at 12 Mile Beach also appear conformable which indicates the mudstone is Waiomo Formation. The abundant laminations seen in this area are likely due to the high energy environment and plentiful supply of sediment from the hills to the west in this area of the basin.

There was one issue when making this decision and that was regarding the Jay conglomerates in DH 621. Proper analysis of the conglomerates has not been undertaken in this thesis but

the question was raised as to why 10m+ of Jay conglomerates occur only several km from 12 Mile Beach but don't occur at 12 Mile Beach themselves. At 12 Mile Beach the Morgan Formation sits unconformably on Greenland Group basement. These conglomerates are essentially indistinguishable and it is only the conformity with the Waiomo Formation above which allows for the identification of this conglomerate as Morgan Formation. It may be that any Jay conglomerate was reworked into the Morgan conglomerates in this location or the Jay conglomerate was never deposited in this location.

2.6 Ford Lake

The Ford Formation is the thinnest and least extensive lacustrine formation studied within the coalfield. As a result it has the least amount of data available and of the poorest quality. Due to the cost of drilling and the lack of extensive economic coal seams within the Jay Formation, most holes don't intersect the Ford Formation resulting in only a small amount of information being made available. The Ford Formation also has a distinct lack of outcrop in comparison to the other mudstones with outcrop seen to the east and north, accessed through Roa Mine. The quality of drill core from the Ford Formation made them difficult to measure and as a result only 1 stratigraphic column was constructed from drill core.

2.6.1 Ford Formation isopach map

A total of 145 drill holes intersect the Ford Formation (Appendix 3). 46 were used to create a new isopach map for the Ford Formation. 14 drill holes were also used that didn't contain Ford Formation but did contain the underlying Jay and overlying Morgan Formations to constrain an inferred lake boundary for the lacustrine deposit

The new Ford Formation isopach map (Figure 2.34) shows a NNE – SSW oriented lake with outcrop in the northern and eastern margins of the coalfield. The isopachs shows the Ford Formation to be truncated by the Roa – Mt Buckley Fault Zone to the east and overall, appear to be quite thin. The overall thickness of the Ford Formation averages approximately 20m with the thickest sediment defining the centre of the Ford Lake.

When closely examined, several areas were highly faulted. The area around Strongman Mine and drill hole 658 had drill holes labelled as containing almost 200m of Ford Formation. The area around 7 Mile Stream and Rewanui Mine shows great discrepancies in thickness

between drill holes due to faulting. Overall it was decided that these areas contained much thinner sediments than previously thought due to the amount of faulting seen in drill core (DH 658).

When comparing the Ford Formation isopach map to earlier isopach maps there are several notable differences. The first major difference is the orientation of the new Ford Lake which is oriented NNE – SSW instead of the NW – SE orientation displayed by Ward (Figure 2.2) and others (Newman 1985; Gage 1952). This new orientation aligns with the isopachs of the other formations within the coalfield. Much of this change in orientation is due to reclassification of the lacustrine deposits at 12 Mile Beach as Waiomo rather than the Ford Formation and due to the removal of faulted sections from the isopach calculations.

The other difference with the revised Ford Formation isopach map is the thickness and the distribution of the formation to the south and west. The most recent, previous Ford isopach map (Ward 1997) shows sediments of up to 140m thick while the revised Ford isopach in Figure 2.34 has a maximum thickness of only 43m in the top north-east corner. This difference is due to factoring in the effects of faulting on sediment thickness which had not been done previously during the construction of older isopachs. The distribution of the Ford Formation has also changed with the additional information from new drill holes showing it to extend further south and south-west but not towards the north-west. Instead this area has been classified as Waiomo Formation.

2.6.2 Ford Formation sedimentology

The quality of drill core made it impossible to accurately log the Ford Formation in three of the four holes it is found in a the NZP&M core store. However, field observations were also made at Roa Mine.

Central block

The Ford Formation within DH 658 (Figure 2.35) in the central block begins in the upper Jay Formation which shows fine, brown sandstone with vertical fossilised rootlet traces indicating that this sandstone was formed in a sub-aerial environment. Flooding of the rootlets likely occurred in a flood plain environment due to river avulsion before lake level rise flooded the area.

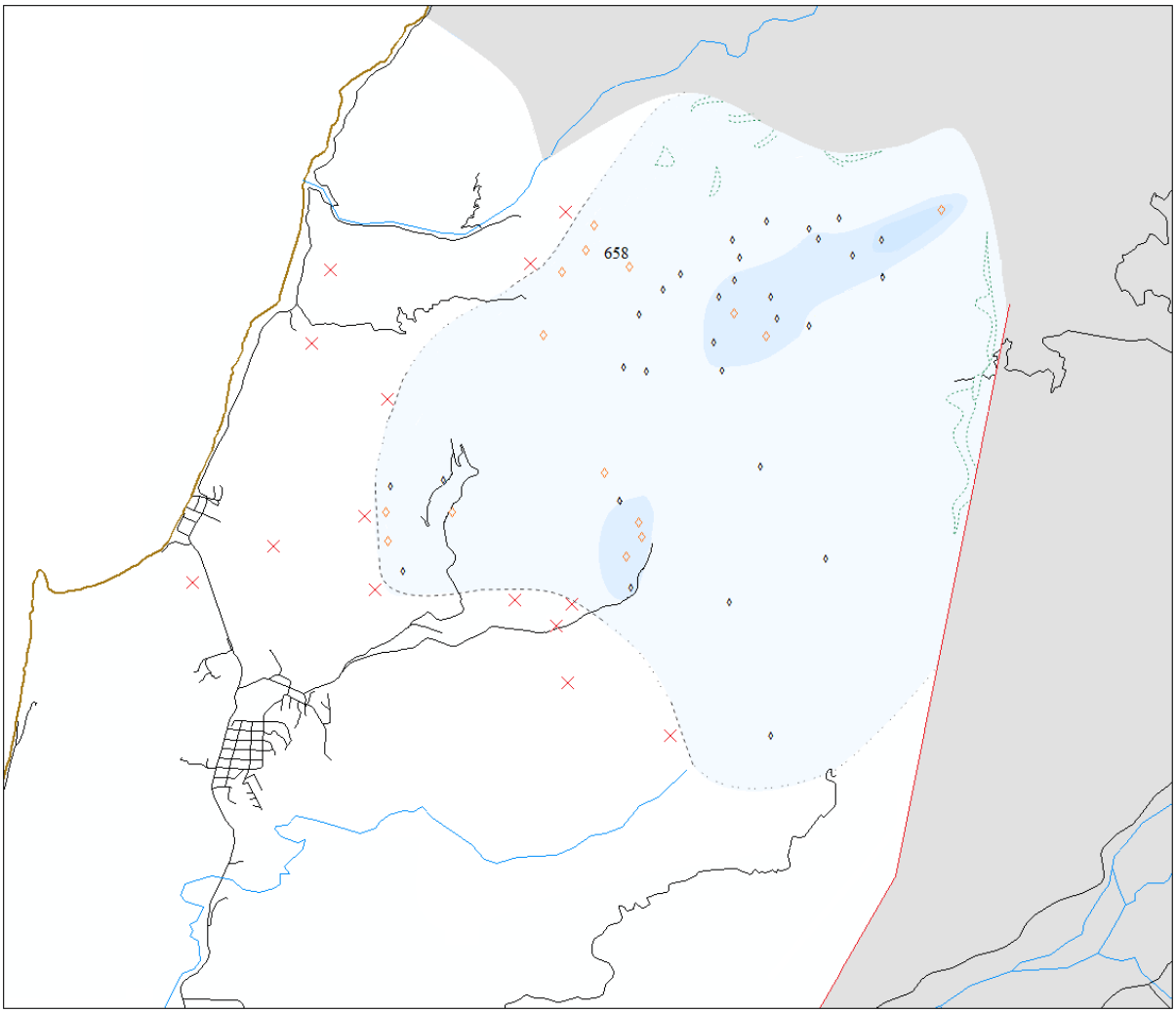

Figure 2.34. Revised isopach model of the Ford Formation showing a NNE – SSW oriented lake.

Unfortunately the true contact is obscured due to faulting placing Ford Formation massive mudstone against Jay Formation sandstones at 308m. This is followed by over 13m of presumed massive mudstone (facies 1a) due to poor recovery of core. There were numerous faulted zones throughout the core and the core itself was broken. At 294m there is a sheared contact between the massive mudstone and a sandier faintly laminated section that is interpreted as a proximal turbidite (facies 2a). This grades quickly back to another few metres of broken massive mudstone. The top few meters of core show another faulted contact between the more massive mudstone and the overlying Morgan Formation. Granule conglomerate bedding grades to sandstone and is interpreted as formed from crevasse splays as flooding and river avulsion occurred in a meandering river delta plain (facies 3c).

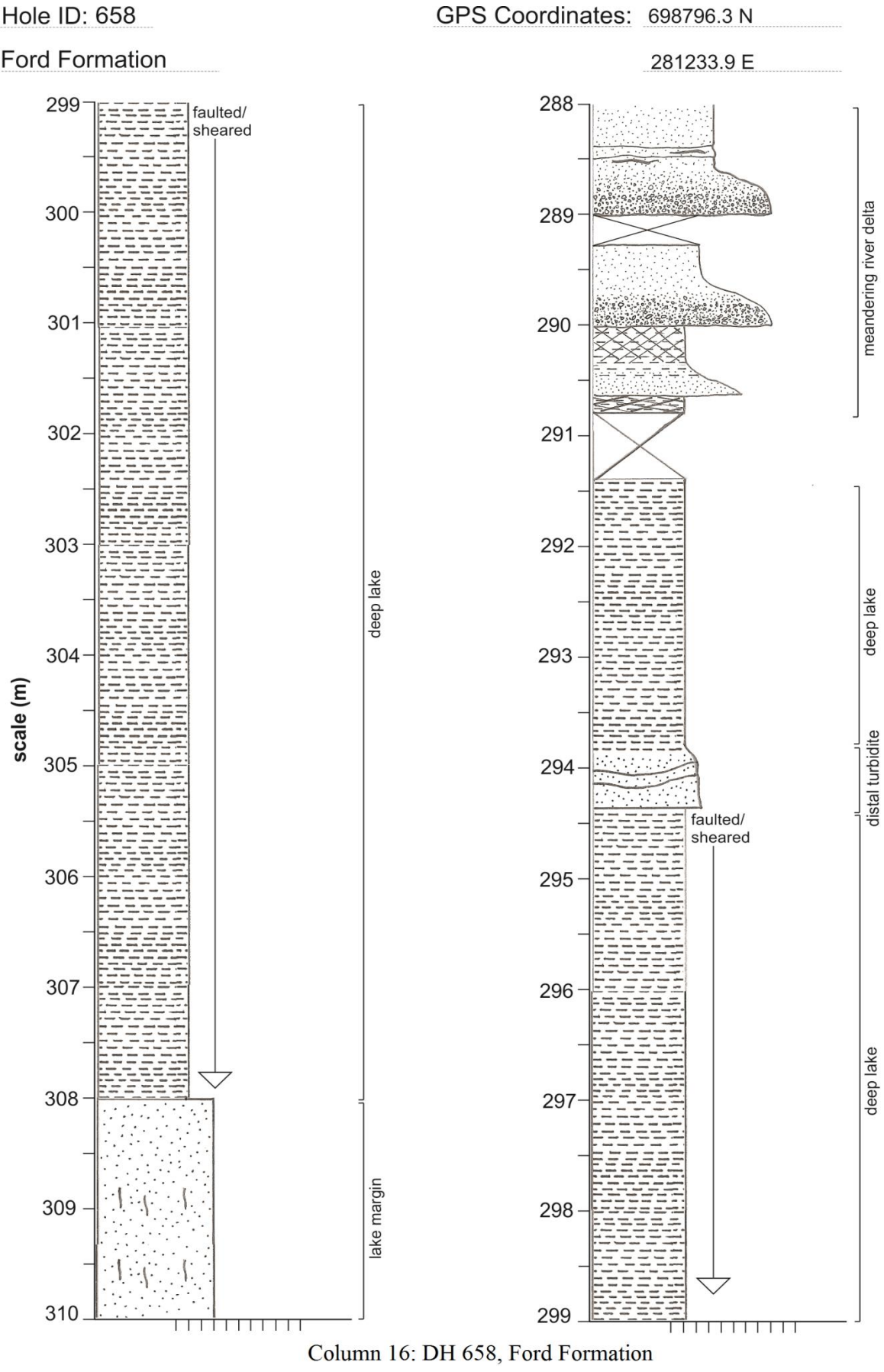

Figure 2.35. DH 658 stratigraphic column.

Eastern block

Outcrop of the Ford Formation at Roa Mine in the eastern block is limited to thin, faulted sections less than 10m (Figure 2.36). The Ford Formation in this area appears to be bedded brown siltstone which grades over 3m into the underlying Jay Formation. This contact shows an increase in grain size to laminated medium sandstones with organics with thin, clast supported pebble conglomerate lenses up to 2m across.

Figure 2.36.Ford Formation outcrop at Roa Mine. Thickness of 10m in this location.

2.7 Revision to nomenclature

2.7.1 Revision to Goldlight Nomenclature

Previous work mapped the Goldlight Formation as comprising only mudstone which limits its extent. In the northwest especially, massive mudstone facies are entirely absent and replaced by a lake edge environment affected by numerous steeper slope processes including debris flows. The presence of sub-aqueous turbidites, well-preserved ripples, reversely graded mouth bar deposits and freshwater mussel fossils in sandstone and conglomerate interbeds are all evidence that the sedimentology of the Goldlight Mudstone is not just massive mudstone. Future work into the basin should acknowledge this, particularly when dealing in the northwest corner where the Goldlight Formation is currently mapped as Rewanui and Dunollie Formation. All other areas of the basin show a gradual flooding of the

basin from Goldlight to Rewanui time and the gradual infilling with mouth bar and shallow lake edge facies from Goldlight to Dunollie time. However, in 10 Mile Creek, this period is marked by thick debris flow and conglomeratic facies, a possible indication of faulting in the area which doesn't fit in with the current tectonic model for the basin. Revisions to the overall basin model discussed later take these anomalies into account.

2.7.2 Revision to Waiomo and Ford Formation Distribution

Original mapping of the Greymouth Coalfield assigned the 12 Mile Beach mudstone as Waiomo Formation (Gage 1952; Nathan 1978). Unpublished revisions undertaken by Ward (1997) relabelled these mudstones as Ford Formation due to their resemblance to the well-laminated Ford Formation bedding seen further to the east. Current mapping convention aligns with the original mapping however the changes suggested by Ward (1997) highlight the sedimentological issues in accurately identifying the mudstones within the coalfield. This issue doesn't just involve the 12 Mile Beach section but can be applied to all three lacustrine mudstones due to their common representation as massive mudstones.

Evidence was outlined in the previous sections to suggest the 12 Mile Beach section is in fact massive mudstone although these won't be repeated in detail here. Instead evidence suggests that although sedimentology of the Waiomo Formation at this location bears greater resemblance to the Ford Formation, stratigraphically it is improbable for the Ford Formation to extend westward past Strongman Mine. The Ford Formation is instead confined to the central, eastern and southern blocks of the Greymouth Coalfield (Figure 2.5).

2.8 Discussion

2.8.1 Distribution of Lithofacies

The distribution of drill holes and outcrop has allowed for the distribution of lithofacies from within the basin to be better understood. The overall trend shows coarser grained sediments to the west with massive mudstone, organic rich siltstone and distal turbidites to the east.

Stratigraphic columns from the Waiomo and Goldlight Formations in the north-western corner show numerous debris flow, mouth bar and coarse grained turbidites within the formations themselves while the transition to fluvial formations includes boulder size conglomerates and meter wide Waiomo Formation rip up clasts. These deposits are an

indication of a very high energy system with undercutting occurring into the partial solidified Waiomo Formation.

In the centre of the coalfield from Strongman to Roa Mine, the primary lithofacies are massive mudstone and distal turbidites. The transition to under and overlying formations are gradual and include flooded peat bogs, organic rich siltstone and very thin, fine grained distal turbidites. These deposits indicate a lower energy environment, with deposition controlled by the low angle of topography in the centre of the basin. Dying peat bogs which are common in this location were slowly flooded by increasing lake level and as lake level dropped, rivers began to feed sediment further into the basin resulting in laminated sandstones and siltstones.

The area south of Spring Creek Mine is very similar to what was described for the centre of the basin with very thick massive mudstone seen within the Goldlight Formation and organic rich siltstone and laminated sandstone seen in both the Waiomo and Goldlight Formations. Sedimentology show a basin high in the southwest corner which allowed for the formation of a very thick section of organic siltstone with in the Goldlight Formation. This basin high is also represented by the very thin Waiomo and Ford Sediments around Spring Creek.

The eastern section of the coalfield around Roa Mine was the least studied due to lack of drill holes and outcrop availability. Unfortunately access could not be gained to this area during the time of this thesis.

2.8.2 Implications for basin geometry

When comparing these results to the current tectonic model for the basin, there appears to be several inconsistencies. The primary inconsistency is whether the basin bounding fault was to the east around Roa Mine as modelled (Ward 1997; Nathan 1978). If this were true, we would expect to see high energy shoreline deposits which are normally associated with faulting on the eastern side of the basin. Instead we see them to the west only. The other issue is if faulting in the east controlled deposition we would expect to see the formations thin out towards the shoreline against alluvial fan deltas off the uplifted fault scarp. Instead the new isopach maps show thick mudstones abruptly truncated against the Roa – Mt Buckley Fault zone which indicates offset by this younger fault zone. These findings are in line with recent work undertaken on the Greymouth Coalfield (Suggate 2014) which shows a down-warping

basin extending across the location of the future Roa-Mt Buckley Fault Zone (Figure 2.37).

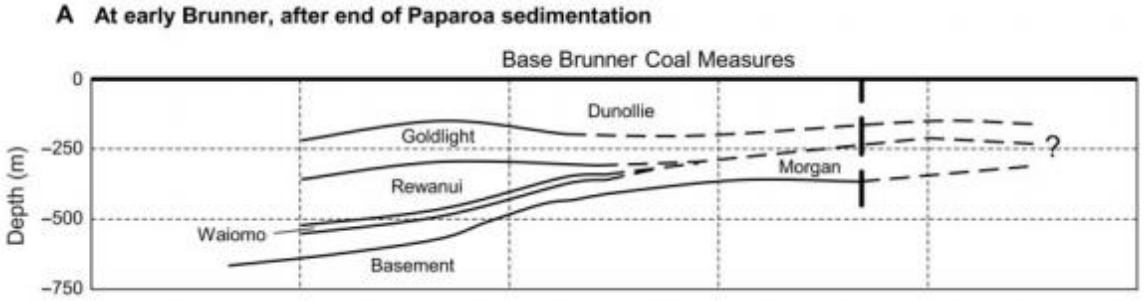

Figure. 2.37. Pre-Brunner development along the eastern side of the basin, adapted from Suggate 2014.

The other issue is as a result of the new isopach map for the Ford Formation. There is now a lack of evidence for a change in basin orientation during deposition of the Ford Formation. Instead it appears this change occurred before deposition of the Paparoa Coal Measures as the underlying Hawks Crag Breccia and Metamorphic Core Complex do appear to oriented perpendicular to the Late Cretaceous formations (Ward 1997; Sager & Palin 2011).

2.9 Conclusions

The sedimentology of the Paparoa Coal Measures lacustrine mudstones was analysed allowing for lithofacies associations to be described and new isopach maps to be constructed. Stratigraphic columns that encompass all three mudstones highlight variations in sedimentology across the coalfield corresponding to distance from lake edge and steepness of slope across the shoreline. Revised isopach maps, which include updated drill hole information, appear to show discrepancies in basin orientation which may have further implications for regional tectonics.

Stratigraphic columns highlight the distribution of individual lithofacies across the coalfield. The northwest corner, which includes the Waiomo and Goldlight Formations, is lacking in massive mudstone. Instead high energy deposits including thick proximal turbidites and debris flows are common. There is also a lack of organic rich siltstone and the lake shore is instead represented by medium micaceous sandstone and conglomerates. In the central, eastern and southern sections of the coalfield massive mudstone facies can be found in all three lacustrine formations. Coal and organic rich sediment are common. There is also a lack

of coarse grained sedimentary rocks and distal turbidites are numerous. In the Waiomo Formation to the east, gravel can be seen which has been derived from the Morgan volcanics around Roa Mine. The south-western edge of the basin shows abundant fossil fragments and a basin high is interpreted due to the lack of Ford and Waiomo Formations and shallowing of the Goldlight Formation.

Isopach maps show three NNE – SSW oriented lakes. This indicates that there was no change in basin orientation during the deposition of the Paparoa Coal Measures. Instead it appears that this change in basin orientation occurred before the deposition of the mudstones. Revisions to mudstone thickness when creating the isopachs also show all three lakes are truncated by the eastern Roa – Mt Buckley Fault zone. This preliminary analysis along with the distribution of lithofacies indicates that fault control during deposition was to the northwest.

Chapter 3 Source Rock Geochemistry

3.1Introduction

Several favourable environments exist for the formation of source rocks. In a marine environment, estuaries, isolated seas and ocean shelves can all provide the necessary conditions for source rock generation. On land, coal and carbonaceous shales which form in sub-aerial environments can be potential source rocks (Taranaki Basin) as are lacustrine shales and mudstones (Zimmerle 1995). The latter forms in tectonically controlled depressions although preservation of organic material, which is essential for a good source rock, requires a low energy environment and lake water anoxia (Allen & Allen 1990). Because of this, the best lacustrine source rocks are fine grained and are often found in the deepest section of the lake (Zimmerle 1995).

Numerous studies over the last few decades have looked into New Zealand source rocks and have found the majority of source rocks being coaly rocks or marine mudstones and shales (Sykes et al. 2013; Killops et al 1994; Herzer et al 1999). Both terrestrial and marine source rocks in New Zealand have been known to produce hydrocarbons however Taranaki is the only place currently producing on a commercial level. Discoveries have also been made in the Canterbury and Great South Basins (Killops 2010) and the West Coast of the South Island (Newman et al 1997, 1999) and the East Coast of the North Island (Elgar 1997).

The presence of petroleum in the Greymouth area has been acknowledged since the early 1900's (Morgan 1911). Seeps along the Kotuku Anticline which are currently being drilled by Mosman Oil and Gas Limited have shown that hydrocarbon generation is possible from the underlying Paparoa Coal Measures (Gage 1956). Identification of key biomarkers indicate these seeps are derived from terrestrial coals (Hirner & Lyon 1989; Frankenberger et al. 1994).

The Paparoa Coal Measures are relatively well studied due to their accessibility, however most other potential lacustrine source rocks across New Zealand are significantly understudied. Preliminary exploration work has identified possible Cretaceous aged lacustrine mudstones in several other New Zealand Basins including the Great South Basin, Canterbury Basin and Taranaki Basin, (Killops 1994, 2010). Due to the similarities in age and depositional setting between the Paparoa Coal Measures and other lacustrine mudstone

bearing basins, it may be assumed than any discoveries relating to the source rock potential of the Paparoa Coal Measures also can be applied to these basins.

3.2 Methodology

3.2.1. Sample collection

A total of 40 samples (Table 3.1) were collected from various drill holes throughout the Greymouth Coalfield (Figure 3.1). Drill hole selection was limited to what was retained in the New Zealand Petroleum & Minerals Core Store in Featherston.

Sampling parameters were based on lithology, thickness and availability of each mudstone. Cost of geochemical testing was also a factor with only the 40 samples allocated for collection and analysis. To maximise results, all samples were taken from massive mudstone and shale facies as opposed to the laminated or transitional facies of the lakes deposits. The reason being, traditional lacustrine source rocks are very fined grained mudstones as the environment required for excellent source rock generation coincides with the environment of deposition of massive mudstone. Where available, more than one sample was taken from each mudstone based on the thickness of each formation in that drill hole. This was most commonly done at the top and bottom of the mudstone formation but on occasion 3 samples were taken from within the much thicker, massive Goldlight Formation.

The actual presence of each mudstone formation within the drill holes also played an important role in sample selection. The Ford Formation was only present in 3 drill holes, resulting in 5 samples. From the Waiomo Formation, 13 samples were collected from 9 drill holes and 22 samples were collected from the Goldlight Formation which presented in 12 drill holes. Although the overall volume of sampling was small it is hoped this study will be seen as a preliminary investigation which will encourage future research into the lacustrine mudstones as a source rock.

3.2.2. Sample preparation

Samples were crushed at the University of Canterbury to a particle size of 1-3mm using a mortar and pestle. From this a small, representative portion was crushed to a fine powder for analysis at GNS Laboratories in Lower Hutt. Between crushing, the mortar and pestle was

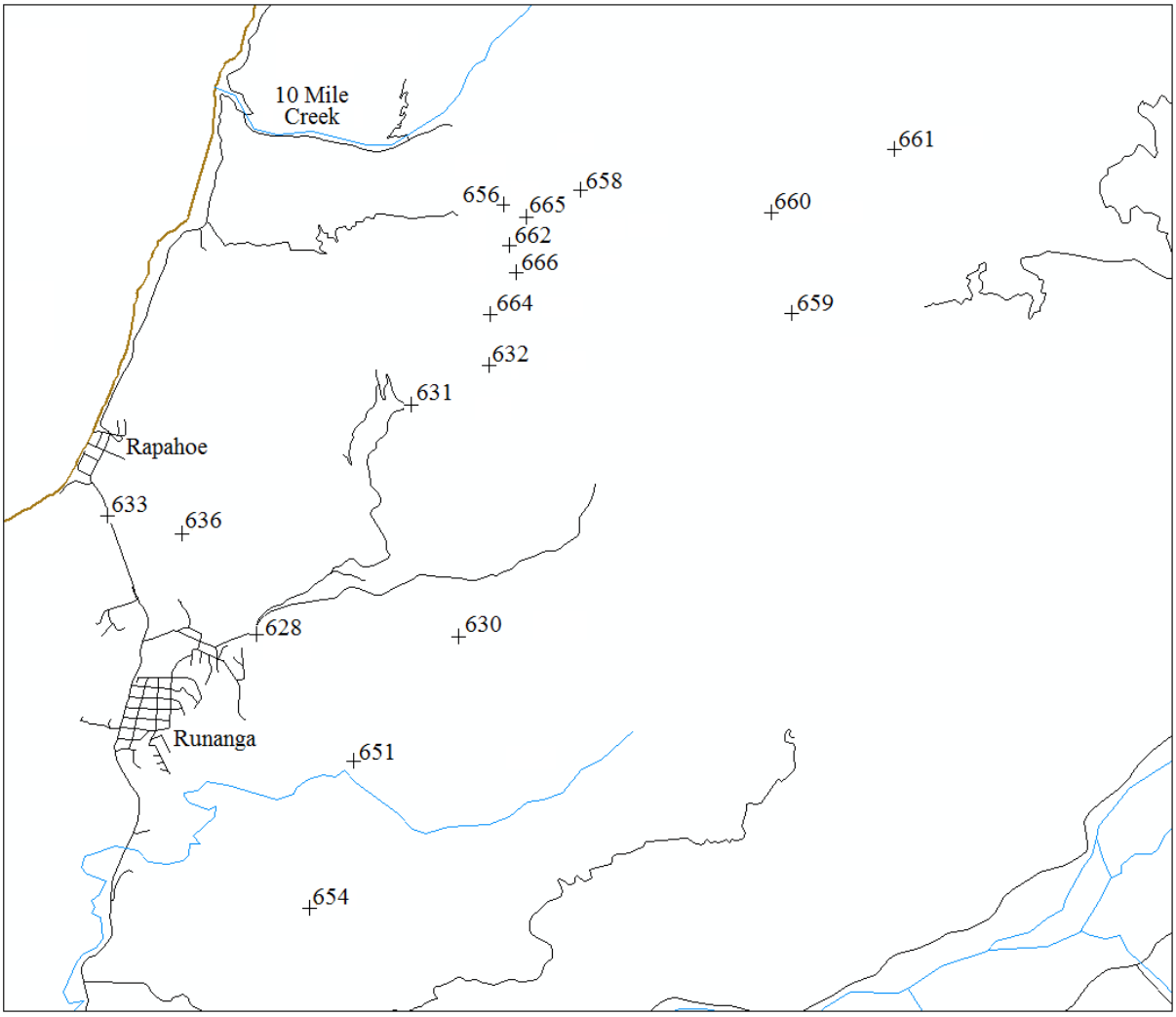

Figure 3.1. Sample locations for source rock analysis on the Paparoa Coal Measure mudstones.

cleaned thoroughly and dried with paper towels and a hot forced air blow dryer. The samples are currently stored at GNS in Lower Hutt.

3.2.3. Analytical procedures

Analysis was undertaken on the crushed mudstone samples at GNS Science in Lower Hutt (New Zealand) using a Source Rock Analyzer (SRA). The SRA uses programmed pyrolysis to determine source rock characteristics of the crushed rock by heating samples until they are at variable levels of degradation, (Horsfield et al. 1983). SRA is comparable in technique and results to the more common Rock-Eval Pyrolysis, however SRA uses oxidation, as opposed

to chemical digestion to measure TOC. The methodology used in this study was based on that described by Peters (1986).

HOLE ID_ DEPTH (m)	Weight (mg)	Formation		HOLE ID_ DEPTH (m)	Weight (mg)	Formation
628_248	83.5	Goldlight		659_245	77.2	Waiomo
630_252-5	81.5	Waiomo		659_249	78.7	Waiomo
631_93-6	82.6	Goldlight		659_376-4	78.2	Ford
631_120-1	80.8	Goldlight		659_393	75.2	Ford
631b_139-8	55.1	Goldlight		660_8-2	77.8	Goldlight
632_214-6	80.5	Goldlight		660_43-2	78.7	Goldlight
632_235	81	Goldlight		660_68	76.5	Goldlight
632_245	79.9	Goldlight		660_192	79.2	Waiomo
632_587-8	81.7	Waiomo		660_212-4	79.9	Waiomo
632_606	100	Waiomo		660_278-4	99	Ford
633_368	79.2	Goldlight		660_336-5	76.8	Ford
636_195-97	79.8	Goldlight		661_30-15	77	Waiomo
636_249-8	80.8	Goldlight		661_48-8	75.3	Waiomo
651_470	81.9	Goldlight		662_48-9	77	Goldlight
654_649-6	79.9	Goldlight		662_116-6	75.2	Goldlight
654_862-7	79.8	Waiomo		664_78-9	75.7	Goldlight
656_461-8	78.8	Waiomo		664_157-5	75.1	Goldlight
658_251	80.1	Waiomo		665_3-8	79.8	Goldlight
658_303	79.4	Ford		666_9	78.3	Goldlight
659_233	78.8	Waiomo		666_144-9	75.9	Goldlight

Table 3.1. Sample weight, hole ID, depth and formation for SRA.

When undertaking source rock analysis, it is essential to consider the measured weight of the samples being tested as this has a direct impact on detection limit problems (Tambach et al. 2009). High volumes of organic material within the mudstone, which commonly coincide with dark colouration, negatively affect the reliability of the overall result. For standard samples with lower organic matter, the standard sample weight must be between 90 and 103mg to ensure testing is regulated. However, when crushing samples, the colour of several samples was noted as being dark which could indicate a high volume of organics within the sample. To compensate this, it was decided to reduce sample weights to around 80mg. On the contrary, some samples were notably lighter in colour when compared with standard samples and as this may indicate less organic material, sample weight was increased to 100mg.

Samples were run over a period of 3 days with each sample taking approximately 45 minutes to complete pyrolysis and oxidation. As each sample is heated a number of events are expected to occur (Thul 2012):

- At approximately 300ºc, any free hydrocarbons within the sample are volatised and measured resulting in the S1 peak (Figure 3.2). As these volatiles are released, they are transferred through the carrier tube by Nitrogen into the Flame Ionisation Detector (FID).
- As the temperature steadily climbs to 650ºC the kerogen "cracks" and releases remaining hydrocarbons and oxygen. These are measured as the S2 peak (Figure 3.2).
- During this stage, the oxygen decomposes early from ~390ºC and the resulting CO2 is measured as the S3 peak (Figure 3.2) within the IR detector.
- The remaining organic matter that remains after the S2 peak is then oxidised. This represents the S4 peak and is again measured in the IR detector.

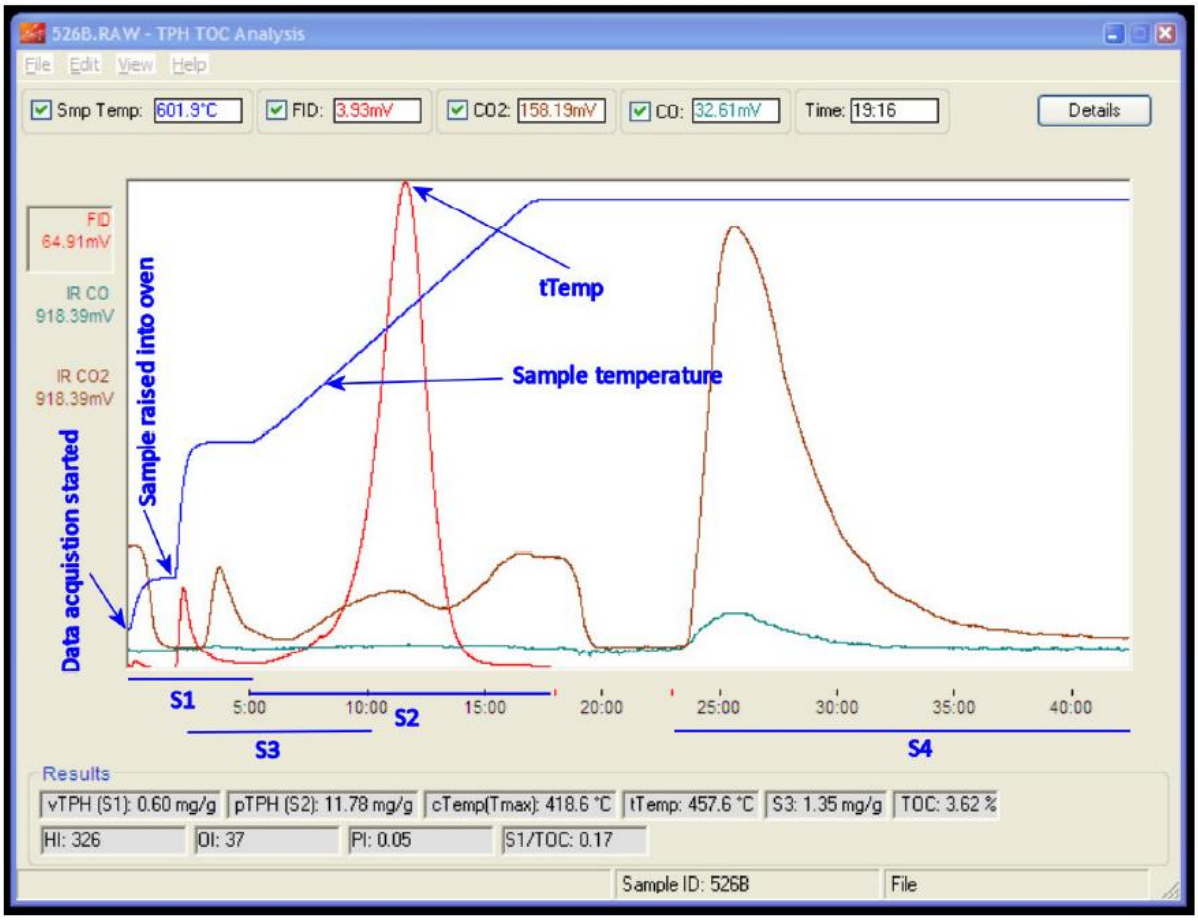

Figure 3.2. Example graph of preliminary SRA results.

3.2.4 Calculated parameters

TOC

Total Organic Carbon (TOC) describes the quantity of organic material within the sample as a percentage. TOC includes both kerogen and bitumen and is a good indicator of how organic rich a source rock is (Peters & Cassa 1994). However, not all organic matter included in TOC can be converted to hydrocarbon.

Tmax

Tmax is a measure of thermal maturity of the source rock (Peters & Cassa 1994). It is determined by the oven temperature at the time of the S2 peak and is influenced by the type of organic matter present within the source rock. Tmax values can also be used in correlation with known temperatures for the onset of expulsion of oil and gas.

Production Index

Production index or PI is commonly referred to as the transformation ratio i.e. how much kerogen is converted into free hydrocarbons (Peters & Cassa 1994). PI increases with maturity as long as expulsion does not occur. Due to its relationship with maturity values, PI can also be used as a general indicator of source rock maturity.

PI is calculated as follows:

$$PI = [S1/(S1+S2)]$$

Values over 0.2 combined with low Tmax results (<445ºC) are considered to be anomalous (Peters & Cassa 1994). Instead, the ratio of PI and Tmax should be positive.

Hydrogen Index

Hydrocarbon index or HI represents the normalised hydrogen content within sample. HI values correspond to the oil-generative potential of the rock with high HI values equalling higher oil generation potential. HI is calculated using TOC and S2 values:

$$HI = (S2x100)/TOC$$

HI primarily allows for identification of kerogen type (Peters & Cassa 1994). From this information, the main expelled product can also be identified. Type I and some type II kerogens are oil prone, type II and type III kerogens are gas prone (or mixed) and type IV kerogens are incapable of hydrocarbon generation (Peters & Cassa 1994).

Oxygen Index

Oxygen index is used to determine the amount of oxygen within the kerogen by measuring CO2 output during S3 (Nunez-Betelu & Baceta 1994). It is calculated from the ratio of oxygen versus TOC:

$$OI = (S3x100)/TOC$$

High OI values are usually found in Type III kerogens but may also be as a result of weathering which elevates S3 (Peters & Cassa 1994). OI values over 100 may also be an indication of terrestrial organic matter which will directly impact HI results. This can give an indication of the organic matter origin with the source rock.

A summary table (Table 3.2) outlines the key measured parameters based on their classification type and their corresponding potential. The main parameters which measure petroleum potential are S1, S2 and TOC. TOC is the most commonly used as is S2. A source rock with "excellent" petroleum potential is considered to have a TOC over 4 wt.% or an S2 value over 20. In comparison, very low TOC (<0.5wt.%) and S2 (<2.5wt.%) are considered to have "poor" petroleum potential.

To measure kerogen type, HI values are commonly used (Peters & Cassa 1994). The preferred kerogen type is Type I as it commonly results in oil as the expelled product. HI values over 600 mg HC/g TOC represent this Type I kerogen. Very low HI values (<50 mg HC/g TOC) are unlikely to produce any oil or gas products and are known as Type IV kerogens.

To measure the maturity of a source rock, several parameters can be used. Commonly when discussing coal maturity, the Suggate Rank scale (Sr) is used while Tmax is more often used to describe petroleum source rock maturity. PI can also be used in conjunction with Tmax. Ideally, potential source rocks are found in the "Mature" range – early, peak and late maturity

as this means the rock has started to expel hydrocarbons but can also still expel hydrocarbons. Because of this, the ideal Tmax temperature would be 435 - 460ºc.

Summary table of key parameters (adapted from Peters & Cassa 1994)			
Petroleum potential parameters			
	S1	S2	TOC
Poor	0 - 0.5	0 - 2.5	0 - 0.5
Fair	0.5 - 1	2.5 - 5	0.5 - 1
Good	1 - 2	5 - 10	1 - 2
Very Good	2 - 4	10 - 20	2 - 4
Excellent	>4	>20	>4
Kerogen Type and character of expelled products			
	HI	S2/S3	Expelled product
I	>600	>15	Oil
II	300 - 600	10 - 15	Oil
II/IIIb	200 - 300	5 - 10	Mixed
III	50 - 200	1 - 5	Gas
IV	<50	<1	None
Thermal maturation parameters			
	Ro%	Tmax	PI
Immature	0.2 - 0.6	<435	<0.10
Mature - Early	0.6 - 0.65	435 - 445	0.10 - 0.25
Mature - Peak	0.65 - 0.9	445 - 450	0.25 - 0.40
Mature - Late	0.9 - 1.35	450 - 470	>0.40
Postmature	>1.35	>470	-

Table 3.2. Summary table of key parameters and their values adapted from Peters & Cassa (1994).

3.3. Results and interpretation

3.3.1 Pyrolysis Results

Pyrolysis analysis of the lacustrine mudstones is shown in Appendix B. The mudstones show a range in values depending on the parameter measured (Table 3.3). One notable exception is sample 656_461.8 which showed favourable results in many of the tested parameters.

3.3.2 Petroleum potential parameter results

Of the three parameters used for determining petroleum potential, TOC and S2 are the most commonly used. As S1 measures free hydrocarbons it does not account for the total potential of the source rock. When describing petroleum potential results the terminology in the left had column of Table 4 is commonly used.

S1

S1 results are varied across each individual mudstone. The Ford Formation S1 results (Table 3.3) ranged from 0.59 in sample 659_393 to 0.15 in sample 658_303. The average and median of the Ford Formation S1 results are 0.4 and 0.42 respectively. These results are classed as Poor to Fair (Table 3.2). The Waiomo Formation S1 results vary from 1.49 (sample 656_461.8) to 0.41 (sample 632_587.8). The average for the Waiomo S1 results is 0.71 while the median is 0.6. Based on the average result, the petroleum potential from S1 is classed as Fair while sample 656_461.8 is classified as Good (Table 4). The Goldlight Formation results range from 0.67 (sample 660_43.2) to 0.10 (sample 633_368). The overall average is 0.3 which would be considered Fair for petroleum potential (Table 4). The median value is 0.29.

S2

S2 results are more favourable than S1 results (Table 3.3). The S2 results for the Ford Formation range from 5.24 (sample 658_303) down to 0.90 (sample 660_278.4). The average S2 result of 2.0 is classed as Poor although the highest value would be considered as Good (Table 3.2). The median result is 1.18. The Waiomo S2 results show greater variation in values compared to the Ford Formation. The highest value of 25.08 (sample 656_461.8) is considered to be Excellent while the lowest value 0.8 (661_30.15) is Poor. The average S2 result for the Waiomo Formation is 6.23 (Good) and the median value is 5.16. The Goldlight Formation S2 results range from 7.49 (sample 632_214.6) to 2.66 (sample 631b_139.8). The average is 4.83 (Fair) while the median is 4.62.

ID	vTPH(S1)	pTPH(S2)	cTemp(Tmax)	tTemp	S3	TOC	HI	OI	PI	BI
628_248	0.16	3.68	429	468.2	2.02	2.09	176	97	0.04	8
630_252-5	0.60	7.52	443	482.2	0.48	3.02	249	16	0.07	20
631_120-1	0.20	4.78	434	472.6	1.80	2.26	211	80	0.04	9
631_93-6	0.18	3.29	433	472.1	1.18	1.77	185	66	0.05	10
631b_139-8	0.25	2.66	431	469.8	4.37	2.01	132	217	0.08	12
632_214-6	0.36	7.49	434	472.6	0.81	2.66	282	30	0.05	14
632_235	0.30	5.16	427	465.8	1.57	2.42	213	65	0.05	12
632_245	0.31	7.61	436	475.4	0.53	2.76	275	19	0.04	11
632_587-8	0.41	4.25	450	488.5	1.18	1.67	255	71	0.09	25
632_606	0.65	5.16	440	479.4	1.26	1.77	292	71	0.11	37
633_368	0.10	3.41	429	468.1	2.90	1.89	181	154	0.03	5
636_195-97	0.15	4.72	430	468.6	2.36	2.26	209	104	0.03	7
636_249-8	0.18	4.47	431	469.7	1.36	2.09	214	65	0.04	9
651_470	0.30	4.76	432	470.9	0.99	2.23	213	44	0.06	13
654_649-6	0.31	3.94	444	483	1.43	2.30	172	62	0.07	13
654_862-7	0.93	6.63	444	482.6	0.71	2.62	253	27	0.12	35
656_461-8	1.49	25.08	442	480.9	0.75	4.54	552	16	0.06	33
658_251	0.53	7.76	452	490.6	1.39	2.50	311	55	0.06	21
658_303	0.15	5.24	456	495.1	1.58	2.56	204	62	0.03	6
659_233	0.92	3.51	467	506	1.04	3.08	114	34	0.21	30
659_245	0.86	2.11	465	504	0.47	1.77	119	27	0.29	49
659_249	0.52	8.31	441	480.1	0.53	2.65	313	20	0.06	20
659_376-4	0.50	1.28	466	504.7	1.87	1.43	90	131	0.28	35
659_393	0.59	1.16	465	504.4	2.29	1.37	84	167	0.34	43
660_192	0.59	2.55	458	496.5	1.95	2.12	120	92	0.19	28
660_212-4	0.64	6.51	455	494.1	0.30	2.78	234	11	0.09	23
660_278-4	0.41	0.90	462	501.4	2.39	1.01	90	237	0.31	41
660_336-5	0.42	1.18	463	502.3	2.48	1.39	85	179	0.26	30
660_43-2	0.67	3.85	450	489.1	0.46	2.38	162	19	0.15	28
660_68	0.54	3.74	451	490.3	1.28	2.65	141	48	0.13	20
660_8-2	0.51	4.39	451	490	1.01	2.74	160	37	0.10	19
661_30-15	0.51	0.80	471	510	1.46	1.17	68	125	0.39	44
661_48-8	0.53	0.85	474	512.7	0.90	1.21	70	75	0.38	44
662_116-6	0.29	6.54	434	472.9	0.51	2.69	244	19	0.04	11
662_48-9	0.29	3.96	437	475.6	1.62	2.30	172	71	0.07	13
664_157-5	0.29	5.49	430	469.3	0.89	2.58	213	35	0.05	11
664_78-9	0.40	7.35	435	473.6	1.24	2.93	251	42	0.05	14
665_3-8	0.27	5.26	437	475.6	1.34	2.95	178	45	0.05	9
666_144-9	0.32	5.18	429	467.6	1.36	2.44	213	56	0.06	13
666_9	0.23	4.51	430	468.9	1.25	2.25	200	56	0.05	10
Averages	0.45	4.93	444.63	483.63	1.38	2.28	197.50	71.18	0.12	20.83

Table 3.3. Summary results table for source rock analysis of the Paparoa Coal Measure lacustrine mudstones.

Toc

TOC results across all three mudstones were varied. The Ford Formation has TOC values (Table 3.3) in the range of 2.56 wt.% (sample 658_303) to 1.01 wt.% (660_278.4) and are classed from Very Good to Good (Table 4). The average is 1.6 wt.% (Good) and the median is 1.39 wt.%. The Waiomo Formation has one Excellent result of 4.54 wt.% (sample

656_461.8) and the lowest result is1.17 wt.% (Good). The average TOC is 2.38 wt.%, and the median is 2.50 wt.%.indicating the Waiomo Formation has Very Good petroleum potential. The Goldlight Formation has results ranging from 2.95 wt.% (Very Good) to 1.77 wt.% (Good). All but two of the Goldlight Formation TOC results are above 2 wt.%. The average TOC for the Goldlight Formation is 2.39 wt.% (Very Good) while the median is 2.34 wt.%.

3.3.3 Thermal Maturation Parameter results

Tmax is the most common source rock maturity index as it also gives an indication of what stage of hydrocarbon generation and expulsion the rocks are currently experiencing (Peters & Cass 1994). Tmax and the lesser used PI can be compared to the common system of ranking coals based on vitrinite reflectance, otherwise known as Suggate Rank (Sr or Ro).

Tmax

Tmax results vary in all three mudstones (Table 3.3). The Ford Formation shows the highest results with a range from 456ºC to 466ºC indicating the formation is post-mature. The average and median results are 462.6 ºC and 463.3 ºC respectively. The Waiomo Formation has a much greater range in values from 441 ºC to 474 ºC. This indicates that the source rocks within the Waiomo are early-mature to pos-tmature. As a general trend, Tmax temperatures showed an increase towards the northeast for the Waiomo Formation. The average and median values are 453.89 ºC (Late-mature) and 451.6 ºC. The Goldlight Formation results also vary in range. The maximum Tmax result is 451 ºC while the lowest is 426.8 ºC indicting the Goldlight ranges froms immature to post-mature depending on locality. The average Tmax for the Goldlight Formation is 435.08 ºC (Early-mature) while the median is 433.35 ºC.

PI

The PI results from the Ford Formation (Table 3.3) show a range in maturity values from 0.03 to 0.34 indicating the source rocks are immature to peak – mature. The average and median PI results are 0.2 and 0.28 with the average indicating the Ford Formation is early – mature. The Waiomo Formation also shows a broad range of PI results from 0.06 to 0.39 indicating the rocks are immature to peak – mature. The average PI is 0.15 while the median

is 0.11 indicating an early – mature source rock. The Goldlight Formation results are also low with all but 3 samples displaying PI values under 0.10. The maximum value obtained is 0.15 (early – mature) while the lowest result is 0.03 (immature). The average and median for the Goldlight Formation are 0.06 and 0.05 respectively indicating an immature source rock.

3.3.4 Kerogen type and source results

HI

The Ford Formation exhibits low HI results across all but 1 of its results (Table 3.3). The highest value of 204 mg HC/g TOC indicates the organic material is derived from Type II/IIIb kerogens and would result in mixed gas and oil products. All other results are under 100 mg HC/g TOC indicating the presence of Type III kerogens and a gas prone source rock. The average and median HI results (110 mg HC/g TOC and 90 mg HC/g TOC) highlight the effect of the best sample inflating the overall average. The Waiomo Formation HI results are again highly variable with the highest value of 552 mg HC/g TOC indicating the presence of Type II oil prone kerogens while the lowest value of 68 mg HC/g TOC is indicative of Type III gas prone kerogens. The average and median HI results are 226.9 mg HC/g TOC and 249 mg HC/g TOC respectively and highlights a skew in data caused by two low results. Additional micro-petrographic analysis was undertaken on sample 656_461.8 which has the highest result and showed that the organic matter is heavily dominated by alginate (telaginite and lamalginite from *Botryococcus* and *Pediastrum*) and also contain fragments of vitrodetrinite and inertodetrinite of terrestrial origin. The Goldlight Formation results show little variation with the highest and lowest values being 282 mg HC/g TOC and 132 mg HC/g TOC respectively. These Type II/IIIb and Type III kerogens result in a gas prone and mixed source rock. The average and median values for the Goldlight are 199. 8 mg HC/g TOC and 204.5 mg HC/g TOC.

OI

The OI results for the Ford Formation show a range in values from 62 to 237 (Table 3.3) indicating organic matter was predominantly derived from terrestrial material which is unlikely to be productive. The Waiomo Formation results are more positive with all but one of the sample exhibiting results over 100. The highest and lowest results are 125 and 11. The average was 49 while the median is 34, brought down by several very low results under 20.

The Goldlight Formation OI results are similar to the Waiomo Formation results with all but three of the samples under 100. The lowest value is 19 while the highest is 217. The average and median results are 65 and 56.

3.3.5. Petroleum potential parameter interpretations

S2

The comparison of S2 peaks was done on three samples to highlight the relationship between S2 and source potential (Graph 3.1). All three samples chosen had similar Tmax values but varying TOC and HI values. The green curve of sample 656_461.8 (Waiomo) is much narrower than the other two curves of samples 662_48.9 (blue curve) and 654_649.6 (red curve) from the Goldlight Formation. Broader widths are an indication of broader activation energies which is directly related to kerogen type (Ehinola et al. 2005; Jarvie 1991). In this case, it appears that the Waiomo sample is likely derived from a narrow range of Type I and Type II kerogens, with micro-petrographic analysis verifying this. In comparison, the other samples appear to contain type III kerogens, inferred from their wider curves and asymmetry (Jarvie 1991). Type III kerogens come from the vitrinite macerals group which are usually composed of terrestrial plant and leaf material, (Peters & Cassa 1994).

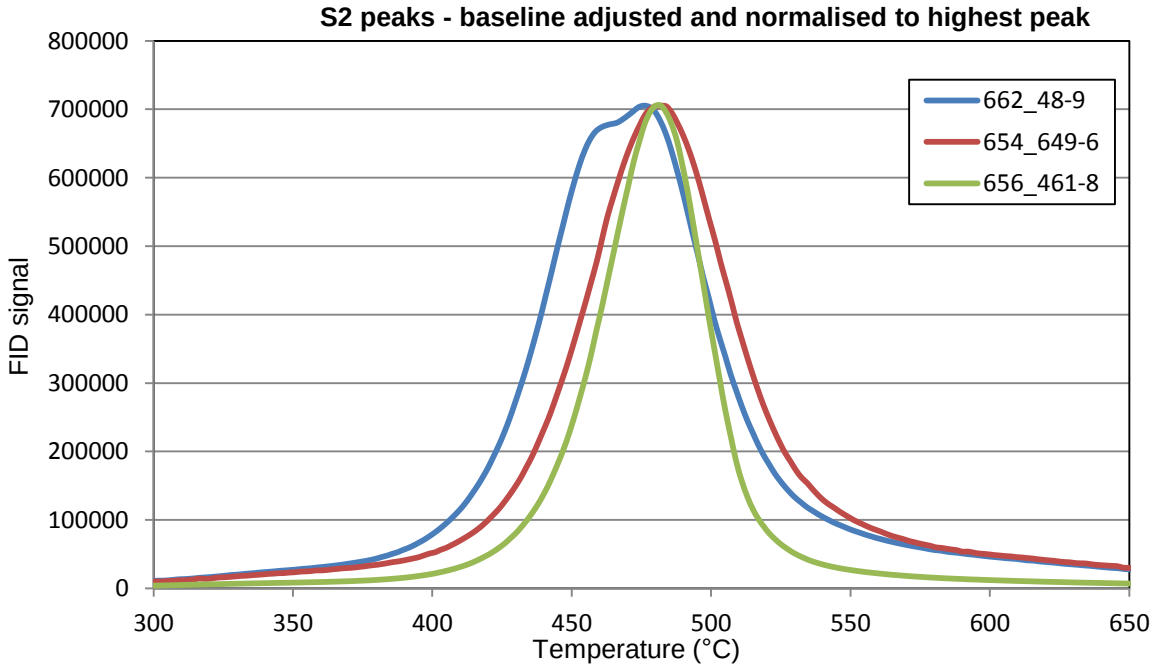

Graph 3.1. Normalised S2 curves for 3 samples. 656_461.8 has a much thinner S2 curve indicating a much smaller range for activation energy distribution. Blue and red are from the Goldlight Formation, green is from Waiomo Formation.

TOC vs S2

TOC vs S2 plots are another useful tool for evaluating the properties from Rock-Eval Pyrolysis. These two petroleum potential parameters can be used to normalise HI data using the regression line equations (Graph 3.2 and 3.3).Graph 3.2 shows the results for all 40 tested samples while Graph 3.3 shows only the samples which are in the early-mature or immature range based on Tmax values (<445ºC). This was done to exclude the more mature samples which are no longer at their maximum petroleum potential. By excluding these samples, the Ford Formation is excluded from the analysis due to its high Tmax results. When comparing these plots with HI results, there is a strong relationship, however the S2 vs TOC plotted values are slightly lower than the corresponding HI values.

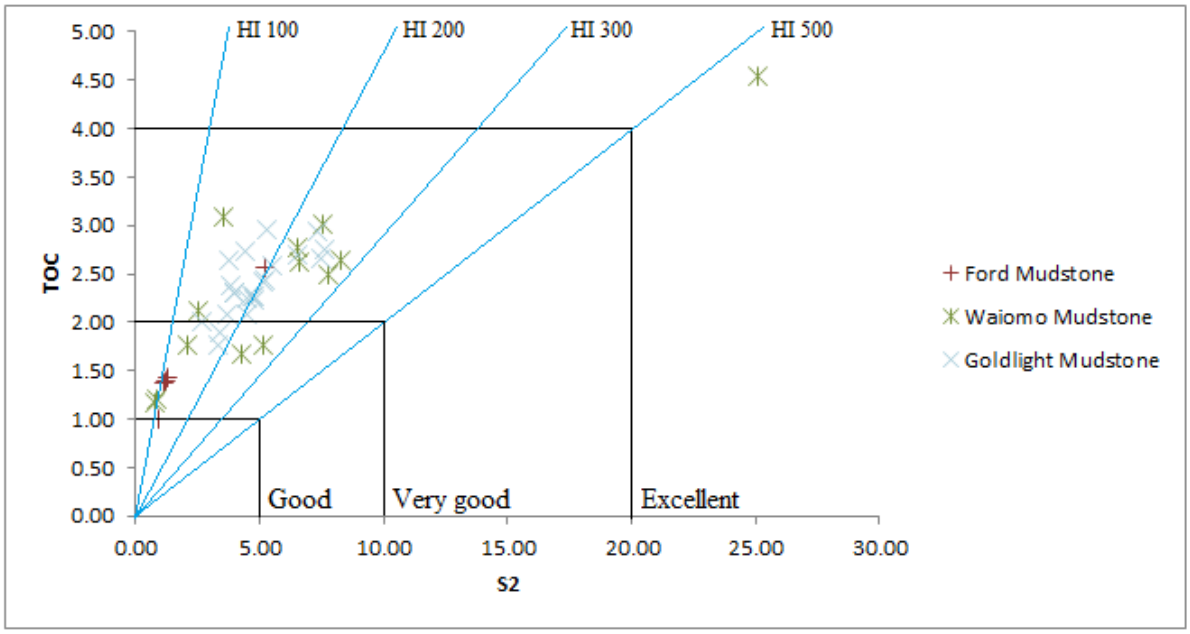

Graph 3.2. S2 vs TOC for all samples. The Ford Formation has the lowest corresponding HI values, the Waiomo Formation results are the most diverse and the Goldlight Formation results are well defined between 100 mg HC/g TOC and 300 mg HC/g TOC. These plotted results match favourable with measured HI results.

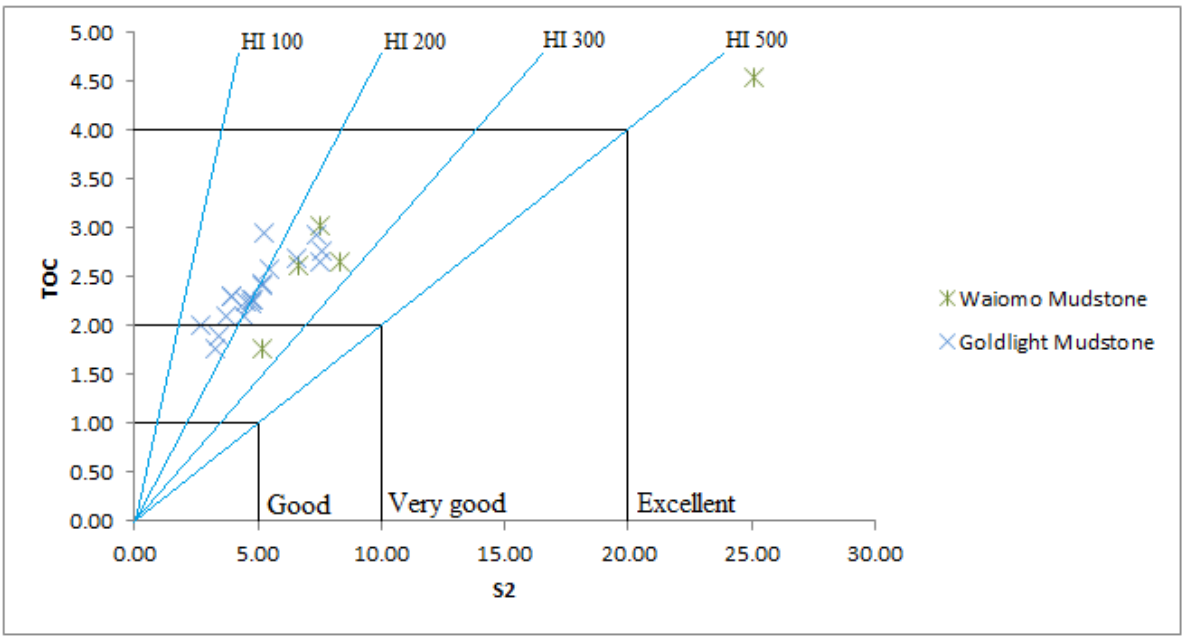

Graph 3.3. S2 versus TOC plot of samples with Tmax values under 445 ºC. The Waiomo Formation results show slightly higher corresponding HI values the Goldlight Formation.

3.3.6 Thermal Maturation Parameters interpretation

Tmax vs Sr

Due to numerous studies on coal rank within the Greymouth Coalfield there is sufficient data to allow for comparisons between Tmax and coal rank (Sr). Specifics regarding coal rank are outlined in Suggate (2002). Coal rank studies within the Rewanui Coals indicate an increase in rank from west to east (Figure 3.3). The most mature mudstone samples (661_48.8, 661_30.15, 659_233) were located around Roa Mine in the northeast corner of the coalfield and maturity values decreased to the southwest. Thermal maturity contour maps were made for each lacustrine formation (Figures 3.4, 3.5, 3.6) to compare with the coal maturity maps of the Rewanui Formation from Suggate and Boyd (2012) (Figure 3.3).

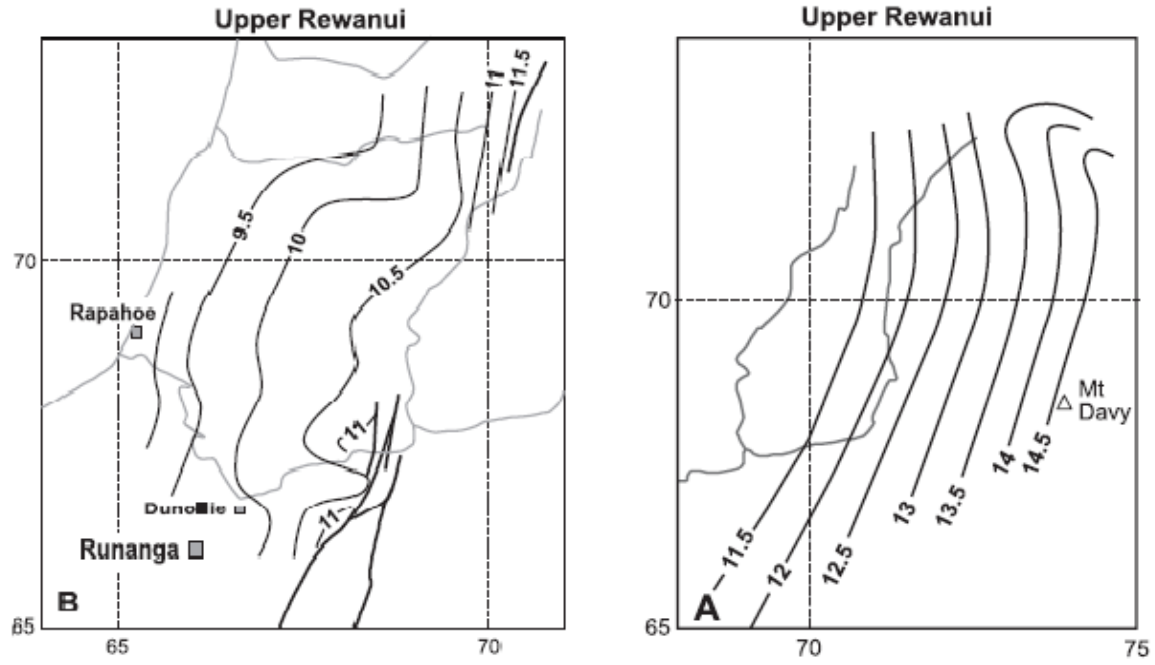

Figure 3.3. Thermal maturity contour map for the Rewanui Coals (Suggate & Boyd 2012). B is located to the southwest, A is located to the east.

The Ford Formation rank contour map (Figure 3.4) show a rank increase towards the east however it is constrained by only a very small number of drill holes in the northern section of the coalfield.

The Waiomo Formation rank contour map (Figure 3.5) is based on 8 drill holes and also shows an increase in rank towards the east. When comparing the ranks of the Waiomo and Ford formations from DH 656, the Ford Formation shows a slight increase in rank contour values than the Waiomo Formation due to the greater burial depth. This is also seen in DH 660 and 659 but with a smaller difference between the two. Around 7 Mile Stream, the Waiomo Formation exhibits slightly higher rank values than the Rewanui Coal from Figure 11 due to the Waiomo Formations stratigraphic position below the Rewanui Coals.

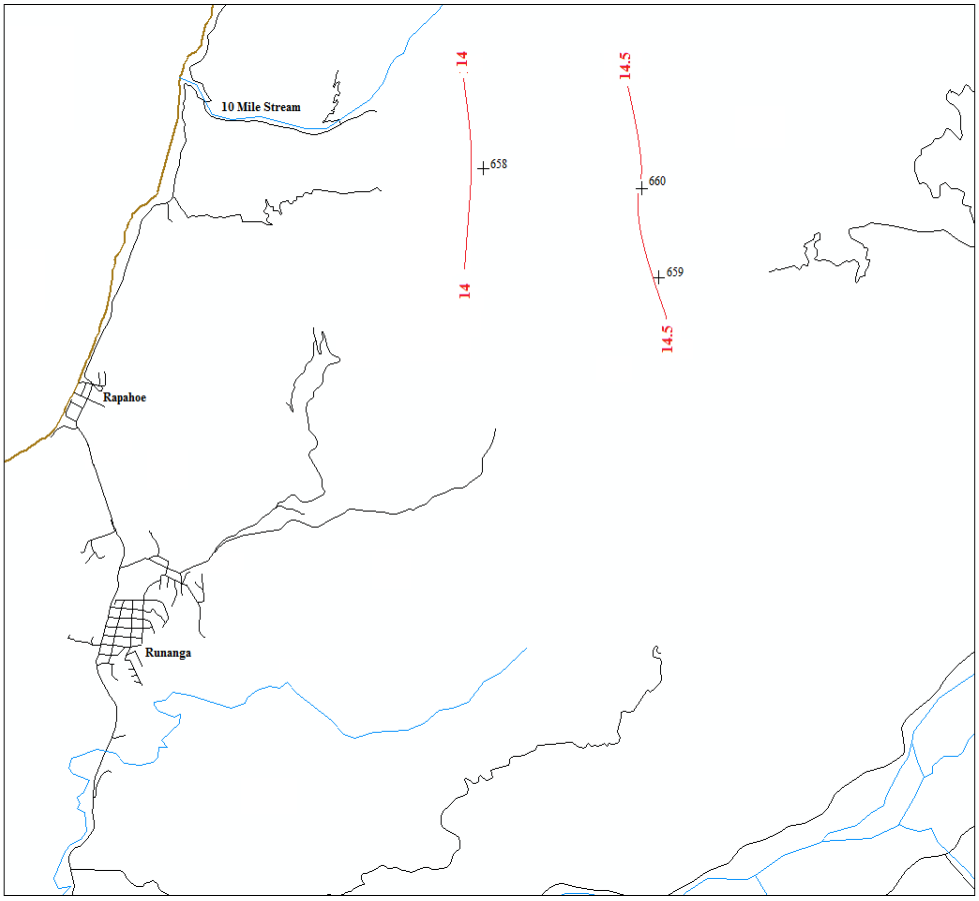

Figure 3.4. Rank contour map of the Ford Formation showing an increase towards the east.

The Goldlight Formation rank contour map (Figure 3.6) is constrained by 12 drill holes with most located on the western side of the coalfield. Again, these rank contour intervals show an increase to the east and have slightly lower values when compared to the Ford or Waiomo Formations in the same drill hole due to the Goldlight Formation's shallower burial depth. The western drill hole ranks are comparable to those from the Waiomo Formation.

Comparisons between the coal rank data and the mudstone rank contours show many similarities. When trying to determine the rank of the mudstones in areas of limited data it would be satisfactory to apply coal rank information to the mudstones.

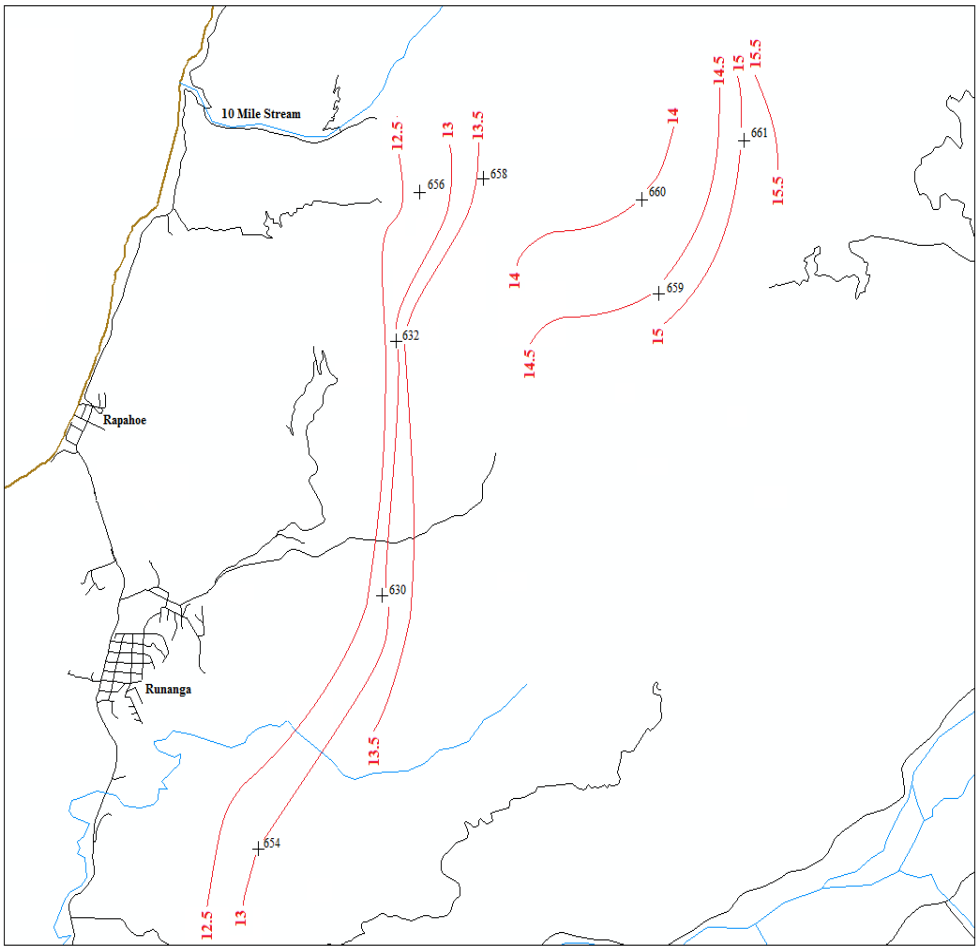

Figure 3.5. Rank contour map of the Waiomo Formation showing an increase towards the east. Values are similar in the 7 Mile Stream area to the Rewanui Coals from (Figure 3.3).

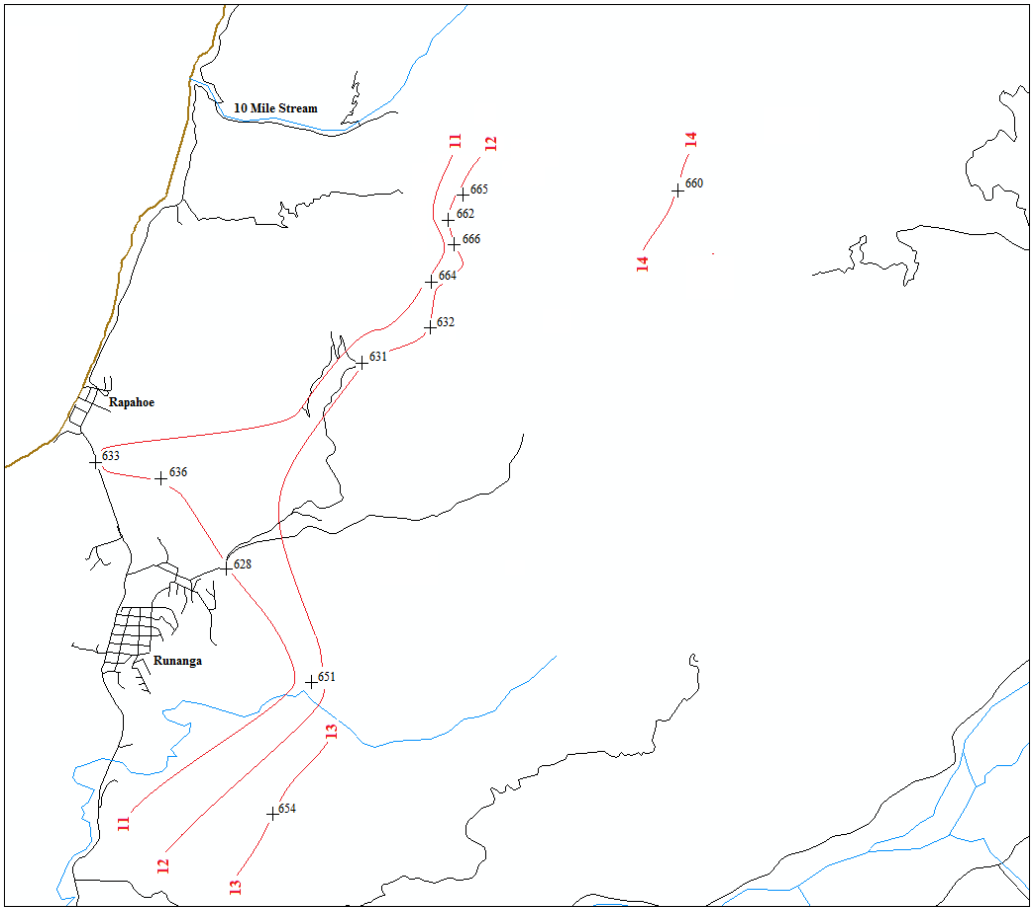

Figure 3.6. Rank contour map of the Goldlight Mudstone showing limited contour intervals in the east but Ro is well constrained to the west. Rank contours are lower

Tmax vs PI

By cross plotting Tmax vs PI, a fairly well constrained positive relationship can be seen where an increase in Tmax corresponds to an increase in Production Index. (Graph 3.4). There is one slight outlier in sample 658_303 which has a relatively high Tmax temperature (456 ºC) yet has the lowest PI value of 0.03. This negative relationship seen in sample 658_303 is an indication that the sample didn't have a high amount of the kerogens which easily break down during heating.

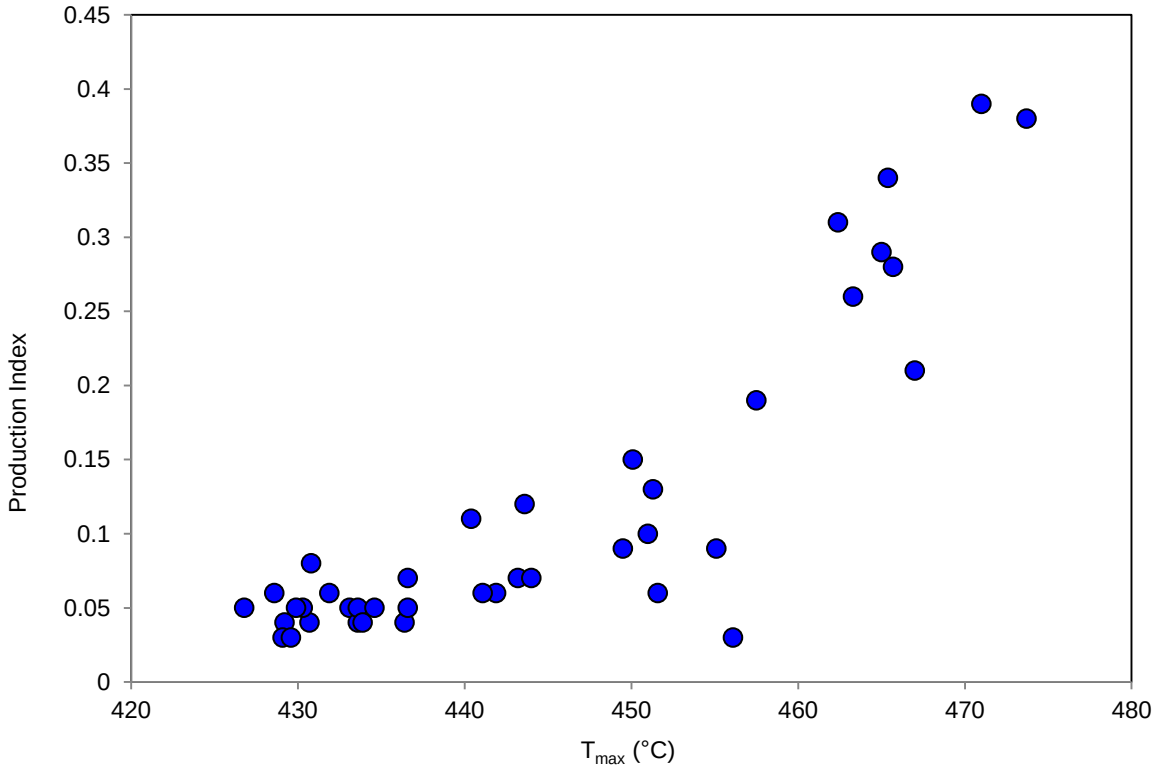

Graph 3.4. Cross plot of Tmax vs PI showing a strong, positive relationship between the two parameters.

3.3.7 Kerogen type and source interpretations

HI vs Tmax

When plotting HI versus Tmax, some interesting results can be seen (Graph 3.5). As HI represents the oil generative potential of a rock meaning HI values are expected to be highest in immature source rocks and to decrease with the onset of hydrocarbon generation (Sykes & Snowdon 2002). There is a clear trend where HI values increase with increasing temperatures as onset of oil generation occurs which is unusual.

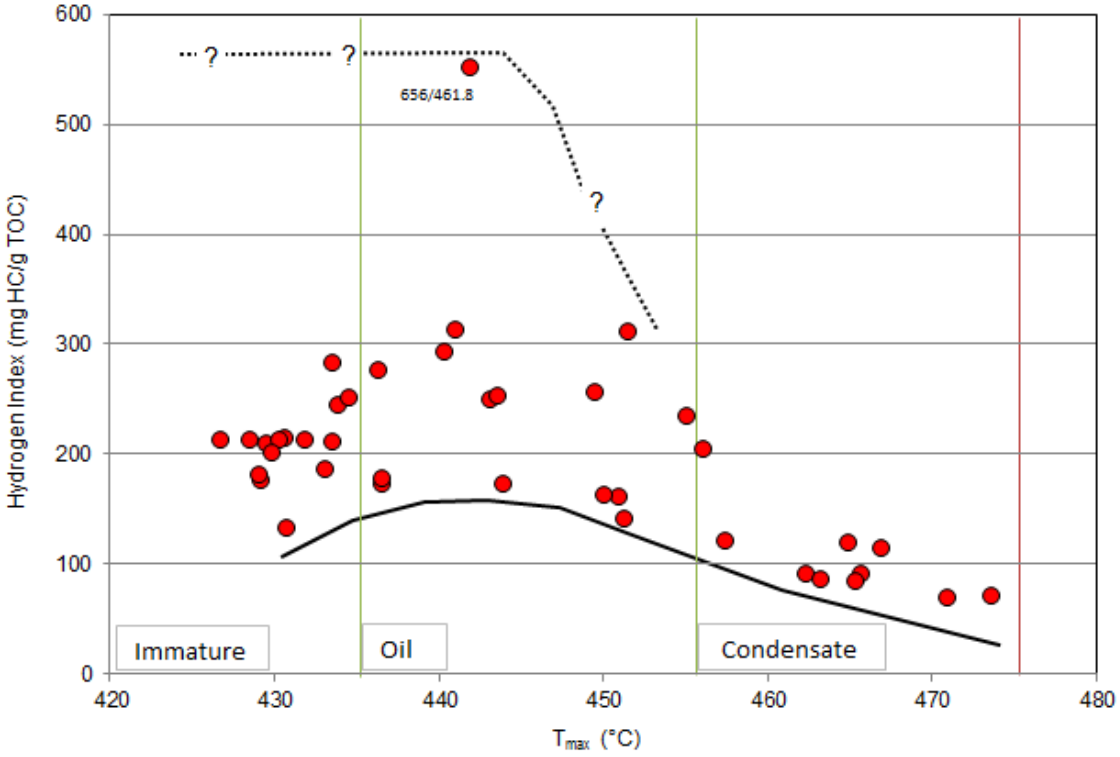

Graph 3.5 Tmax vs HI showing sample plots against oil and gas window.

This initial increase in HI with temperature is also seen in New Zealand coals when plotting HI versus Tmax (Sykes & Snowden 2002). The work done on the NZ coals has shown that the likely cause for the increase seen above is due to rearrangement of the coal molecules during diagenesis and catagenesis (Sykes & Snowdon 2002). As this happens within the coal, new higher energy bonds form which result in an increase in hydrocarbon generative potential. Given the similarity of the trends it suggests that a similar reaction may occur to the organic material within the mudstones. Based on this information, some of the immature low HI samples may actually have higher HI values once they reach the oil window (Graph 5) and subsequently, samples with higher HI values currently within the oil window may have had lower HI values when they were still immature. This could indicate the Paparoa Coal Measures actually have higher HI values than what has been indicated in the results.

HI vs OI

Using HI and OI, the mudstone organic material can be characterised using the van Krevelen diagram (Graph 3.6). This has traditionally been used for coals (Suggate 2002) but the same principle can be applied to lacustrine mudstones as another way to interpret and display information on kerogen type

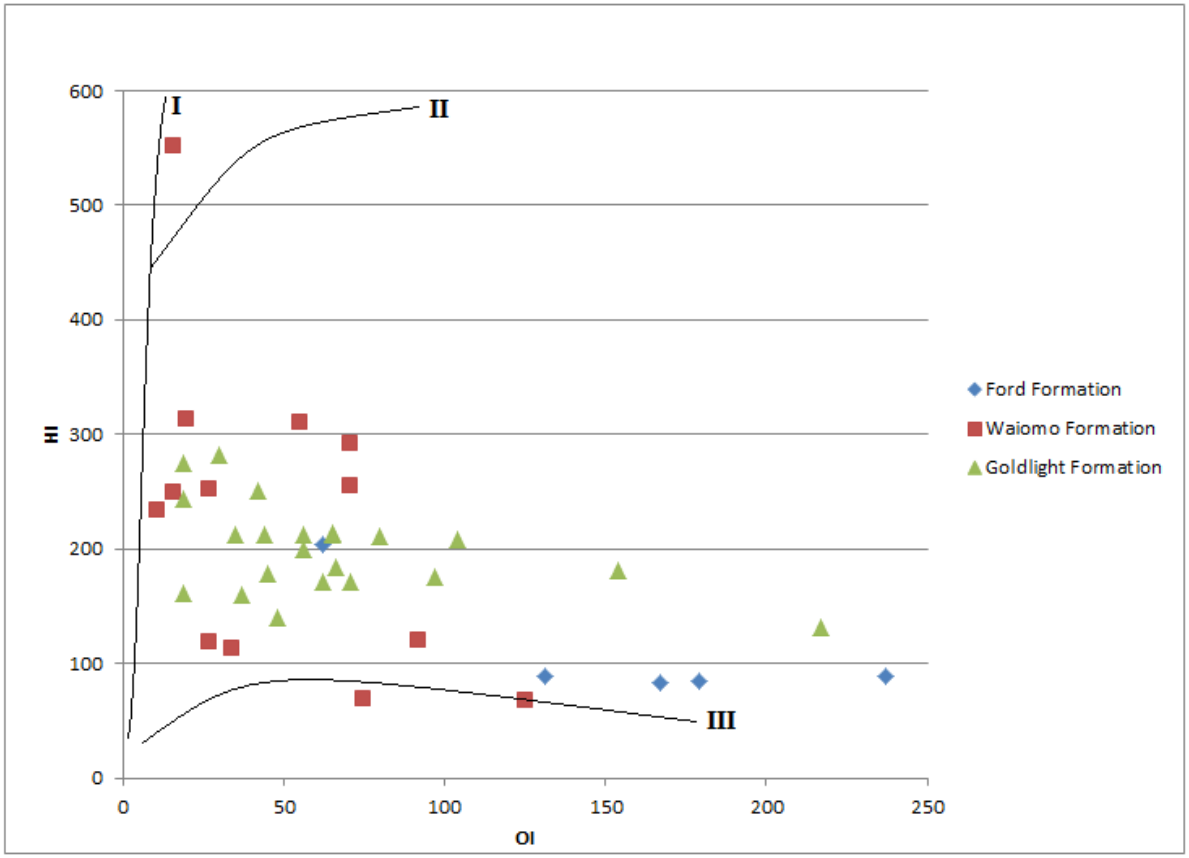

Graph 3.6. Cross plot of OI vs HI overlain by van Krevelen diagram highlighting type of kerogen. Modified from Sykes and Johansen.

One Waiomo sample (656_461.8) is and outlier in the Type I kerogen field and is the only definitive oil prone sample. The other samples are spread out with lower HI's and a range of OI values plotting in the mixed Type II and Type III kerogen field. The Ford Formation has the lowest HI results and thus corresponds to Type III kerogens. The Waiomo and Goldlight Formations have higher HI results with the Goldlight showing a smaller range of HI values compared to the Waiomo Formation. The results for the Goldlight Formation combined with is low Tmax results indicate it could be a possible shale gas resource.

3.4 Discussion

3.4.1 Summary of main results

Results for the three lacustrine mudstones showed a range of values across the main tested parameters: **TOC**, **HI** and **Tmax.**

TOC values for the Ford Formation are the lowest on average of the three lacustrine mudstones with a value of 1.6 wt.%. In comparison, the Waiomo Formation has a TOC average of 2.38% and the Goldlight has an average TOC of 2.39 wt.%. Both the Waiomo and Goldlight Formations have high enough TOC values to be considered as potential source rocks on this parameter alone.

HI results for the Ford Formation are poor with an average value of 110 mg HC/g TOC which is inflated by one sample with a HI value of 204 mg HC/g TOC. All other values are under 100 mg HC/g TOC which is an indication that any expelled product would be gas prone. The Waiomo Formation has a broad range of HI values from 552 mg HC/g TOC to 66 mg HC/g TOC. The highest value indicates the presence of type I or type II kerogens which are oil prone whereas the lowest value of 66 mg HC/g TOC is low enough to be non-producing. The average HI value for the Waiomo is 226 mg HC/g TOC suggesting in the possible expulsion of wet gas products. The Goldlight Formation has an HI average of 199 mg HC/g TOC with all values between 132 mg HC/g TOC and 282 mg HC/g TOC. This would make the Goldlight Formation gas prone, derived from Type II and Type III kerogens.

The final key parameter is **Tmax**. Overall, results show the Ford Formation to be late-mature with a Tmax value of 463ºC. The Waiomo Formation is also late-mature but with a value of 453ºC. The Goldlight Formation appears to be early-mature with a much lower Tmax value of 435ºC. This overall decrease in Tmax from the Ford to the Goldlight Formation is to be expected given the stratigraphic order of the mudstone as the Ford has experienced the greatest burial depth.

3.4.2 International comparisons

There are several well-known and well-studied examples of lacustrine source rocks and potential source rocks around the world including but not limited to the Green River Formation (USA), the Qingshankou and Nenjiang Formations (China) and the Kissenda Shale (Africa). These international examples are selected for comparison due to their range in

geochemical properties and values as well as all being considered viable source rocks. It is important to compare Paparoa mudstones with these global examples, to determine the overall potential of the Ford, Waiomo and Goldlight Formations.

Comparisons to the Green River Formation

The Green River Formation is one of the most prolific lacustrine source rocks in the world with deposits found across 3 states in the USA (Ruble et al 2001). It is comprised of 3 units; the lower and middle member, the central saline facies and upper member and the upper transitional beds (Keighley 2003). Sedimentology of the Green River Formation shows three distinct facies association subdivisions: fluvial lacustrine, fluctuating profundal and evaporative (Smith et al. 2008).

Geochemical results from the Green River Formation are highly variable. Average TOC results across most of the members within the Green River Formation are 6.3 wt.% (Ruble et al. 2001) while values of 47 wt.% have been recorded from some locations. These high TOC values are uncommon in lacustrine and marine source rocks and are approaching the TOC measurements normally seen in coaly source rocks (Sykes & Snowdon 2002). HI values from the Green River Formation are also usually high with the average HI recorded as 900 mg HC/g TOC. This clearly indicates that Type I oil prone kerogens were dominant within the Green River Formation (Ruble et al. 2001). Tmax values from the Green River Formation are all under 440 ºC, which indicates the source rocks are early mature at most.

When you compare these values to the Paparoa Group mudstones, there is a clear difference. The most promising sample (656_461.8) which has a TOC of 4.54 wt.% is well below the average from the Green River Formation yet is still considered to have enough organic material to produce hydrocarbons given the right conditions. The highest HI seen in this study has a value of 552 mg HC/g TOC which makes it oil prone but with a slightly broader geochemical composition (Peters & Cassa 1994). As shown earlier, the Paparoa Coal Measures mudstones exhibit a range in maturity levels. The Goldlight Formation has an average Tmax of 435 ºC which is slightly lower than that seen within the Green River Formation while the Waiomo and Ford Formations are over mature.

The Green River Formation is considered to be the best lacustrine source rock in the world and these geochemical properties attest to that. In comparison, the Paparoa Coal Measures mudstone results appear to be poor however some of the results measured within the Waiomo

Formation are comparable to those seen within the Green River Formation. From this it can be determined that although the Paparoa mudstones may not be as profitable as the Green River Formation, it does show some characteristics of a commercial source rock given the results from the Waiomo sample 656_461.8 and the maturity of the Goldlight Formation.

Comparisons to the Qingshankou and Nenjiang Formations

The rift basins of northern China have been considered as a petroleum source for several decades (Bechtel et al. 2012). Thick and laterally continuous lacustrine deposits are found throughout much of the Songliao basin and were deposited during the Late Cretaceous (Song et al. 2013) with organic rich zones forming shales within the Qingshankou and Nenjiang Formations, (Bechtel et al. 2012). Geochemical results show that the Qingshankou and Nenjiang Formations are organic rich and dominated by Type I kerogens in the more organic rich oil shales,(Fleet et al. 1988; Bechtel et al. 2012). The Qingshankou Formation has TOC values ranging from 0.75 wt.% up to 23.8 wt.% in the more organic rich oil shales while the HI values are typically within 400 – 700 mg HC/g TOC (Bechtel et al. 2012). The Nenjiang Formation shows less variation within its results with TOC values ranging from 0.75 wt.% – 11.85 wt.% (averaging <1.7 wt.% for the majority of the Formation) and HI values averaging 300 mg HC/g TOC (high HI of 750 mg HC/g TOC in the lower shales), (Bechtel et al. 2012).

The Songliao Basin shales show a much broader range within the TOC and HI results compared to the Paparoa Mudstones especially for the TOC results. The TOC and HI results from the Qingshankou Formation are still more favourable than the Paparoa mudstones but the Nenjiang Formation shares many similar geochemical properties to the Waiomo and Goldlight Formations especially. TOC averages within the Waiomo and Goldlight are higher on average than those within producing the Nenjiang Formation.

The Nengjiang and Qingshankou Formations are considered to be excellent source rocks (Jia et al. 2013; Jia et al. 2013) and also exhibit similar geochemical properties as the Paparoa Mudstones. As mentioned, the Waiomo and Goldlight Formations have higher average TOC and similar HI results to the Nengjiang Formation. Based on these comparisons it appears that the Waiomo and Goldlight Formations could also be considered as an excellent source rock but would be gas prone as opposed to oil prone like the Songliao Basin shales.

Comparisons to the Kissenda Formation

The Kissenda Formation within the Gabon Basin in Africa is considerably less studied than the other global examples presented in this chapter. The shales were deposited in an Early Cretaceous rift system associated with the initial opening of the Atlantic Ocean (Pedentchouk et al 2004). The Kissenda Formation exhibits a range of TOC and HI values (Kuo 1994; Pedentchouk et al. 2004). TOC values range from 1.12 wt.% to 7.89 wt.% with an average of 4.2 wt.%. HI values are from 496 mg HC/g TOC - 690 mg HC/g TOC with an average of HI value of 609 mg HC/g TOC. Tmax averages show that the shale has reached early to peak maturity with all Tmax results between 434ºC and 445ºC.

The Kissenda Formation shows more favourable results on average in comparison to the Ford, Waiomo and Goldlight Formations. The Kissenda shales appear to be oil prone in comparison to the gas prone Goldlight and Waiomo Formations. Although the Kissenda Formation is not a proven source rock (due to lack of information) it is more favourable than the Paparoa Coal Measure mudstones. However it is probable that both Kissenda and Paparoa mudstones were deposited in the same basin setting and therefore the Paparoa mudstones deserve analysis. .

3.5 Conclusions

The Paparoa Coal Measure lacustrine mudstones have been analysed for their hydrocarbon potential and to gain a better understanding of New Zealand non-marine source rocks. Results for each mudstone are varied with some expected and some unexpected results.

The Ford Formation has the lowest average values across all parameters with TOC and HI results under 1.6 wt.% and 110 mg HC/g TOC respectively. OI results also show that the organic material within the Ford Formation is terrestrial in origin and had undergone weathering during burial. This information, combined with high Tmax temperatures, shows that the Ford is low in organic material, the quality of the organic matter is of poor quality and it is post mature.

The Waiomo Formation has higher averages than the Ford Formation with a TOC value of 2.38 wt.% and a HI value of 226 mg HC/g TOC. Tmax temperatures indicate the Formation has just reached late maturity. The Waiomo also shows a broader range of values, particularly HI, which could indicate the presence of several difference source materials.

The one notable result (sample 656_461.9) from the Waiomo Formation had a high TOC of 4.54 wt.% and a HI value of 552 mg HC/g TOC. This sample compares favourably to other known lacustrine source rocks around the world. The presence of well-preserved organic material which is derived from alginite also indicates an anoxic lake environment which is commonly thought of as the ideal preservation environment during lacustrine source rock formation.

The Goldlight Formation results are to the Waiomo Formation except there is no high outlier. TOC average for the Goldlight was 2.39 wt.% with an average HI of 200 mg HC/g TOC however some HI results were in the low 300's and could potentially indicate oil prone source rocks. Tmax results show that the Goldlight Formation has just reached early maturity and it may be considered as a potential shale gas resource.

Preliminary results show that the conditions for the formation and preservation of high quality lacustrine source rocks existed during the deposition of the Paparoa Coal Measures and are likely to exist within other Late Cretaceous syn-rift sequences in other New Zealand Basins. In addition, the kerogen quality, range of maturities and accessibility of the Paparoa lacustrine units make them a potential unconventional shale gas and oil resource in their own right.

Chapter 4 Tectonic setting and petroleum potential

4.1 Summary of results

4.1.1 Sedimentology

Sedimentology of the Paparoa Group lacustrine mudstones has shown variations in facies associations across the basin, with further implications for basin formation and depositional environment. The lacustrine deposits on the western side of the coalfield are characterised by coarse yellow sandstone, laminated proximal turbidites and conglomeratic debris flows. The fluvial facies in this location are high energy alluvial fans with thick clast supported boulder to cobble conglomerate. These facies are characteristic of a high energy shoreline fan delta environment, with abundant sediment supply fed by uplifted highlands to the WNW. In the central and eastern sections of the basin, massive mudstone facies are prevalent along with thin distal turbidites, carbonaceous mudstone and thin, split coal seams. These deposits indicate a low energy, deep water lacustrine environment. During the maximum flooding time for the lake, the central and eastern sections would have contained deep lakes, abundant distal turbidites and sediment was supplied through meandering river deltas. During the other phases of lake development, migrating river deltas were evident as were isolated peat bogs. In the south, massive mudstone was more prevalent as was abundant organics supplied from a basin high in the southwest.

Distribution of lithofacies provides valuable information on tectonic controls during basin development. From this, the dominant fault controlling basin formation is interpreted as being located to the northwest. Due to the cross-cutting of the Roa – Mt Buckley fault zone it is hard to say whether an alternative fault system was present to the east. If it did exist, it would have been further east than the current basin boundary.

Analysis of the sedimentology of the individual mudstone formations was controlled by outcrop availability and drill core availability. The Ford Formation is thinner than originally thought (<50 m) and contains abundant organic fragments, siltstone laminations and massive mudstone and is interpreted to have formed in a shallow, low energy lacustrine environment. The abundant leaf fossils within the core indicate a steady influx of organic matter into the lake. Due to lack of outcrop and the depth of the Ford Formation, it was only described in one poor quality drill hole. Other drill core was available but of insufficient quality.

Stratigraphic columns for the Waiomo Formation cover most areas of the coalfield and show massive mudstone and faintly bedded siltstone facies in the south and east which grade to marshy, organic siltstone at the underlying and overlying contacts. Towards the north-west, the Waiomo Formation lacks massive mudstone and instead is characterised by numerous thinly bedded turbidite deposits with gradational contacts between the under and overlying formations marked by the inclusion of fluvial delta front conglomerates, rip-up clasts and debris flows. This northwest corner also contains the thickest Waiomo sediment at ~60m. The central and eastern sections of the lake formed in an environment with meandering rivers feeding organic rich sediment into the lake and shallow slopes allowing for the formation of thin, distal turbidites. The southern extent of the lack is limited to around Spring Creek Mine where it is commonly laminated and shows soft sediment deformation. The area to the west appears to indicate a period of active uplift forming steep slopes seen through the higher energy debris flows, proximal turbidites, boulder conglomerate fan deltas and large rip up clasts. Relief in this area would have been higher leading to alluvial fan formation and steep underwater slopes. Imbrication and pinching out of sandstone beds indicate flow direction from the NNW and give an approximate location for the basin bounding fault system.

Outcrop and drill hole data is abundant for the Goldlight Formation in comparison to the older lacustrine formations. The Goldlight Formation in almost all areas is identified as a massive dark grey mudstone up to 180m thick. The reclassified transitional facies which are now included in the Goldlight Formation include distal turbidites, meandering river deltas and organic rich siltstones. In the north-west section of the coalfield, the Goldlight Formation has previously been mislabelled due to the absence of massive mudstone facies. Instead the Goldlight Formation in the northwest is characterised by brown, very fine to medium laminated sandstone with thick proximal turbidites and debris flows. This area is assigned as the north-western edge of the Goldlight Lake.

The very thick, massive mudstone indicates that the Goldlight Formation was the most extensive lake within the Paparoa Group and covered the entirety of the outcropping coalfield. Hemipelagic sedimentation was the primary form of deposition for the massive mudstone facies while the thin laminations and organic rich siltstone formed from turbidity currents and fluvial discharge. In the north-west, the coarser grained sedimentary rocks indicate a higher energy shoreline fan delta environment. The thick proximal turbidites indicate a high angle slope in this area which allowed for the transport of large quantities of unstable sediment. Similarly the large, angular debris flow conglomerates are an indication of

sub-aerial slope failure, with the conglomerates transported into the lake along steep alluvial fans. In the eastern and southern margins, the lake appears to extend outside the coalfield given the thick Goldlight Formation sediments which are truncated by the Roa – Mt Buckley Fault Zone.

In addition to these results, allocation of the 12 Mile Beach mudstone was also made. Due to the lack of drill hole data in this area it has been difficult to stratigraphically correlate the 12 Mile Beach mudstone with either the Ford or Waiomo Formations. Based on the pinching out of the Ford Formation at Strongman Mine, the lack of Ford Formation in DH 621 at 10 Mile Creek and the conformity of the conglomerates at the beach with the mudstone, the 12 Mile Beach mudstone is assigned to the Waiomo Formation. Although this aligns with current mapping convention (Nathan 1978; Nathan et al. 2002), recognising the lack of Ford Formation past Strongman Mine has not been officially done before.

4.1.2 Isopach maps

New sediment thickness isopachs were created from updated drill hole data to represent the current thickness of the three lacustrine mudstone formations. As well as accounting for new drill hole information, revisions to sedimentology were also taken into consideration with the Waiomo Formation at 12 Mile Beach and the greater Goldlight Formation facies being included.

The Ford Formation isopach (Figure 2.34)), originally thought to have formed in a NW – SE oriented basin (Ward 1997; Newman 1985; Gage 1952), now looks to have formed in a NNE – SSW oriented basin, the same orientation as the other lacustrine mudstones. The thickness of the Ford Formation is also very different to the Ford mudstone in older isopachs which showed thickness extents of up to 180m (Ward 1997). Earlier isopachs didn't account for thickening or thinning of the formations by faulting which has led to an arbitrary thickness in the majority of drill holes. By accounting for this as much as possible it appears the Ford Formation is thinner and smaller than originally thought and has no thick, massive mudstone facies. Facies distributions suggest deposition in an NNE – SSW oriented basin rather than the originally interpreted WNW - ESE oriented basin (Ward 1997). The Ford Formation also appears to be cut by the Roa – Mt Buckley Fault Zone in the east.

When constructing the Waiomo Formation isopach the 12 Mile Beach section was also included which was not previously assigned as Waiomo (Ward 1997; Newman 1985). New

drill hole data also identified the Waiomo Formation around Spring Creek Mine, allowing for the lake to encroach further westward. In the east, the Waiomo isopach is also cut by the eastern Roa – Mt Buckley Fault Zone across the thickest, deepest water facies. The overall size and thickness of the Waiomo Formation around Spring Creek Mine is around 40m; the thickest section outside of the northwest corner (60m). A minor increase in lake size as compared to the Ford Lake can be seen towards the south near the Grey River. The major difference between the Waiomo and Ford Formation isopachs is towards the west where the Waiomo Formation is thicker and extends past Strongman Mine. This westward extension may mark a time of basin growth as the lake increased in size.

In contrast to the Ford and Waiomo Formation isopachs, the Goldlight Formation is much thicker and more extensive, covering the entirety of the coalfield. In the east, the Goldlight isopach shows mudstones over 160m thick sitting sharply against the eastern fault zone. Sediment thickness gradually decreases towards the west indicating that the current eastern boundary of the coalfield may have been the centre of the Goldlight Lake. Younger tectonic uplift along the eastern margin of the coalfield has eroded a significant portion of the Goldlight Formation however it may be found further south under younger sediment.

There are two major interpretations taken from the construction of new isopach maps. The first is the orientation of the Ford Formation which aligns with the orientation of the other mudstones. From this it appears there was no change in basin orientation during the formation of the Paparoa Group. The other major interpretation surrounds the eastern fault zone which cross-cuts all three mudstones. With deep lake mudstones sitting against the fault zone, it indicates that not only was lake extent greater than previously thought but the basin bounding fault to the east may not have existed. The extent of the Paparoa Coal Measures to the east of the Roa – Mt Buckley Fault Zone is unknown as is the possibility for an eastern fault zone. When combining this information with the sedimentology data, it appears dominant fault control for the formation of the Paparoa Group was to the northwest.

4.1.3 Geochemistry

Source rock analysis was undertaken on 40 samples obtained from the Paparoa Coal Measure lacustrine mudstones which showed a variety of results with varying implications for future work.

The Ford Formation results showed generally low TOC and HI values. High OI values were interpreted as samples that had undergone alteration before burial which also decreases the quality and amount of hydrocarbons within the Ford Formation. The samples were post mature, indicating that any hydrocarbons that would have been generated have been released. The overall potential for the Ford Formation based on geochemistry was poor.

The results for the Waiomo Formation were considered to be better on average with one excellent result in sample 656_461.8 at Strongman Mine. This sample had high TOC (>4 wt.%) and was made mostly from alginate – a Type I, oil-prone kerogen. The other Waiomo Formation samples showed average TOC of 2.38 wt.% and mid range HI values, indicating a possible gas-prone source rock. The main conclusion drawn from the Waiomo Formation results is that sample 656_461.8 indicates that the necessary conditions for deposition and preservation of organic-rich, oil prone material was occurring within the lakes at some stage. This information can be applied to lacustrine mudstones in other New Zealand petroleum basins which may also contain organic-rich source rocks.

The Goldlight Formation had very similar results to the Waiomo Formation with the exception of sample 656_461.8. Average TOC was 2.39 wt.% while HI results showed gas prone Type II / III kerogens. Although these values are not as high as other currently producing lacustrine source rocks, the Goldlight Formation may be considered as a possible shale gas target based on its geochemical results and Tmax values.

4.2 Basin tectonic setting

Previous studies on the area around the Paparoa Coal Measures have highlighted two quite distinct orientations for basin bounding faults based on isopach maps of the coal-bearing units (Ward 1997; Newman 1985; Gage 1952). Faults oriented in a WNW – ESE direction are commonly associated with the Paparoa Metamorphic Core Complex (Herd 2007; Sagar & Palin 2011; Schulte et al. 2014) and the Tutaki half graben which lies directly west of the Paparoa Coal Measures offshore (Bishop 2010). Onshore and in relation to the Paparoa Coal Measures, these structures show a similar trend to the Jay and Ford Formation isopach maps of Gage (1952) Newman (1985) and Ward (1997) and the underlying Hawkes Crag Breccia of the Pororari Group (Bishop 2010). The second primary fault orientation is NNE-SSW, in line with the younger Paparoa Coal Measure Formations, the revised Ford Formation

orientation and the basin bounding transfer faults for the Tutaki Basin (Bishop 2010; Ward 1997).

There are several theories for the change in orientation between the older Paparoa Core Complex and Tutaki Basin faults and the younger Paparoa Coal Measures faults. The first involves a dramatic 90º change to the primary extension direction from N - S to E – W during deposition of the Paparoa Coal Measures (Bishop 2010). Alternatively, a large change in orientation may not have been necessary, with a small change in extension direction being accommodated as oblique movement on the NNE – SSW previously transform faults (Bishop 2010, Laird 1994). This idea also highlights the presence of possible transtensional faults in the northern Taranaki Basin. The revised orientation of the Ford Formation suggests that there was no dramatic change in basin orientation and that the Paparoa Coal Measures were deposited in a single structural basin type its life span.

Reconstructions of New Zealand relating to Tasman Sea spreading (Figure 4.1) show a narrow corridor along the west coast of New Zealand that aligns parallel with the primary extension direction during this time (Laird 1994; Bishop 2010). Although these paleo-reconstructions indicate the possibility for the formation of a transtensional basin, the Paparoa Coal Measures has always been thought of as having formed in a pure rift basin setting (Ward 1997; Newman 1985; Gage 1952). To gain a better understanding of basin formation, traits specific to each basin model need to be identified within the Paparoa Coal Measures. Many characteristics for rift and transtensional basins are interchangeable making it difficult to provide evidence for either basin type. Key features to be discussed include facies distributions across the basin, intra-basin faulting, adjacent depocentres and sedimentary cycles controlled by subsidence.

4.2.1 Rift Basins

Rift or extensional basins are more common in the literature than transtensional basins with many well-known modern and ancient examples in the sedimentary record. Surficial rift basins and flank uplifts result from stretching of the underlying lithosphere (Leeder 1995) and are ideal depositional sinks for sediment. Lithospheric stretching is the result of either passive rifting, where localised stresses arise along plate edge forces, or active rifting which involves upwelling of mantle melt and eruptive volcanics (Leeder 1995). Although intrusives and volcaniclastics have been found within the Paparoa Coal Measures, these are rare and it

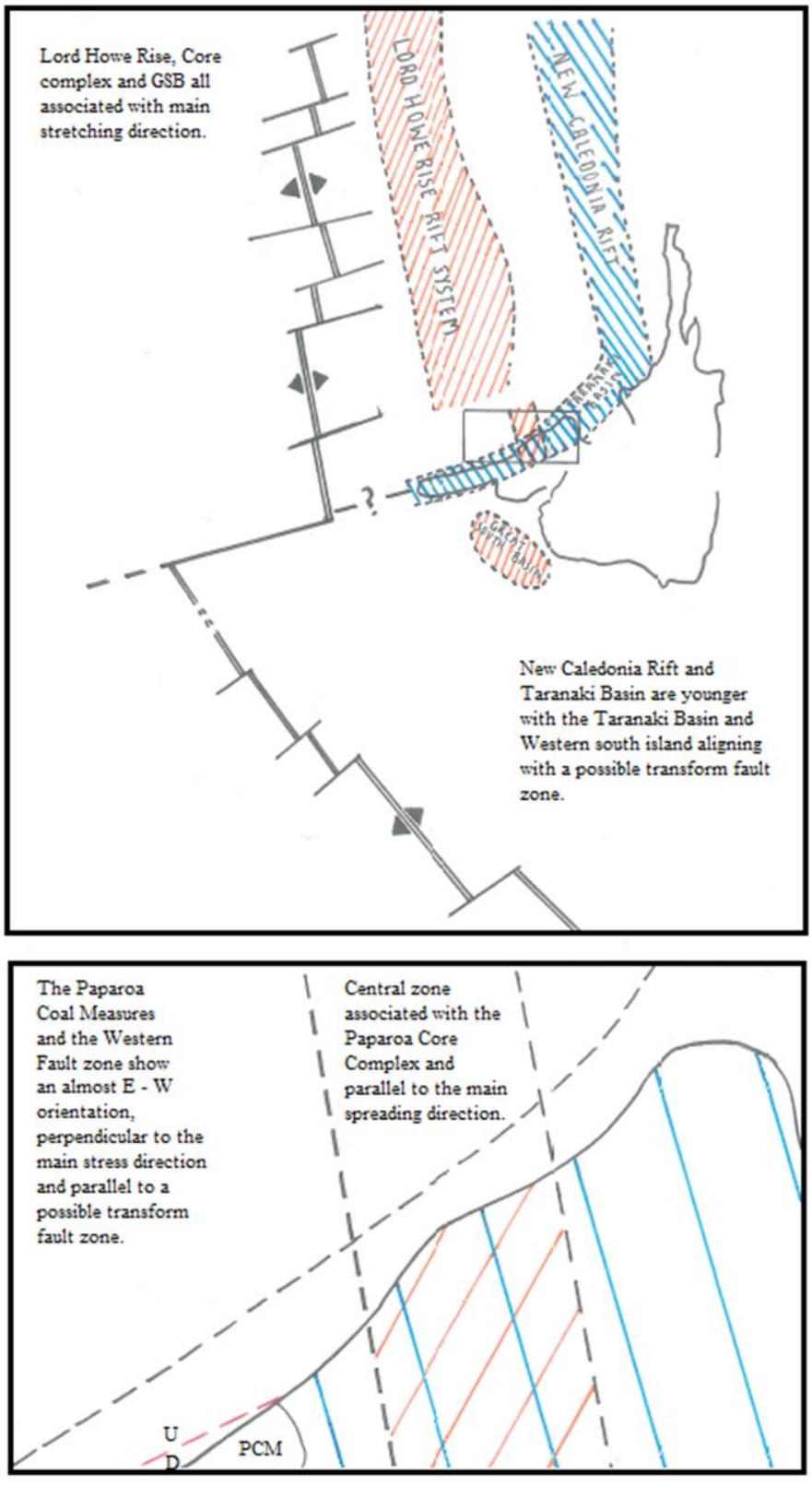

Figure 4.1 Reconstruction of the Tasman Sea spreading centre highlighting the late-Cretaceous sediments (blue) which overlie the older mid-Cretaceous extensional features (orange), adapted from Laird (1994). The northern rift system is opening faster than the southern rift.

is determined the Paparoa sequence was formed in relation to passive rifting associated with Tasman Sea spreading (Bradshaw & Laird 2004). The evolution of rift basins follows an idealised sequence of events from initiation as a continental rift basin to a later stage oceanic spreading centre. Initial crustal stretching and thinning of the lithosphere without extensional faulting is known as a sag basin or immature continental basin (Allen & Allen 1990). These sag basins can then develop into fault controlled rifts then passive margins and oceanic spreading centres. The latter stage passive margins form as oceanic lithosphere upwells into the rift axis which begins the final transition to an oceanic spreading centre.

Continental thinning and stretching which accompanies the formation of rifts results in the formation of grabens and half grabens (Frisch et al. 2011). Grabens and half grabens are depressions, bounded by fault controlled slopes (Figure 4.2) on one or both sides of the basin. The initiation phase of fault growth within the basin is characterised by small-displacement, isolated normal faults which form low angle surface topography. The next stage of development involves the initiation of fault growth and eventual linkage of these structures (Gawthorpe & Leeder 2000). Displacement is eventually localised to the largest fault zones. In the final stage of fault development, faults along the basin margin are continuous and through-going, with major displacement accommodated along the basin margins. Minor faults within the basin become inactive. This stage of fault development leads to major graben and half graben depocentres which become the predominant catchment zones for sediment.

The nature of rift basins allows for the formation of multiple fault zones within the basin, with crustal blocks in between. These blocks undergo rigid deformation and tilting, allowing for the formation of isolated depocentres within the greater basin area (Leeder 1995). As extension continues, stress is commonly transferred onto the inner hanging-wall faults (Figure 4.2), resulting in the “death” of the foot-wall fault. With limited growth on the foot-wall, erosion and incision forms lower relief (Gawthorpe & Leeder 2000).

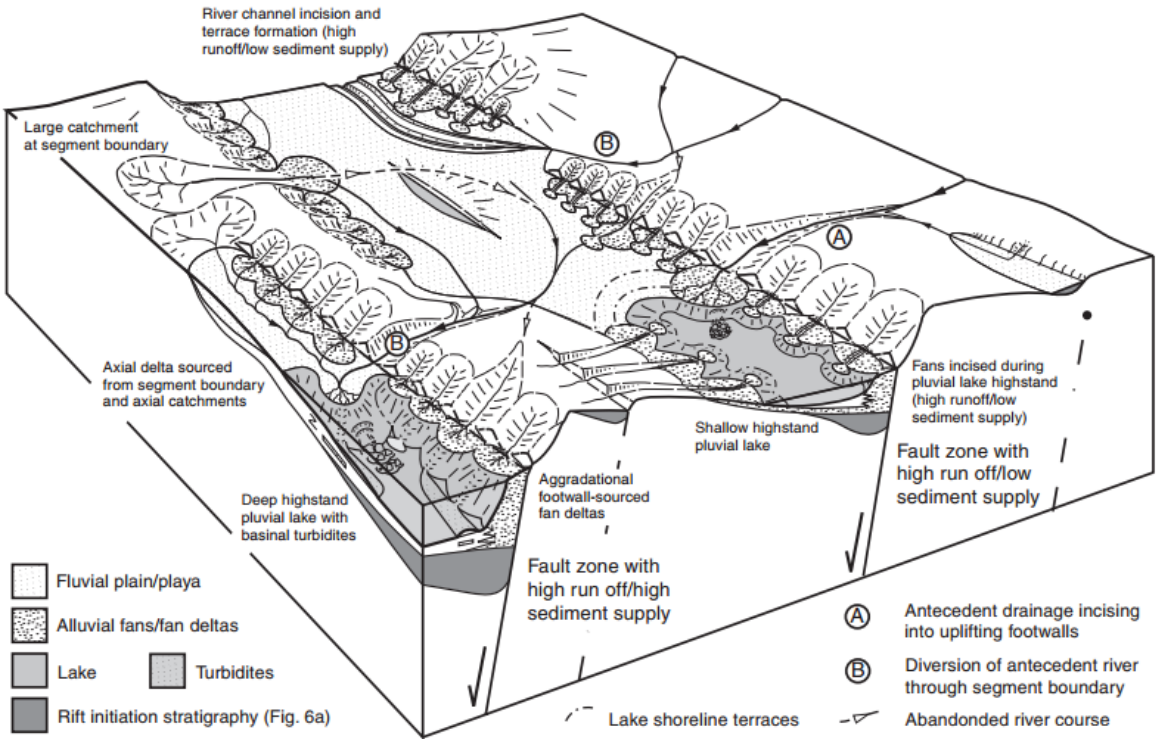

Figure 4.2. Tectono-sedimentary evolution of a through-going continental rift basin (Gawthorpe & Leeder 2000). Interaction of faults leads to enlargement of basin and subsequent depositional settings including lakes. High energy sediments are source from the footwall (A and B) while the low angle hanging wall sources finer, low energy sediments.

The formation of a half graben commonly results in an asymmetrical basin where the faulted foot-wall margin is steeper and produces higher energy sediments than the un-faulted hanging-wall hinge side (Figure 4.3).This has a major impact on deposition and facies distribution across the basin (Gawthorpe & Leeder 2000). Other factors which control deposition include climate, subsidence rates, rock type, catchment morphology and basin geometry (Gawthorpe & Leeder 2000; Connell, 2010).

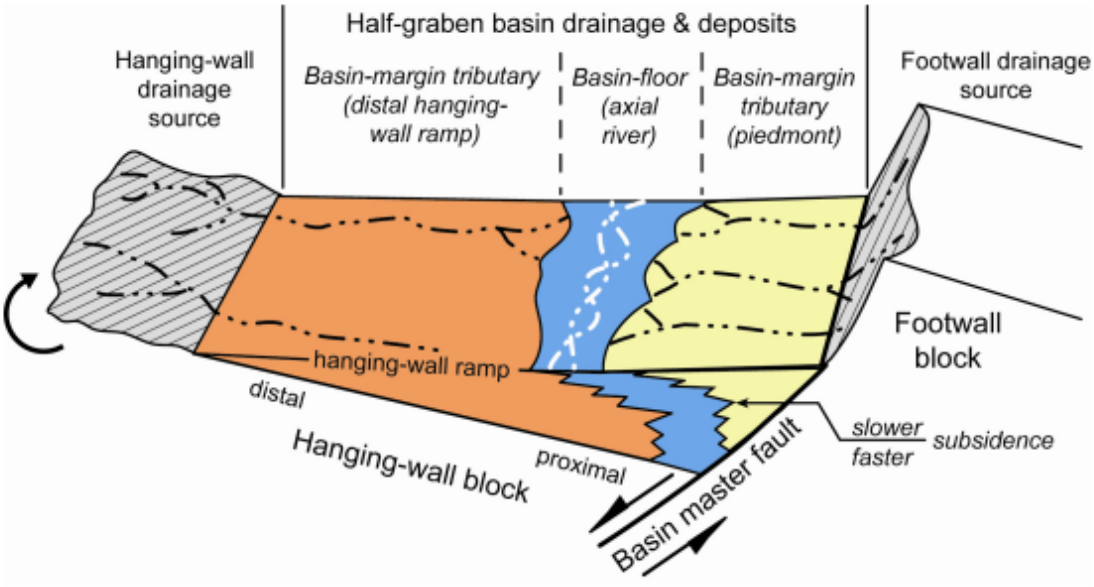

Figure 4.3. Common deposition of fluvial systems in a half graben basin (Connell 2010).

Within the basin, the type of drainage system plays a crucial role in the formation of a lacustrine and fluvial environment. Drainage systems which terminate within the basin result in the formation of lakes and are known as interior drainage systems. Conversely, if the basin is open and drainage systems (rivers) form it is known as axial through drainage (Leeder 1995). These depositional environments create very different lithofacies. Fluctuations between open and closed drainage systems occur primarily due to subsidence rates and tilting of fault blocks and result in alternating fluvial and lacustrine sequences (Leeder 1995).

Sediment transported from the steeply dipping foot-wall drainage area forms coarse grained alluvial fan deposits along the active source area. Due to the change in slope angle, rapid deposition occurs at the base of the footwall. In times when transverse or parallel drainage occurs through the basin centre, sediment is then transferred onto the basin floor) through rivers (Figure 4.3. In comparison, a closed system with a central lacustrine environment allows for the formation of delta fans and sediment is transported down slope through turbidites, debris flows and hemipelagic sedimentation (Leeder 1999).

Sediment supplied from the shallow dipping hanging wall is finer grained due to the lower energy environment (Einsele 1992) although the source land is much larger (Leeder 1995). Alluvial fans are low angle and broad, as are fan deltas. Slight incision and channelization may occur due to fault block tilting (Gawthorpe & Leeder 2000).

4.2.2 Transtensional basins

Transtensional basins are not as widely described as rift basins. Due to the nature of plate motions and stress directions, strike slip faults commonly have a transpressional (convergent) or transtensional (divergent) component (Allen & Allen 1990). Complicated fault relationships including basin step overs and fault bending lead to the formation of localised sedimentary basins (Leeder 1999). Subsidence within these basins is rapid, particularly closest to the main strike slip fault fragment. Offset of the main basin bounding faults also results in changes to source area (Leeder 1999).

Although strike slip faults may be laterally extensive, strike slip basins are localised and small. For transtensional basins which involve extension, a common mode of formation is within releasing bends (Figure 4.4). As fault blocks move past each other, extension occurs (Nilsen & Sylvester 1995; Allen & Allen 1990). This is emphasised if an extensional component is involved as seen in Figure 4.4 and often results in multiple depocentres and basin asymmetry (Wu et al. 2008). Basin asymmetry within transtensional basins occurs in the same manner as that within rift basins. Faulting is dominant on one side of the basin resulting in a high angle footwall and a low angle hanging wall. Intrabasin tectonics are more complex and will have a greater impact within transtensional basins as they remain active through the evolution of the basin (Wu et al. 2008).

Initiation of a transtensional basin begins with minor shearing in the area between the dominant strike slip faults (Wu et al. 2008). These shears eventually join and create the main faults which flank the primary depression. Continued shearing allows for subsidence along the now established basin bounding faults. These eventually undergo oblique extension and segmented sidewall faulting begins. The final stage of transtensional basin initiation involves the initiation of the cross basin fault system and formation of opposing depocentres (Wu et al. 2008). As with rift basins, if extension continues and the basin widens, spreading ridges comparable to oceanic spreading centres may form (Einsele 1992).

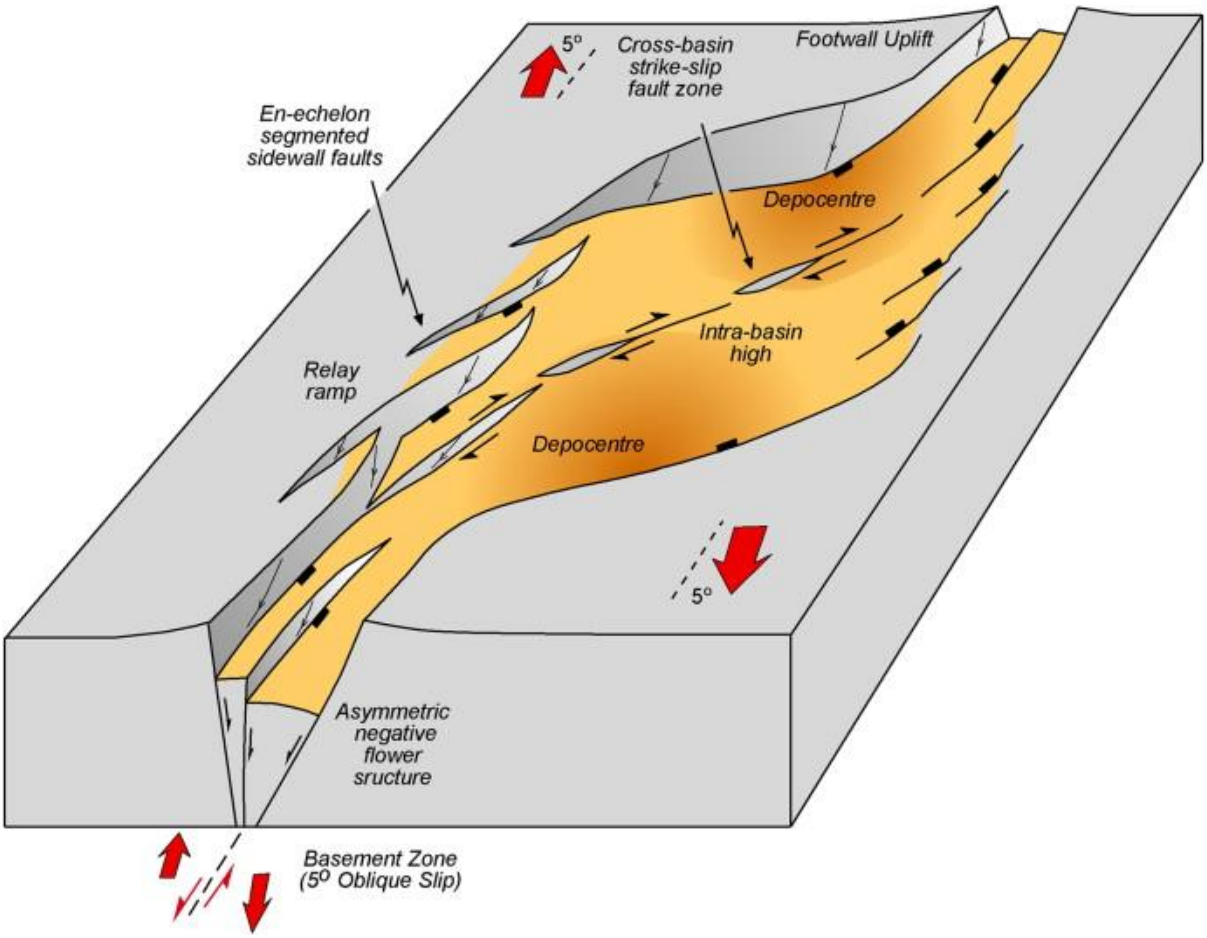

Figure 4.4. Releasing bend, transtensional basin showing complicated fault relationships due to lateral shearing and rotation (Wu et al. 2008).

The nature of shearing to form transtensional basins often results in the formation of asymmetrical basins with multiple depocentres and intra-basin highs (Wu et al. 2008). These features all have an impact on depositional systems within the basin.

Transpressional basins are often narrow and deep however conglomerates and breccias are often located near active fault zones highlighting asymmetry within the basin (Figure 4.5). Other common sedimentological features seen with strike slip or transtensional basins are rapid subsidence, stratigraphic mismatch, lateral facies changes and variations in stratigraphic thickness (Bridges & Castle 2003).

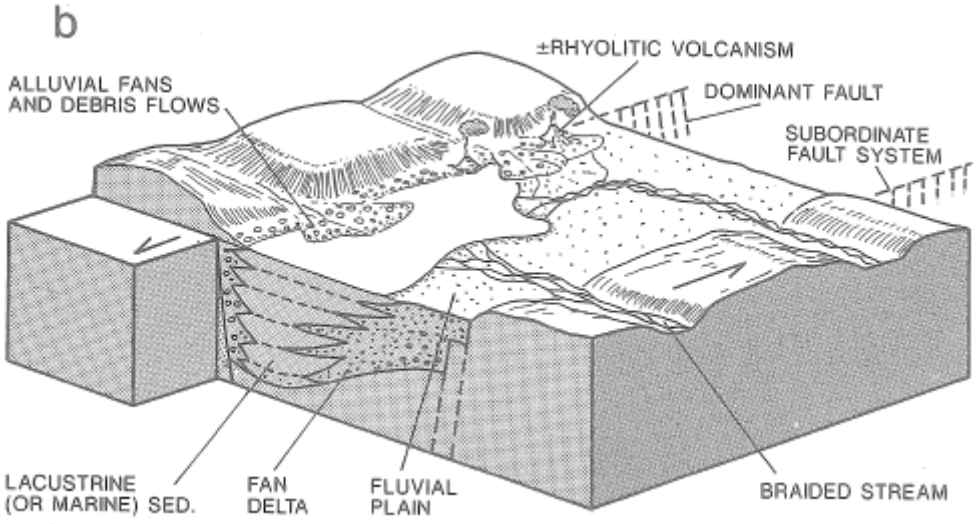

Figure 4.5. Deposition within a strike slip basin with minor extension (Einsele 1992).

As with rift basins, asymmetry plays one of the greatest roles in deposition. Coarse grained alluvial fans and debris flows are often located along fault controlled margins while low angle deltas and fluvial facies are found on the opposite hanging wall (Einsele 1992). As seen in Figure 4.5, facies distributions within are transtensional basins are very similar to those seen in rift basins due to the asymmetrical nature of the basin (Allen & Allen 1990; Bridges & Castle 2003). This leads to steep, coarse grained conglomeratic alluvial fans on the foot-wall side and shall delta fans on the hanging-wall side. Lake location is also focused against the foot-wall basin margin (Einsele 1992).

4.2.3 Paparoa Basin tectonic setting

Although plate reconstructions indicate the potential for a transtensional basin setting, comparisons between sedimentology and corresponding depositional environments should be made to indicate direct evidence for either basin type.

Primary evidence that the Paparoa Coal Measures were deposited in an extensional basin is the distribution of facies across the basin (Gage 1952; Ward 1997; Newman 1985; Suggate 2014). The conglomerates and other coarse grained sediments to the northwest and massive mudstone and coal in the east indicate a half graben or asymmetrical basin where faulting is controlled by one side only (Leeder 1999; Leeder 1995; Gawthorpe & Leeder 2000). These

half grabens are most commonly associated with rifting but have also been identified in strike slip basins (Nilsen & Sylvester 1995) although asymmetry within strike slip basins is more complicated. Given the Roa-Mt Buckley Fault Zone has truncated the eastern side of the basin, it is impossible to determine whether the Paparoa Coal Measures were deposited in a graben or half graben setting. Either scenario conforms with both basin models.

Other evidence for a rift basin setting is the relationship between fluvial and lacustrine sedimentary cycles. Due to subsidence rates which increase and decrease in accordance with the life of the rift basin, a common sedimentary sequence seen within rifts is a fluvial > lacustrine > fluvial pattern (Gawthorpe & Leeder 2000). This is seen and repeated several times within the Paparoa Coal Measures with the four fluvial and three lacustrine formations. As this pattern is controlled by subsidence rates vs. sediment supply and depends on activity of the basin bounding fault, it can also be found in transtensional basins (Wu et al. 2008; Leeder 1999; Gawthorpe & Leeder 2000; Nilsen & Sylvester 1995).

There are two primary forms of evidence in favour of transtensional basins, the first being intra-basin faulting and uplift (Wu et al. 2008). Previous work on the Paparoa Coal Measures has highlighted a complex basin high in the centre of the basin (Figure 4.6). Due to the complexities involved with oblique shearing, a central horst feature may form in transtensional basins due to the nature of oblique shearing (Wu et al. 2008). However, extensional basins may exhibit a similar feature through the stacking of normal tilted fault blocks within a half graben (Einsele 1992; Leeder 1995; Leeder 1999; Gawthorpe & Leeder 2000). Although this feature can be seen in extensional basins it is only in the initiation and fault linkage stage (Gawthorpe & Leeder 2000; Einsele 1992). Established rift basins lack intra-basin horst features.

Related to the formation of a central horst feature seen within transtensional basins is the formation of dual depocentres (Wu et al. 2008). Modelling of transtensional basins has shown this to be a key feature which separates it from other similar basin types (Wu et al. 2008). Dual depocentres are found in the revised Waiomo Formation isopach which shows two distinct areas of different sedimentary thickness within the lake. Dual depocentres are also proposed to explain the variations between the Eastern and Western Compositional suites of the Rewanui Formation (Ward 1997).

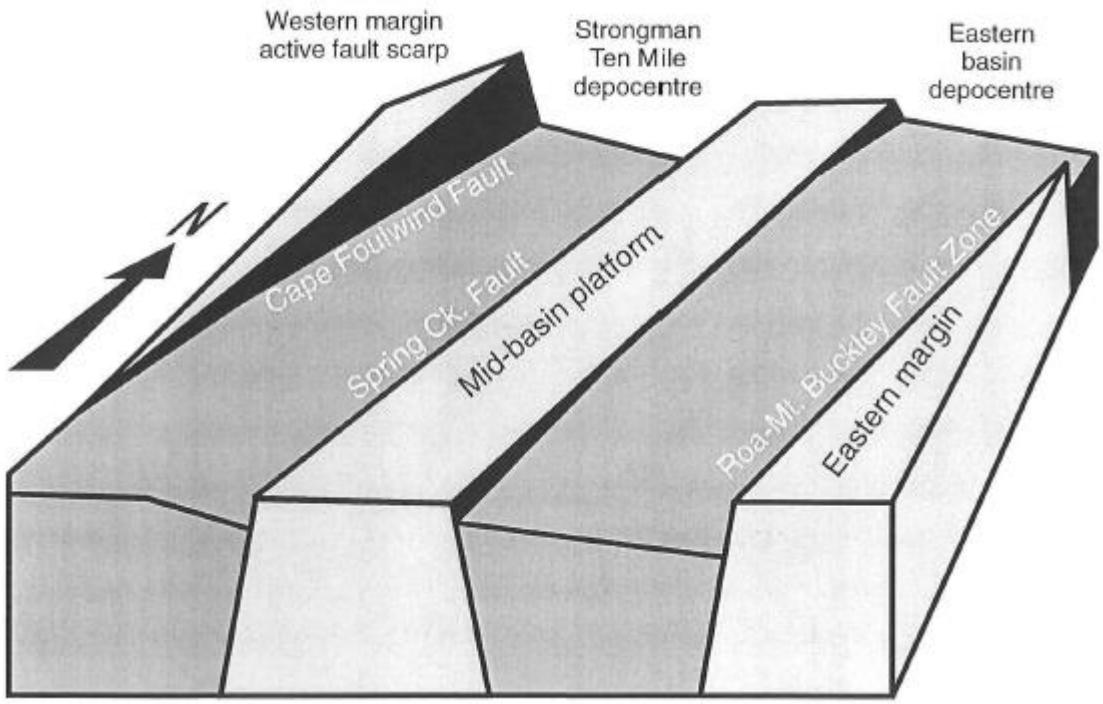

Figure 4.6. Basin model for the Paparoa Coal Measures (Ward 1997) showing a central horst feature.

Although the characteristics outlined are more common in either a pure rift or transtensional basin, all features can be explained by processes that occur in both basin types. Because of this, it is impossible to infer basin type from the sedimentary record alone within the Paparoa Coal Measures. Instead, analysis of faults and sense indicators throughout the zone in question will likely result in a greater insight into the formation of the area. Although sedimentology does not present any clear outcome, revisiting the initial plate reconstructions (Laird 1994; Bishop 2010) may lead to greater conclusions.

For the Paparoa Coal Measures to be formed in a pure rift setting, primary extension for this basin would be required to change from the N-S orientation seen during formation of the Metamorphic Core Complex to E-W for the formation of the Paparoa Coal Measures. This 90º change in orientation must have occurred before deposition of the Paparoa Coal Measures as indicated by the revised lacustrine isopachs which show all lakes to be oriented NNE-SSW. Given the ~15 Ma gap in time between deposition of the underlying Hawks Crag Breccia and the Paparoa Coal Measures (Gage 1952; Nathan 1978) a change may have occurred in this time. Although a 90º change seems improbable, there are several examples of

past and present spreading centres where this is occurring and are known as triple junctions (Wolfenden 2004; Bird 1999).

The most well-known example of a triple junction is the Afar triple junction, which currently forms the Red Sea, Gulf of Aden and the East African Rift Zone (Figure 4.7). Here the Arabian, Nubian and Somalian plates are rifting apart resulting in a complex zone with each rift at approximately 120º angles from each other (Wolfenden 2004). For the Paparoa Coal Measures to form in an extensional basin, a third rift arm would need to project from the Taranaki Basin area to form a complete triple junction (Figure 4.6).

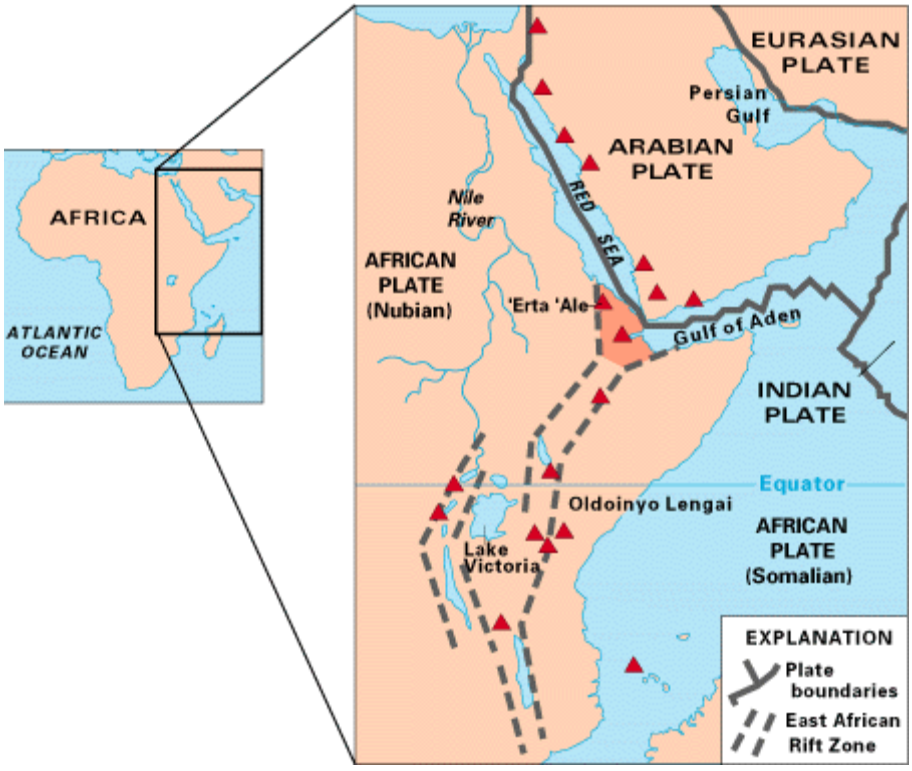

Figure 4.7 Afar Triple Junction showing three diverging plates. (USGS).

To create a transtensional basin, no great change in extension direction would need to occur. Instead primary movement would be accommodated on the transform faults formed through the initial stage of N–S extension of the Metamorphic Core Complex. Differential movement between the northward moving plates on either side of Proto–New Zealand would create strike slip movement along the fault zone resulting in a transtensional basin.

Comparisons of sedimentology within rift and transtensional basins have yielded no clear out come. No evidence for offset has been found to strongly support a transtensional regime however, the active nature of New Zealand tectonics has reactivated most faults along New Zealand's West Coast. Any strike slip motion has likely been erased by younger tectonic regimes. Instead the primary argument for transtension revolves around the plate reconstructions. Although 90º changes in extension direction can occur, in the case of the Paparoa Coal Measures, this does not make sense geologically. The proximity to a major spreading centre (Figure 4.1) and an inactive subduction zone to the east would create 6 micro-plates within close proximity to each other. There is also no direct evidence for a third, failed rift system projecting through the central north island which is needed for a triple junction model. Instead it appears a minor change in extension direction occurred and allowed for primary movement to be accommodated along transfer faults from the Metamorphic Core Complex. Given the lack of information to the east of the coalfield, it is impossible to determine the exact location of the eastern bounding fault zone which would represent the eastern limb of the transtensional fault system.

4.3 The Paparoa Coal Measures as an analogue for New Zealand Late Cretaceous rift basins.

Overall results show that the Paparoa Coal Measure mudstones could be a potential lacustrine source rock given the results found within the Waiomo and Goldlight Formations. In addition, the results obtained from 656_461.8 show that the environment necessary for the formation of high quality source rocks also occurred during deposition. As well as applying these results directly to the Paparoa Coal Measures, they can also be used to interpret and determine the source rock potential of other understudied Late Cretaceous lacustrine mudstones in offshore New Zealand basins (Figure 4.8).

Basic seismic interpretations and drilling have shown that there are several Late Cretaceous age basins around New Zealand which exhibit similar basin structures to that seen in Greymouth Coalfield. These include the Great South Basin, offshore Taranaki Basin and the lesser known Bellona and Solander Basins. Early basin fill in these basins is thought to be from fluvial and lacustrine systems with a marine influence into the Paleocene and Eocene (Uruski 2010), mirroring the sequence seen in the Greymouth Coalfield (Gage 1952; Nathan 1978).

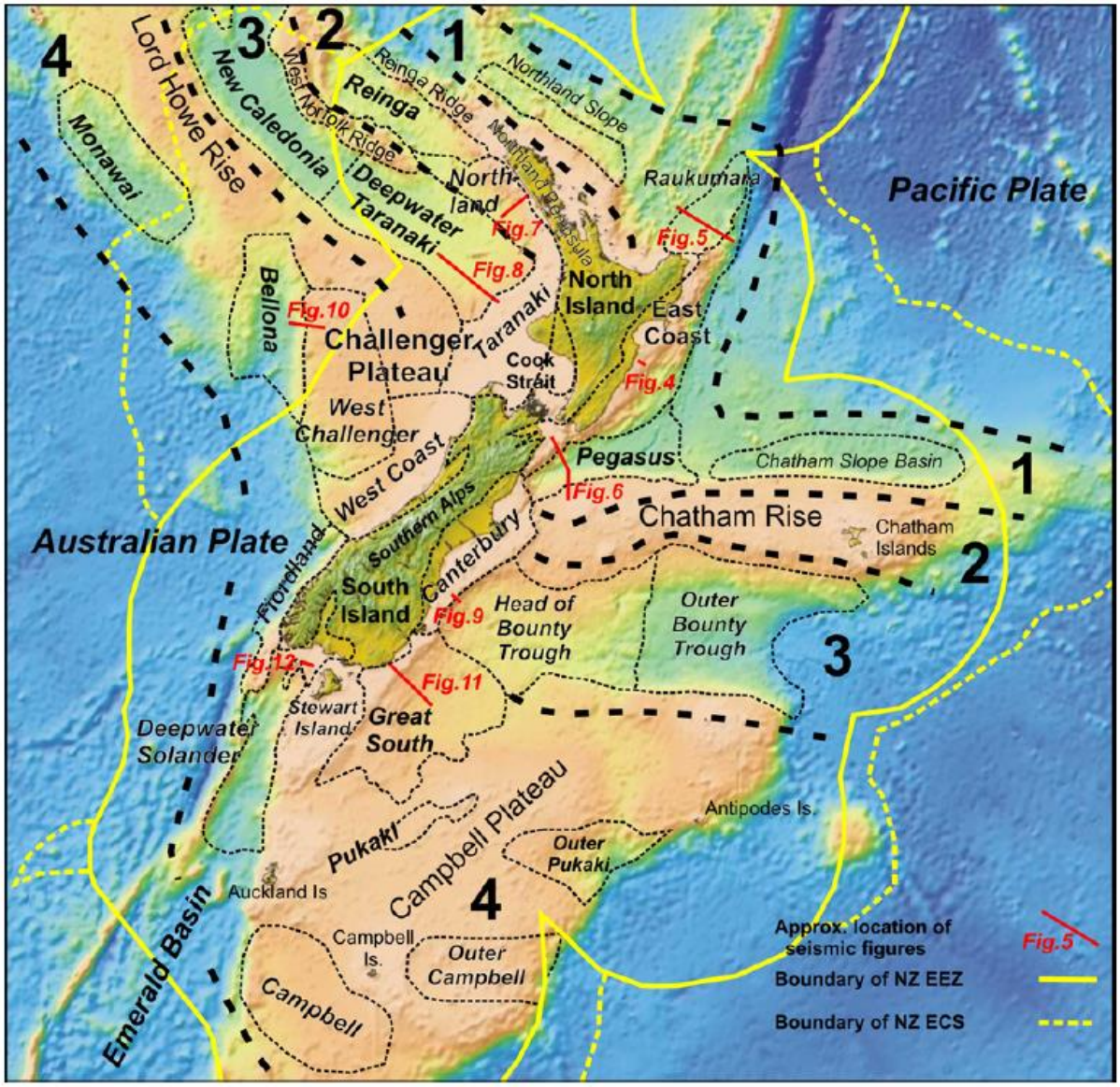

Figure 4.8. Map of New Zealand basins. Specific basins which exhibit evidence of Late Cretaceous source rocks include the Great South Basin, offshore Taranaki Basin, Bellona Basin and the Deepwater Solander Basin. (Uruski 2010).

4.3.1 Petroleum potential of rift basins

For the purposes of this section, all basins which exhibit rift basin characteristics through subsidence and/or normal faulting (rift basins, transtensional or strike slip basins, sag basins) will be classed as rift basins. Sedimentology has shown that both rifts and transtensional or

pull apart basins shown very similar characteristics and are difficult to distinguish in the sedimentary record.

Rift basins are known as sediment sinks which create profitable source rocks. The relationship between subsidence, sediment fill and accommodation space creates very thick sedimentary sequences of fluvial and lacustrine sediments which often also contain coal and coaly source rocks (Kelts 1988; Gawthorpe & Leeder 2000; Allen & Allen 1990). Late stage rift basins transitioning to passive margins undergo marine influence during deposition resulting in marine source rocks. Throughout all stages of the rift basin life cycle, reservoir rocks can also be created and are often interpreted as delta fans, fluvial sandstones and shallow marine sandstones. Reservoir rocks require high permeability and porosities so are often sandy in nature (Allen & Allen 1990; Moosavi et al. 2014). Within the Greymouth area, Oligocene limestones are also known to contain small quantities of oil, derived from the Paparoa Coals (Morgan 1911).

4.3.2 The Taranaki Basin and comparisons to the Paparoa Basin

The Taranaki Basin, as New Zealands only producing basin, has been extensively studied for several decades. Basement rocks vary greatly from east to west but include the Murihiku Terrane and plutonic rocks of the Median Tectonic Zone (Mortimer et al. 2010). The Murihiku Terrane formed in a proposed fore-arc setting and is composed of volcanic derived sandstones and siltstones. Occasional conglomerates and volcanic tuff can be found (Roser et al. 2002). The Carboniferous to Early Cretaceous Median Tectonic Zone represents a period of active rifting and mantle upwelling along the western margin of New Zealand resulting in predominantly plutonic rocks which are found extensively throughout New Zealand (Mortimer et al. 1999; Mortimer et al. 2010).

The initiation of Tasman Sea spreading allowed for the formation of localised grabens and half grabens in a similar setting to the Paparoa Coal Measures. Late Cretaceous source and reservoir rocks (Figure 4.9) were deposited in the form of coal and coaly source rocks, potential lacustrine mudstones, deltas and sandstones (PBE; Higgs et al. 2010).

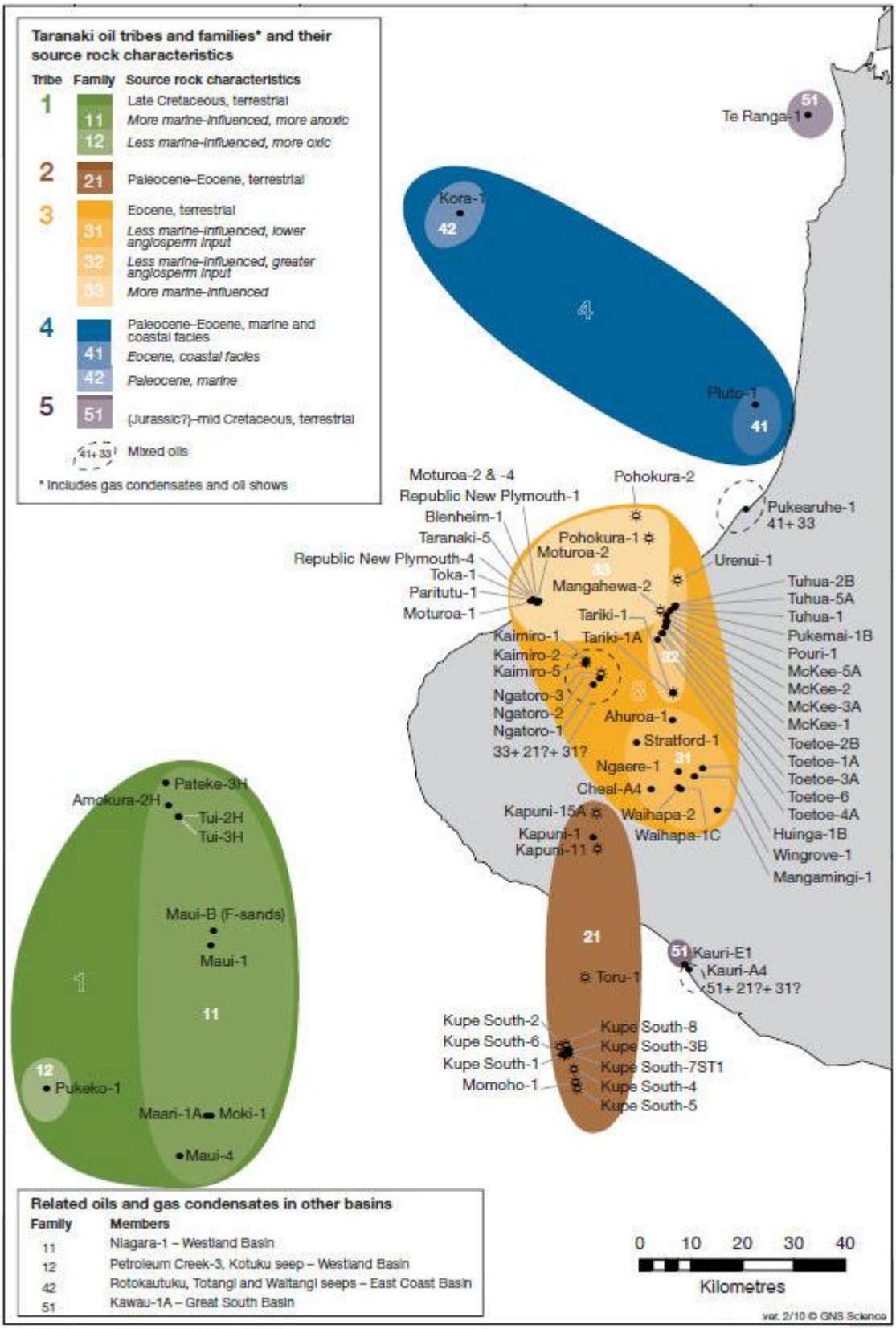

Figure 4.9. Location map for Taranaki source rocks. Late-Cretaceous terrestrial rocks located in Green.

This continued through the Paleocene into the Eocene with localised marine transgressions affecting source rock quality and geochemistry (Sykes et al. 2014). Continued subsidence allowed for the formation of thick turbidite sequences which are now common reservoir rocks as are limestones and shallow marine sandstones (PBE).

Although the primary source rocks within the Taranaki Basin are Eocene in age (PBE, Sykes et al. 2014), Late Cretaceous sediments have been recognised (Higgs et al. 2010). A lack of drill hole data that reaches depth has meant main interpretations have been made using seismic data (PBE) as well as observing limited outcrop onshore (Higgs et al. 2010). In comparison, there are over 1000 drill holes available for the Greymouth Coalfield with over 450 analysed in this study. Outcrop availability in Greymouth is also greater with easy access into many parts of the coalfield through mine roads and public walkways.

Given the similarities in basin formation and potential source rock characteristics of Taranaki and Greymouth, the Paparoa Coal Measures should be considered as another potential location for outcrop and drill hole analysis of Late Cretaceous source rocks. The information gained from the Paparoa Coal Measures can be applied to Taranaki to gain a better understanding of these sediments, given the lack of drill hole data and limited seismic data available in Taranaki. This need not be applied to only the lacustrine mudstones in the Paparoa Coal Measures but also to the coaly source rocks which are also known to produce hydrocarbons. Specifically, sedimentology has enhanced our understanding of Late Cretaceous half graben formation, as well as given an indication for potential lacustrine source rock size and distribution. Geochemical analysis has highlighted the potential for lacustrine source rocks to be found in New Zealand basins and analogous lacustrine rocks are inferred to exist in deepwater Taranaki Basin (Uruski 2010). Given the availability of data and access, the Paparoa coals and their modes for formation and burial history should also be considered as an analogue for Taranaki Basin.

4.3.3 Hydrocarbon potential for other Late Cretaceous New Zealand rift basins.

The Paparoa Coal Measure lacustrine mudstone may also be used to predict the source rock potential of minor Late Cretaceous rift basins offshore of New Zealand. Seismic data has highlighted the possibility for Late Cretaceous fluvial and lacustrine sediments to exist in three other basins; the Great South Basin of the southeast coast of the South Island, the

Bellona Basin to the west of Taranaki and Challenger Plateau and the Deepwater Solander Basin south of Fiordland (Uruski 2010; Killops et al. 1997).

The Great South Basin off the coast of the South Island has been of interest for several decades with several wells drilled and several thousand km of seismic acquired (Killops et al. 1997; Uruski 2010). This has identified a very thick sequence of terrestrial and transgressive Cretaceous syn-rift sediments which contain sandstones, mudstones and coal (Uruski 2010; PBE). There is also the possibility of thinner lacustrine sediments to have accumulated in smaller and more isolated syn-rift centres (Sahoo et al. 2014).

The Solander Basin appears to have all necessary conditions for petroleum generation and trapping with the potential source rocks coming from lacustrine, fluvial and coaly Cretaceous sediment (Uruski 2010). Evidence for organic rich lacustrine units can also be found in younger Eocene rocks which are found onshore in the northern section of the Basin with these Eocene shales being used for oil during the 1940's (Uruski 2010).

The Bellona Basin follows the same trend as the West Coast and Solander Basins but there is very little additional information available. Plate reconstructions have shown that the Bellona Basin may have formed adjacent to the Gippsland Basin in Australia (Uruski 2010). Using current knowledge on the Gippsland Basin, it is likely that the Bellona Basin contains a similar sequence of Cretaceous to Late Cretaceous coals, lacustrine shales and marginal marine shales (Bhattacharjee 2005). Further investigation into the Solander and Bellona basins should be considered given these preliminary results.

Although little information is available regarding other Late Cretaceous lacustrine mudstones in New Zealand, preliminary analysis indicates these basins may contain the terrestrial rift sediments. If lacustrine mudstones were found in the Great South, Bellona and Deepwater Solander Basins, geochemical analysis of the equivalent Paparoa mudstones indicate they could be productive with moderate to high TOC values and a range of HI and Tmax values.

4.4 Conclusions

Sedimentology of the Paparoa Coal Measures lacustrine mudstones has shown variations in facies distribution across the Greymouth Coalfield and has greater implications for basin formation and regional tectonics. The north-western corner of the Greymouth Coalfield shows predominantly coarse grained alluvial fan conglomerates, debrites with meter wide rip

up clasts, channelised quartzose sandstone and thick proximal turbidites. In comparison, the central, eastern and southern sections display massive mudstone that can be up to 180m thick with coal, carbonaceous mudstone and fluvial medium sandstones within the under and overlying coal bearing formations.

Revised isopachs maps show that any change in basin orientation had to occur prior to the deposition of the Paparoa Coal Measures as the Ford Formation now suggests a basin oriented in a NNE – SSW direction. This conforms with the other lacustrine formation isopach maps indicating that the basin didn't change orientation during its lifespan. Isopach maps also highlight the abrupt end of the Paparoa Coal Measure mudstone along the eastern basin boundary as they are truncated by the Roa – Mt Buckley Fault Zone while still thick and fine grained.

Sedimentology and isopach mapping has indicated that primary fault control during formation of the Paparoa Coal Measures was to the northwest. The Roa –Mt Buckley Fault Zone was concluded to be a younger feature that has offset the Paparoa Coal Measures post-deposition.

I interpret a transtensional tectonic regime, instead of a pure rift regime, for the Paparoa Coal Measures based on plate reconstructions and the lack of a change in basin orientation during its formation. This indicates that any change would have needed to be post Metamorphic Core Complex but prior to Paparoa Coal Measures deposition. Analysis of the sedimentology with comparisons to both rift and transtensional basin deposits has shown no conclusive interpretation can be drawn from sedimentology alone. Re-examination of the plate reconstructions showed a rift basin setting was possible but required a triple junction plate boundary to the north of Taranaki Basin. In comparison, a transtensional basin setting would require only a small change in extension direction and movement would be accommodated by transform faults which formed in conjunction with earlier rifting along the West Coast. Based on this evidence and the unlikelihood of a triple junction to the north of Taranaki Basin, a transtensional tectonic setting is preferred for the formation of the Paparoa depositional basin.

Analysis also has been undertaken on the Paparoa Coal Measure mudstones to determine their suitability as a lacustrine source rock. Results are varied across the lacustrine formations although the Waiomo Formation contains one excellent sample that is comparable to other world-renowned lacustrine source rocks. The Ford Formation overall is considered to be a

poor source rock due to its low TOC values, low HI values and over-maturity. The Waiomo Formation contains favourable TOC and HI results but is too mature and expulsion of hydrocarbons has likely occurred. The Goldlight Formation shows favourable TOC and HI results and due to its low maturity could be considered as a potential shale gas resource especially given its nature as a massive mudstone and its thickness of up to 180m.

Sedimentology and source rock analysis has highlighted important results relevant to not only the Paparoa Coal Measures but to wider New Zealand Late Cretaceous sedimentary basins. Source rock analysis has shown that Late Cretaceous lacustrine rocks do exist in New Zealand and may be found in other basins which show signs of containing similar sedimentary rocks. Greater implications regarding sedimentology and basin formation can also be applied to the Taranaki Basin. Although Taranaki Basin contains New Zealands only producing petroleum system, lack of outcrop and water depths mean many areas of the basin are understudied, particularly those which contain Late Cretaceous sediments. Given the similarities between the Greymouth Coalfield sedimentary sequence and those in Taranaki Basin, the Paparoa Coal Measures should be considered as a new analogue for Late Cretaceous rift or transtensional basins in New Zealand.

Acknowledgments

First and foremost I would like to thank GNS for the funding of my thesis and Solid Energy for allowing me use of all of their drill hole data. Specifically I would like to thank Richard Sykes for giving his time and resources to this project. Without his support the source rock analysis wouldn't have been possible.

Thanks to my supervisors Dr Kari Bassett and Dr Tim Moore for lending their technical knowledge and expertise to this project and especially to Kari who always looked happy even after my 5th surprise visit for the day. Thanks for also giving me a kick in the pants when I spent so long deciding what to focus on.

Other staff members who offered their support include Rob Spiers for his timely creation of thin sections, Dr Anekant Wandres for obtaining the Holy Bible that is Gage 1952 and Cathy and Sasha for gear assistance. For advice I want to thank Jarg, Andy Nicol and John Bradshaw.

Outside of University I would like to thank the geo's at Spring Creek Mine, especially Jolene and Rick for escorting us up and down the mine sites when they already have a full plate. Thanks to Johnny McNee for your advice and the old Gage maps. Also thanks to Jane Newman for everything you know about Greymouth.

Thanks to Dan Willmott and Vincent at the NZP&M core store in Featherston. You guys were super busy but always made sure there was core waiting for me to log. Thanks as well for the rides over the hill all the way back to Wellington!

Finally, I want to thank all my family for their constant encouragement and support. Specifically to Jenny, Steve and Jo (and everyone else) for editing my chapters over Christmas and New Year's, thanks to Dad for constantly reminding me I haven't actually got to Perth yet and thanks to Will for tolerating me over the last few years. Also thanks to Fraser for being a very intelligent field assistant.

References

Allen PA, Allen JR 1992. Basins due to lithospheric stretching. In: Allen PA, Allen JR 1992. Basin Analysis: Principles & Applications. Blackwell Scientific Publications. 43 – 92.

Arnott RW 2010. Deep marine sediments and sedimentary systems In: James NP, Dalrymple RW Facies Models 4. Geological Association of Canada 295 – 322.

Beglinger SE, van Wees JD, Cloetingh S, Doust H 2012. Tectonic subsidence history and source-rock maturation in the Campos Basin, Brazil. Petroleum Geoscience 18: 153 – 172.

Behctel A, Jia J, Strobl SAI, Sachsenhofer RF, Liu Z, Gratzer R, Puttmann W 2012. Paleoenvironmental conditions during deposition of the Upper Cretaceous oil shale sequences in the Songliao Basin (NE China): Implications from geochemical analysis. Organic Geochemistry 46: 76 – 95.

Bennett MR, Doyle P, Mather AE 1996. Dropstones: their origin and significance. Palaeogeography, Palaeoclimatology, Palaeoecology 121: 331 – 339.

Bhattacharjee SK 2005. Unlocking the Gippsland Basin. Offshore 65: 112 – 117.

Bhattacharya JP 2010. Deltas In: James NP, Dalrymple RW Facies Models 4. Geological Association of Canada 233 – 264.

Bishop DJ 2010. Extensional tectonism and magmatism during the middle Cretaceous to Paleocene, North Westland, New Zealand. New Zealand Journal of Geology and Geophysics 35: 81 – 91.

Bird RT, Tebbens SF, Kleinrock MC, Naar DF 1999. Episodic triple-junction migration by rift propagation and microplates. Geology 27: 911 – 914.

Blair TC 1999. Sedimentology of the debris-flow dominated Warm Spring Canyon alluvial fan, Death Valley, California. Sedimentology 46: 941 – 965.

Boggs S 2006.Continental (terrestrial) environments. In: Boggs S Fourth Ed Principles of Sedimentology and Stratigraphy 245 – 287.

Bridges RA, Castle JW 2003. Local and regional tectonic control on sedimentology and stratigraphy in a strike-slip basin: Miocene Temblor Formation of the Coalinga Area, California, USA. Sedimentary Geology 158: 271 – 297.

Browne GH, Kennedy EM, Constable RM, Raine JI, Crouch EM, Sykes R 2008. An outcrop-based study of the economically significant Late Cretaceous Rakopi Formation, northwest Nelson, Taranaki Basin, New Zealand. New Zealand Journal of Geology & Geophysics 51: 295 – 315.

Carroll AR, Bohacs KM 2001. Lake-type controls on petroleum source rock potential in nonmarine basins. The American Association of Petroleum Geologists 85: 1033 – 1053.

Cas RAF, Wright JV 1987. Volcanic successions, modern and ancient: a geological approach to processes, products, and successions. Allen & Unwin, Boston; London.

Chang TS, Chun SS 2012. Micro-characteristics of sustained, fine-grained lacustrine turbidites in the Cretaceous Hwangsan Tuff, SW Korea. Geosciences Journal 16: 409 – 420.

Collier RJ, Johnston JH 1991. The identification of possible hydrocarbon source rocks, using biomarker geochemistry, in the Taranaki basin, New Zealand. Journal of Southeast Asian Earth Science 5: 231 – 239.

Collinson JD 1996. Alluvial sediments In: : Reading HG Third Ed Sedimentary Environments: Processes, Facies and Stratigraphy 37 – 82.

Connell SD 2010. Fluvial Sedimentation in Continental Half Grabens. Doctor of Philosophy, University of New Mexico, Albuquerque, USA.

Crews SG 1990. Structure, syntectonic sedimentation, and stratigraphy of asymmetrical non-marine basins. Doctor of Philosophy, University of Wyoming, USA.

Demaison G, Huizinga BJ 1994. Genetic classification of Petroleum systems using three factors: Charge, Migration, and Entrapment. The Petroleum System – from source to trap: AAPG vol 60: 73 – 89.

Diessel CFK 1992. Coal-bearing depositional systems. Springer-Verlag, New York; Berlin.

Ehinola OA, Sonibare OO, Falode OA, Awofala BO 2005. Hydrocarbon Potential and Thermal maturity of Nkporo Shale from the Lower Benue Trough, Nigeria. Journal of Applied Sciences Vol 5: 689 – 695.

Einsele G 1992. Sedimentary Basins: evolution, facies and sedimentary budget. Springer-Verlag, New York; Berlin.

Elgar NE 1997. Petroleum geology and geochemistry of oils and possible source rocks of the Southern East Coast Basin, New Zealand. Doctor of Philosophy, Victoria University of Wellington.

Feng J DATE. Source rock characterisation of the Green River oil shale, Piceance Creek Basin, Colorado. Masters Thesis, Colorado School of Mines, Colorado, USA.

Frankenberger A, Brooks RR, Varela-Alvarez H, Collen JD, Filby RH, Fitzgerald SL 1994. Classification of some of New Zealand crude oils and condensates by means of their trace element contents. Applied Geochemistry 9: 65 – 71.

Frisch W, Meschede M, Blakey R 2011. Continental Graben Structures. Plate Tectonics: 27 – 41.

Gage M 1952. The Greymouth Coalfield. New Zealand Geological Survey 45.

Gaina C, Müller DR, Royer J, Stock J, Hardebeck J, Symonds P 1998. The tectonic history of the Tasman Sea: A puzzle with 13 pieces. Journal of geophysical research 103: 12412 – 12433.

Gawthorpe RL, Leeder MR 2000. Tectono-sedimentary evolution of active extensional basins. Basin Research 12: 195 – 218.

Giba M, Nicol A, Walsh, JJ 2010. Evolution of faulting and volcanism in a back-arc basin and its implications for subduction processes. Tectonics 29.

Henrich R, Hüneke H 2011. Hemipelagic advection and periplatform sedimentation. Developments in Sedimentology 63: 353 – 396.

Herd MEJ 2007. Continental Extensional Tectonics – The Paparoa Metamorphic Core Complex of Westland, New Zealand. Master of Science, University of Canterbury, New Zealand.

Herzer RH, Sykes R, Killops SD, FUnnell RH, Burggraf DR, Townend J, Raine JI, Wilson GJ 1999. Cretaceous carbonaceous rocks from the Norfolk Ridge system, Southwest

Pacific: implications for the regional petroleum potential. New Zealand Journal of Geology & Geophysics 42: 57 – 73.

Higgs KE, Arnot MJ, Browne GH, Kennedy EM 2010. Reservoir potential of Late Cretaceous terrestrial to shallow marine sandstones, Taranaki Basin, New Zealand. Marine and Petroleum Geology 27: 1849 – 1871.

Hirner AV, Lyon G 1989. Stable isotope geochemistry of crude oils and of possible source rocks from New Zealand – 1: Carbon. Applied Geochemistry 4: 109 – 120.

Horsfield B, Dembicki Jr H, Ho TTY 1983. Some potential applications of pyrolysis to basin studies. Journal Geology society of London 140: 431-443.

Image: Afar Triple Junction. Taken from USGS website: http://pubs.usgs.gov/gip/dynamic/East_Africa.html

Jarvie DM 1991. Factors affecting Rock-Eval derived kinetic parameters. Chemical Geology 93: 77 – 99.

Jia J, Bechtel A, Liu Z, Strobl SA, Sun P, Sachsenhofer RF 2013. International Journal of Coal Geology 113: 11 – 26.

Jia J, Liu Z, Bechtel A, Strobl SA, Sun P 2013. Tectonic and climate control of oil shale deposition in the Upper Cretaceous Qingshankou Formation (Songliao Basin, NE China). International Journal of Earth Sciences 102: 1717 – 1734.

Jiamo F, Guoying S, Dehan L. Organic geochemical characteristics of major types of terrestrial petroleum source rocks in China. In: Fleet AJ, Kelts K, Talbot MR 1988. Lacustrine petroleum source rocks. Geological Society special publication 40: 279 – 289.

Johnston JH, Collier RJ, Maidment AI 1991. Coals as source rocks for hydrocarbon generation in the Taranaki Basin, New Zealand: a geochemical biomarker study. Journal of Southeast Asian Earth Sciences 5 283 – 289.

Jones HL, Hajek EA 2007. Characterising avulsion stratigraphy in ancient alluvial deposits. Sedimentary Geology 202: 124 – 137.

Keighley D, Flint S,Howell J, Moscariello A 2003. Sequence Stratigraphy in lacustrine basins: A model for part of the Green River Formation (Eocene), southwest Uinta Basin, Utah, USA. Journal of Sedimentology Research 73: 987 – 1006.

Kelts K 1988. Environments of deposition of lacustrine petroleum source rocks: an introduction. In: Fleet AJ, Kelts K, Talbot MR 1988. Lacustrine petroleum source rocks. Geological Society special publication 40: 3 – 26.

Killops SD, Cook RA, Sykes R, Boudou JP 2010. Petroleum potential and oil-source correlation in the Great South and Canterbury Basins. New Zealand Journal of Geology and Geophysics 40: 405 – 423.

Killops SD, Woodhouse AD, Weston RJ, Cook RA 1994. A geochemiscal appraisal of oil generation in the Taranaki Basin, New Zealand. AAPG Bulletin 78: 1560 – 1585.

Knight J 2009. Significance of soft-sediment clasts in glacial outwash, Puget Sound, USA. Sedimentary Geology 220: 126 – 133.

Laird MG 1994. Geological aspects of the opening of the Tasman Sea. In: van der Lingen GJ, Swanson KM, Muir RJ 1994. Evolution of the Tasman Sea Basin. 1 – 18.

Laird MG, Bradshaw JD 2004. The Break-up of a Long-term Relationship: the Cretaceous Separation of New Zealand from Gondwana. Gondwana Research 7: 273 – 286.

Leeder MR 1995. Continental Rifts and Proto-Oceanic Rift Troughs. In: Busby CJ, Ingersoll RV 1995. Tectonics of Sedimentary Basins. Blackwell Science. 119 – 148.

Leeder MR 1999. Sedimentology in Sedimentary Basins. In: Leeder MR, Sedimentology and Sedimentary Basins: From Turbulence to Tectonics. Blackwell Science. 497 – 530.

Lung – Chuan K 1994. Lower Cretaceous lacustrine source rocks in northern Gabon: effect of organic facies and thermal maturity on crude oil quality. Organic Geochemistry 22: 257 – 273.

MacEachern JA, Pemberton SG, Gingras MK, Bann KL 2010. Ichnology and Facies models. In: James NP, Dalrymple RW Facies Models 4. Geological Association of Canada 19 – 58.

Makaske B, Smith DG, Berendsen HJA 2002. Avulsions, channel evolution and floodplain sedimentation rates of the anastomosing upper Colombia River, British Colombia, Canada. Sedimentology 49: 1049 – 1071.

Marshall JEA, Brown JF, Hindmarsh S 1986. Hydrocarbon source rock potential of the Devonian rocks of the Orcadian Basin. Scottish Journal of Geology 21: 301-320.

McNee JT 1997. Structural geology of the Rapahoe Sector, Greymouth coalfield, West Coast, New Zealand. Masters Thesis, University of Canterbury, New Zealand.

Miall A 2010. Alluvial deposits. In: James NP, Dalrymple RW Facies Models 4. Geological Association of Canada 105 – 138.

Moosavi SA, Goshtasbi K, Kazemzadeh E 2014. Relaitonship between porosity and permeability with stress using pore volume compressibility characteristic of reservoir rocks. Arabian Journal of Geosciences 7: 231 – 239.

Mortimer N, Nathan S, Jongens R, Kawachi Y, Ryland C, Cooper AF, Stewart M, Randall S 2013. Regional metamorphism of the Early Palaeozoic Greenland Group, South Westland, New Zealand. New Zealand Journal of Geology and Geophysics 56: 1 – 15.

Mortimer N, Tulloch AJ, Ireland TR 2010. Basement geology of the Taranaki and Wanganui Basins, New Zealand. New Zealand Journal of Geology and Geophysics 40: 223 – 236.

Mortimer N, Tulloch AJ, Spark RN, Ladley E, Allibone A, Kimbrough DL 1999. Overview of the Median Batholith, New Zealand: a new interpretation of the geology of the Median Tectonic Zone and adjacent rocks.

Muir RJ, Bradshaw JD, Weaver, SD, Laird MG 2000. The influence of basement structure on the evolution of the Taranaki Basin in New Zealand. Journal of Geological Society, London 157: 1179 – 1185.

Nathan S 1978. Sheet S44 Greymouth (1st Edition). "Geological Map of New Zealand 1:63,360". Department of Scientific and Industrial Research, Wellington, New Zealand.

Nathan S, Rattenbury MS, Suggate RP 2002. Geology of the Greymouth Area. Institute of Geological & Nuclear Sciences 1:250000 geological map 12.' 1 sheet + 58 p.

Newman J 1985. Paleoenvironments, coal properties and their interrelationships in the Paparoa and selected Brunner Coal Measures on the West Coast of the South Island. Doctor of Philosophy, University of Canterbury, New Zealand.

Newman J, Boreham CJ, Ward SD, Murray AP, Bal AA 1999. Floral Influences on the Petroleum source potential of New Zealand Coals. Coalbed Methane: Scientific, Environmental and Economic Evaluation 461 – 492.

Newman J, Price LC, Johnston JH 1997. Hydrocarbon source potential and maturation in Eocene New Zealand vitrinite-rich coals: insights from traditional coal analyses and rock-eval and biomarker studies. Journal of Petroleum Geology 20 137 – 163.

Nielsen LH, Peterson HI, Thai ND, Duc NA, Fyhn MBW, Boldreel LO, Tuan HA, Lindström, Hien LV 2007. A Middle-Upper Miocene fluvial-lacustrine rift sequence in the Song Ba Rift, Vietnam: an analogue to oil prone, small-scale continental rift basins. Petroleum Geoscience 13: 145 – 168.

Nilsen TH, Sylvetser AG 1995. Strike-slip Basins. In: Busby CJ, Ingersoll RV 1995. Tectonics of Sedimentary Basins. Blackwell Science. 425 – 458.

Nunez-Betelu L, Baceta JI 1994. Basics and Application of Rock-Eval/TOC Pyrolysis: an example from the uppermost Paleocene/lowermost Eocene In The Basque Basin, Western Pyrenees. Natural Science 46: 43 – 62.

Pedentchouk N, Freeman KH, Harris NB, Clifford DJ, Grice K 2004. Sources of alkylbenzenes in Lower Cretaceous lacustrine source rocks, West African rift Basins. Organic Geochemistry 35: 33 – 45.

Peters KE 1986. Guidelines for evaluating petroleum source rock using programmed pyrolysis. AAPG Bulletin 70: 318 – 329.

Peters KE, Cassa MR 1994. Applied source rock geochemistry. The Petroleum System – from source to trap: AAPG Memoir 60.

Peterson HI, Anderson C, Anh PH, Bojeson-Koefoed JA, Nielsen LH, Nytoft HP, Rosenberg P, Thanh L 2000. Petroleum potential of Oligocene lacustrine mudstones and coals at Dong Ho, Vietnam Đ an outcrop analogue to terrestrial source rocks in the greater Song Hong Basin. Journal of Asian Earth Sciences 19: 135 – 154.

Petroleum Basin Explorer (PBE), GNS Science. Accessed from http://data.gns.cri.nz/pbe/index.html#HTML:Content/PBE_Home.html.

Powell TJ 1986. Petroleum geochemistry and depositional setting of lacustrine source rocks. Marine and Petroleum Geology 3: 200 – 219.

Renaut RW, Gierlowski-Kordesch EH 2010. Lakes. In: James NP, Dalrymple RW Facies Models 4. Geological Association of Canada 541 – 575

Roser BP, Coombs DS, Korsch RJ, Campbell JD 2002. Whole-rock geochemical variations and evolution of the arc-derived Murihiku Terrane, New Zealand. Geological Magazine 139: 665 – 685.

Ross DJK, Bustin RM 2009. The importance of shale composition and pore structure upon gas storage potential of shale gas reservoirs. Marine and Petroleum Geology 26: 916 – 927.

Ruble TE, Lewan MD, Philp RP 2001. New insights on the Green River petroleum system in the Uinta Basin from hydrous pyrolysis experiments. AAPG Bulletin 85: 1333 – 1371.

Sager MW, Palin JM 2011. Emplacement, metamorphism, deformation and affiliation of mid-Cretaceous Orthogneiss from the Paparoa Metamorphic Core Complex lower-plate, Charleston, New Zealand. New Zealand Journal of Geology and Geophysics 54: 273 – 289.

Sahoo TR, King PR, Blank KJ, Strogen DP, Sykes R 2014. Tectono-sedimentsry evolution and source rock distribution of the mid to Late Cretaceous succession in the Great South Basin, New Zealand. APPEA 2014: 259 – 274.

Saneyoshi M, Nakayama K, Tetsuya S, Yoshihiro S, Hidemi I 2006. Half graben filling processes in the early phase of continental rifting: The Miocene Namurungule Formation of the Kenya Rift. Sedimentary Geology 186: 111 – 131.

Sara WA 1963. Reserves of bituminous coal in the Liverpool and Paparoa areas, Greymouth Coalfield. New Zealand Journal of Geology and Geophysics 6: 566 -581.

Schulte DO, Ring U, Thomson SN, Glodny J, Carrad H 2014. Two-stage development of the Paparoa Metamorphic Core Complex, West Coast, South Island, New Zealand: Hot continental extension preceeds sea-floor spreading by ~25.my. Lithosphere 6: 177 – 194.

Shanmugan G 2002. Ten turbidite myths. Earth Science Reviews 58: 311 – 341.

Sletten K, Blikra LH, Ballantyne CK, Nesje A, Dahl SO 2003. Holocene debris flows recognized in a lacustrine sedimentary succession: sedimentology, chronostratigraphy and cause of triggering. Holocene 13: 907.

Smith ME, Carroll AR, Singer BS 2008. Synoptic reconstruction of a major ancient lake system: Eocene Green River Formation, western United States. GSA Bulletin 120: 54 – 84.

Song Z, Qin Y, George SC, Wang L, Guo J, Feng Z 2013. A biomarker study of depositional paleoenvironments and source inputs for the massive formation of Upper Cretaceous lacustrine source rocks in the Songliao Basin, China. Palaeogeography, Palaeoclimatology, Palaeoecology 385: 137 – 151.

Stahl T 2014. Active Tectonics and Geomorphology of the central South Island, New Zealand: Earthquake Hazards of Reverse Faults. Doctor of Philosophy, University of Canterbury, New Zealand.

Stow DAV, Reading HG, Collinson JD 1996. Deep seas In: Reading HG, Third Ed Sedimentary Environments: Processes, Facies and Stratigraphy 395 – 453

Suggate RP 1959. Paparoa mine area, Greymouth Coalfield: Swelling properties and reserves of coal. New Zealand Journal of Geology and Geophysics 2: 355 – 367.

Suggate RP 2002. Application of Rank (Sr), a maturity index based on chemical analyses of coals. Marine and Petroleum Geology 19: 929 – 950.

Suggate RP, Boyd RJ 2012. Greymouth Coalfield, New Zealand: vertical coal rank gradients, depths of burial and paleotemperatures. New Zealand Journal of Geology and Geophysics 55: 111 – 126.

Suggate RP 2014. Extensional basin development and subsequent inversion in Greymouth Coalfield. New Zealand Journal of Geology and Geophysics: 1 – 12.

Sykes R, Johansen PE. Maturation characteristics of the New Zealand coal band: Part 1 – Evolution of Oil and Gas products.

Sykes R, Snowdon LR 2002. Guidelines for assessing the petroleum potential of coaly source rocks using Rock-Eval pyrolysis. Organic Geochemistry 33: 1441 – 1455.

Sykes R, Volk, H, George SC, Ahmed M, Higgs KE, Johansen PE, Snowdon LR 2013. Marine influence helps preserve the oil potential of coaly source rocks: Eocene Mangahewa Formation, Taranaki Basin, New Zealand. Organic Geochemistry 66: 140 – 163.

Tambach TJ, Veld H, Griffioen J 2009. Influence of HCI/HF treatment on organic matter in aquifer sediments: A Rock-Eval pyrolysis study. Applied Geochemistry 24: 2144 – 2151.

Thul D 2012. Niobara source rock maturity in the Denver Basin: A study of differential heating and tectonics on petroleum prospectivity using programmed pyrolysis. Masters thesis Colorado School of Mines, Colorado, USA.

Turkman I, Aksoy E, Taşgin CK 2007. Alluvial and lacustrine facies in an extensional basin: The Miocene of Malataya basin, eastern Turkey. Journal of Asian Earth Science 30: 181 – 198.

Umhoefer PJ, Schwennicke T, Del Margo MT, Ruiz-Geraldo G, Ingle Jr. JC, McIntosh W 2007. Transtensional fault-termination basins: an important basin type illustrated by the Pliocene San Jose Island basin and related basins in the southern Gulf of California, Mexico. Basin Research 19: 297 – 322.

Uruski CL 2008. Deepwater Taranaki, New Zealand: Structural development and petroleum potential. Exploration Geophysics 39: 94 – 107.

Uruski CL 2010. New Zealand's deepwater frontier. Marine and Petroleum Geology 27: 2005 – 2026.

Ward SD 1997. Lithostratigraphy, palynostratigraphy and basin analysis of the Late Cretaceous to early Tertiary Paparoa Group, Greymouth Coalfield, New Zealand. Doctor of Philosophy, University of Canterbury, New Zealand.

Wolfenden E, Ebinger C, Yirgu G, Deino A, Ayalew D 2004. Evolution of the northern Main Ethiopian rift: basin of a triple junction. Earth and Planetary Science Letters 224: 213 – 228.

Wu JE, McClay K, Whitehouse P, Dooley T 2008. 4D analogue modelling of transtensional pull-apart basins. Marine and Petroleum Geology 26: 1608 – 1623.

Zhongsheng Li 2002. Mineralogy and trace elements of the Cretaceous Greymouth coals and their combustion products. Doctor of Philosophy, University of Canterbury, New Zealand.

Zimmerle W 1995.Sedimentology of rocks important to hydrocarbon exploration. In: Zimmerle W, Petroleum Sedimentology. Klumwer Academic Publishers 108 – 167.

Appendix 1 Stratigraphic columns

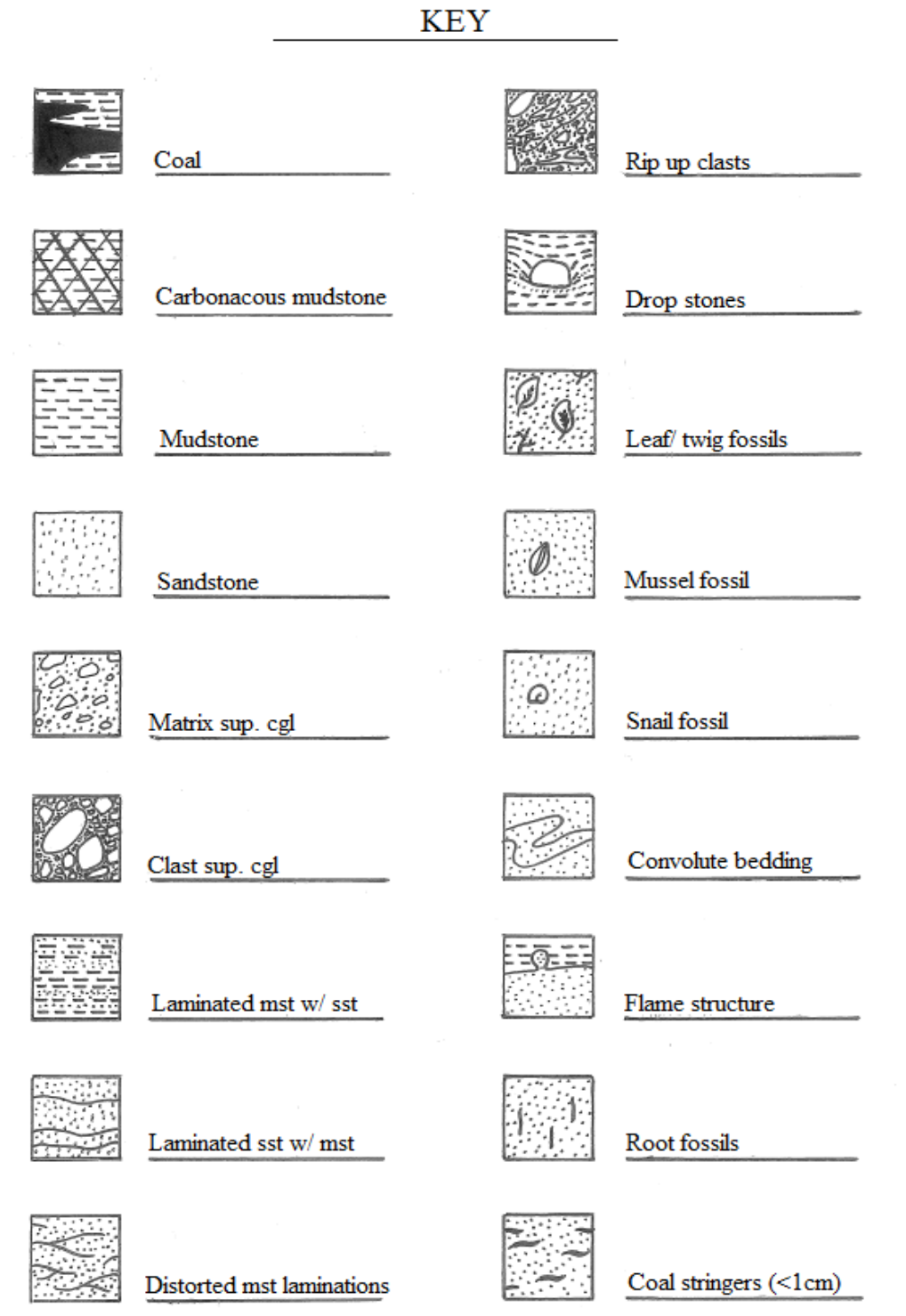

Figure A.1 Stratigraphic column key.

Hole ID: 631 GPS Coordinates: 695938.7 N

Goldlight Formation 278428.7 E

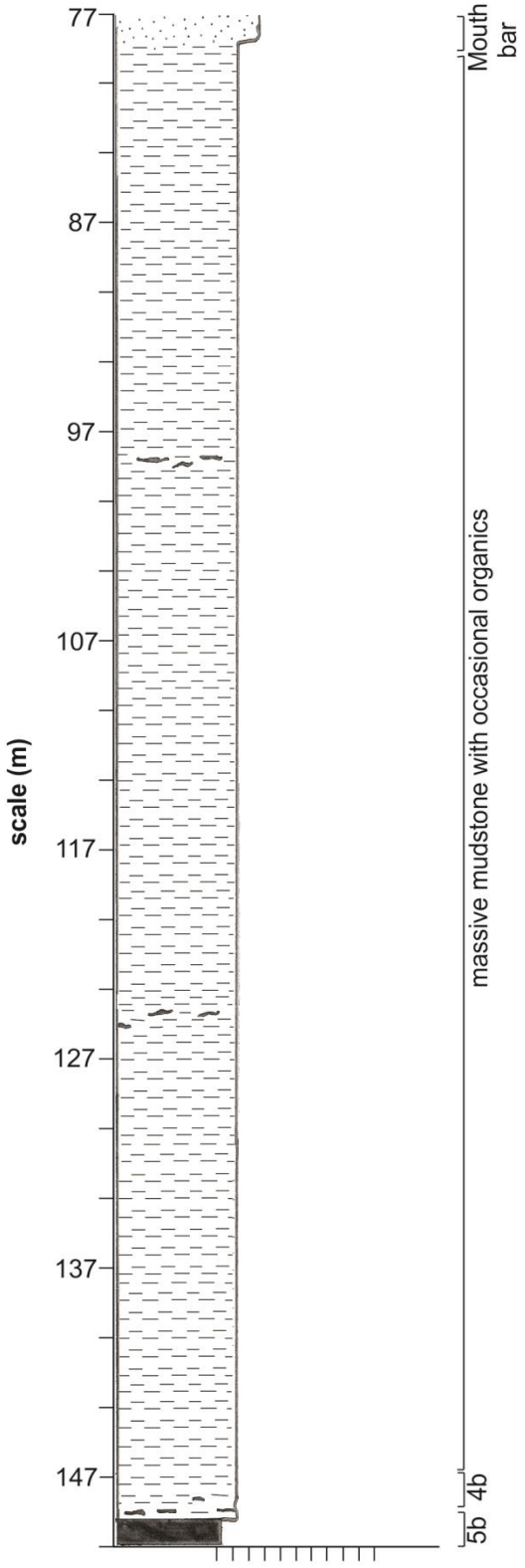

Figure A.2 DH 631. Facies 5b and 4b correspond to peat bog and lake edge respectively.

Hole ID: 632

Waiomo Formation

GPS Coordinates: 696166.53 N

279975.62 E

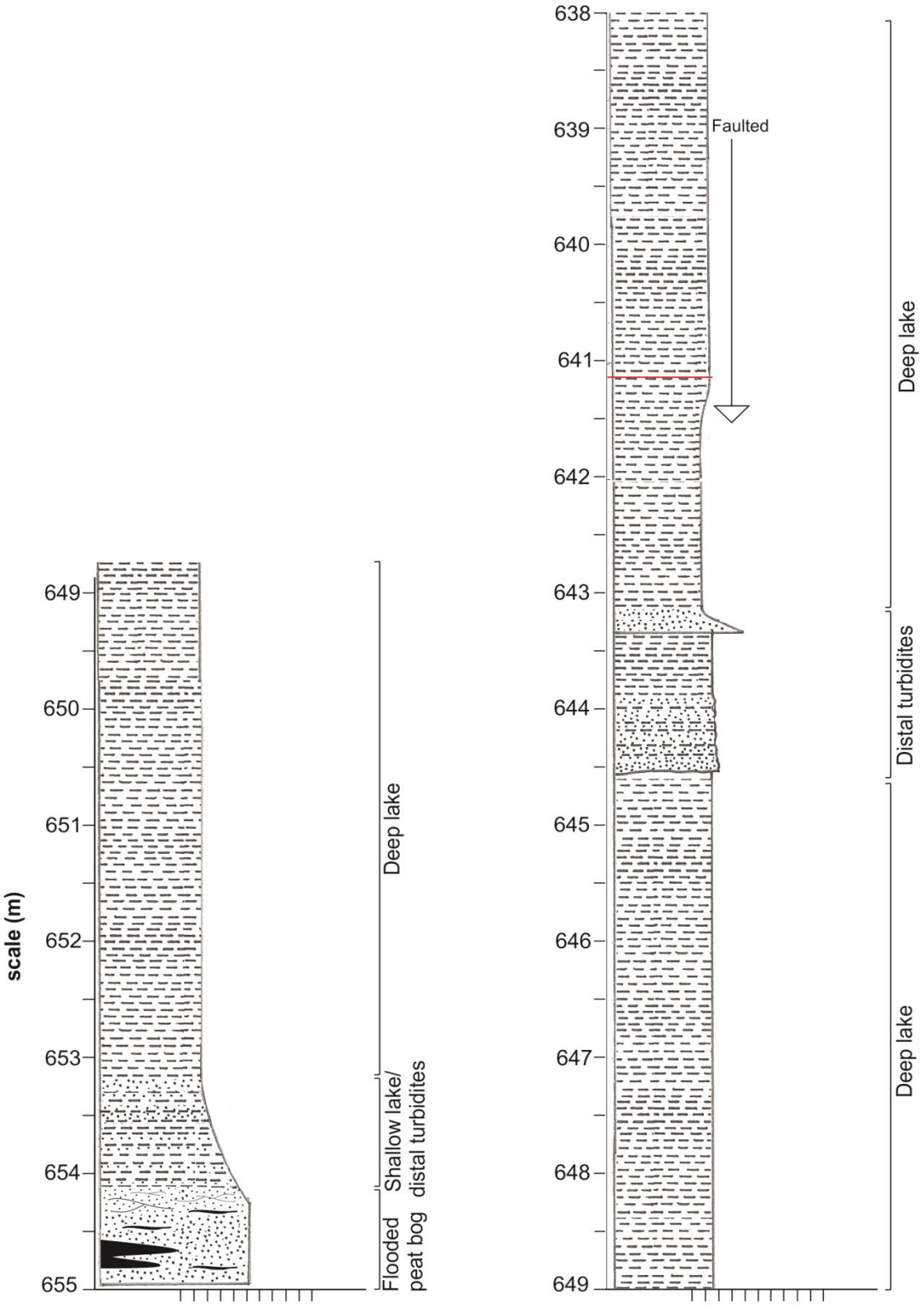

Figure A.3 DH 632.

Hole ID: 632

Waiomo Formation

GPS Coordinates: 696166.53 N

279975.62 E

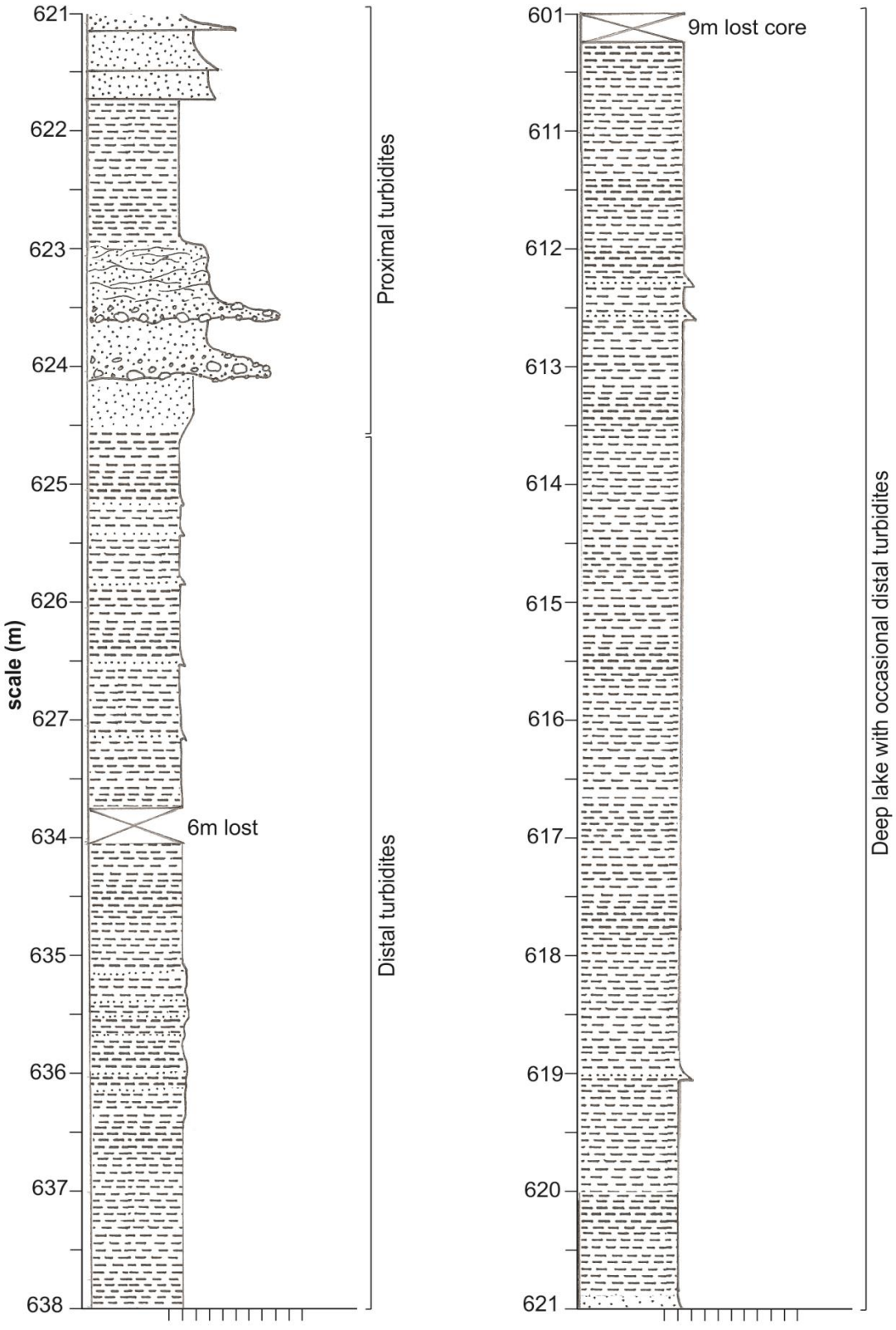

Figure A.3 DH 632.

Hole ID: 632

Waiomo Formation

GPS Coordinates: 696166.53 N

279975.62 E

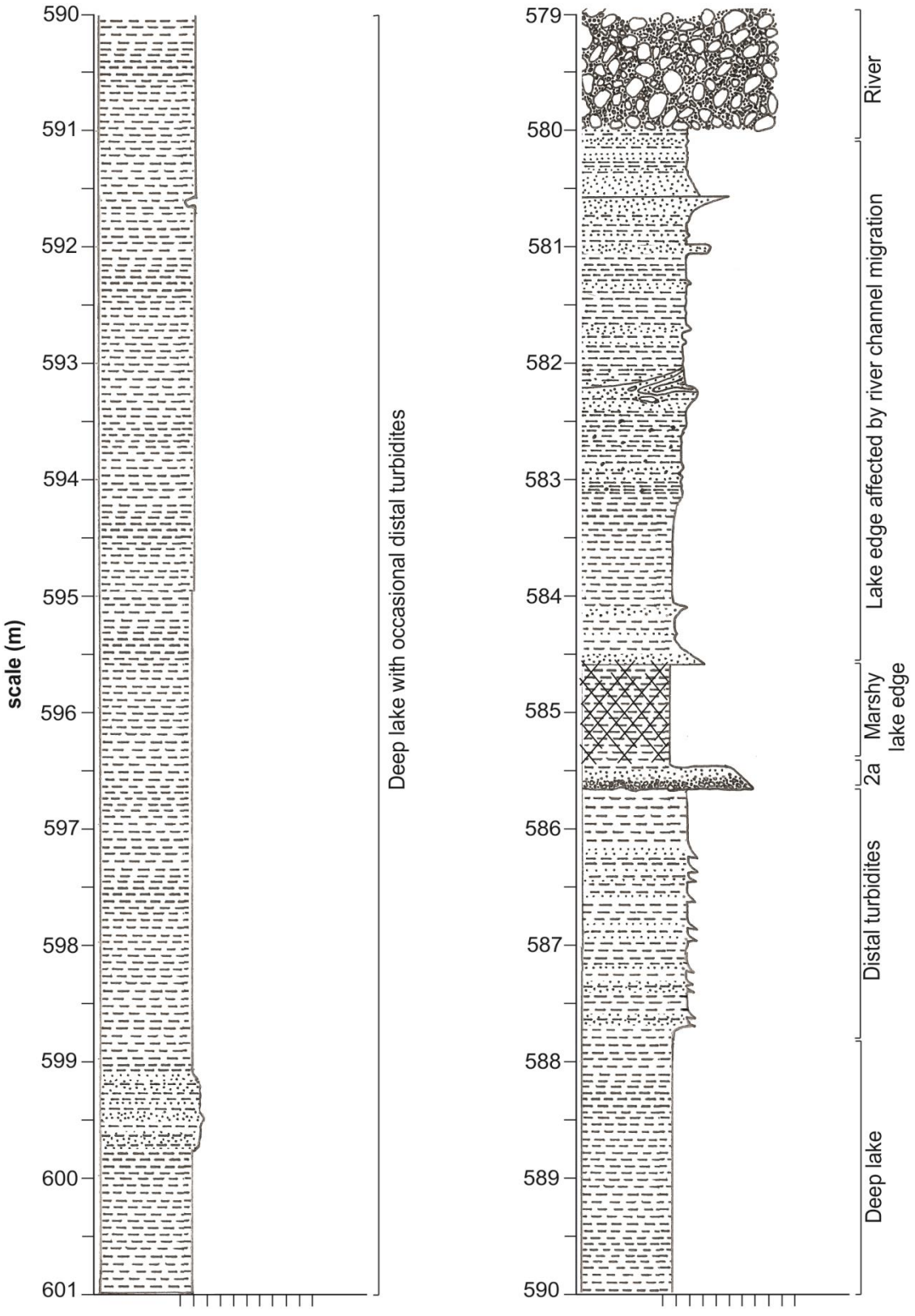

Figure A.3 DH 632.

Location: 10 Mile Creek

GPS Coordinates: 696166.53 N

Waiomo Formation

279975.62 E

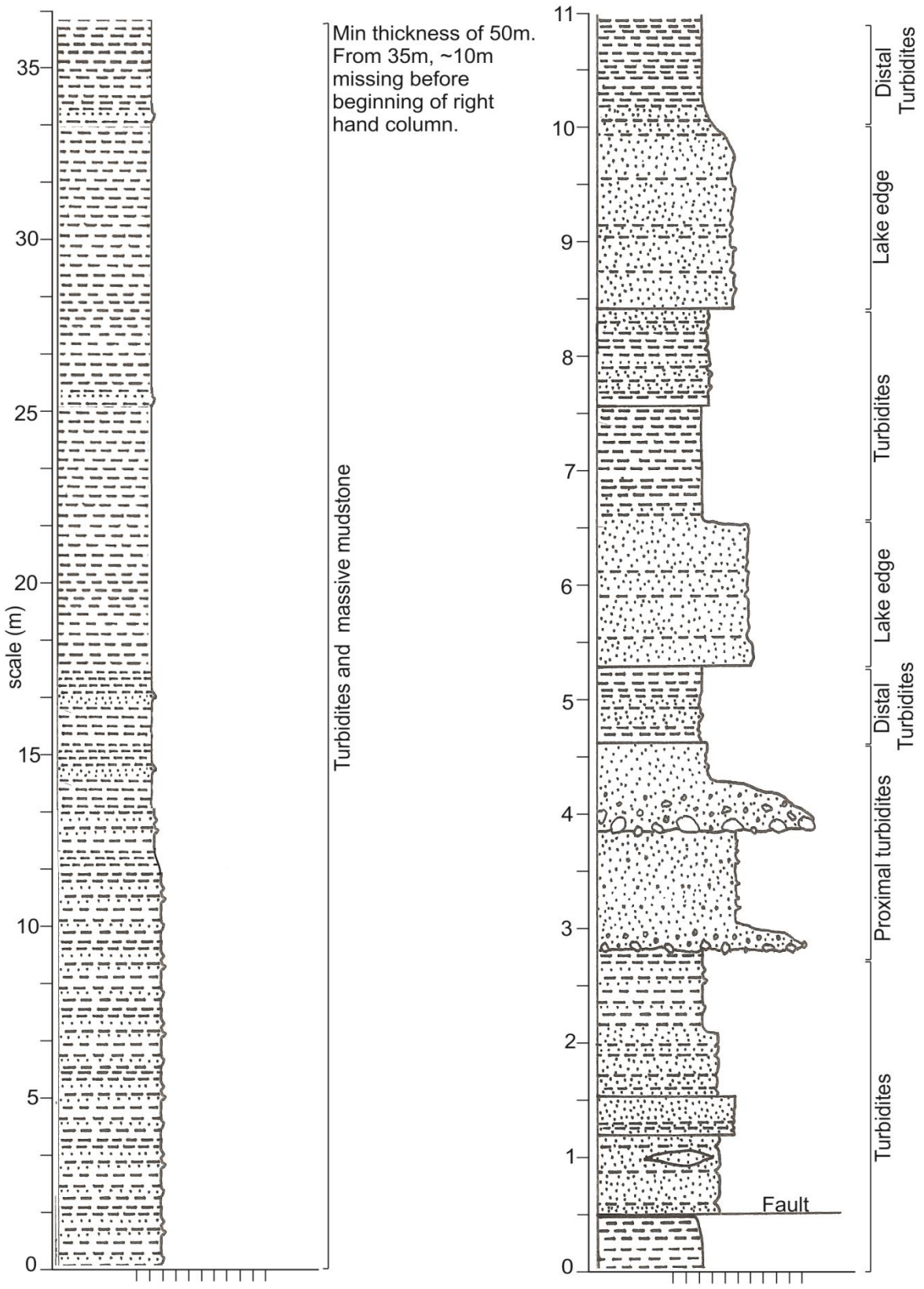

Figure A.4 10 Mile Creek (now collapsed).

Location: 12 Mile Beach

GPS Coordinates: 701123.6 N

Waiomo Mudstone (Close up)

276964.5 E

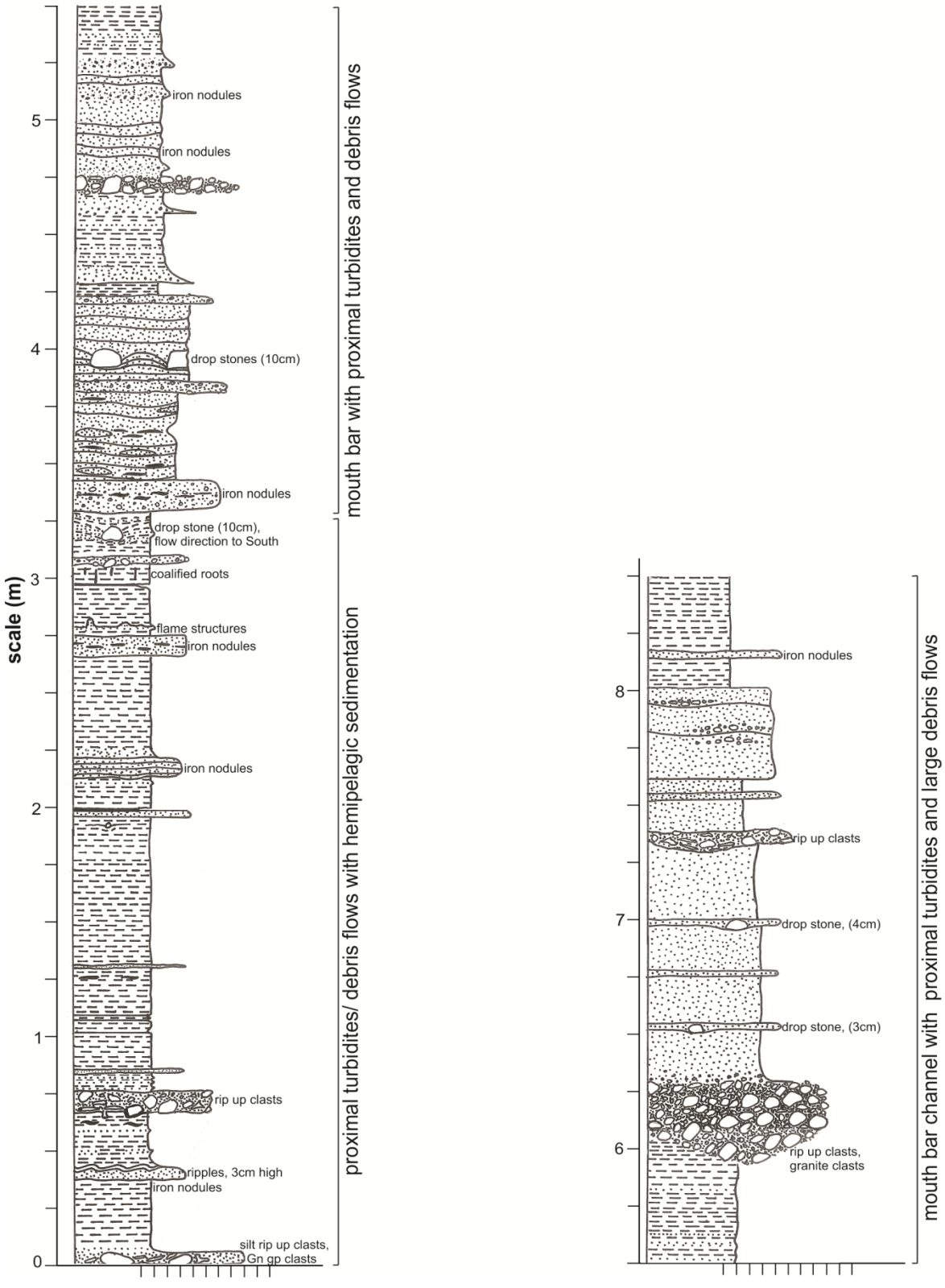

Figure A.5 Close up, upper Waiomo Formation, 12 Mile Beach.

Appendix 2 SRA plots

SR Analyzer (SRA -TOC) - TPH TOC Analysis v6.5.117

Sample ID: 628_248 **Acq. Type**: TPH **Weight**: 83.5 **Crucible**: 4
Depth: 248.0 (Measured) **Lithology**: None **Sample Type**: Core **Well Name**: 628
Acq. Date: July 17 2014 / 3:59:35 PM

Data: C:\SRA JOBS\SRA049_Greymouth lacustrine mudstones_17072014\628_248.RAW
Method: C:\Program Files\Thermal Station\GNS 300-650 STD 160000.sram
Sequence: C:\Program Files\Thermal Station\Data\SRA049 Greymouth lacustrine mudstones 17072014\SRA049 Greymouth lacustrine mudstones 17072014.sras
Method Information: Initial Temp: 300 °C -- Initial Time: 3 -- Rate : 25.0 °C/Min -- Final Temp: 650 °C -- Final Time: 1 Min -- OxiPurge: 5 Min -- OxiTime: 20 Min -- OxiTemp: 630 °C
FID Temp: 325 °C
FID Gain: Low (10^6)

Calibration Standard Information: Standard Name: 160000 TOC tTemp: 455.0 °C pTPH (S2): 12.43 mg/g S3: 0.79 mg/g S4: 22.40 mg/g
Operator: R Sykes **Instrument name**: SRA -TOC

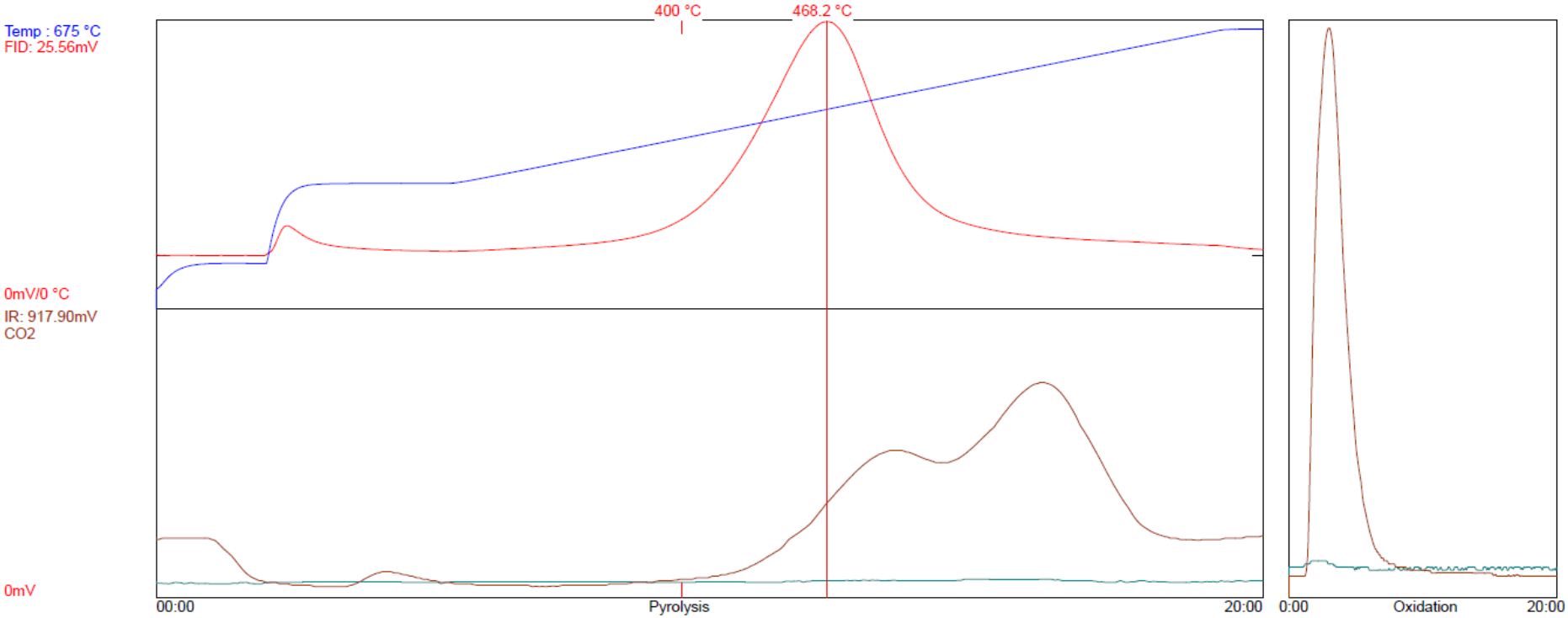

vTPH(S1):.16mg/g pTPH(S2): 3.68mg/g cTemp(Tmax): 429.2°C tTemp:468.2°C S3:2.02mg/g TOC:2.09 % HI:176 OI:97 PI:0.04 S1/TOC:0.08

Monday, 21 July 2014 17:35:18

SR Analyzer (SRA -TOC) - TPH TOC Analysis v6.5.117

Sample ID: 630_252-5 **Acq. Type**: TPH **Weight**: 81.5 **Crucible**: 5
Depth: 252.5 (Measured) **Lithology**: None **Sample Type**: Core **Well Name**: 630
Acq. Date: July 17 2014 / 4:54:21 PM

Data: C:\SRA JOBS\SRA049_Greymouth lacustrine mudstones_17072014\630_252-5.RAW
Method: C:\Program Files\Thermal Station\GNS 300-650 STD 160000.sram
Sequence: C:\Program Files\Thermal Station\Data\SRA049 Greymouth lacustrine mudstones 17072014\SRA049 Greymouth lacustrine mudstones 17072014.sras
Method Information: Initial Temp: 300 °C -- Initial Time: 3 -- Rate : 25.0 °C/Min -- Final Temp: 650 °C -- Final Time: 1 Min -- OxiPurge: 5 Min -- OxiTime: 20 Min -- OxiTemp: 630 °C
FID Temp: 325 °C
FID Gain: Low (10^6)

Calibration Standard Information: Standard Name: 160000 TOC tTemp: 455.0 °C pTPH (S2): 12.43 mg/g S3: 0.79 mg/g S4: 22.40 mg/g
Operator: R Sykes **Instrument name**: SRA -TOC

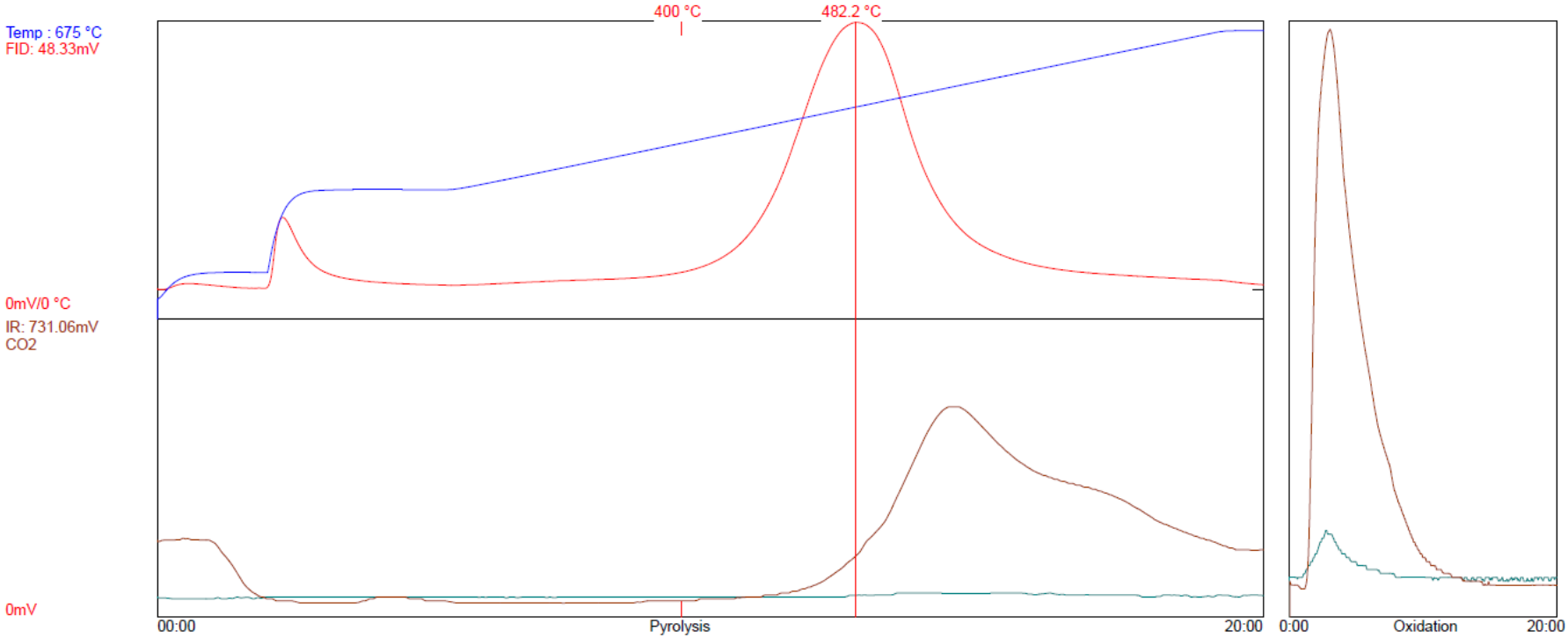

vTPH(S1):.60mg/g pTPH(S2): 7.52mg/g cTemp(Tmax): 443.2°C tTemp:482.2°C S3:.48mg/g TOC:3.02 % HI:249 OI:16 PI:0.07 S1/TOC:0.20

Monday, 21 July 2014 17:36:01

SR Analyzer (SRA -TOC) - TPH TOC Analysis v6.5.117

Sample ID: 631_93-6 **Acq. Type**: TPH **Weight**: 82.6 **Crucible**: 6
Depth: 93.6 (Measured) **Lithology**: None **Sample Type**: Core **Well Name**: 631
Acq. Date: July 17 2014 / 5:49:05 PM

Data: C:\SRA JOBS\SRA049_Greymouth lacustrine mudstones_17072014\631_93-6.RAW
Method: C:\Program Files\Thermal Station\GNS 300-650 STD 160000.sram
Sequence: C:\Program Files\Thermal Station\Data\SRA049 Greymouth lacustrine mudstones 17072014\SRA049 Greymouth lacustrine mudstones 17072014.sras
Method Information: Initial Temp: 300 °C -- Initial Time: 3 -- Rate : 25.0 °C/Min -- Final Temp: 650 °C -- Final Time: 1 Min -- OxiPurge: 5 Min -- OxiTime: 20 Min -- OxiTemp: 630 °C
FID Temp: 325 °C
FID Gain: Low (10^6)

Calibration Standard Information: Standard Name: 160000 TOC tTemp: 455.0 °C pTPH (S2): 12.43 mg/g S3: 0.79 mg/g S4: 22.40 mg/g
Operator: R Sykes **Instrument name**: SRA -TOC

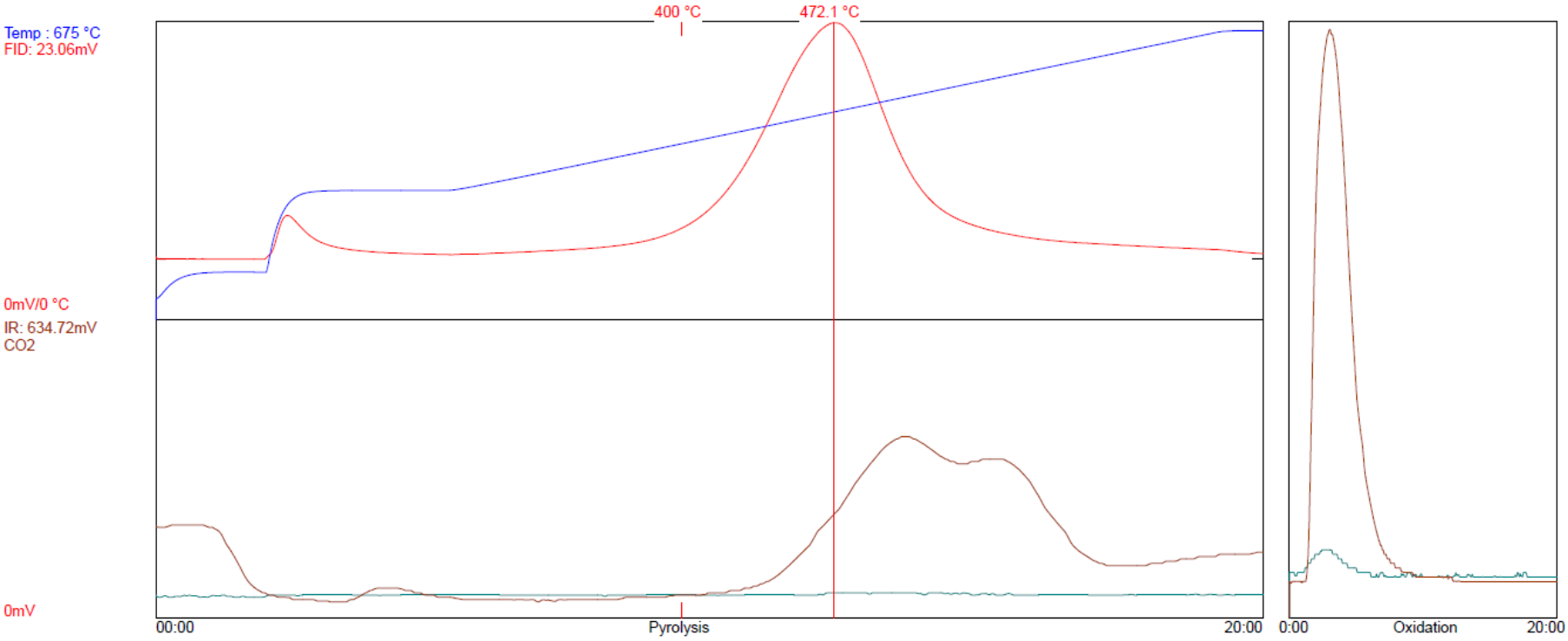

vTPH(S1):.18mg/g pTPH(S2): 3.29mg/g cTemp(Tmax): 433.1°C tTemp:472.1°C S3:1.18mg/g TOC:1.77 % HI:185 OI:66 PI:0.05 S1/TOC:0.10

Monday, 21 July 2014 17:36:55

SR Analyzer (SRA -TOC) - TPH TOC Analysis v6.5.117

Sample ID: 631_120-1 **Acq. Type**: TPH **Weight**: 80.8 **Crucible**: 7
Depth: 120.1 (Measured) **Lithology**: None **Sample Type**: Core **Well Name**: 631
Acq. Date: July 17 2014 / 6:43:52 PM

Data: C:\SRA JOBS\SRA049_Greymouth lacustrine mudstones_17072014\631_120-1.RAW
Method: C:\Program Files\Thermal Station\GNS 300-650 STD 160000.sram
Sequence: C:\Program Files\Thermal Station\Data\SRA049 Greymouth lacustrine mudstones 17072014\SRA049 Greymouth lacustrine mudstones 17072014.sras
Method Information: Initial Temp: 300 °C -- Initial Time: 3 -- Rate : 25.0 °C/Min -- Final Temp: 650 °C -- Final Time: 1 Min -- OxiPurge: 5 Min -- OxiTime: 20 Min -- OxiTemp: 630 °C
FID Temp: 325 °C
FID Gain: Low (10^6)

Calibration Standard Information: Standard Name: 160000 TOC tTemp: 455.0 °C pTPH (S2): 12.43 mg/g S3: 0.79 mg/g S4: 22.40 mg/g
Operator: R Sykes **Instrument name**: SRA -TOC

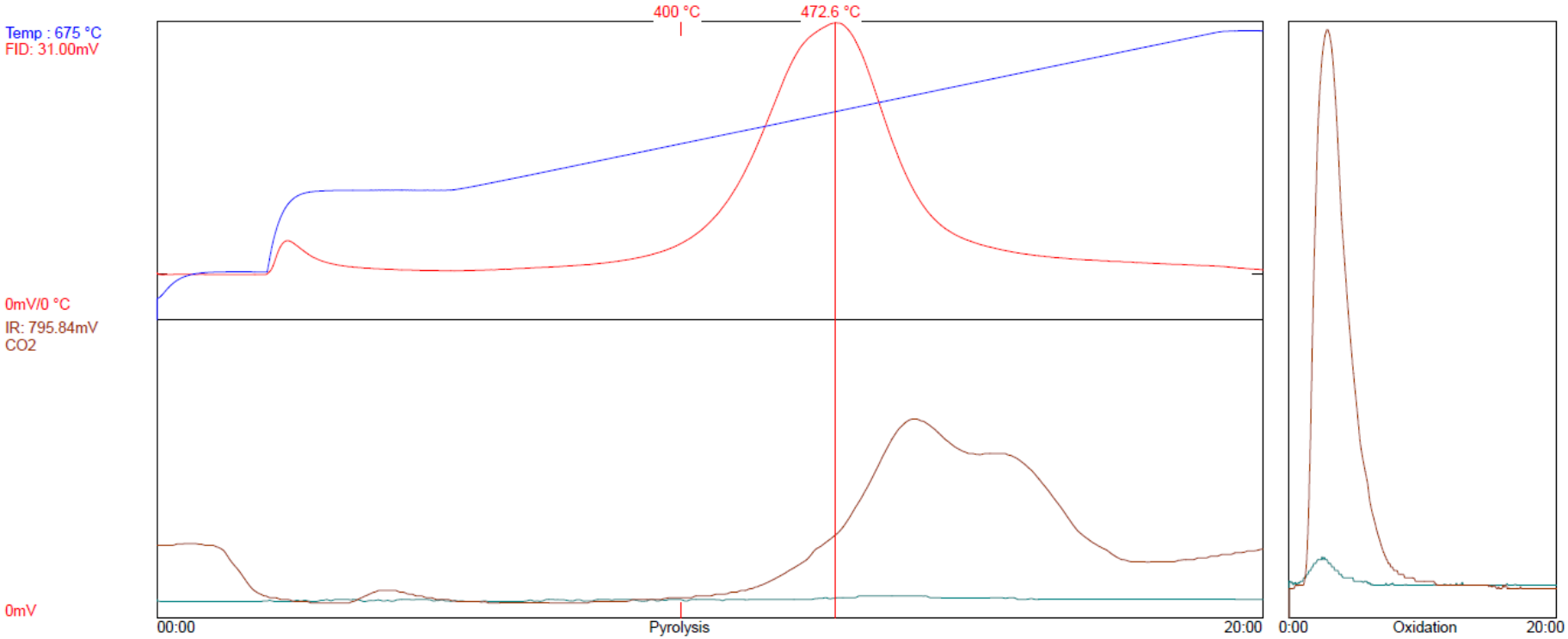

vTPH(S1):.20mg/g pTPH(S2): 4.78mg/g cTemp(Tmax): 433.6°C tTemp:472.6°C S3:1.80mg/g TOC:2.26 % HI:211 OI:80 PI:0.04 S1/TOC:0.09

Monday, 21 July 2014 17:37:19

SR Analyzer (SRA -TOC) - TPH TOC Analysis v6.5.117

Sample ID: 631b_139-8 **Acq. Type**: TPH **Weight**: 55.1 **Crucible**: 26
Depth: 139.8 (Measured) **Lithology**: None **Sample Type**: Core **Well Name**: 631
Acq. Date: July 21 2014 / 2:16:33 PM

Data: C:\SRA JOBS\SRA049C_Greymouth lacustrine mudstones_20072014\631b_139-8.RAW
Method: C:\Program Files\Thermal Station\GNS 300-650 STD 160000.sram
Sequence: C:\Program Files\Thermal Station\Data\SRA049C Greymouth lacustrine mudstones 20072014\SRA049C Greymouth lacustrine mudstones 20072014.sras
Method Information: Initial Temp: 300 °C -- Initial Time: 3 -- Rate : 25.0 °C/Min -- Final Temp: 650 °C -- Final Time: 1 Min -- OxiPurge: 5 Min -- OxiTime: 20 Min -- OxiTemp: 630 °C
FID Temp: 325 °C
FID Gain: Low (10^6)

Calibration Standard Information: Standard Name: 160000 TOC tTemp: 455.0 °C pTPH (S2): 12.43 mg/g S3: 0.79 mg/g S4: 22.40 mg/g
Operator: R Sykes **Instrument name**: SRA -TOC

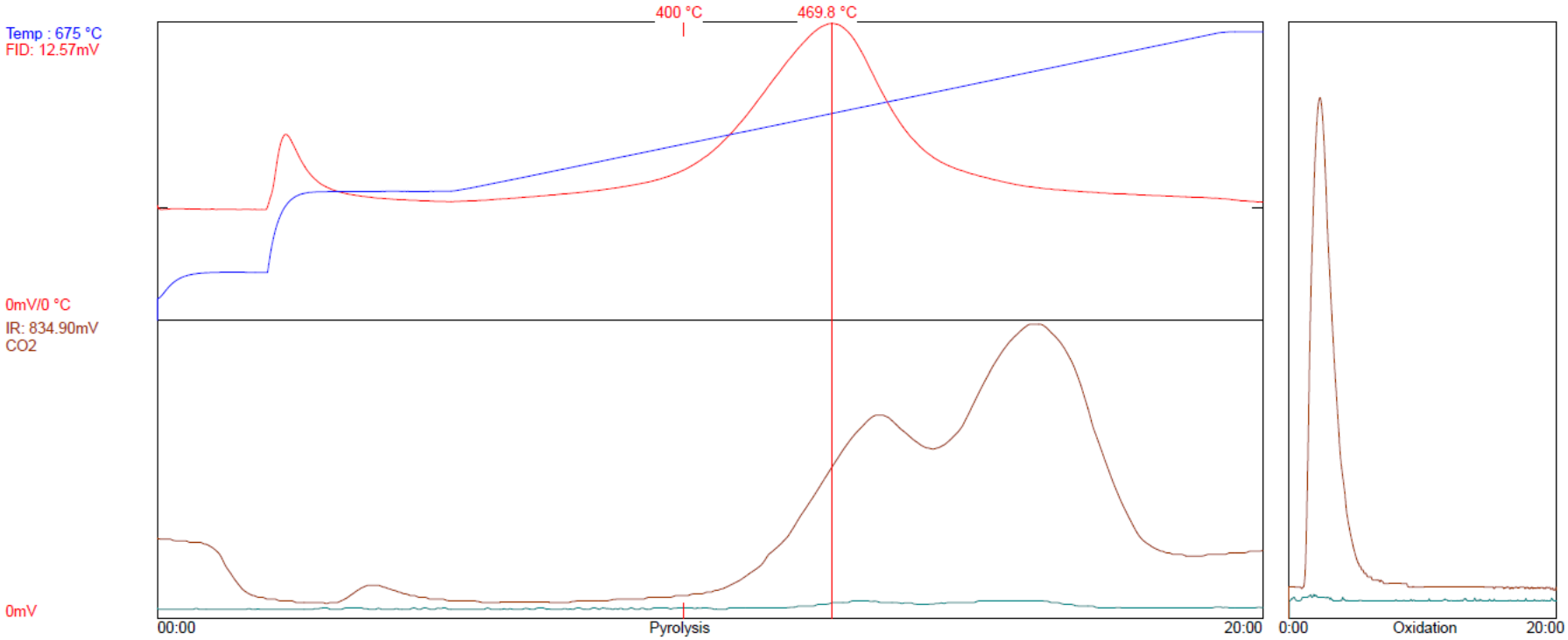

vTPH(S1):.25mg/g pTPH(S2): 2.66mg/g cTemp(Tmax): 430.8°C tTemp:469.8°C S3:4.37mg/g TOC:2.01 % HI:132 OI:217 PI:0.08 S1/TOC:0.12

Monday, 21 July 2014 17:49:55

SR Analyzer (SRA -TOC) - TPH TOC Analysis v6.5.117

Sample ID: 632_214-6 **Acq. Type**: TPH **Weight**: 80.5 **Crucible**: 9
Depth: 214.6 (Measured) **Lithology**: None **Sample Type**: Core **Well Name**: 632
Acq. Date: July 17 2014 / 8:33:39 PM

Data: C:\SRA JOBS\SRA049_Greymouth lacustrine mudstones_17072014\632_214-6.RAW
Method: C:\Program Files\Thermal Station\GNS 300-650 STD 160000.sram
Sequence: C:\Program Files\Thermal Station\Data\SRA049 Greymouth lacustrine mudstones 17072014\SRA049 Greymouth lacustrine mudstones 17072014.sras
Method Information: Initial Temp: 300 °C -- Initial Time: 3 -- Rate : 25.0 °C/Min -- Final Temp: 650 °C -- Final Time: 1 Min -- OxiPurge: 5 Min -- OxiTime: 20 Min -- OxiTemp: 630 °C
FID Temp: 325 °C
FID Gain: Low (10^6)

Calibration Standard Information: Standard Name: 160000 TOC tTemp: 455.0 °C pTPH (S2): 12.43 mg/g S3: 0.79 mg/g S4: 22.40 mg/g
Operator: R Sykes **Instrument name**: SRA -TOC

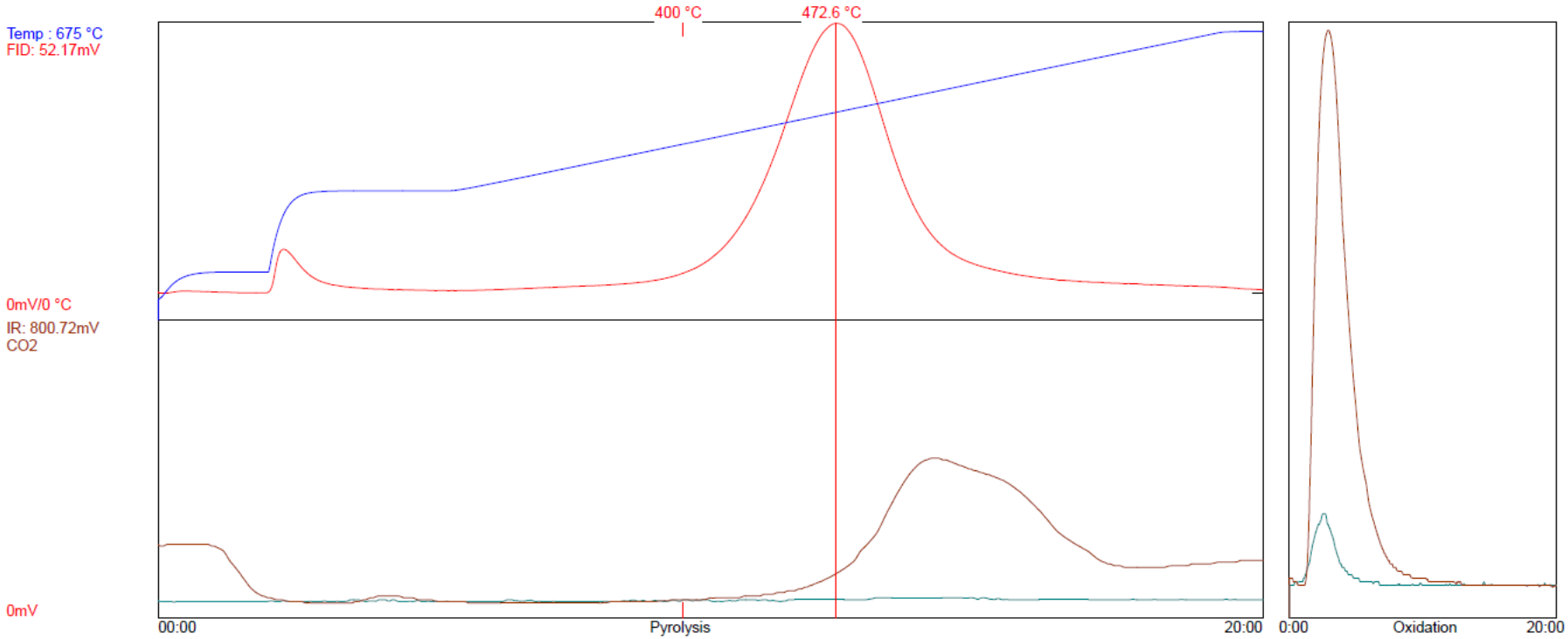

vTPH(S1):.36mg/g pTPH(S2): 7.49mg/g cTemp(Tmax): 433.6°C tTemp:472.6°C S3:.81mg/g TOC:2.66 % HI:282 OI:30 PI:0.05 S1/TOC:0.14

Monday, 21 July 2014 17:38:35

SR Analyzer (SRA -TOC) - TPH TOC Analysis v6.5.117

Sample ID: 632_235 **Acq. Type**: TPH **Weight**: 81.0 **Crucible**: 10
Depth: 235 (Measured) **Lithology**: None **Sample Type**: Core **Well Name**: 632
Acq. Date: July 17 2014 / 9:28:36 PM

Data: C:\SRA JOBS\SRA049_Greymouth lacustrine mudstones_17072014\632_235.RAW
Method: C:\Program Files\Thermal Station\GNS 300-650 STD 160000.sram
Sequence: C:\Program Files\Thermal Station\Data\SRA049 Greymouth lacustrine mudstones 17072014\SRA049 Greymouth lacustrine mudstones 17072014.sras
Method Information: Initial Temp: 300 °C -- Initial Time: 3 -- Rate : 25.0 °C/Min -- Final Temp: 650 °C -- Final Time: 1 Min -- OxiPurge: 5 Min -- OxiTime: 20 Min -- OxiTemp: 630 °C
FID Temp: 325 °C
FID Gain: Low (10^6)

Calibration Standard Information: Standard Name: 160000 TOC tTemp: 455.0 °C pTPH (S2): 12.43 mg/g S3: 0.79 mg/g S4: 22.40 mg/g
Operator: R Sykes **Instrument name**: SRA -TOC

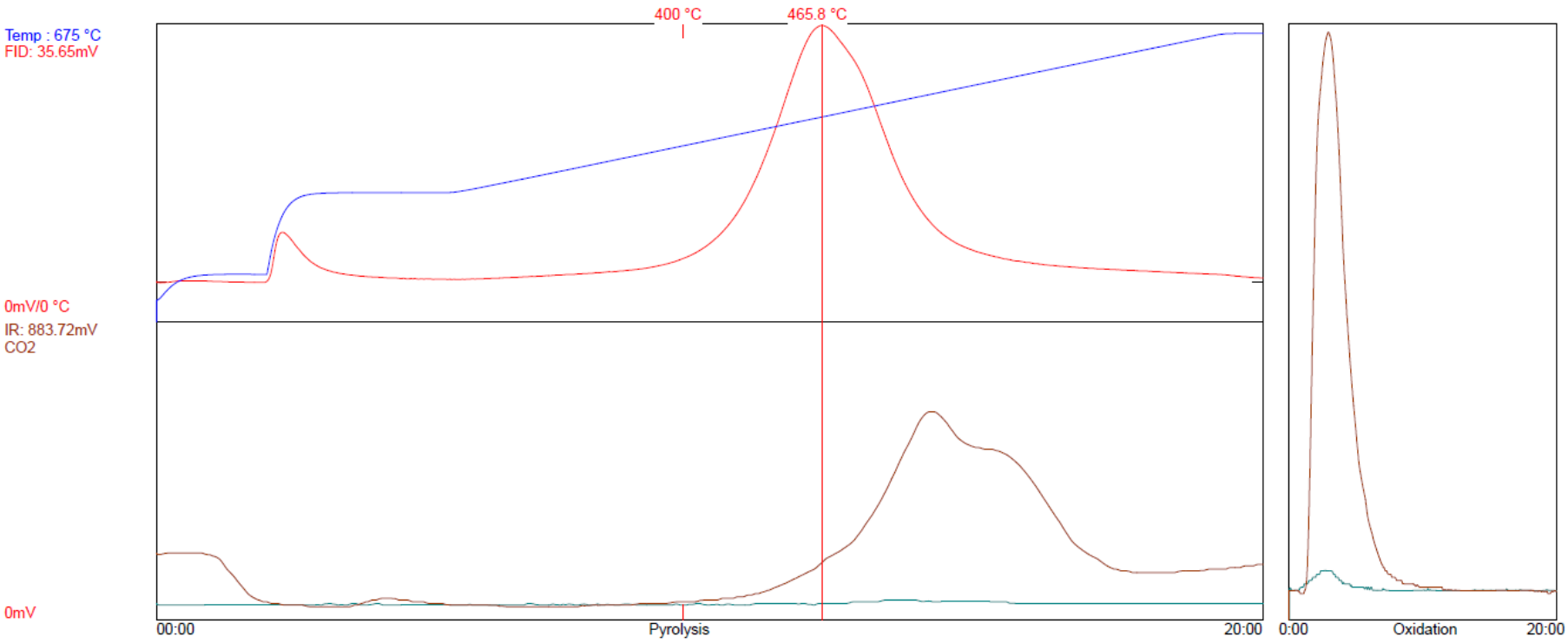

vTPH(S1):.30mg/g pTPH(S2): 5.16mg/g cTemp(Tmax): 426.8°C tTemp:465.8°C S3:1.57mg/g TOC:2.42 % HI:213 OI:65 PI:0.05 S1/TOC:0.12

Monday, 21 July 2014 17:39:07

SR Analyzer (SRA -TOC) - TPH TOC Analysis v6.5.117

Sample ID: 632_245 **Acq. Type**: TPH **Weight**: 79.9 **Crucible**: 11
Depth: 245.0 (Measured) **Lithology**: None **Sample Type**: Core **Well Name**: 632
Acq. Date: July 17 2014 / 10:23:16 PM

Data: C:\SRA JOBS\SRA049_Greymouth lacustrine mudstones_17072014\632_245.RAW
Method: C:\Program Files\Thermal Station\GNS 300-650 STD 160000.sram
Sequence: C:\Program Files\Thermal Station\Data\SRA049 Greymouth lacustrine mudstones 17072014\SRA049 Greymouth lacustrine mudstones 17072014.sras
Method Information: Initial Temp: 300 °C -- Initial Time: 3 -- Rate : 25.0 °C/Min -- Final Temp: 650 °C -- Final Time: 1 Min -- OxiPurge: 5 Min -- OxiTime: 20 Min -- OxiTemp: 630 °C
FID Temp: 325 °C
FID Gain: Low (10^6)

Calibration Standard Information: Standard Name: 160000 TOC tTemp: 455.0 °C pTPH (S2): 12.43 mg/g S3: 0.79 mg/g S4: 22.40 mg/g
Operator: R Sykes **Instrument name**: SRA -TOC

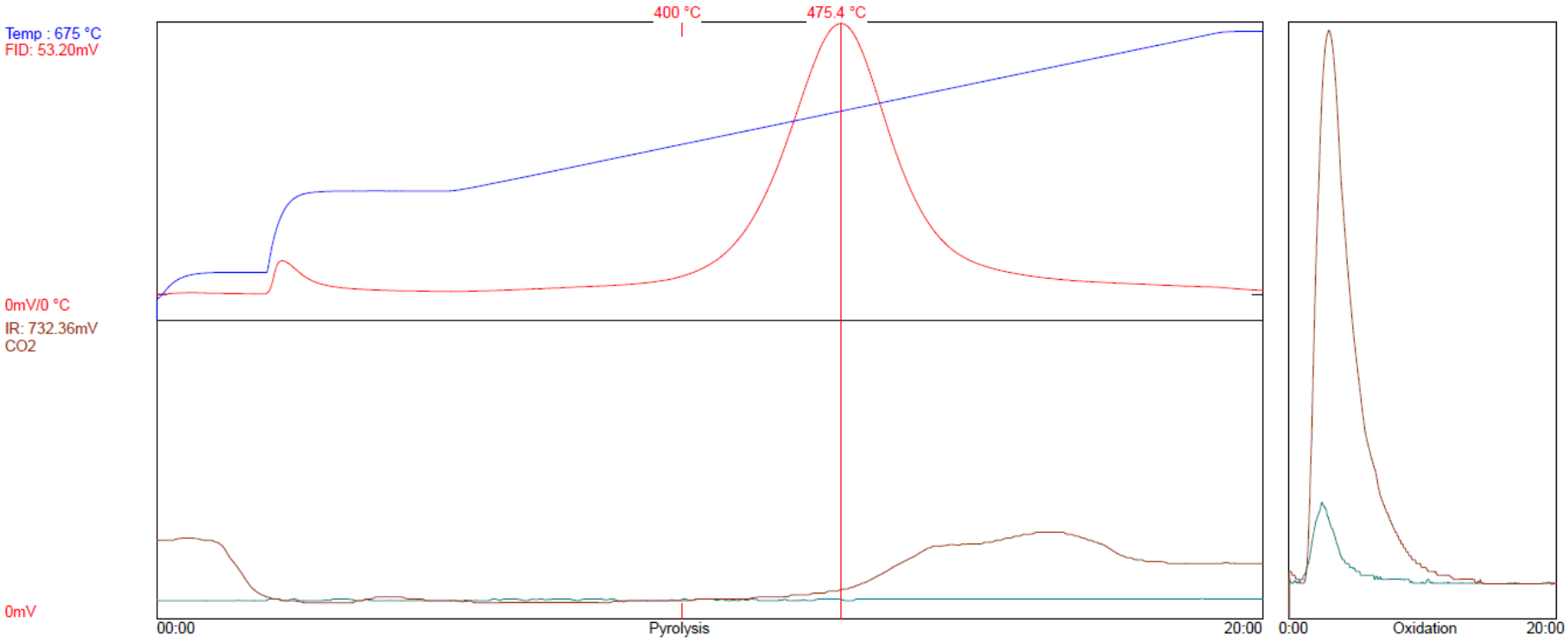

vTPH(S1):.31mg/g pTPH(S2): 7.61mg/g cTemp(Tmax): 436.4°C tTemp:475.4°C S3:.53mg/g TOC:2.76 % HI:275 OI:19 PI:0.04 S1/TOC:0.11

Monday, 21 July 2014 17:39:33

SR Analyzer (SRA -TOC) - TPH TOC Analysis v6.5.117

Sample ID: 632_587-8 **Acq. Type**: TPH **Weight**: 81.7 **Crucible**: 12
Depth: 587.8 (Measured) **Lithology**: None **Sample Type**: Core **Well Name**: 632
Acq. Date: July 17 2014 / 11:18:02 PM

Data: C:\SRA JOBS\SRA049_Greymouth lacustrine mudstones_17072014\632_587-8.RAW
Method: C:\Program Files\Thermal Station\GNS 300-650 STD 160000.sram
Sequence: C:\Program Files\Thermal Station\Data\SRA049 Greymouth lacustrine mudstones 17072014\SRA049 Greymouth lacustrine mudstones 17072014.sras
Method Information: Initial Temp: 300 °C -- Initial Time: 3 -- Rate : 25.0 °C/Min -- Final Temp: 650 °C -- Final Time: 1 Min -- OxiPurge: 5 Min -- OxiTime: 20 Min -- OxiTemp: 630 °C
FID Temp: 325 °C
FID Gain: Low (10^6)

Calibration Standard Information: Standard Name: 160000 TOC tTemp: 455.0 °C pTPH (S2): 12.43 mg/g S3: 0.79 mg/g S4: 22.40 mg/g
Operator: R Sykes **Instrument name**: SRA -TOC

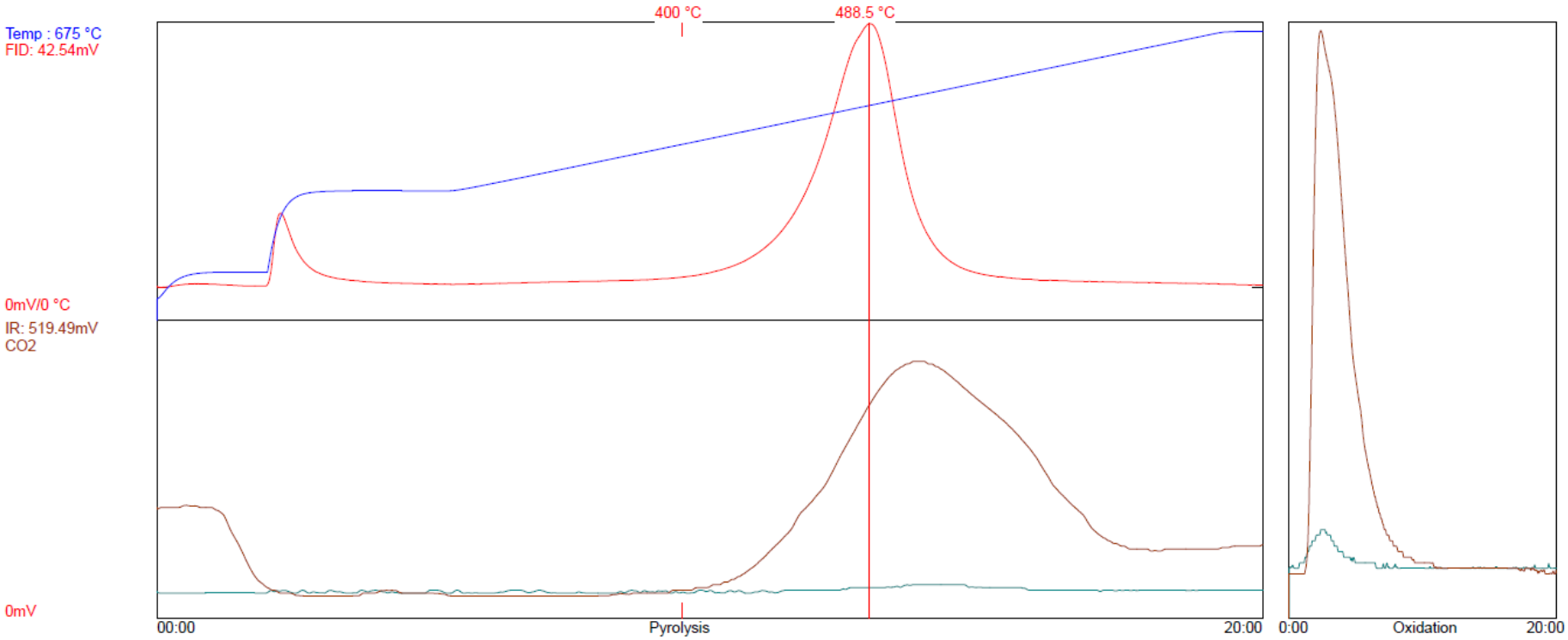

vTPH(S1):.41mg/g pTPH(S2): 4.25mg/g cTemp(Tmax): 449.5°C tTemp:488.5°C S3:1.18mg/g TOC:1.67 % HI:255 OI:71 PI:0.09 S1/TOC:0.25

Monday, 21 July 2014 17:40:09

SR Analyzer (SRA -TOC) - TPH TOC Analysis v6.5.117

Sample ID: 632_606 **Acq. Type**: TPH **Weight**: 100.0 **Crucible**: 13
Depth: 606 (Measured) **Lithology**: None **Sample Type**: Core **Well Name**: 632
Acq. Date: July 18 2014 / 12:12:45 AM

Data: C:\SRA JOBS\SRA049_Greymouth lacustrine mudstones_17072014\632_606.RAW
Method: C:\Program Files\Thermal Station\GNS 300-650 STD 160000.sram
Sequence: C:\Program Files\Thermal Station\Data\SRA049 Greymouth lacustrine mudstones 17072014\SRA049 Greymouth lacustrine mudstones 17072014.sras
Method Information: Initial Temp: 300 °C -- Initial Time: 3 -- Rate : 25.0 °C/Min -- Final Temp: 650 °C -- Final Time: 1 Min -- OxiPurge: 5 Min -- OxiTime: 20 Min -- OxiTemp: 630 °C
FID Temp: 325 °C
FID Gain: Low (10^6)

Calibration Standard Information: Standard Name: 160000 TOC tTemp: 455.0 °C pTPH (S2): 12.43 mg/g S3: 0.79 mg/g S4: 22.40 mg/g
Operator: R Sykes **Instrument name**: SRA -TOC

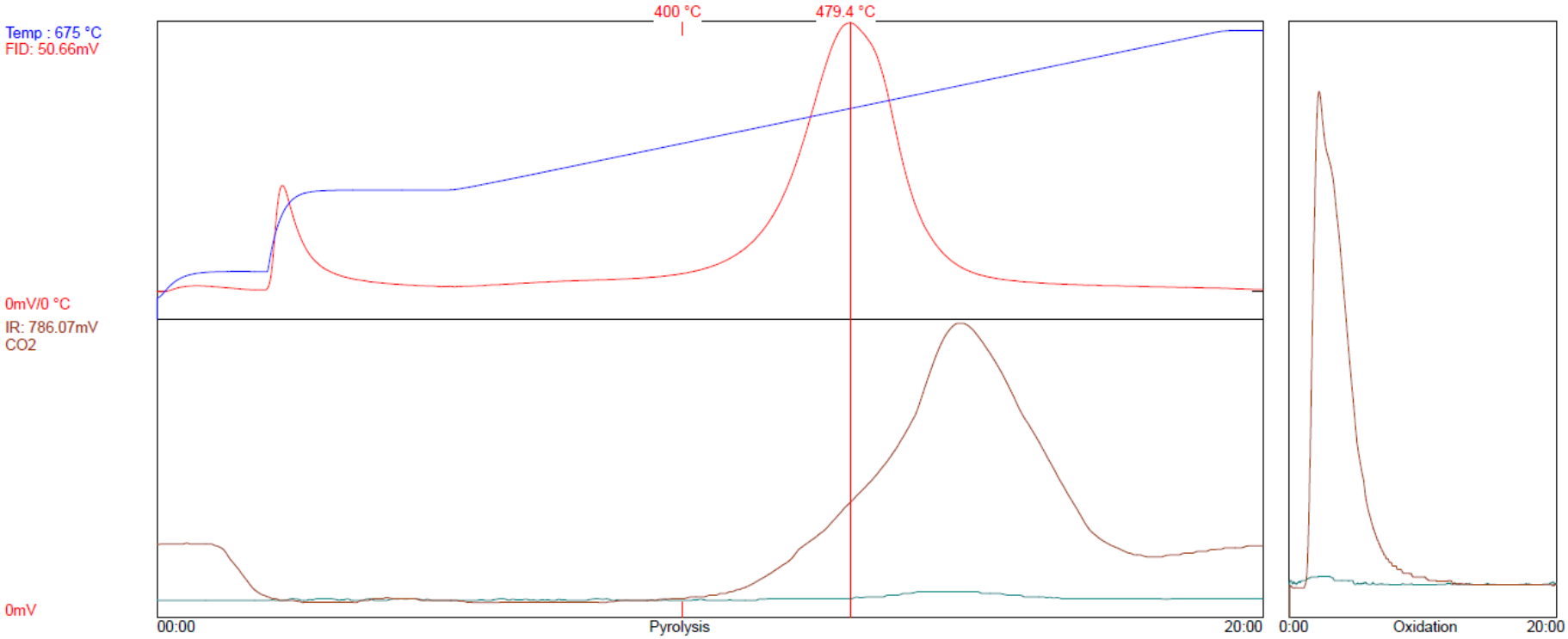

vTPH(S1):.65mg/g pTPH(S2): 5.16mg/g cTemp(Tmax): 440.4°C tTemp:479.4°C S3:1.26mg/g TOC:1.77 % HI:292 OI:71 PI:0.11 S1/TOC:0.37

Monday, 21 July 2014 17:40:37

SR Analyzer (SRA -TOC) - TPH TOC Analysis v6.5.117

Sample ID: 633_368 **Acq. Type**: TPH **Weight**: 79.2 **Crucible**: 15
Depth: 368 (Measured) **Lithology**: None **Sample Type**: Core **Well Name**: 633
Acq. Date: July 18 2014 / 2:02:23 AM

Data: C:\SRA JOBS\SRA049_Greymouth lacustrine mudstones_17072014\633_368.RAW
Method: C:\Program Files\Thermal Station\GNS 300-650 STD 160000.sram
Sequence: C:\Program Files\Thermal Station\Data\SRA049 Greymouth lacustrine mudstones 17072014\SRA049 Greymouth lacustrine mudstones 17072014.sras
Method Information: Initial Temp: 300 °C -- Initial Time: 3 -- Rate : 25.0 °C/Min -- Final Temp: 650 °C -- Final Time: 1 Min -- OxiPurge: 5 Min -- OxiTime: 20 Min -- OxiTemp: 630 °C
FID Temp: 325 °C
FID Gain: Low (10^6)

Calibration Standard Information: Standard Name: 160000 TOC tTemp: 455.0 °C pTPH (S2): 12.43 mg/g S3: 0.79 mg/g S4: 22.40 mg/g
Operator: R Sykes **Instrument name**: SRA -TOC

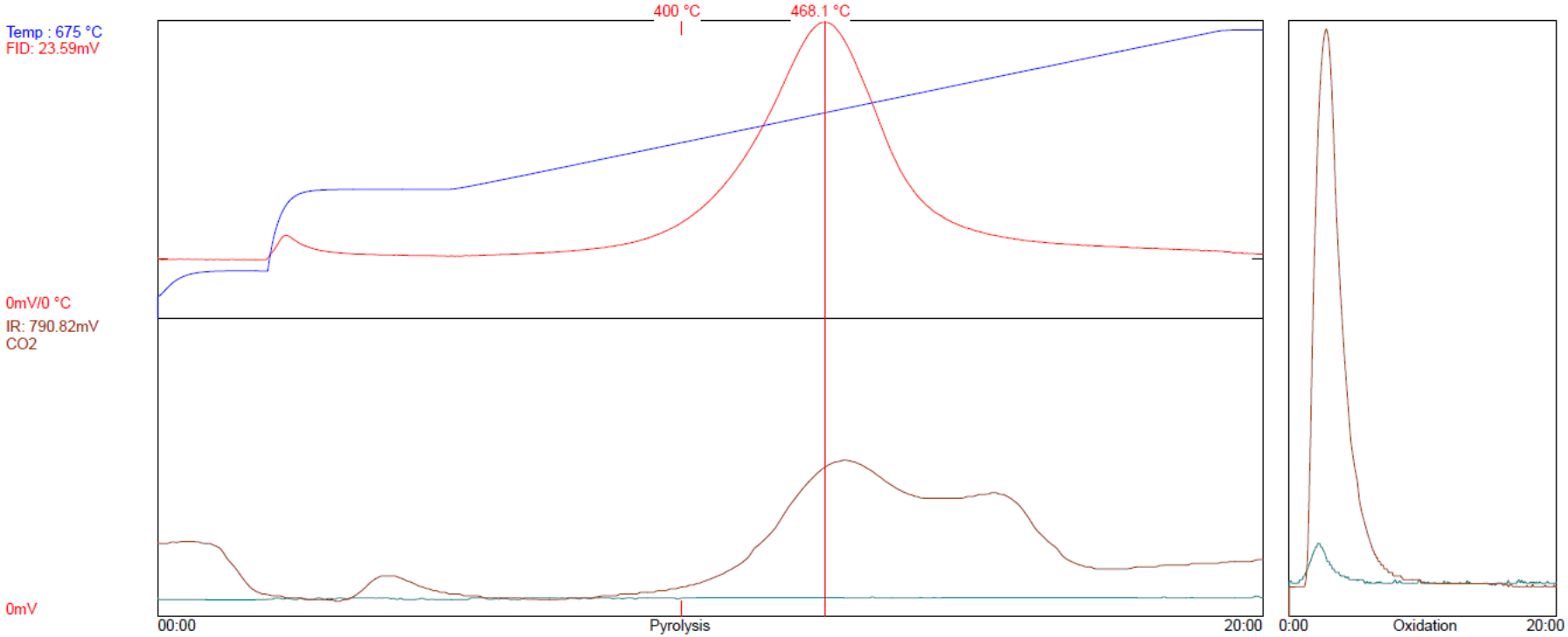

vTPH(S1):.10mg/g pTPH(S2): 3.41mg/g cTemp(Tmax): 429.1°C tTemp:468.1°C S3:2.90mg/g TOC:1.89 % HI:181 OI:154 PI:0.03 S1/TOC:0.06

Monday, 21 July 2014 17:41:17

SR Analyzer (SRA -TOC) - TPH TOC Analysis v6.5.117

Sample ID: 636_195-97 **Acq. Type**: TPH **Weight**: 79.8 **Crucible**: 16
Depth: 195.97 (Measured) **Lithology**: None **Sample Type**: Core **Well Name**: 636
Acq. Date: July 18 2014 / 2:57:07 AM

Data: C:\SRA JOBS\SRA049_Greymouth lacustrine mudstones_17072014\636_195-97.RAW
Method: C:\Program Files\Thermal Station\GNS 300-650 STD 160000.sram
Sequence: C:\Program Files\Thermal Station\Data\SRA049 Greymouth lacustrine mudstones 17072014\SRA049 Greymouth lacustrine mudstones 17072014.sras
Method Information: Initial Temp: 300 °C -- Initial Time: 3 -- Rate : 25.0 °C/Min -- Final Temp: 650 °C -- Final Time: 1 Min -- OxiPurge: 5 Min -- OxiTime: 20 Min -- OxiTemp: 630 °C
FID Temp: 325 °C
FID Gain: Low (10^6)

Calibration Standard Information: Standard Name: 160000 TOC tTemp: 455.0 °C pTPH (S2): 12.43 mg/g S3: 0.79 mg/g S4: 22.40 mg/g
Operator: R Sykes **Instrument name**: SRA -TOC

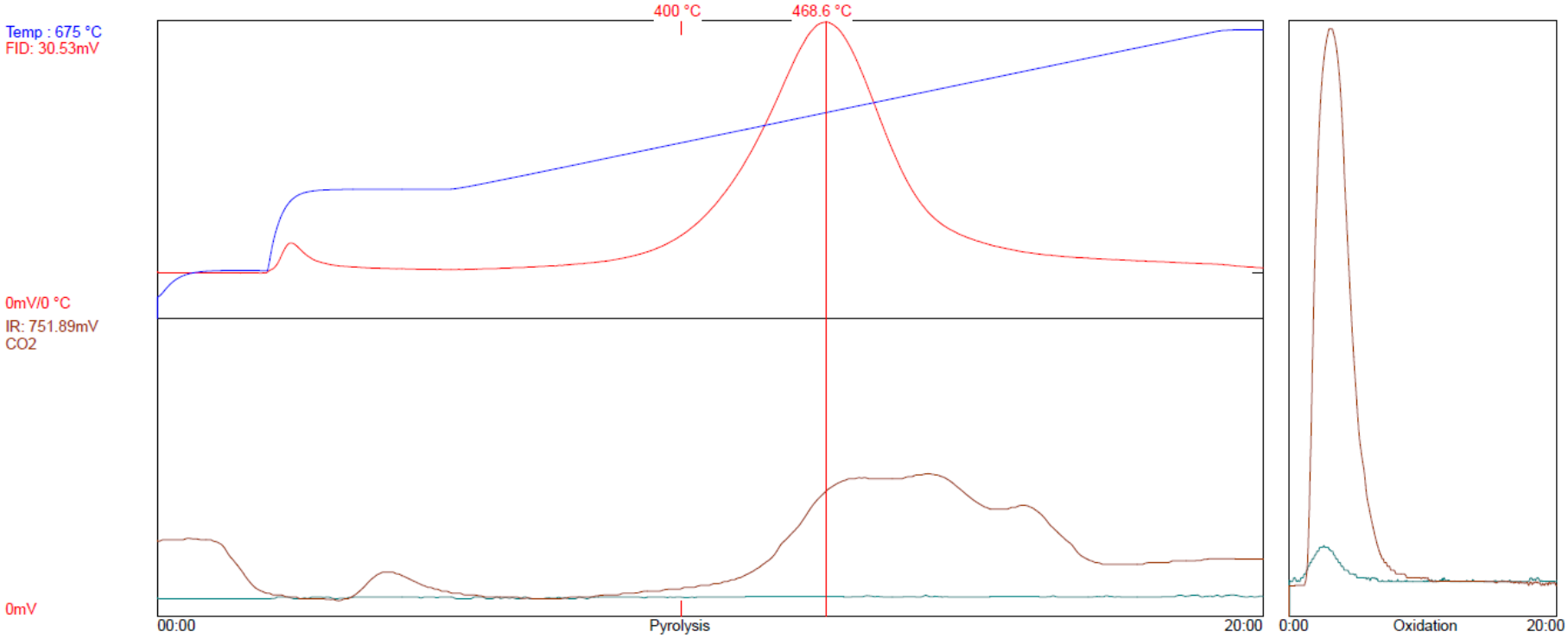

vTPH(S1):.15mg/g pTPH(S2): 4.72mg/g cTemp(Tmax): 429.6°C tTemp:468.6°C S3:2.36mg/g TOC:2.26 % HI:209 OI:104 PI:0.03 S1/TOC:0.07

Monday, 21 July 2014 17:41:44

SR Analyzer (SRA -TOC) - TPH TOC Analysis v6.5.117

Sample ID: 636_249-8 **Acq. Type**: TPH **Weight**: 80.8 **Crucible**: 17
Depth: 249.8 (Measured) **Lithology**: None **Sample Type**: Core **Well Name**: 636
Acq. Date: July 18 2014 / 3:51:52 AM

Data: C:\SRA JOBS\SRA049_Greymouth lacustrine mudstones_17072014\636_249-8.RAW
Method: C:\Program Files\Thermal Station\GNS 300-650 STD 160000.sram
Sequence: C:\Program Files\Thermal Station\Data\SRA049 Greymouth lacustrine mudstones 17072014\SRA049 Greymouth lacustrine mudstones 17072014.sras
Method Information: Initial Temp: 300 °C -- Initial Time: 3 -- Rate : 25.0 °C/Min -- Final Temp: 650 °C -- Final Time: 1 Min -- OxiPurge: 5 Min -- OxiTime: 20 Min -- OxiTemp: 630 °C
FID Temp: 325 °C
FID Gain: Low (10^6)

Calibration Standard Information: Standard Name: 160000 TOC tTemp: 455.0 °C pTPH (S2): 12.43 mg/g S3: 0.79 mg/g S4: 22.40 mg/g
Operator: R Sykes **Instrument name**: SRA -TOC

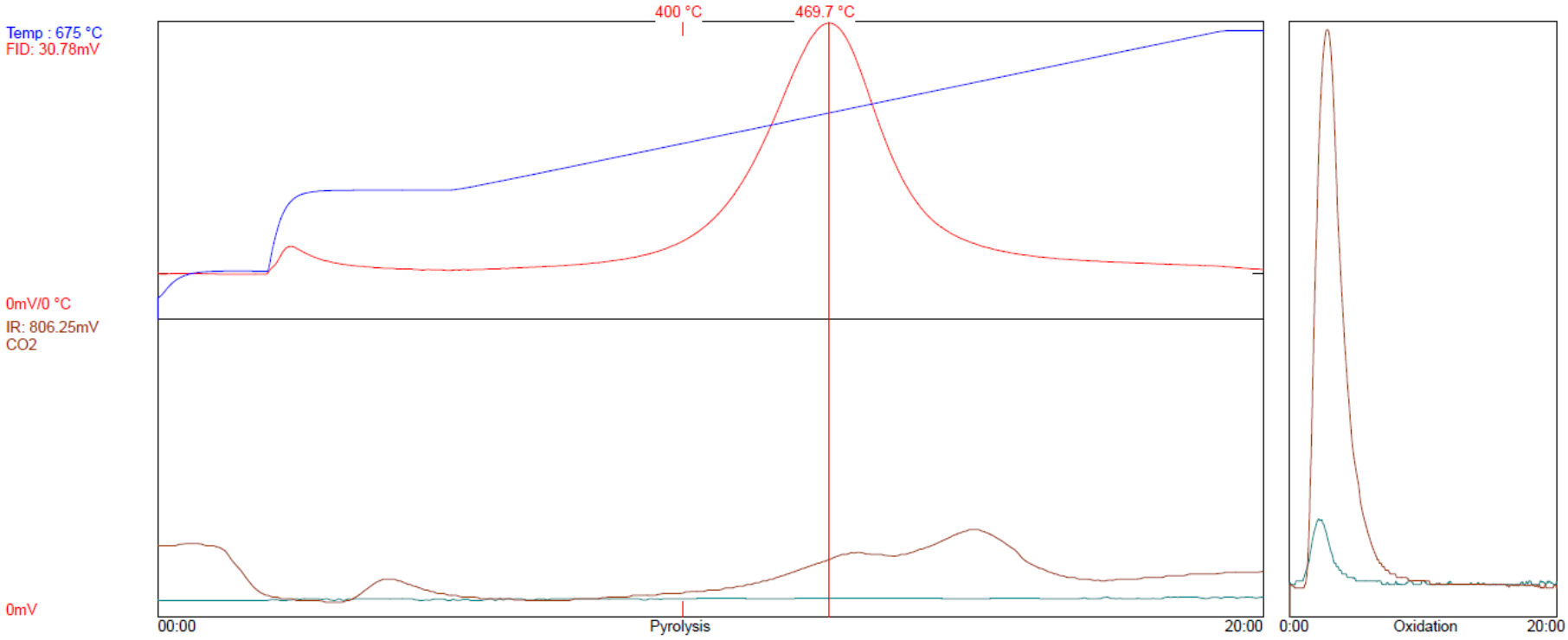

vTPH(S1):.18mg/g pTPH(S2): 4.47mg/g cTemp(Tmax): 430.7°C tTemp:469.7°C S3:1.36mg/g TOC:2.09 % HI:214 OI:65 PI:0.04 S1/TOC:0.09

Monday, 21 July 2014 17:42:57

SR Analyzer (SRA -TOC) - TPH TOC Analysis v6.5.117

Sample ID: 651_470 **Acq. Type**: TPH **Weight**: 81.9 **Crucible**: 18
Depth: 470.0 (Measured) **Lithology**: None **Sample Type**: Core **Well Name**: 651
Acq. Date: July 18 2014 / 4:46:35 AM

Data: C:\SRA JOBS\SRA049_Greymouth lacustrine mudstones_17072014\651_470.RAW
Method: C:\Program Files\Thermal Station\GNS 300-650 STD 160000.sram
Sequence: C:\Program Files\Thermal Station\Data\SRA049 Greymouth lacustrine mudstones 17072014\SRA049 Greymouth lacustrine mudstones 17072014.sras
Method Information: Initial Temp: 300 °C -- Initial Time: 3 -- Rate : 25.0 °C/Min -- Final Temp: 650 °C -- Final Time: 1 Min -- OxiPurge: 5 Min -- OxiTime: 20 Min -- OxiTemp: 630 °C
FID Temp: 325 °C
FID Gain: Low (10^6)

Calibration Standard Information: Standard Name: 160000 TOC tTemp: 455.0 °C pTPH (S2): 12.43 mg/g S3: 0.79 mg/g S4: 22.40 mg/g
Operator: R Sykes **Instrument name**: SRA -TOC

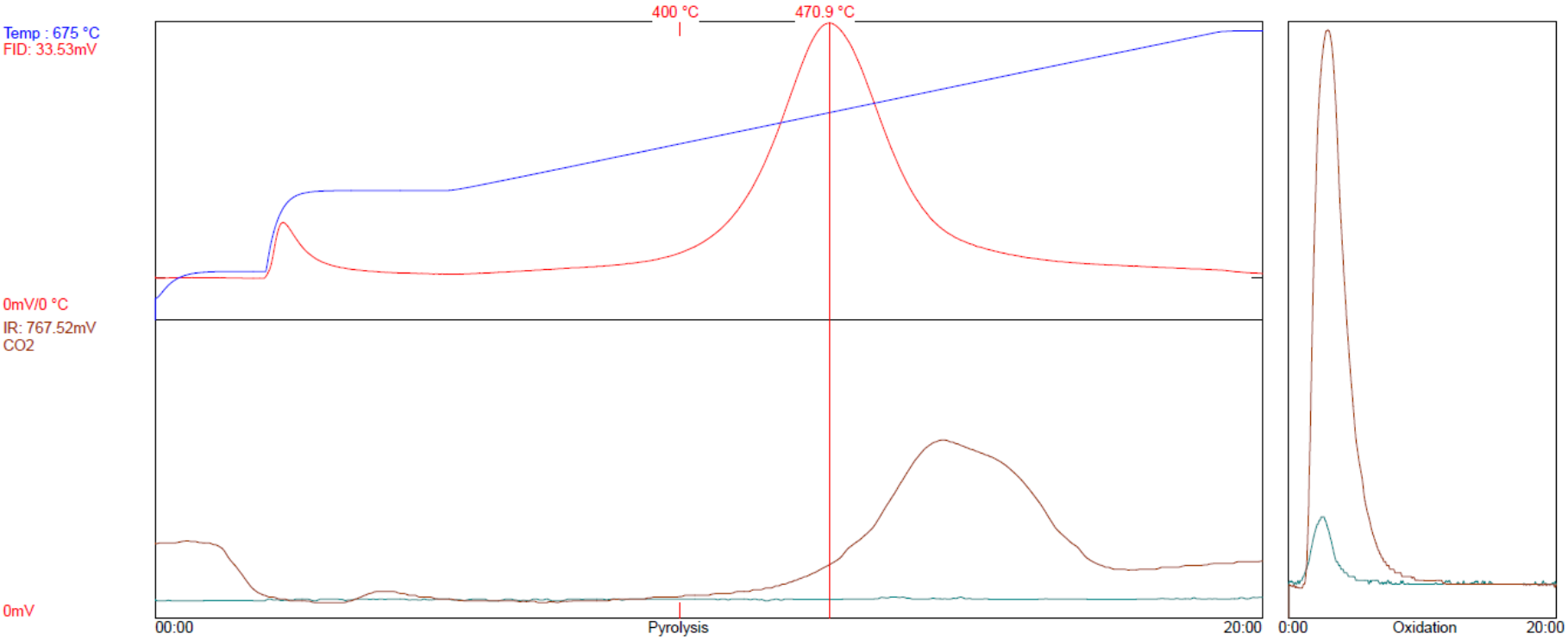

vTPH(S1):.30mg/g pTPH(S2): 4.76mg/g cTemp(Tmax): 431.9°C tTemp:470.9°C S3:.99mg/g TOC:2.23 % HI:213 OI:44 PI:0.06 S1/TOC:0.13

Monday, 21 July 2014 17:44:33

SR Analyzer (SRA -TOC) - TPH TOC Analysis v6.5.117

Sample ID: 654_649-6 **Acq. Type**: TPH **Weight**: 79.9 **Crucible**: 19
Depth: 649.6 (Measured) **Lithology**: None **Sample Type**: Core **Well Name**: 654
Acq. Date: July 18 2014 / 5:41:25 AM

Data: C:\SRA JOBS\SRA049_Greymouth lacustrine mudstones_17072014\654_649-6.RAW
Method: C:\Program Files\Thermal Station\GNS 300-650 STD 160000.sram
Sequence: C:\Program Files\Thermal Station\Data\SRA049 Greymouth lacustrine mudstones 17072014\SRA049 Greymouth lacustrine mudstones 17072014.sras
Method Information: Initial Temp: 300 °C -- Initial Time: 3 -- Rate : 25.0 °C/Min -- Final Temp: 650 °C -- Final Time: 1 Min -- OxiPurge: 5 Min -- OxiTime: 20 Min -- OxiTemp: 630 °C
FID Temp: 325 °C
FID Gain: Low (10^6)

Calibration Standard Information: Standard Name: 160000 TOC tTemp: 455.0 °C pTPH (S2): 12.43 mg/g S3: 0.79 mg/g S4: 22.40 mg/g
Operator: R Sykes **Instrument name**: SRA -TOC

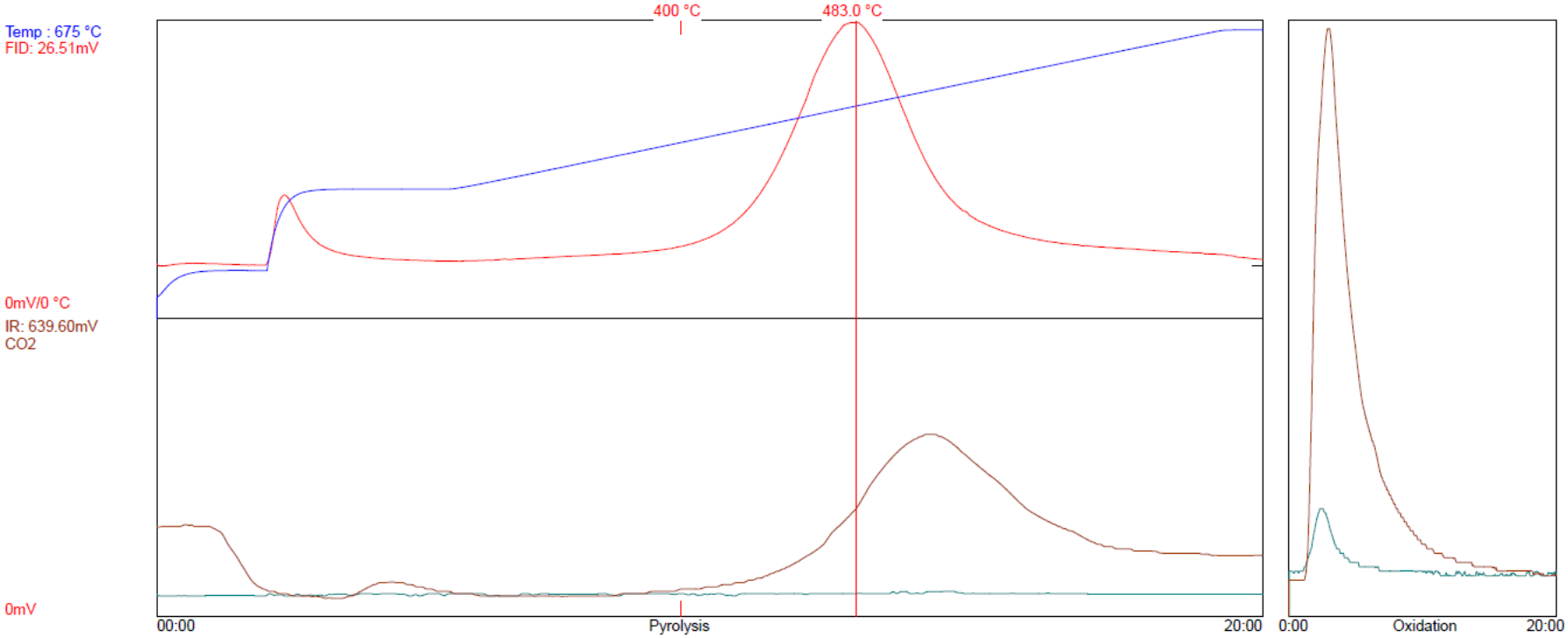

vTPH(S1):.31mg/g pTPH(S2): 3.94mg/g cTemp(Tmax): 444.0°C tTemp:483.0°C S3:1.43mg/g TOC:2.30 % HI:172 OI:62 PI:0.07 S1/TOC:0.14

Monday, 21 July 2014 17:45:16

SR Analyzer (SRA -TOC) - TPH TOC Analysis v6.5.117

Sample ID: 654_862-7 **Acq. Type**: TPH **Weight**: 79.8 **Crucible**: 20
Depth: 862.7 (Measured) **Lithology**: None **Sample Type**: Core **Well Name**: 654
Acq. Date: July 18 2014 / 6:36:06 AM

Data: C:\SRA JOBS\SRA049_Greymouth lacustrine mudstones_17072014\654_862-7.RAW
Method: C:\Program Files\Thermal Station\GNS 300-650 STD 160000.sram
Sequence: C:\Program Files\Thermal Station\Data\SRA049 Greymouth lacustrine mudstones 17072014\SRA049 Greymouth lacustrine mudstones 17072014.sras
Method Information: Initial Temp: 300 °C -- Initial Time: 3 -- Rate : 25.0 °C/Min -- Final Temp: 650 °C -- Final Time: 1 Min -- OxiPurge: 5 Min -- OxiTime: 20 Min -- OxiTemp: 630 °C
FID Temp: 325 °C
FID Gain: Low (10^6)

Calibration Standard Information: Standard Name: 160000 TOC tTemp: 455.0 °C pTPH (S2): 12.43 mg/g S3: 0.79 mg/g S4: 22.40 mg/g
Operator: R Sykes **Instrument name**: SRA -TOC

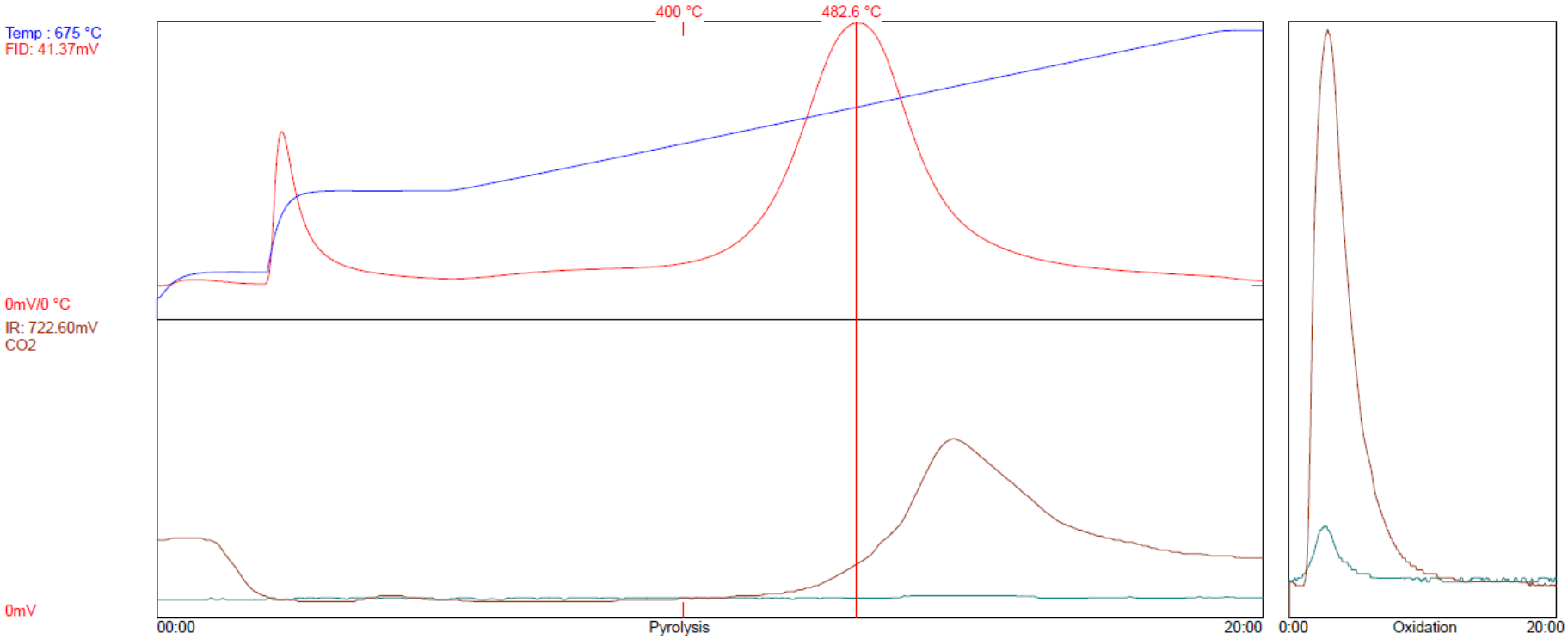

vTPH(S1):.93mg/g pTPH(S2): 6.63mg/g cTemp(Tmax): 443.6°C tTemp:482.6°C S3:.71mg/g TOC:2.62 % HI:253 OI:27 PI:0.12 S1/TOC:0.35

Monday, 21 July 2014 17:45:50

SR Analyzer (SRA -TOC) - TPH TOC Analysis v6.5.117

Sample ID: 656_461-8 **Acq. Type**: TPH **Weight**: 78.8 **Crucible**: 21
Depth: 461.8 (Measured) **Lithology**: None **Sample Type**: Core **Well Name**: 656
Acq. Date: July 18 2014 / 7:30:49 AM

Data: C:\SRA JOBS\SRA049_Greymouth lacustrine mudstones_17072014\656_461-8.RAW
Method: C:\Program Files\Thermal Station\GNS 300-650 STD 160000.sram
Sequence: C:\Program Files\Thermal Station\Data\SRA049 Greymouth lacustrine mudstones 17072014\SRA049 Greymouth lacustrine mudstones 17072014.sras
Method Information: Initial Temp: 300 °C -- Initial Time: 3 -- Rate : 25.0 °C/Min -- Final Temp: 650 °C -- Final Time: 1 Min -- OxiPurge: 5 Min -- OxiTime: 20 Min -- OxiTemp: 630 °C
FID Temp: 325 °C
FID Gain: Low (10^6)

Calibration Standard Information: Standard Name: 160000 TOC tTemp: 455.0 °C pTPH (S2): 12.43 mg/g S3: 0.79 mg/g S4: 22.40 mg/g
Operator: R Sykes **Instrument name**: SRA -TOC

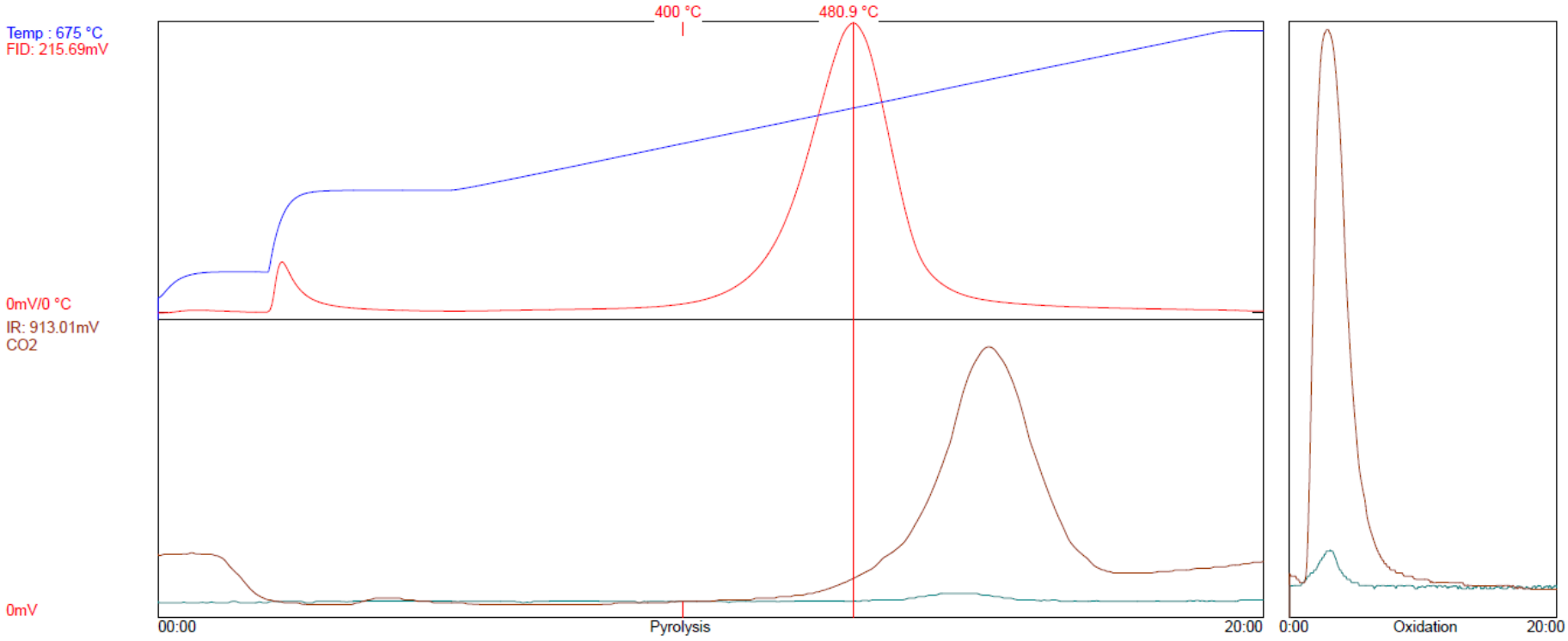

vTPH(S1):1.49mg/g pTPH(S2): 25.08mg/g cTemp(Tmax): 441.9°C tTemp:480.9°C S3:.75mg/g TOC:4.54 % HI:552 OI:16 PI:0.06 S1/TOC:0.33

Monday, 21 July 2014 17:46:28

SR Analyzer (SRA -TOC) - TPH TOC Analysis v6.5.117

Sample ID: 658_251 **Acq. Type**: TPH **Weight**: 80.1 **Crucible**: 22
Depth: 251.0 (Measured) **Lithology**: None **Sample Type**: Core **Well Name**: 658
Acq. Date: July 18 2014 / 8:25:29 AM

Data: C:\SRA JOBS\SRA049_Greymouth lacustrine mudstones_17072014\658_251.RAW
Method: C:\Program Files\Thermal Station\GNS 300-650 STD 160000.sram
Sequence: C:\Program Files\Thermal Station\Data\SRA049 Greymouth lacustrine mudstones 17072014\SRA049 Greymouth lacustrine mudstones 17072014.sras
Method Information: Initial Temp: 300 °C -- Initial Time: 3 -- Rate : 25.0 °C/Min -- Final Temp: 650 °C -- Final Time: 1 Min -- OxiPurge: 5 Min -- OxiTime: 20 Min -- OxiTemp: 630 °C
FID Temp: 325 °C
FID Gain: Low (10^6)

Calibration Standard Information: Standard Name: 160000 TOC tTemp: 455.0 °C pTPH (S2): 12.43 mg/g S3: 0.79 mg/g S4: 22.40 mg/g
Operator: R Sykes **Instrument name**: SRA -TOC

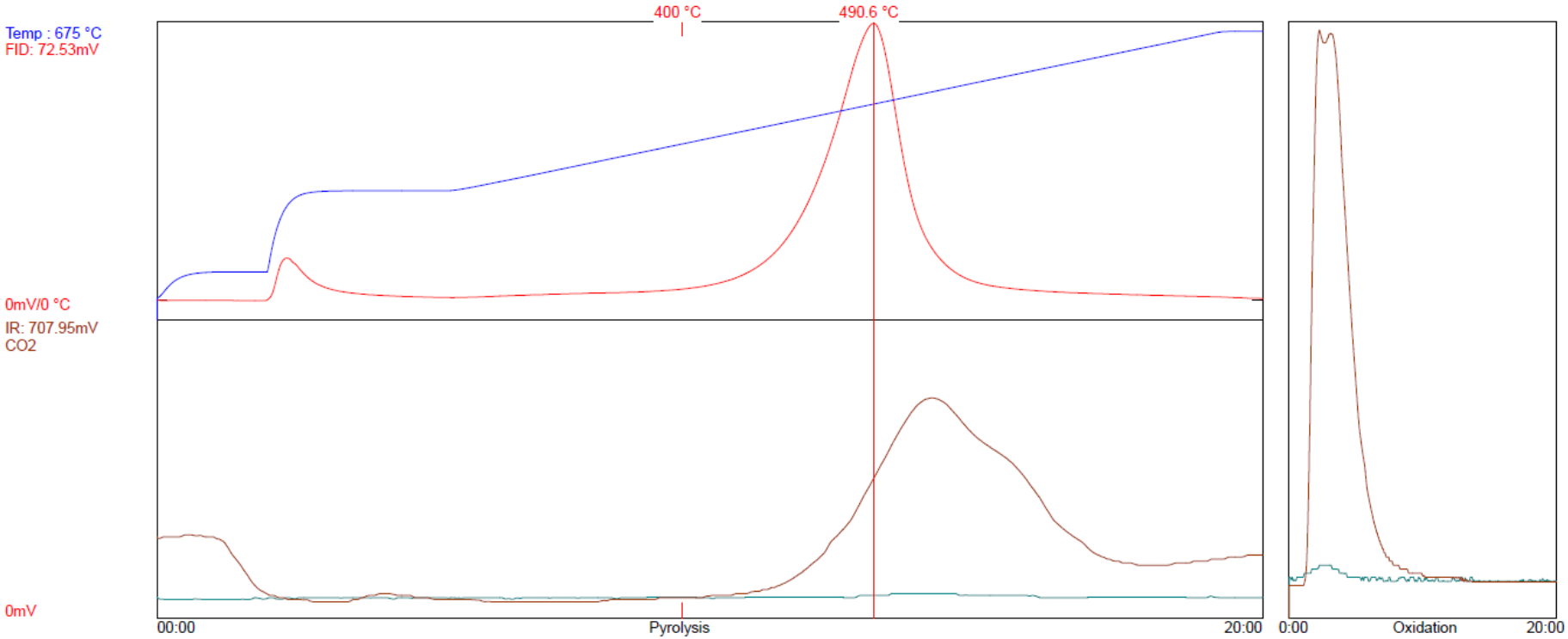

vTPH(S1):.53mg/g pTPH(S2): 7.76mg/g cTemp(Tmax): 451.6°C tTemp:490.6°C S3:1.39mg/g TOC:2.50 % HI:311 OI:55 PI:0.06 S1/TOC:0.21

Monday, 21 July 2014 17:47:04

SR Analyzer (SRA -TOC) - TPH TOC Analysis v6.5.117

Sample ID: 658_303 **Acq. Type**: TPH **Weight**: 79.4 **Crucible**: 23
Depth: 303.0 (Measured) **Lithology**: None **Sample Type**: Core **Well Name**: 658
Acq. Date: July 18 2014 / 9:20:03 AM

Data: C:\SRA JOBS\SRA049_Greymouth lacustrine mudstones_17072014\658_303.RAW
Method: C:\Program Files\Thermal Station\GNS 300-650 STD 160000.sram
Sequence: C:\Program Files\Thermal Station\Data\SRA049 Greymouth lacustrine mudstones 17072014\SRA049 Greymouth lacustrine mudstones 17072014.sras
Method Information: Initial Temp: 300 °C -- Initial Time: 3 -- Rate : 25.0 °C/Min -- Final Temp: 650 °C -- Final Time: 1 Min -- OxiPurge: 5 Min -- OxiTime: 20 Min -- OxiTemp: 630 °C
FID Temp: 325 °C
FID Gain: Low (10^6)

Calibration Standard Information: Standard Name: 160000 TOC tTemp: 455.0 °C pTPH (S2): 12.43 mg/g S3: 0.79 mg/g S4: 22.40 mg/g
Operator: R Sykes **Instrument name**: SRA -TOC

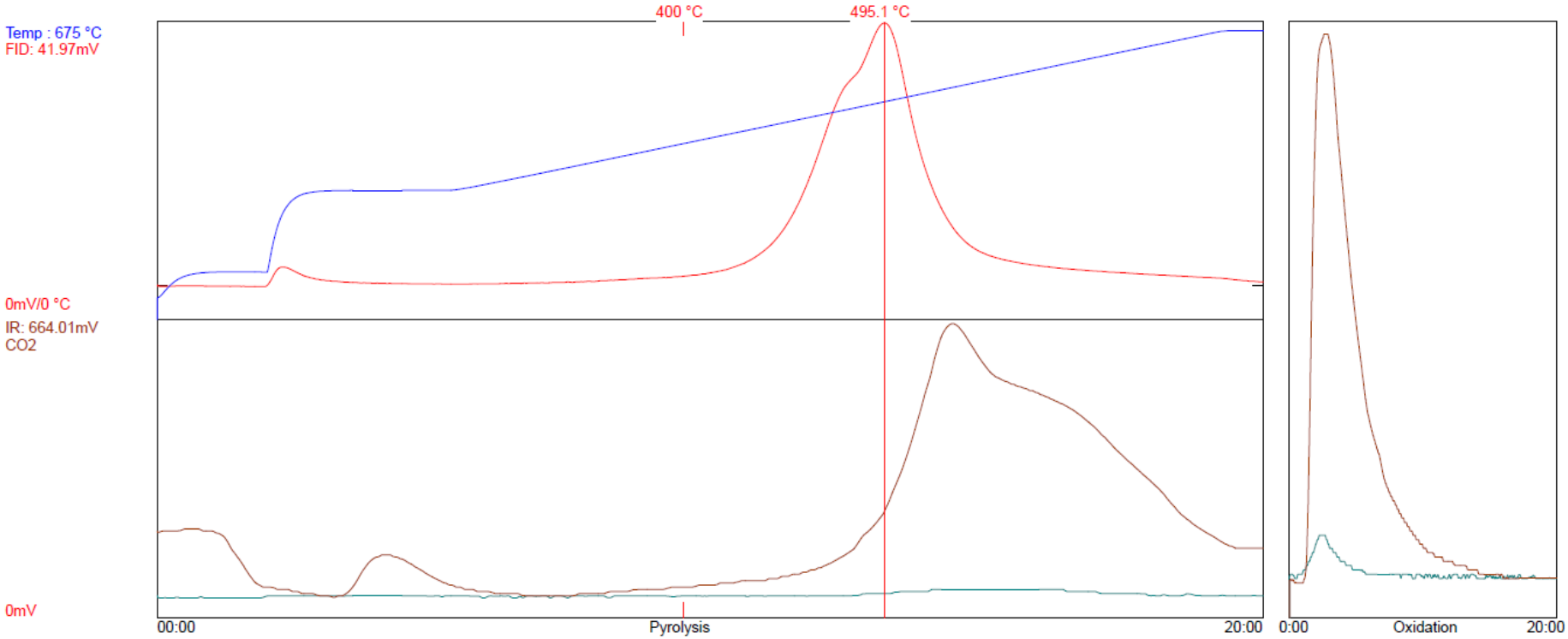

vTPH(S1):.15mg/g pTPH(S2): 5.24mg/g cTemp(Tmax): 456.1°C tTemp:495.1°C S3:1.58mg/g TOC:2.56 % HI:204 OI:62 PI:0.03 S1/TOC:0.06

Monday, 21 July 2014 17:47:34

SR Analyzer (SRA -TOC) - TPH TOC Analysis v6.5.117

Sample ID: 659_233 **Acq. Type**: TPH **Weight**: 78.8 **Crucible**: 24
Depth: 233.0 (Measured) **Lithology**: None **Sample Type**: Core **Well Name**: 659
Acq. Date: July 18 2014 / 10:14:52 AM

Data: C:\SRA JOBS\SRA049_Greymouth lacustrine mudstones_17072014\659_233.RAW
Method: C:\Program Files\Thermal Station\GNS 300-650 STD 160000.sram
Sequence: C:\Program Files\Thermal Station\Data\SRA049 Greymouth lacustrine mudstones 17072014\SRA049 Greymouth lacustrine mudstones 17072014.sras
Method Information: Initial Temp: 300 °C -- Initial Time: 3 -- Rate : 25.0 °C/Min -- Final Temp: 650 °C -- Final Time: 1 Min -- OxiPurge: 5 Min -- OxiTime: 20 Min -- OxiTemp: 630 °C
FID Temp: 325 °C
FID Gain: Low (10^6)

Calibration Standard Information: Standard Name: 160000 TOC tTemp: 455.0 °C pTPH (S2): 12.43 mg/g S3: 0.79 mg/g S4: 22.40 mg/g
Operator: R Sykes **Instrument name**: SRA -TOC

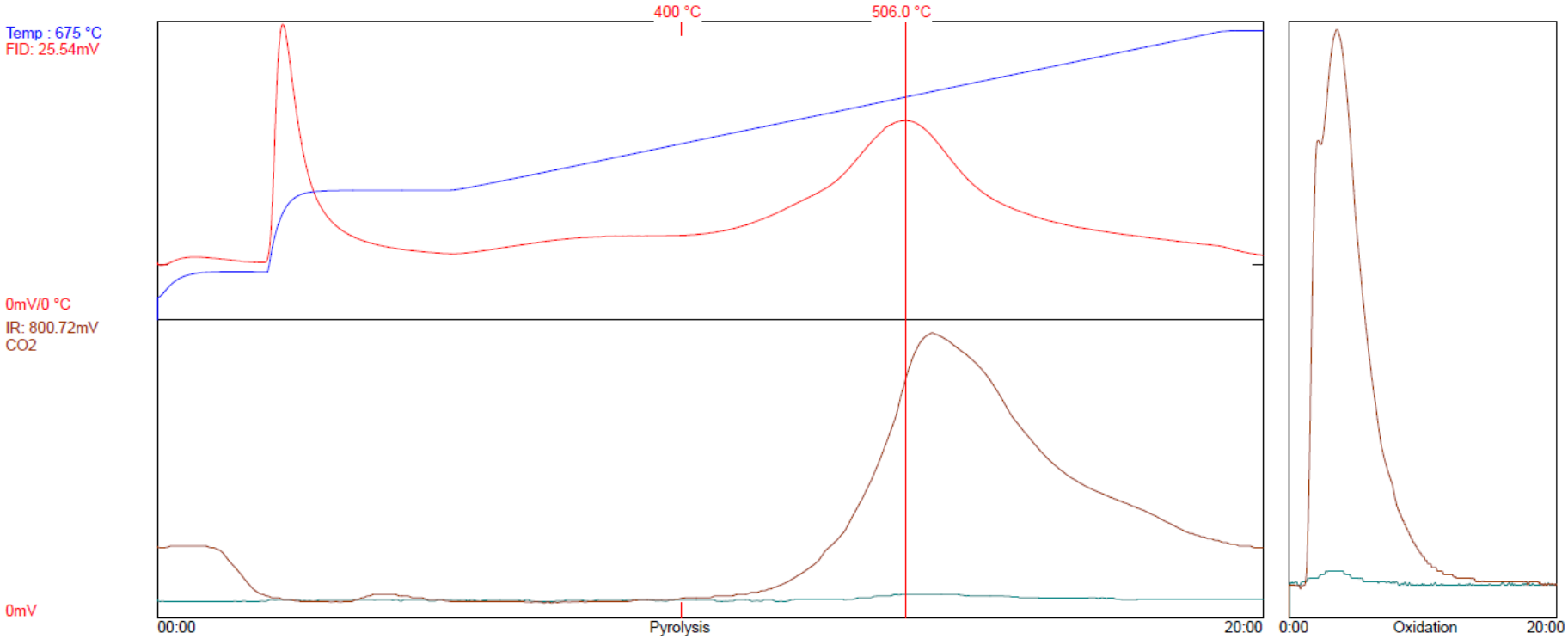

vTPH(S1):.92mg/g pTPH(S2): 3.51mg/g cTemp(Tmax): 467.0°C tTemp:506.0°C S3:1.04mg/g TOC:3.08 % HI:114 OI:34 PI:0.21 S1/TOC:0.30

Monday, 21 July 2014 17:48:32

SR Analyzer (SRA -TOC) - TPH TOC Analysis v6.5.117

Sample ID: 659_245 **Acq. Type**: TPH **Weight**: 77.2 **Crucible**: 4
Depth: 245 (Measured) **Lithology**: None **Sample Type**: Core **Well Name**: 659
Acq. Date: July 20 2014 / 6:11:31 PM

Data: C:\SRA JOBS\SRA049C_Greymouth lacustrine mudstones_20072014\659_245.RAW
Method: C:\Program Files\Thermal Station\GNS 300-650 STD 160000.sram
Sequence: C:\Program Files\Thermal Station\Data\SRA049C Greymouth lacustrine mudstones 20072014\SRA049C Greymouth lacustrine mudstones 20072014.sras
Method Information: Initial Temp: 300 °C -- Initial Time: 3 -- Rate : 25.0 °C/Min -- Final Temp: 650 °C -- Final Time: 1 Min -- OxiPurge: 5 Min -- OxiTime: 20 Min -- OxiTemp: 630 °C
FID Temp: 325 °C
FID Gain: Low (10^6)

Calibration Standard Information: Standard Name: 160000 TOC tTemp: 455.0 °C pTPH (S2): 12.43 mg/g S3: 0.79 mg/g S4: 22.40 mg/g
Operator: R Sykes **Instrument name**: SRA -TOC

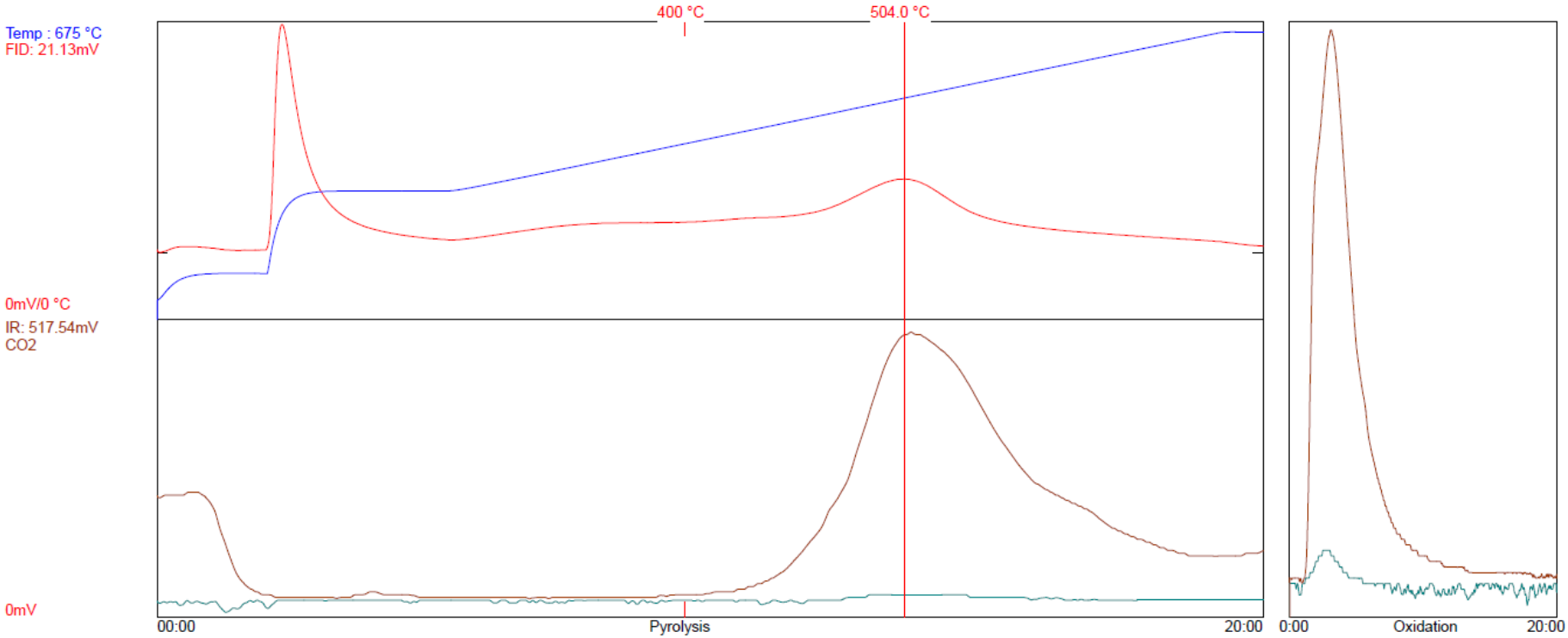

vTPH(S1):.86mg/g pTPH(S2): 2.11mg/g cTemp(Tmax): 465.0°C tTemp:504.0°C S3:.47mg/g TOC:1.77 % HI:119 OI:27 PI:0.29 S1/TOC:0.49

Monday, 21 July 2014 17:51:09

SR Analyzer (SRA -TOC) - TPH TOC Analysis v6.5.117

Sample ID: 659_249 **Acq. Type**: TPH **Weight**: 78.7 **Crucible**: 5
Depth: 249 (Measured) **Lithology**: None **Sample Type**: Core **Well Name**: 659
Acq. Date: July 20 2014 / 7:06:20 PM

Data: C:\SRA JOBS\SRA049C_Greymouth lacustrine mudstones_20072014\659_249.RAW
Method: C:\Program Files\Thermal Station\GNS 300-650 STD 160000.sram
Sequence: C:\Program Files\Thermal Station\Data\SRA049C Greymouth lacustrine mudstones 20072014\SRA049C Greymouth lacustrine mudstones 20072014.sras
Method Information: Initial Temp: 300 °C -- Initial Time: 3 -- Rate : 25.0 °C/Min -- Final Temp: 650 °C -- Final Time: 1 Min -- OxiPurge: 5 Min -- OxiTime: 20 Min -- OxiTemp: 630 °C
FID Temp: 325 °C
FID Gain: Low (10^6)

Calibration Standard Information: Standard Name: 160000 TOC tTemp: 455.0 °C pTPH (S2): 12.43 mg/g S3: 0.79 mg/g S4: 22.40 mg/g
Operator: R Sykes **Instrument name**: SRA -TOC

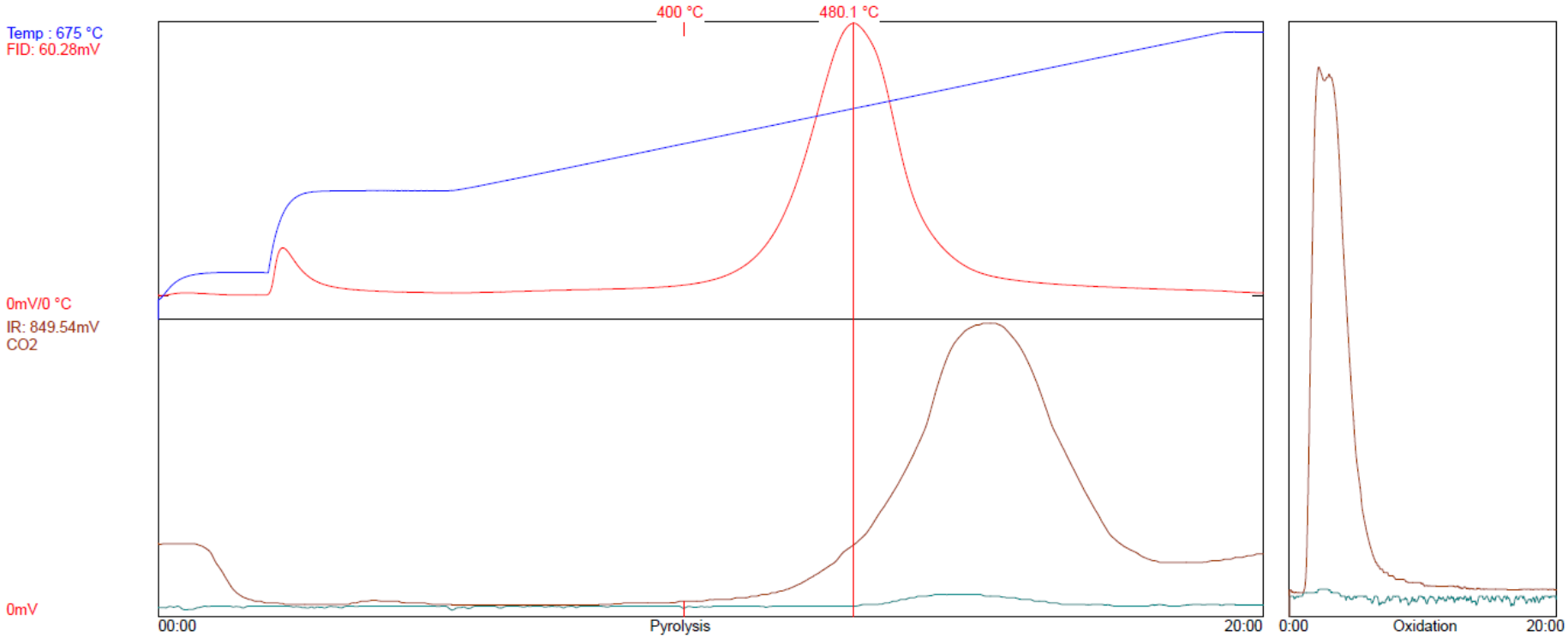

vTPH(S1):.52mg/g pTPH(S2): 8.31mg/g cTemp(Tmax): 441.1°C tTemp:480.1°C S3:.53mg/g TOC:2.65 % HI:313 OI:20 PI:0.06 S1/TOC:0.20

Monday, 21 July 2014 17:51:41

SR Analyzer (SRA -TOC) - TPH TOC Analysis v6.5.117

Sample ID: 659_376-4 **Acq. Type**: TPH **Weight**: 78.2 **Crucible**: 6
Depth: 376.4 (Measured) **Lithology**: None **Sample Type**: Core **Well Name**: 659
Acq. Date: July 20 2014 / 8:01:08 PM

Data: C:\SRA JOBS\SRA049C_Greymouth lacustrine mudstones_20072014\659_376-4.RAW
Method: C:\Program Files\Thermal Station\GNS 300-650 STD 160000.sram
Sequence: C:\Program Files\Thermal Station\Data\SRA049C Greymouth lacustrine mudstones 20072014\SRA049C Greymouth lacustrine mudstones 20072014.sras
Method Information: Initial Temp: 300 °C -- Initial Time: 3 -- Rate : 25.0 °C/Min -- Final Temp: 650 °C -- Final Time: 1 Min -- OxiPurge: 5 Min -- OxiTime: 20 Min -- OxiTemp: 630 °C
FID Temp: 325 °C
FID Gain: Low (10^6)

Calibration Standard Information: Standard Name: 160000 TOC tTemp: 455.0 °C pTPH (S2): 12.43 mg/g S3: 0.79 mg/g S4: 22.40 mg/g
Operator: R Sykes **Instrument name**: SRA -TOC

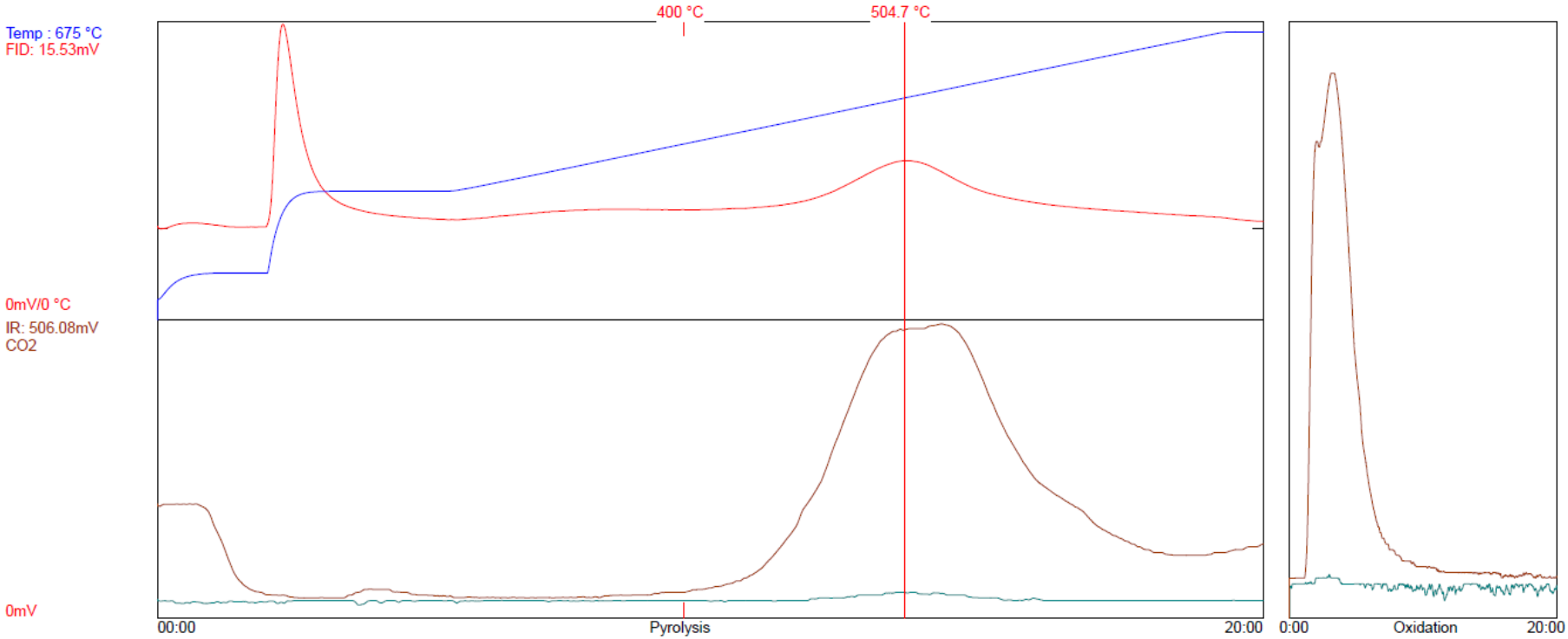

vTPH(S1):.50mg/g pTPH(S2): 1.28mg/g cTemp(Tmax): 465.7°C tTemp:504.7°C S3:1.87mg/g TOC:1.43 % HI:90 OI:131 PI:0.28 S1/TOC:0.35

Monday, 21 July 2014 17:52:24

SR Analyzer (SRA -TOC) - TPH TOC Analysis v6.5.117

Sample ID: 659_393 **Acq. Type**: TPH **Weight**: 75.2 **Crucible**: 7
Depth: 393 (Measured) **Lithology**: None **Sample Type**: Core **Well Name**: 659
Acq. Date: July 20 2014 / 8:55:53 PM

Data: C:\SRA JOBS\SRA049C_Greymouth lacustrine mudstones_20072014\659_393.RAW
Method: C:\Program Files\Thermal Station\GNS 300-650 STD 160000.sram
Sequence: C:\Program Files\Thermal Station\Data\SRA049C Greymouth lacustrine mudstones 20072014\SRA049C Greymouth lacustrine mudstones 20072014.sras
Method Information: Initial Temp: 300 °C -- Initial Time: 3 -- Rate : 25.0 °C/Min -- Final Temp: 650 °C -- Final Time: 1 Min -- OxiPurge: 5 Min -- OxiTime: 20 Min -- OxiTemp: 630 °C
FID Temp: 325 °C
FID Gain: Low (10^6)

Calibration Standard Information: Standard Name: 160000 TOC tTemp: 455.0 °C pTPH (S2): 12.43 mg/g S3: 0.79 mg/g S4: 22.40 mg/g
Operator: R Sykes **Instrument name**: SRA -TOC

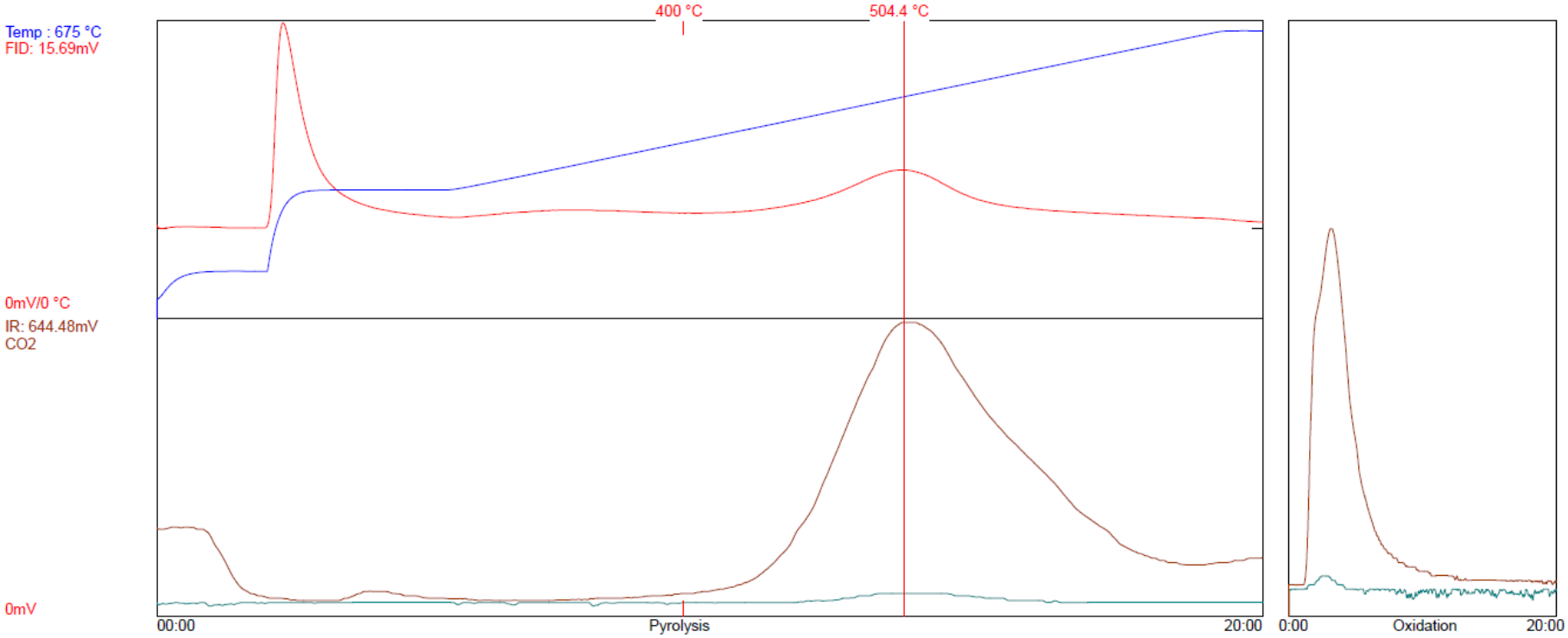

vTPH(S1):.59mg/g pTPH(S2): 1.16mg/g cTemp(Tmax): 465.4°C tTemp:504.4°C S3:2.29mg/g TOC:1.37 % HI:84 OI:167 PI:0.34 S1/TOC:0.43

Monday, 21 July 2014 17:52:48

SR Analyzer (SRA -TOC) - TPH TOC Analysis v6.5.117

Sample ID: 660_8-2 **Acq. Type**: TPH **Weight**: 77.8 **Crucible**: 8
Depth: 8.2 (Measured) **Lithology**: None **Sample Type**: Core **Well Name**: 660
Acq. Date: July 20 2014 / 9:50:43 PM

Data: C:\SRA JOBS\SRA049C_Greymouth lacustrine mudstones_20072014\660_8-2.RAW
Method: C:\Program Files\Thermal Station\GNS 300-650 STD 160000.sram
Sequence: C:\Program Files\Thermal Station\Data\SRA049C Greymouth lacustrine mudstones 20072014\SRA049C Greymouth lacustrine mudstones 20072014.sras
Method Information: Initial Temp: 300 °C -- Initial Time: 3 -- Rate : 25.0 °C/Min -- Final Temp: 650 °C -- Final Time: 1 Min -- OxiPurge: 5 Min -- OxiTime: 20 Min -- OxiTemp: 630 °C
FID Temp: 325 °C
FID Gain: Low (10^6)

Calibration Standard Information: Standard Name: 160000 TOC tTemp: 455.0 °C pTPH (S2): 12.43 mg/g S3: 0.79 mg/g S4: 22.40 mg/g
Operator: R Sykes **Instrument name**: SRA -TOC

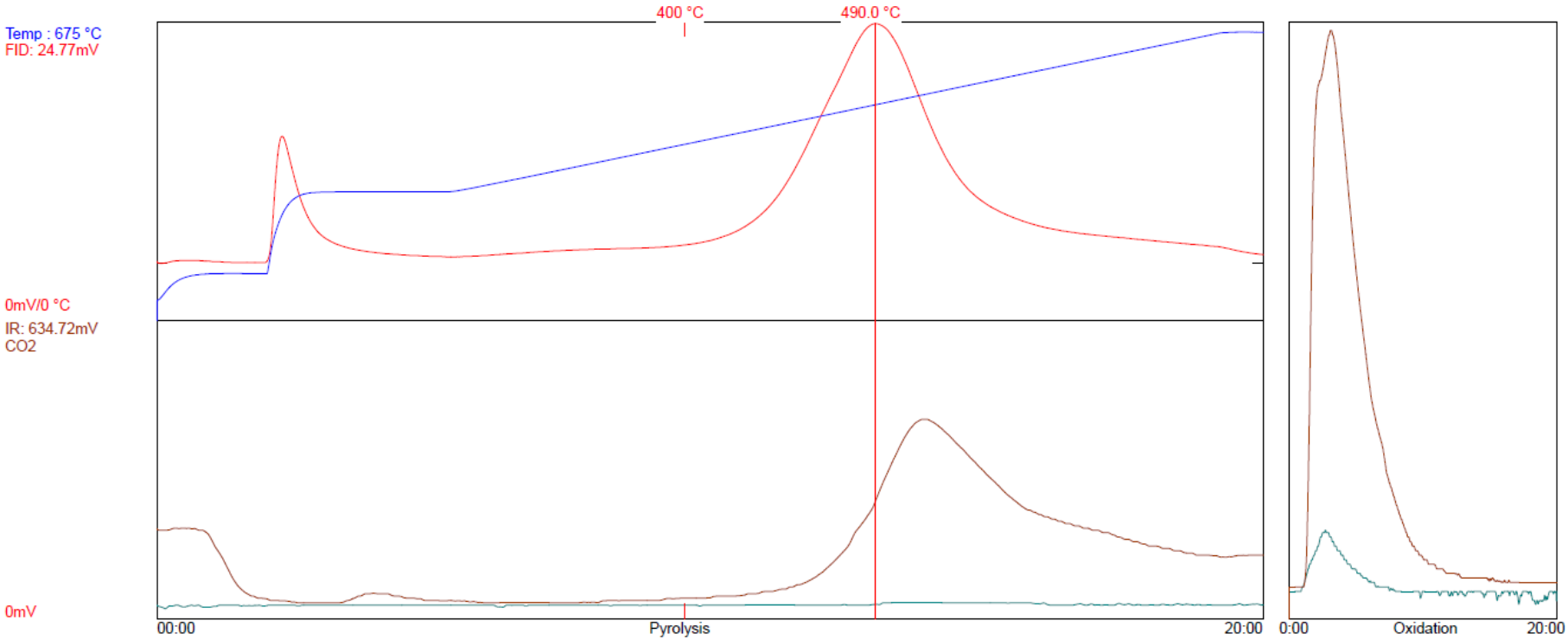

vTPH(S1):.51mg/g pTPH(S2): 4.39mg/g cTemp(Tmax): 451.0°C tTemp:490.0°C S3:1.01mg/g TOC:2.74 % HI:160 OI:37 PI:0.10 S1/TOC:0.19

Monday, 21 July 2014 17:53:20

SR Analyzer (SRA -TOC) - TPH TOC Analysis v6.5.117

Sample ID: 660_43-2 **Acq. Type**: TPH **Weight**: 78.7 **Crucible**: 9
Depth: 43.2 (Measured) **Lithology**: None **Sample Type**: Core **Well Name**: 660
Acq. Date: July 20 2014 / 10:45:35 PM

Data: C:\SRA JOBS\SRA049C_Greymouth lacustrine mudstones_20072014\660_43-2.RAW
Method: C:\Program Files\Thermal Station\GNS 300-650 STD 160000.sram
Sequence: C:\Program Files\Thermal Station\Data\SRA049C Greymouth lacustrine mudstones 20072014\SRA049C Greymouth lacustrine mudstones 20072014.sras
Method Information: Initial Temp: 300 °C -- Initial Time: 3 -- Rate : 25.0 °C/Min -- Final Temp: 650 °C -- Final Time: 1 Min -- OxiPurge: 5 Min -- OxiTime: 20 Min -- OxiTemp: 630 °C
FID Temp: 325 °C
FID Gain: Low (10^6)

Calibration Standard Information: Standard Name: 160000 TOC tTemp: 455.0 °C pTPH (S2): 12.43 mg/g S3: 0.79 mg/g S4: 22.40 mg/g
Operator: R Sykes **Instrument name**: SRA -TOC

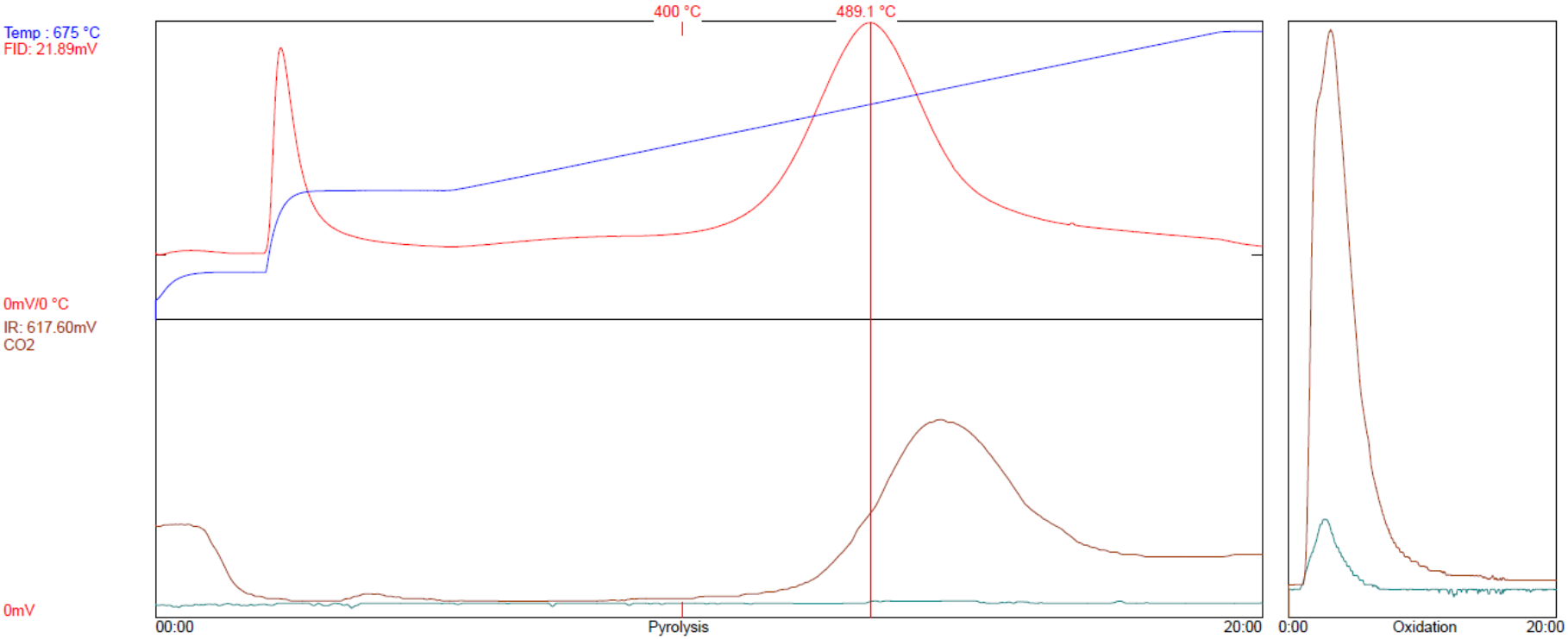

vTPH(S1):.67mg/g pTPH(S2): 3.85mg/g cTemp(Tmax): 450.1°C tTemp:489.1°C S3:.46mg/g TOC:2.38 % HI:162 OI:19 PI:0.15 S1/TOC:0.28

Monday, 21 July 2014 17:54:01

SR Analyzer (SRA -TOC) - TPH TOC Analysis v6.5.117

Sample ID: 660_68 **Acq. Type**: TPH **Weight**: 76.5 **Crucible**: 10
Depth: 68 (Measured) **Lithology**: None **Sample Type**: Core **Well Name**: 660
Acq. Date: July 20 2014 / 11:40:30 PM

Data: C:\SRA JOBS\SRA049C_Greymouth lacustrine mudstones_20072014\660_68.RAW
Method: C:\Program Files\Thermal Station\GNS 300-650 STD 160000.sram
Sequence: C:\Program Files\Thermal Station\Data\SRA049C Greymouth lacustrine mudstones 20072014\SRA049C Greymouth lacustrine mudstones 20072014.sras
Method Information: Initial Temp: 300 °C -- Initial Time: 3 -- Rate : 25.0 °C/Min -- Final Temp: 650 °C -- Final Time: 1 Min -- OxiPurge: 5 Min -- OxiTime: 20 Min -- OxiTemp: 630 °C
FID Temp: 325 °C
FID Gain: Low (10^6)

Calibration Standard Information: Standard Name: 160000 TOC tTemp: 455.0 °C pTPH (S2): 12.43 mg/g S3: 0.79 mg/g S4: 22.40 mg/g
Operator: R Sykes **Instrument name**: SRA -TOC

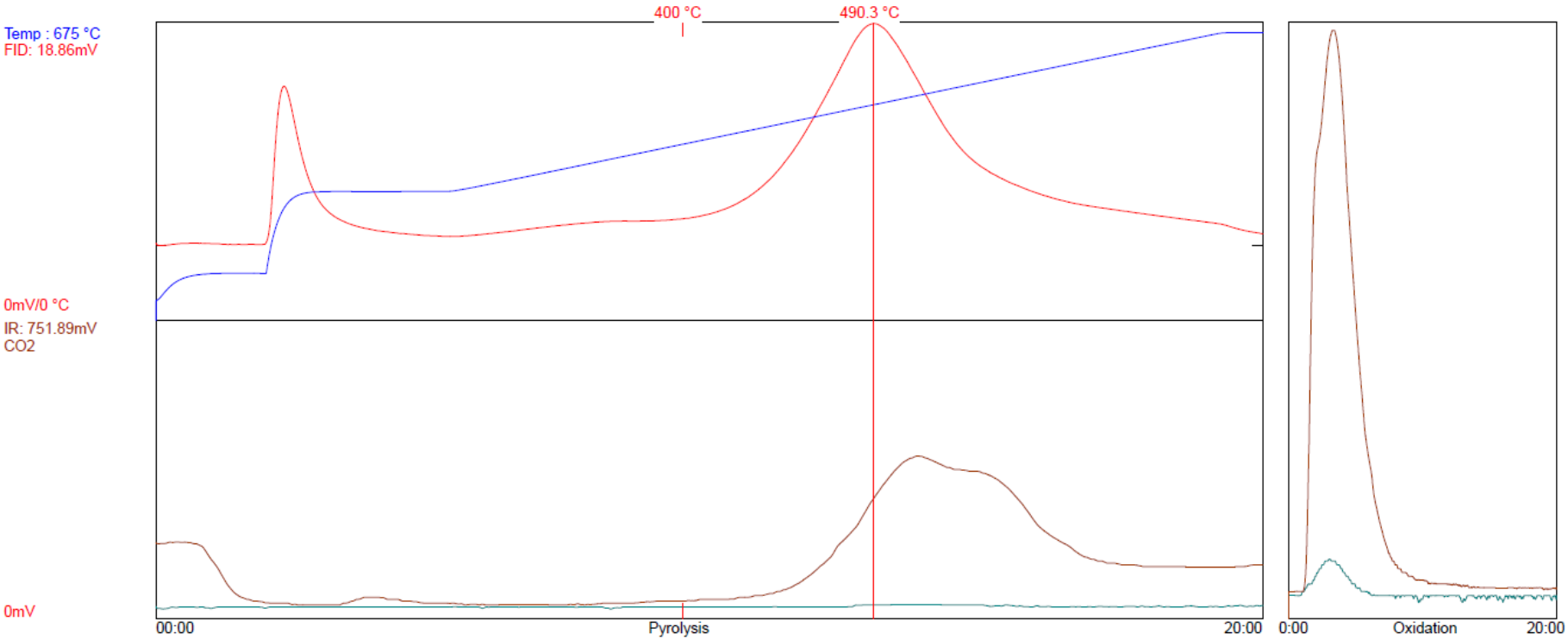

vTPH(S1):.54mg/g pTPH(S2): 3.74mg/g cTemp(Tmax): 451.3°C tTemp:490.3°C S3:1.28mg/g TOC:2.65 % HI:141 OI:48 PI:0.13 S1/TOC:0.20

Monday, 21 July 2014 17:54:35

SR Analyzer (SRA -TOC) - TPH TOC Analysis v6.5.117

Sample ID: 660_192 **Acq. Type**: TPH **Weight**: 79.2 **Crucible**: 12
Depth: 192 (Measured) **Lithology**: None **Sample Type**: Core **Well Name**: 660
Acq. Date: July 21 2014 / 1:30:02 AM

Data: C:\SRA JOBS\SRA049C_Greymouth lacustrine mudstones_20072014\660_192.RAW
Method: C:\Program Files\Thermal Station\GNS 300-650 STD 160000.sram
Sequence: C:\Program Files\Thermal Station\Data\SRA049C Greymouth lacustrine mudstones 20072014\SRA049C Greymouth lacustrine mudstones 20072014.sras
Method Information: Initial Temp: 300 °C -- Initial Time: 3 -- Rate : 25.0 °C/Min -- Final Temp: 650 °C -- Final Time: 1 Min -- OxiPurge: 5 Min -- OxiTime: 20 Min -- OxiTemp: 630 °C
FID Temp: 325 °C
FID Gain: Low (10^6)

Calibration Standard Information: Standard Name: 160000 TOC tTemp: 455.0 °C pTPH (S2): 12.43 mg/g S3: 0.79 mg/g S4: 22.40 mg/g
Operator: R Sykes **Instrument name**: SRA -TOC

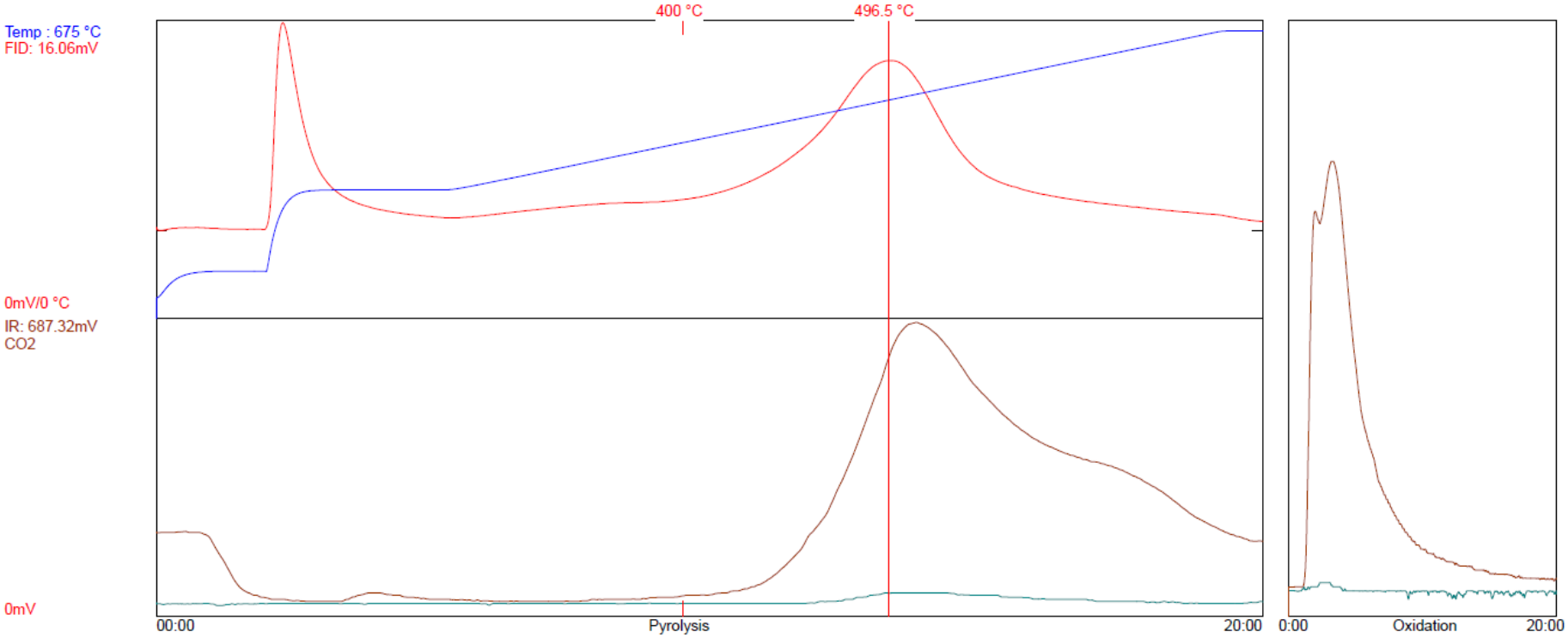

vTPH(S1):.59mg/g pTPH(S2): 2.55mg/g cTemp(Tmax): 457.5°C tTemp:496.5°C S3:1.95mg/g TOC:2.12 % HI:120 OI:92 PI:0.19 S1/TOC:0.28

Monday, 21 July 2014 17:55:01

SR Analyzer (SRA -TOC) - TPH TOC Analysis v6.5.117

Sample ID: 660_212-4 **Acq. Type**: TPH **Weight**: 79.9 **Crucible**: 13
Depth: 212.4 (Measured) **Lithology**: None **Sample Type**: Core **Well Name**: 660
Acq. Date: July 21 2014 / 2:24:47 AM

Data: C:\SRA JOBS\SRA049C_Greymouth lacustrine mudstones_20072014\660_212-4.RAW
Method: C:\Program Files\Thermal Station\GNS 300-650 STD 160000.sram
Sequence: C:\Program Files\Thermal Station\Data\SRA049C Greymouth lacustrine mudstones 20072014\SRA049C Greymouth lacustrine mudstones 20072014.sras
Method Information: Initial Temp: 300 °C -- Initial Time: 3 -- Rate : 25.0 °C/Min -- Final Temp: 650 °C -- Final Time: 1 Min -- OxiPurge: 5 Min -- OxiTime: 20 Min -- OxiTemp: 630 °C
FID Temp: 325 °C
FID Gain: Low (10^6)

Calibration Standard Information: Standard Name: 160000 TOC tTemp: 455.0 °C pTPH (S2): 12.43 mg/g S3: 0.79 mg/g S4: 22.40 mg/g
Operator: R Sykes **Instrument name**: SRA -TOC

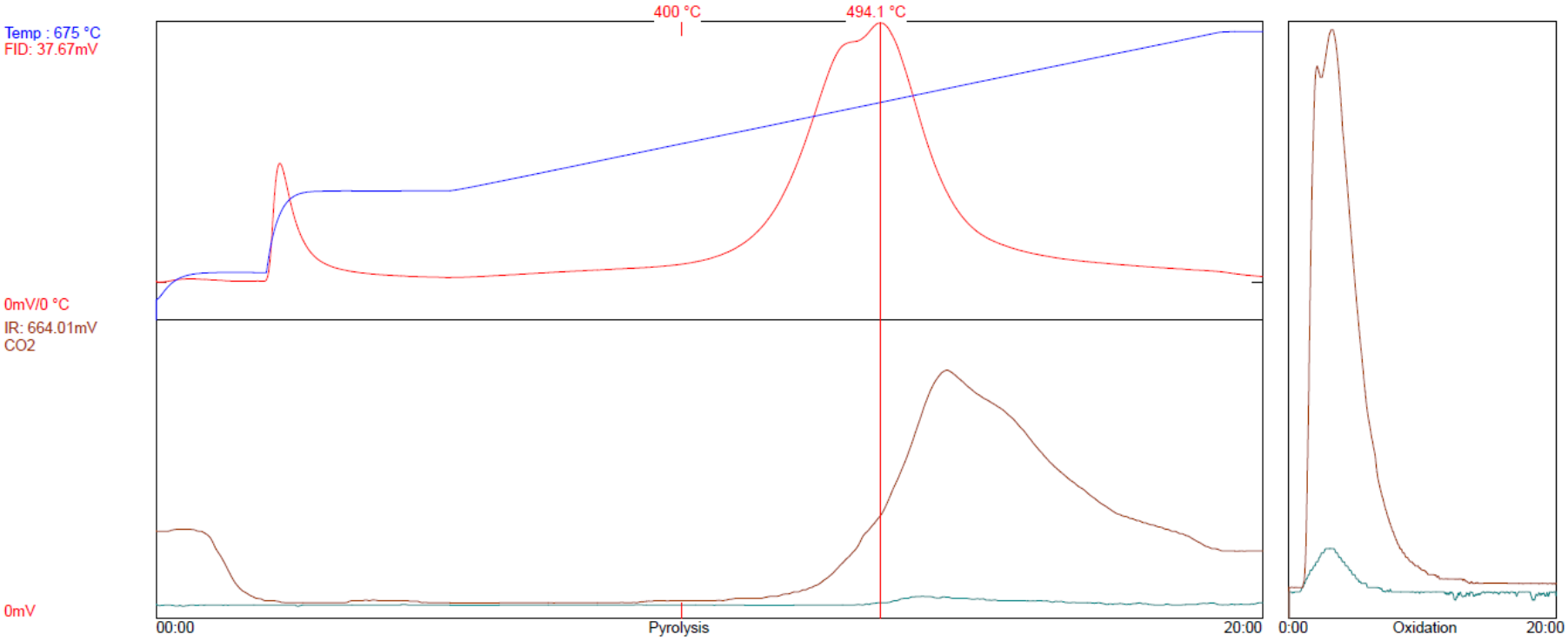

vTPH(S1):.64mg/g pTPH(S2): 6.51mg/g cTemp(Tmax): 455.1°C tTemp:494.1°C S3:.30mg/g TOC:2.78 % HI:234 OI:11 PI:0.09 S1/TOC:0.23

Monday, 21 July 2014 17:55:27

SR Analyzer (SRA -TOC) - TPH TOC Analysis v6.5.117

Sample ID: 660_278-4 **Acq. Type**: TPH **Weight**: 99.0 **Crucible**: 14
Depth: 278.4 (Measured) **Lithology**: None **Sample Type**: Core **Well Name**: 660
Acq. Date: July 21 2014 / 3:19:35 AM

Data: C:\SRA JOBS\SRA049C_Greymouth lacustrine mudstones_20072014\660_278-4.RAW
Method: C:\Program Files\Thermal Station\GNS 300-650 STD 160000.sram
Sequence: C:\Program Files\Thermal Station\Data\SRA049C Greymouth lacustrine mudstones 20072014\SRA049C Greymouth lacustrine mudstones 20072014.sras
Method Information: Initial Temp: 300 °C -- Initial Time: 3 -- Rate : 25.0 °C/Min -- Final Temp: 650 °C -- Final Time: 1 Min -- OxiPurge: 5 Min -- OxiTime: 20 Min -- OxiTemp: 630 °C
FID Temp: 325 °C
FID Gain: Low (10^6)

Calibration Standard Information: Standard Name: 160000 TOC tTemp: 455.0 °C pTPH (S2): 12.43 mg/g S3: 0.79 mg/g S4: 22.40 mg/g
Operator: R Sykes **Instrument name**: SRA -TOC

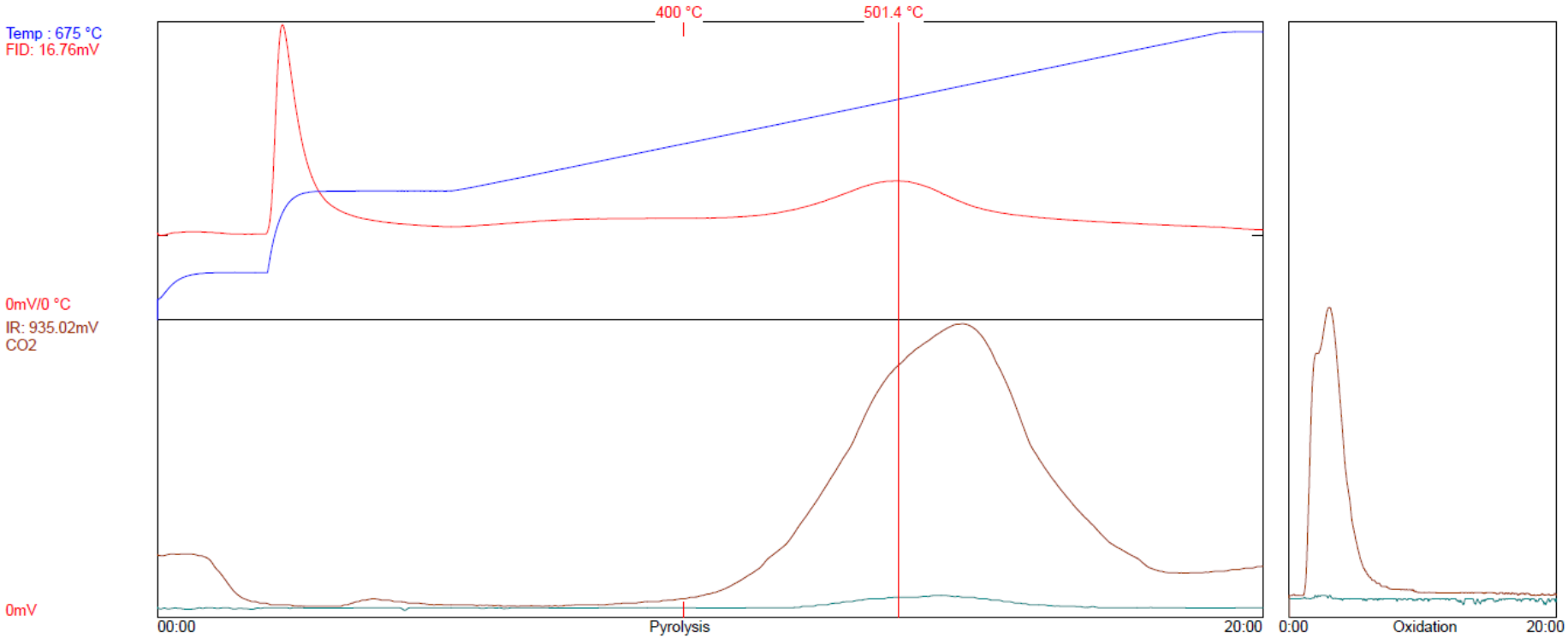

vTPH(S1):.41mg/g pTPH(S2): .90mg/g cTemp(Tmax): 462.4°C tTemp:501.4°C S3:2.39mg/g TOC:1.01 % HI:90 OI:237 PI:0.31 S1/TOC:0.41

Monday, 21 July 2014 17:56:01

SR Analyzer (SRA -TOC) - TPH TOC Analysis v6.5.117

Sample ID: 660_336-5 **Acq. Type**: TPH **Weight**: 76.8 **Crucible**: 15
Depth: 336.5 (Measured) **Lithology**: None **Sample Type**: Core **Well Name**: 660
Acq. Date: July 21 2014 / 4:14:27 AM

Data: C:\SRA JOBS\SRA049C_Greymouth lacustrine mudstones_20072014\660_336-5.RAW
Method: C:\Program Files\Thermal Station\GNS 300-650 STD 160000.sram
Sequence: C:\Program Files\Thermal Station\Data\SRA049C Greymouth lacustrine mudstones 20072014\SRA049C Greymouth lacustrine mudstones 20072014.sras
Method Information: Initial Temp: 300 °C -- Initial Time: 3 -- Rate : 25.0 °C/Min -- Final Temp: 650 °C -- Final Time: 1 Min -- OxiPurge: 5 Min -- OxiTime: 20 Min -- OxiTemp: 630 °C
FID Temp: 325 °C
FID Gain: Low (10^6)

Calibration Standard Information: Standard Name: 160000 TOC tTemp: 455.0 °C pTPH (S2): 12.43 mg/g S3: 0.79 mg/g S4: 22.40 mg/g
Operator: R Sykes **Instrument name**: SRA -TOC

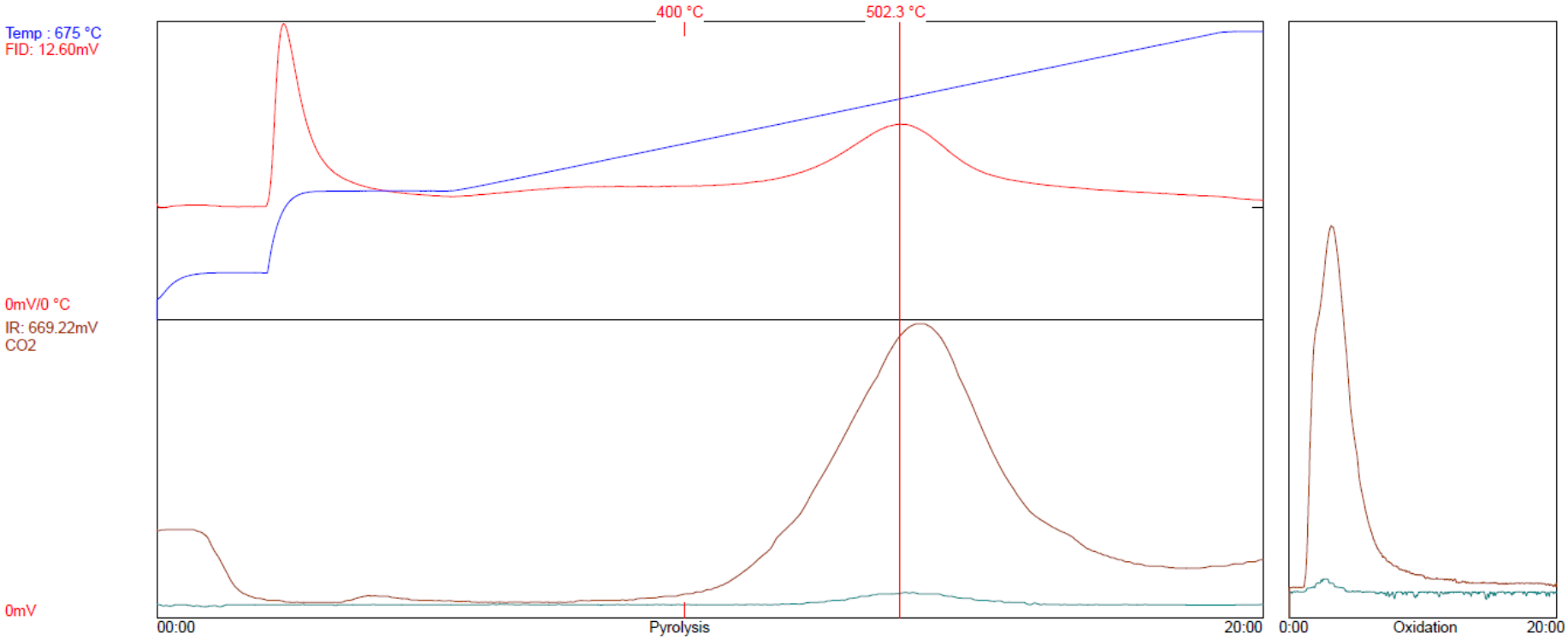

vTPH(S1):.42mg/g pTPH(S2): 1.18mg/g cTemp(Tmax): 463.3°C tTemp:502.3°C S3:2.48mg/g TOC:1.39 % HI:85 OI:179 PI:0.26 S1/TOC:0.30

Monday, 21 July 2014 17:56:29

SR Analyzer (SRA -TOC) - TPH TOC Analysis v6.5.117

Sample ID: 661_30-15 **Acq. Type**: TPH **Weight**: 77.0 **Crucible**: 16
Depth: 30.15 (Measured) **Lithology**: None **Sample Type**: Core **Well Name**: 661
Acq. Date: July 21 2014 / 5:09:11 AM

Data: C:\SRA JOBS\SRA049C_Greymouth lacustrine mudstones_20072014\661_30-15.RAW
Method: C:\Program Files\Thermal Station\GNS 300-650 STD 160000.sram
Sequence: C:\Program Files\Thermal Station\Data\SRA049C Greymouth lacustrine mudstones 20072014\SRA049C Greymouth lacustrine mudstones 20072014.sras
Method Information: Initial Temp: 300 °C -- Initial Time: 3 -- Rate : 25.0 °C/Min -- Final Temp: 650 °C -- Final Time: 1 Min -- OxiPurge: 5 Min -- OxiTime: 20 Min -- OxiTemp: 630 °C
FID Temp: 325 °C
FID Gain: Low (10^6)

Calibration Standard Information: Standard Name: 160000 TOC tTemp: 455.0 °C pTPH (S2): 12.43 mg/g S3: 0.79 mg/g S4: 22.40 mg/g
Operator: R Sykes **Instrument name**: SRA -TOC

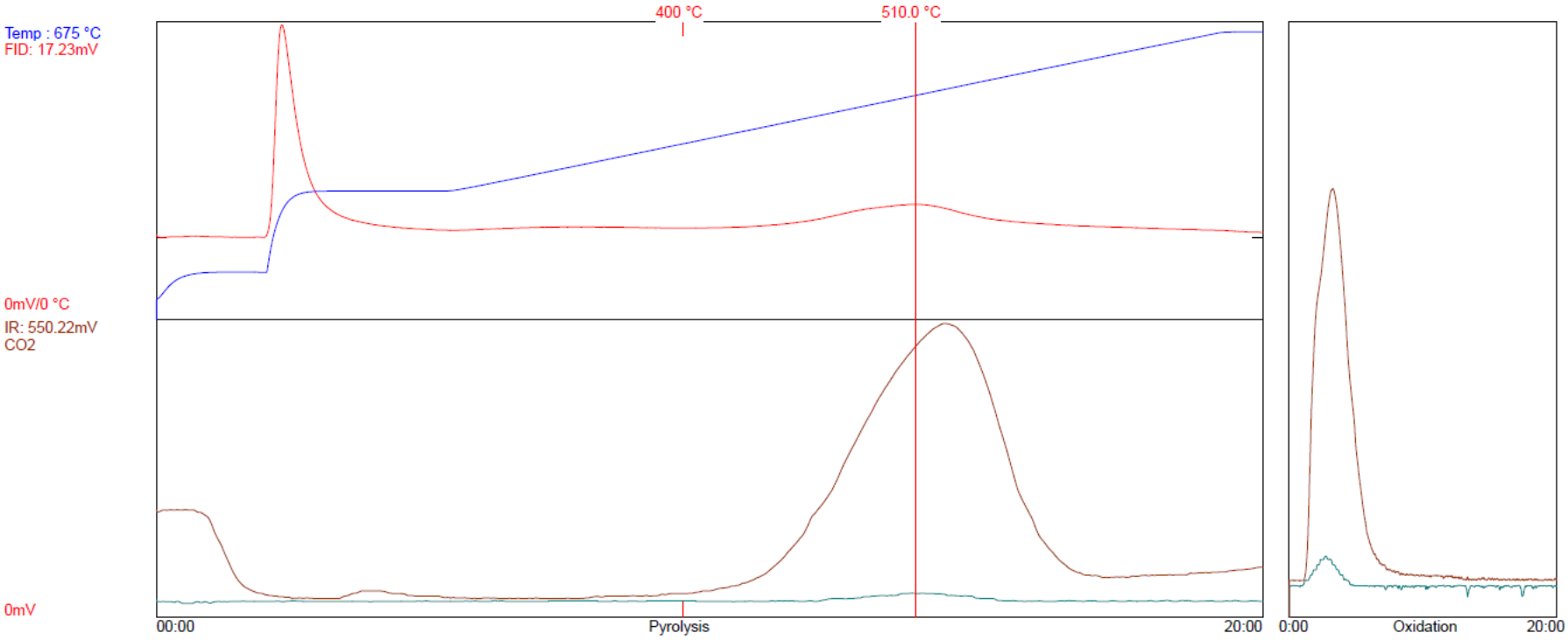

vTPH(S1):.51mg/g pTPH(S2): .80mg/g cTemp(Tmax): 471.0°C tTemp:510.0°C S3:1.46mg/g TOC:1.17 % HI:68 OI:125 PI:0.39 S1/TOC:0.43

Monday, 21 July 2014 17:57:05

SR Analyzer (SRA -TOC) - TPH TOC Analysis v6.5.117

Sample ID: 661_48-8 **Acq. Type**: TPH **Weight**: 75.3 **Crucible**: 17
Depth: 48.8 (Measured) **Lithology**: None **Sample Type**: Core **Well Name**: 661
Acq. Date: July 21 2014 / 6:03:53 AM

Data: C:\SRA JOBS\SRA049C_Greymouth lacustrine mudstones_20072014\661_48-8.RAW
Method: C:\Program Files\Thermal Station\GNS 300-650 STD 160000.sram
Sequence: C:\Program Files\Thermal Station\Data\SRA049C Greymouth lacustrine mudstones 20072014\SRA049C Greymouth lacustrine mudstones 20072014.sras
Method Information: Initial Temp: 300 °C -- Initial Time: 3 -- Rate : 25.0 °C/Min -- Final Temp: 650 °C -- Final Time: 1 Min -- OxiPurge: 5 Min -- OxiTime: 20 Min -- OxiTemp: 630 °C
FID Temp: 325 °C
FID Gain: Low (10^6)

Calibration Standard Information: Standard Name: 160000 TOC tTemp: 455.0 °C pTPH (S2): 12.43 mg/g S3: 0.79 mg/g S4: 22.40 mg/g
Operator: R Sykes **Instrument name**: SRA -TOC

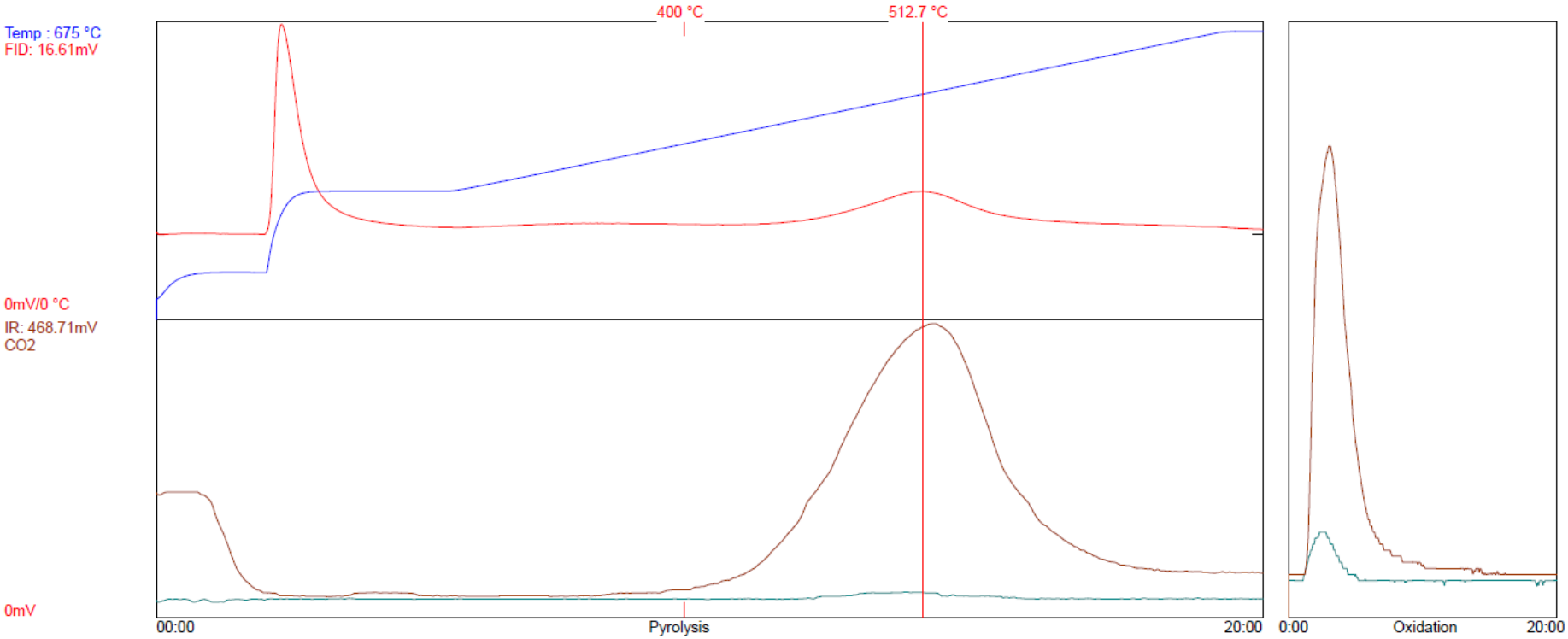

vTPH(S1):.53mg/g pTPH(S2): .85mg/g cTemp(Tmax): 473.7°C tTemp:512.7°C S3:.90mg/g TOC:1.21 % HI:70 OI:75 PI:0.38 S1/TOC:0.44

Monday, 21 July 2014 17:57:30

SR Analyzer (SRA -TOC) - TPH TOC Analysis v6.5.117

Sample ID: 662_116-6 **Acq. Type**: TPH **Weight**: 75.2 **Crucible**: 20
Depth: 116.6 (Measured) **Lithology**: None **Sample Type**: Core **Well Name**: 662
Acq. Date: July 21 2014 / 8:48:09 AM

Data: C:\SRA JOBS\SRA049C_Greymouth lacustrine mudstones_20072014\662_116-6.RAW
Method: C:\Program Files\Thermal Station\GNS 300-650 STD 160000.sram
Sequence: C:\Program Files\Thermal Station\Data\SRA049C Greymouth lacustrine mudstones 20072014\SRA049C Greymouth lacustrine mudstones 20072014.sras
Method Information: Initial Temp: 300 °C -- Initial Time: 3 -- Rate : 25.0 °C/Min -- Final Temp: 650 °C -- Final Time: 1 Min -- OxiPurge: 5 Min -- OxiTime: 20 Min -- OxiTemp: 630 °C
FID Temp: 325 °C
FID Gain: Low (10^6)

Calibration Standard Information: Standard Name: 160000 TOC tTemp: 455.0 °C pTPH (S2): 12.43 mg/g S3: 0.79 mg/g S4: 22.40 mg/g
Operator: R Sykes **Instrument name**: SRA -TOC

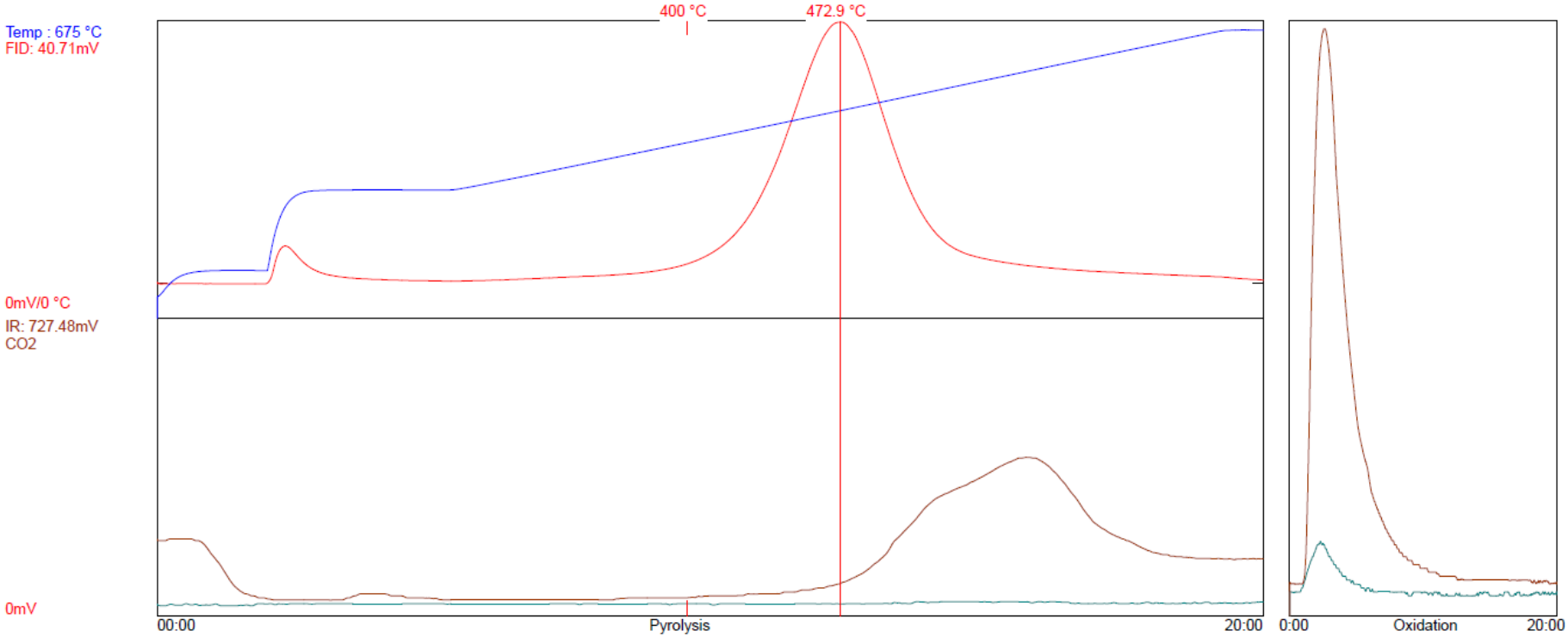

vTPH(S1):.29mg/g pTPH(S2): 6.54mg/g cTemp(Tmax): 433.9°C tTemp:472.9°C S3:.51mg/g TOC:2.69 % HI:244 OI:19 PI:0.04 S1/TOC:0.11

Monday, 21 July 2014 17:58:37

SR Analyzer (SRA -TOC) - TPH TOC Analysis v6.5.117

Sample ID: 662_48-9 **Acq. Type**: TPH **Weight**: 77.0 **Crucible**: 18
Depth: 48.9 (Measured) **Lithology**: None **Sample Type**: Core **Well Name**: 662
Acq. Date: July 21 2014 / 6:58:33 AM

Data: C:\SRA JOBS\SRA049C_Greymouth lacustrine mudstones_20072014\662_48-9.RAW
Method: C:\Program Files\Thermal Station\GNS 300-650 STD 160000.sram
Sequence: C:\Program Files\Thermal Station\Data\SRA049C Greymouth lacustrine mudstones 20072014\SRA049C Greymouth lacustrine mudstones 20072014.sras
Method Information: Initial Temp: 300 °C -- Initial Time: 3 -- Rate : 25.0 °C/Min -- Final Temp: 650 °C -- Final Time: 1 Min -- OxiPurge: 5 Min -- OxiTime: 20 Min -- OxiTemp: 630 °C
FID Temp: 325 °C
FID Gain: Low (10^6)

Calibration Standard Information: Standard Name: 160000 TOC tTemp: 455.0 °C pTPH (S2): 12.43 mg/g S3: 0.79 mg/g S4: 22.40 mg/g
Operator: R Sykes **Instrument name**: SRA -TOC

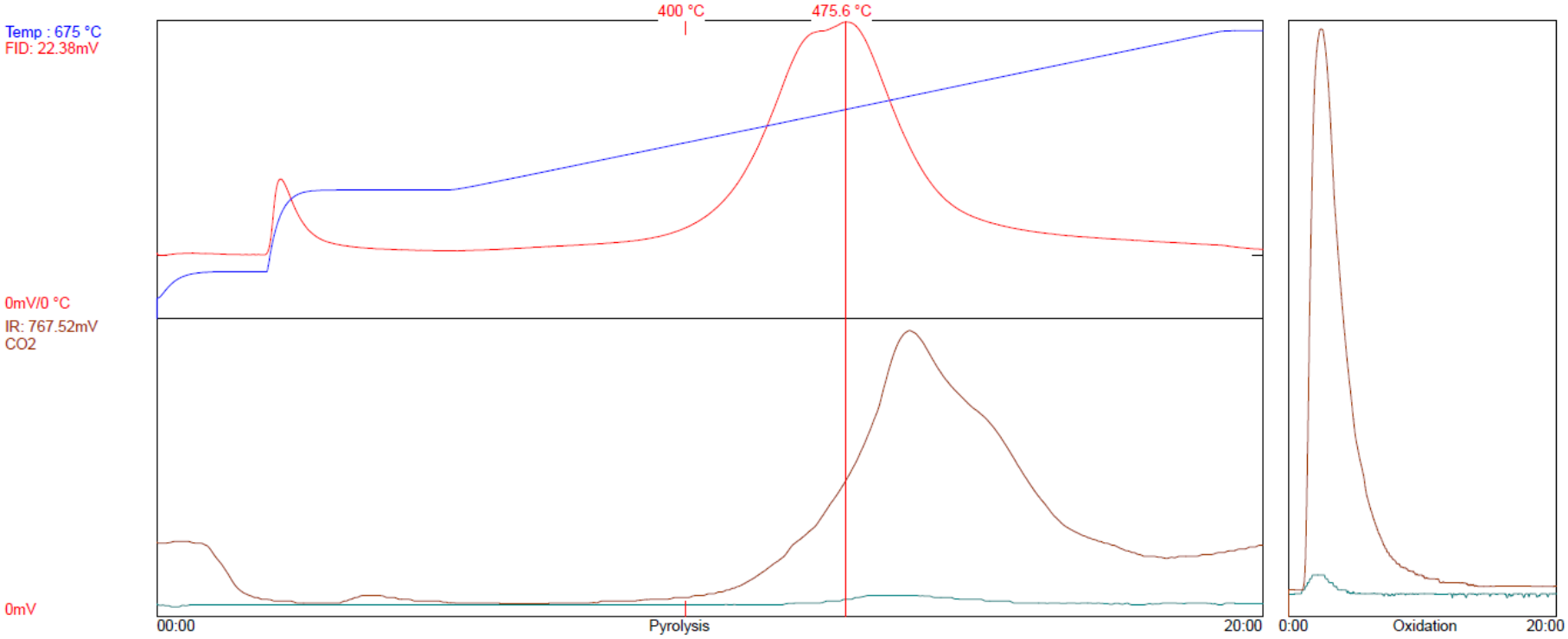

vTPH(S1):.29mg/g pTPH(S2): 3.96mg/g cTemp(Tmax): 436.6°C tTemp:475.6°C S3:1.62mg/g TOC:2.30 % HI:172 OI:71 PI:0.07 S1/TOC:0.13

Monday, 21 July 2014 17:58:04

SR Analyzer (SRA -TOC) - TPH TOC Analysis v6.5.117

Sample ID: 664_78-9 **Acq. Type**: TPH **Weight**: 75.7 **Crucible**: 21
Depth: 78.9 (Measured) **Lithology**: None **Sample Type**: Core **Well Name**: 664
Acq. Date: July 21 2014 / 9:42:55 AM

Data: C:\SRA JOBS\SRA049C_Greymouth lacustrine mudstones_20072014\664_78-9.RAW
Method: C:\Program Files\Thermal Station\GNS 300-650 STD 160000.sram
Sequence: C:\Program Files\Thermal Station\Data\SRA049C Greymouth lacustrine mudstones 20072014\SRA049C Greymouth lacustrine mudstones 20072014.sras
Method Information: Initial Temp: 300 °C -- Initial Time: 3 -- Rate : 25.0 °C/Min -- Final Temp: 650 °C -- Final Time: 1 Min -- OxiPurge: 5 Min -- OxiTime: 20 Min -- OxiTemp: 630 °C
FID Temp: 325 °C
FID Gain: Low (10^6)

Calibration Standard Information: Standard Name: 160000 TOC tTemp: 455.0 °C pTPH (S2): 12.43 mg/g S3: 0.79 mg/g S4: 22.40 mg/g
Operator: R Sykes **Instrument name**: SRA -TOC

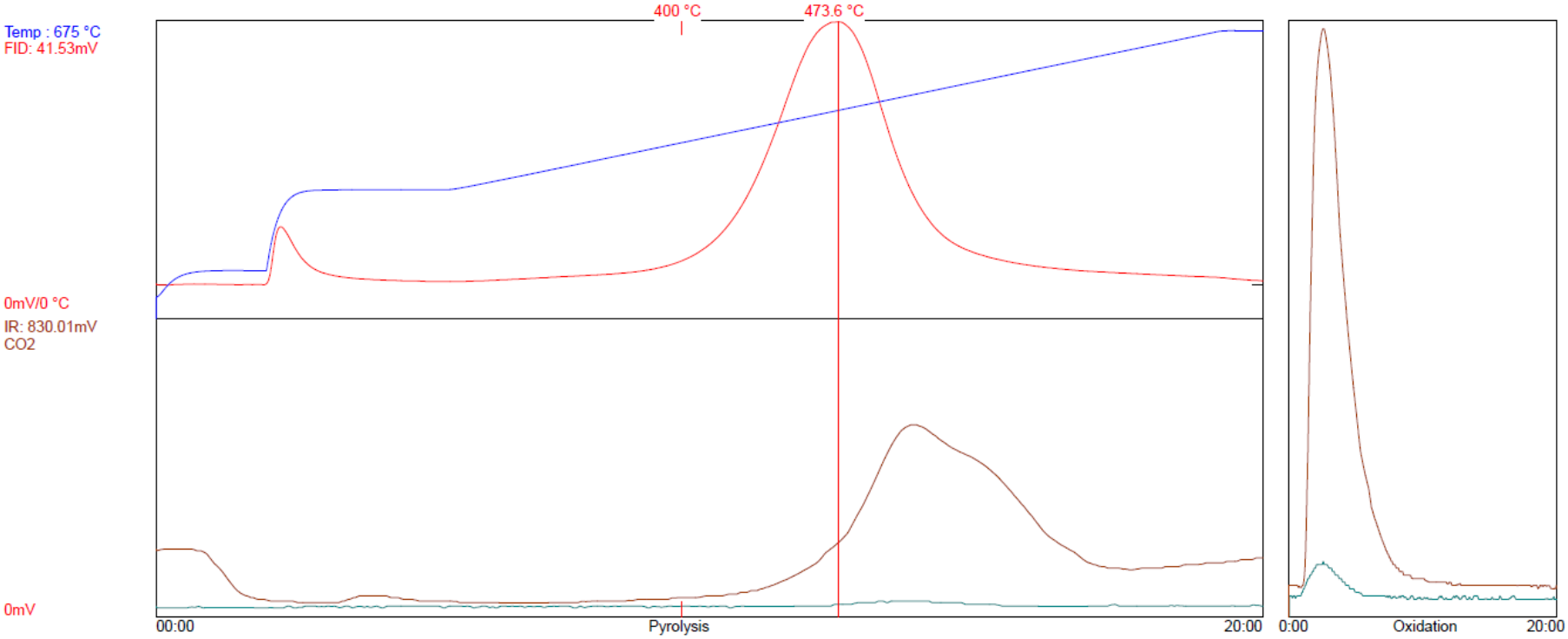

vTPH(S1):.40mg/g pTPH(S2): 7.35mg/g cTemp(Tmax): 434.6°C tTemp:473.6°C S3:1.24mg/g TOC:2.93 % HI:251 OI:42 PI:0.05 S1/TOC:0.14

Monday, 21 July 2014 17:59:07

SR Analyzer (SRA -TOC) - TPH TOC Analysis v6.5.117

Sample ID: 664_157-5 **Acq. Type**: TPH **Weight**: 75.1 **Crucible**: 22
Depth: 157.5 (Measured) **Lithology**: None **Sample Type**: Core **Well Name**: 664
Acq. Date: July 21 2014 / 10:37:36 AM

Data: C:\SRA JOBS\SRA049C_Greymouth lacustrine mudstones_20072014\664_157-5.RAW
Method: C:\Program Files\Thermal Station\GNS 300-650 STD 160000.sram
Sequence: C:\Program Files\Thermal Station\Data\SRA049C Greymouth lacustrine mudstones 20072014\SRA049C Greymouth lacustrine mudstones 20072014.sras
Method Information: Initial Temp: 300 °C -- Initial Time: 3 -- Rate : 25.0 °C/Min -- Final Temp: 650 °C -- Final Time: 1 Min -- OxiPurge: 5 Min -- OxiTime: 20 Min -- OxiTemp: 630 °C
FID Temp: 325 °C
FID Gain: Low (10^6)

Calibration Standard Information: Standard Name: 160000 TOC tTemp: 455.0 °C pTPH (S2): 12.43 mg/g S3: 0.79 mg/g S4: 22.40 mg/g
Operator: R Sykes **Instrument name**: SRA -TOC

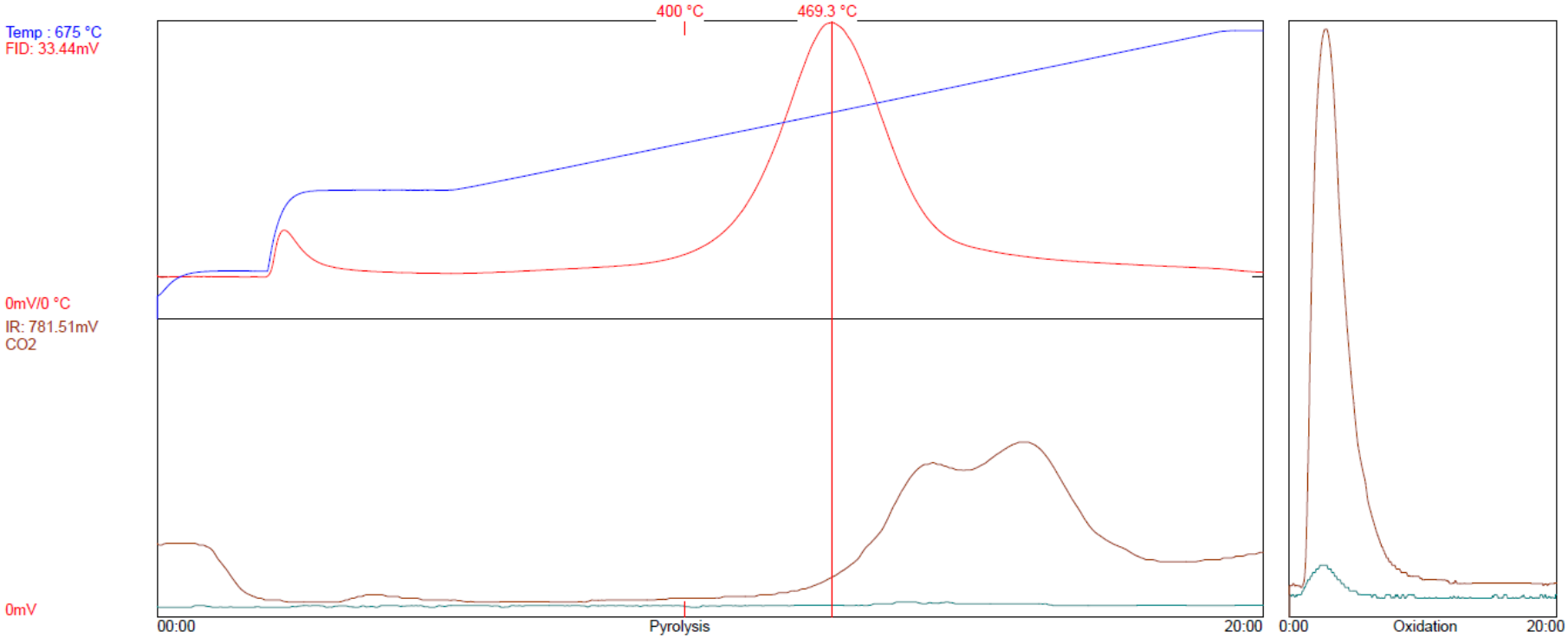

vTPH(S1):.29mg/g pTPH(S2): 5.49mg/g cTemp(Tmax): 430.3°C tTemp:469.3°C S3:.89mg/g TOC:2.58 % HI:213 OI:35 PI:0.05 S1/TOC:0.11

Monday, 21 July 2014 17:59:40

SR Analyzer (SRA -TOC) - TPH TOC Analysis v6.5.117

Sample ID: 665_3-8 **Acq. Type**: TPH **Weight**: 79.8 **Crucible**: 23
Depth: 3.8 (Measured) **Lithology**: None **Sample Type**: Core **Well Name**: 665
Acq. Date: July 21 2014 / 11:32:16 AM

Data: C:\SRA JOBS\SRA049C_Greymouth lacustrine mudstones_20072014\665_3-8.RAW
Method: C:\Program Files\Thermal Station\GNS 300-650 STD 160000.sram
Sequence: C:\Program Files\Thermal Station\Data\SRA049C Greymouth lacustrine mudstones 20072014\SRA049C Greymouth lacustrine mudstones 20072014.sras
Method Information: Initial Temp: 300 °C -- Initial Time: 3 -- Rate : 25.0 °C/Min -- Final Temp: 650 °C -- Final Time: 1 Min -- OxiPurge: 5 Min -- OxiTime: 20 Min -- OxiTemp: 630 °C
FID Temp: 325 °C
FID Gain: Low (10^6)

Calibration Standard Information: Standard Name: 160000 TOC tTemp: 455.0 °C pTPH (S2): 12.43 mg/g S3: 0.79 mg/g S4: 22.40 mg/g
Operator: R Sykes **Instrument name**: SRA -TOC

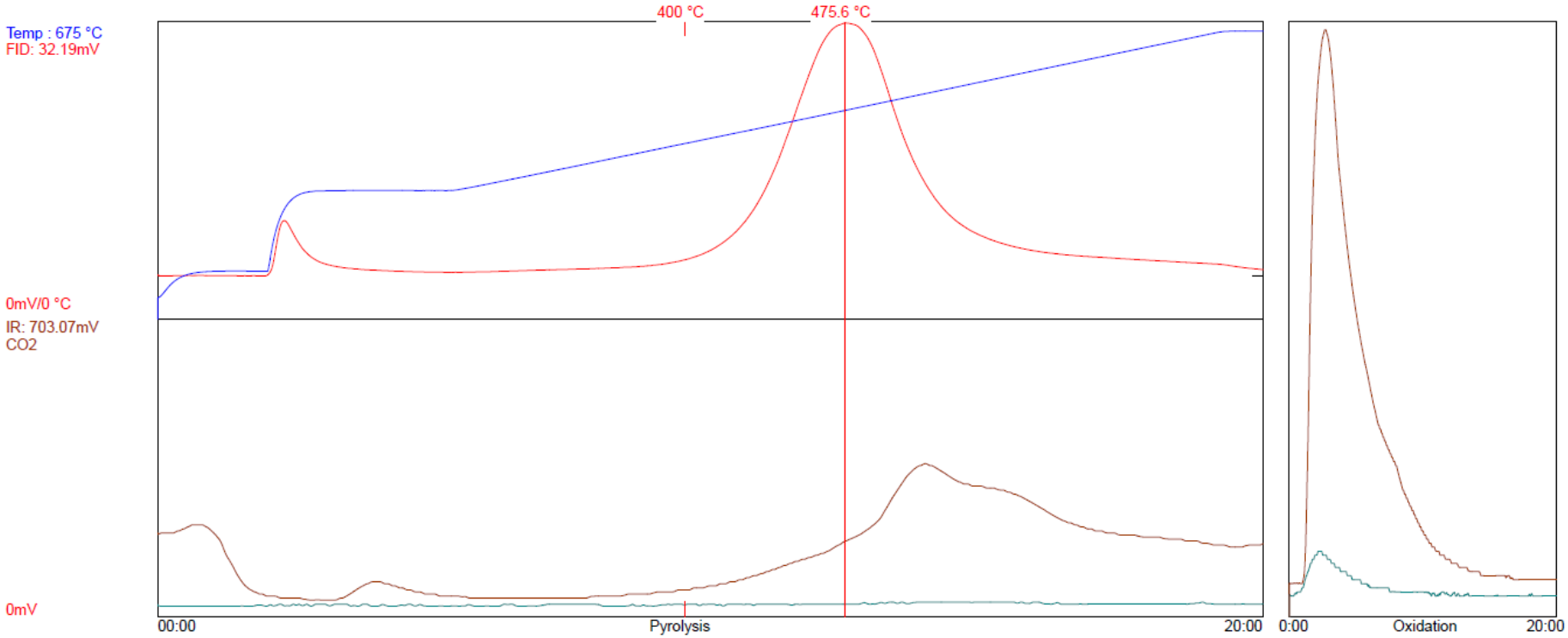

vTPH(S1):.27mg/g pTPH(S2): 5.26mg/g cTemp(Tmax): 436.6°C tTemp:475.6°C S3:1.34mg/g TOC:2.95 % HI:178 OI:45 PI:0.05 S1/TOC:0.09

Monday, 21 July 2014 18:00:10

SR Analyzer (SRA -TOC) - TPH TOC Analysis v6.5.117

Sample ID: 666_9 **Acq. Type**: TPH **Weight**: 78.3 **Crucible**: 24
Depth: 9 (Measured) **Lithology**: None **Sample Type**: Core **Well Name**: 666
Acq. Date: July 21 2014 / 12:27:01 PM

Data: C:\SRA JOBS\SRA049C_Greymouth lacustrine mudstones_20072014\666_9.RAW
Method: C:\Program Files\Thermal Station\GNS 300-650 STD 160000.sram
Sequence: C:\Program Files\Thermal Station\Data\SRA049C Greymouth lacustrine mudstones 20072014\SRA049C Greymouth lacustrine mudstones 20072014.sras
Method Information: Initial Temp: 300 °C -- Initial Time: 3 -- Rate : 25.0 °C/Min -- Final Temp: 650 °C -- Final Time: 1 Min -- OxiPurge: 5 Min -- OxiTime: 20 Min -- OxiTemp: 630 °C
FID Temp: 325 °C
FID Gain: Low (10^6)

Calibration Standard Information: Standard Name: 160000 TOC tTemp: 455.0 °C pTPH (S2): 12.43 mg/g S3: 0.79 mg/g S4: 22.40 mg/g
Operator: R Sykes **Instrument name**: SRA -TOC

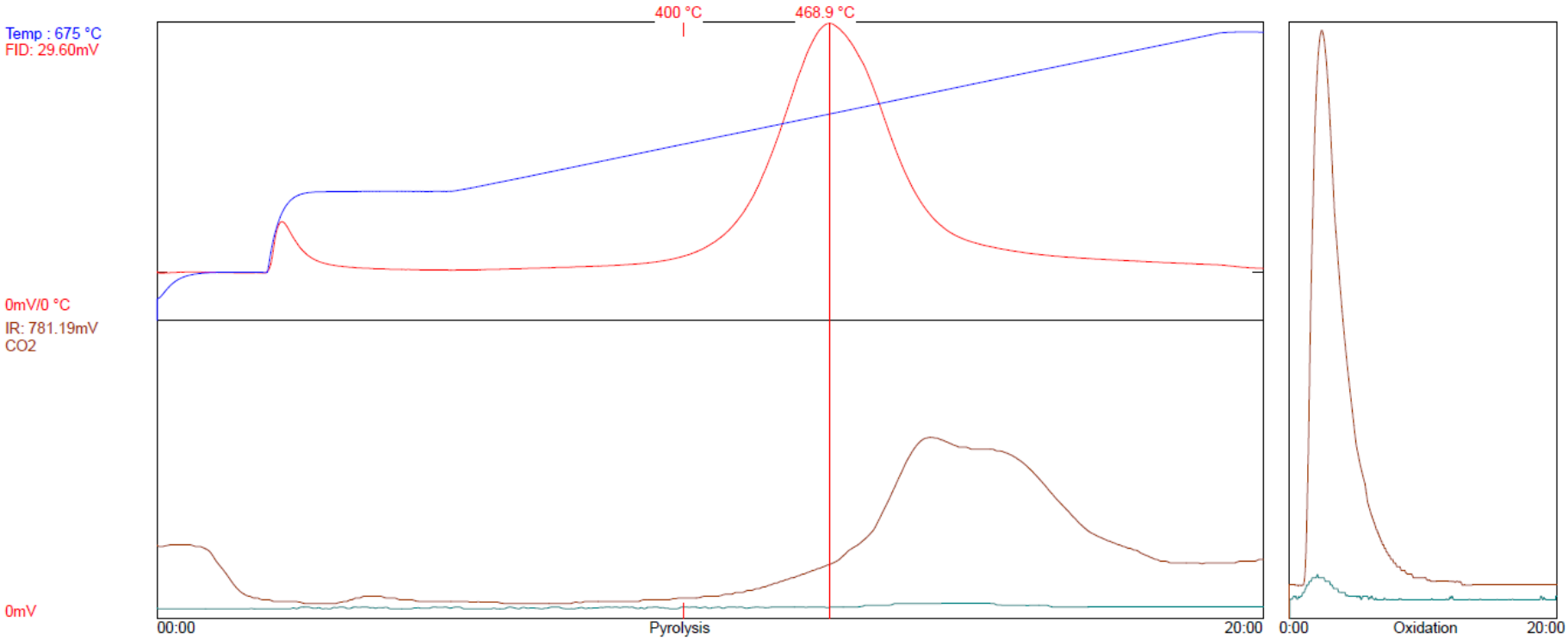

vTPH(S1):.23mg/g pTPH(S2): 4.51mg/g cTemp(Tmax): 429.9°C tTemp:468.9°C S3:1.25mg/g TOC:2.25 % HI:200 OI:56 PI:0.05 S1/TOC:0.10

Monday, 21 July 2014 18:00:58

SR Analyzer (SRA -TOC) - TPH TOC Analysis v6.5.117

Sample ID: 666_144-9 **Acq. Type**: TPH **Weight**: 75.9 **Crucible**: 25
Depth: 144.9 (Measured) **Lithology**: None **Sample Type**: Core **Well Name**: 666
Acq. Date: July 21 2014 / 1:21:51 PM

Data: C:\SRA JOBS\SRA049C_Greymouth lacustrine mudstones_20072014\666_144-9.RAW
Method: C:\Program Files\Thermal Station\GNS 300-650 STD 160000.sram
Sequence: C:\Program Files\Thermal Station\Data\SRA049C Greymouth lacustrine mudstones 20072014\SRA049C Greymouth lacustrine mudstones 20072014.sras
Method Information: Initial Temp: 300 °C -- Initial Time: 3 -- Rate : 25.0 °C/Min -- Final Temp: 650 °C -- Final Time: 1 Min -- OxiPurge: 5 Min -- OxiTime: 20 Min -- OxiTemp: 630 °C
FID Temp: 325 °C
FID Gain: Low (10^6)

Calibration Standard Information: Standard Name: 160000 TOC tTemp: 455.0 °C pTPH (S2): 12.43 mg/g S3: 0.79 mg/g S4: 22.40 mg/g
Operator: R Sykes **Instrument name**: SRA -TOC

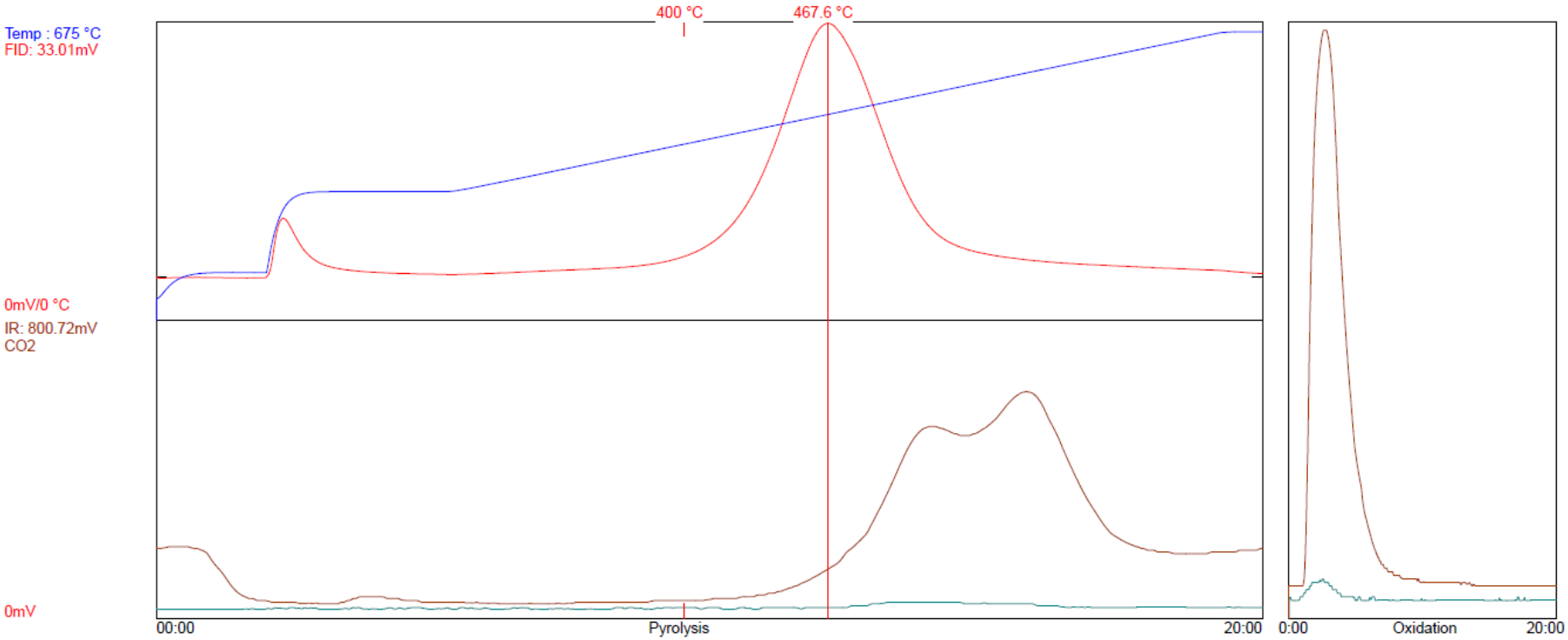

vTPH(S1):.32mg/g pTPH(S2): 5.18mg/g cTemp(Tmax): 428.6°C tTemp:467.6°C S3:1.36mg/g TOC:2.44 % HI:213 OI:56 PI:0.06 S1/TOC:0.13

Monday, 21 July 2014 18:01:28

Appendix 3 Isopach data

Appendix 3.1 Total available drill hole data encompassing all three lacustrine mudstones.

HOLEID	TOP	BOTTOM	STRAT	THICKNESS	EAST	NORTH
92	84.43	106.68	FM	22.25	281249.26	697766.57
92	18.59	45.72	WM	27.13	281249.26	697766.57
241	309.37	369.72	FM	60.35	280344.006	694869.746
241	192.48	222.96	WM	30.48	280344.006	694869.746
246	320.65	417.58	FM	96.93	280283.656	695111.148
246	252.22	277.67	WM	25.45	280283.656	695111.148
262	328.88	366.98	FM	38.1	280197.775	695783.976
262	249.63	273.71	WM	24.08	280197.775	695783.976
265	329.49	341.68	FM	12.19	280195.494	695528.947
265	243.84	264.41	WM	20.57	280195.494	695528.947
318	703.17	826.01	FM	122.84	281676.23	694530.1
318	268.22	398.53	GM	130.31	281676.23	694530.1
318	624.54	657.75	WM	33.21	281676.23	694530.1
342	280.87	418.95	GM	138.08	282067.626	694134.769
342	627.89	648	WM	20.11	282067.626	694134.769
384	185.01	193.85	FM	8.84	280469.716	695247.137
384	111.56	128.02	WM	16.46	280469.716	695247.137
421	81.08	88.71	FM	7.63	281828.63	697714.26
421	0	7.62	WM	7.62	281828.63	697714.26
463	171.3	185.62	FM	14.32	280311.819	695460.174
463	77.72	95.1	WM	17.38	280311.819	695460.174
464	223.723	237.74	FM	14.017	280374.182	695352.549
464	124.968	149.809	WM	24.841	280374.182	695352.549
475	225.86	235.61	FM	9.75	280360.1	695264.035

475	135.64	158.04	WM	22.4	280360.1	695264.035
592	62.64	186.74	GM	124.1	282432.734	695942.173
592	449.96	487.98	WM	38.02	282432.734	695942.173
595	553.36	554.74	FM	1.38	282825.213	696111.757
595	102.93	223.72	GM	120.79	282825.213	696111.757
595	470.23	497.79	WM	27.56	282825.213	696111.757
596	80.8	205.8	GM	125	282636.919	696414.917
596	437.69	460.45	WM	22.76	282636.919	696414.917
600	300.48	425.48	GM	125	281885.99	694946.7
600	689.76	718.11	WM	28.35	281885.99	694946.7
616	761.58	765	FM	3.42	282657.27	695182.27
616	280.3	414.5	GM	134.2	282657.27	695182.27
616	675.13	699.35	WM	24.22	282657.27	695182.27
617	744.09	750	FM	5.91	282537.92	694517.59
617	285	427	GM	142	282537.92	694517.59
617	665.52	692.7	WM	27.18	282537.92	694517.59
618	778.67	782	FM	3.33	282090.56	695351.57
618	354.4	482.5	GM	128.1	282090.56	695351.57
618	706.1	731.19	WM	25.09	282090.56	695351.57
620	784.6	796.1	FM	11.5	282150.03	692510.06
620	367.5	507.6	GM	140.1	282150.03	692510.06
620	722	756	WM	34	282150.03	692510.06
624	267.2	311.7	FM	44.5	277921.67	695311.82
624	5.2	52	GM	46.8	277921.66	695311.81
625	348.2	444.8	GM	96.6	280894.13	692578.54
625	616.4	639	WM	22.6	280894.13	692578.54

635	303	378.8	GM	75.8	277294.78	697002.06
635	648.3	711.2	WM	62.9	277294.77	697002.07
640	396	410.9	FM	14.9	277651.63	694738.63
640	115	186.8	GM	71.8	277651.63	694738.63
641	218.17	342.8	GM	124.63	276541.06	697006.88
641	578.5	628.2	WM	49.7	276541.06	697006.88
642	182	275.1	GM	93.1	275993.33	695406.8
642	325.5	333	WM	7.5	275993.33	695406.8
645	427.9	476.9	FM	49	277307.35	696221.42
645	48	113	GM	65	277307.35	696221.42
647	240.3	281.5	GM	41.2	276119.91	696357.75
647	424.3	427.1	WM	2.8	276119.91	696357.75
649	267.6	325.3	GM	57.7	276339.1	692692.16
649	267.6	325.3	GM	57.7	275469.17	694413.93
656	291.2	489	FM	197.8	279611.06	698455.81
656	246.7	253.5	WM	6.8	279611.06	698455.81
657	549.25	679.6	FM	130.35	279385.71	697517.46
657	0	184.7	GM	184.7	279385.71	697517.46
657	413.6	415.6	WM	2	279385.71	697517.46
658	291.85	309.9	FM	18.05	281233.86	698796.28
658	189.35	252.8	WM	63.45	281233.86	698796.28
659	367.8	490.2	FM	122.4	282737.88	697215.37
659	229.4	252.7	WM	23.3	282737.88	697215.37
660	257.9	282.4	FM	24.5	282567.93	698497.24
660	282.6	408	FM	125.4	283995.66	699255.42
660	0	90.7	GM	90.7	282567.93	698497.24

660	188.1	213.8	WM	25.7	282567.93	698497.24
666	0	146.54	GM	146.54	279689.11	697580.8
666	214.47	215.76	WM	1.29	279689.11	697580.8
690	0	53.5	GM	53.5	279077.82	698548.63
690	214.7	215.4	WM	0.7	279077.82	698548.63
693	0	10.6	GM	10.6	279715.07	698139.93
693	220.1	222.75	WM	2.65	279715.07	698139.93
704	191	296.1	GM	105.1	276504.6	695912.5
704	362.9	368.4	WM	5.5	276504.6	695912.5
707	212	329.3	GM	117.3	276768.91	696462.08
707	506	532	WM	26	276768.91	696462.08
708	73.6	201.7	GM	128.1	277088.88	697401.99
708	449.6	475.4	WM	25.8	277088.88	697402
709	226.4	309.1	GM	82.7	276228.51	697537.45
709	481.65	499.4	WM	17.75	276228.51	697537.45
710	185	258.8	GM	73.8	276457.63	698435.56
710	487	493.4	WM	6.4	276457.63	698435.56
719	180.6	205	FM	24.4	281758.75	698826.38
719	90.8	116.9	WM	26.1	281758.75	698826.38
727	294.2	436.7	GM	142.5	282290.49	694833.3
727	670.85	696.3	WM	25.45	282290.49	694833.3
730	281.4	423.15	GM	141.75	282781.55	694009.53
730	671.85	699.65	WM	27.8	282781.55	694009.53
731	101.75	143.4	GM	41.65	277393.62	697269.18
731	197.37	268.13	GM	70.76	277393.62	697269.18
732	583.55	591.55	FM	8	281609.83	694219.79

732	153.2	286.5	GM	133.3	281609.83	694219.79
732	526.2	552.65	WM	26.45	281609.83	694219.79
734	761.2	771.1	FM	9.9	282859.3	694784.22
734	305	443.8	GM	138.8	282859.3	694784.22
734	684	708.25	WM	24.25	282859.3	694784.22
736	421.85	433.65	FM	11.8	282020.69	695978.73
736	42.1	128.1	GM	86	282020.69	695978.73
736	358.9	383.05	WM	24.15	282020.69	695978.73
746	383.5	446.8	FM	63.3	280213.22	697794.57
746	295.2	311.6	WM	16.4	280213.22	697794.57
759	367.75	374	FM	6.25	280984.61	698460.55
759	293.5	319.5	WM	26	280984.61	698460.55
772	178.35	355.55	GM	177.2	275879.85	694167.22
772	367.2	377.4	GM	10.2	275879.85	694167.22
774	244.49	316.45	GM	71.96	275851.71	694172.49
774	401.9	437.3	GM	35.4	275851.71	694172.49
787	133.83	244.5	GM	110.67	276802.92	695713.82
787	363.73	368.5	WM	4.77	276802.92	695713.82
789	476.42	481.7	FM	5.28	277252.07	695717.18
789	14.7	297.46	GM	282.76	277252.07	695717.18
835	75.79	195.45	GM	119.66	277100.5	694455
835	341.06	341.06	WM	0	277100.5	694455
836	409.74	416.05	FM	6.31	277408.2	694632.14
836	102.5	212.75	GM	110.25	277408.2	694632.14
839	39	145.75	GM	106.75	277042.04	694695.11
839	147.9	153.47	GM	5.57	277042.04	694695.11

853	375.81	393.51	FM	17.7	277513.92	694779.25
853	84	212.65	GM	128.65	277513.92	694779.25
869	123.9	130.9	FM	7	282914.93	698857.88
869	73.5	90.5	WM	17	282914.93	698857.88
876	0	5	GM	5	283182.57	698428.46
876	273.55	294.05	WM	20.5	283182.57	698428.46
878	505.7	510	FM	4.3	277910.73	695841.25
878	151	257.4	GM	106.4	277910.73	695841.25
894	0	75	GM	75	279850.92	698381.46
894	251.7	262.85	WM	11.15	279850.92	698381.46
925	485	494.74	FM	9.74	279975.62	696166.53
925	72.5	242	GM	169.5	279975.62	696166.53
925	394	421	WM	27	279975.62	696166.53
926	424.5	434.26	FM	9.76	280248.46	697258.36
926	0	129.5	GM	129.5	280248.46	697258.36
926	351	373.5	WM	22.5	280248.46	697258.36
933	16	137.5	GM	121.5	278736.6	693898.37
933	290.8	304.3	WM	13.5	278736.6	693898.37
952	261	274.4	FM	13.4	279733.77	698706.36
952	181.5	183.5	WM	2	279733.77	698706.36
974	135	163	FM	28	281248	698570.72
974	40	93.2	WM	53.2	281248	698570.72
977	143	181	FM	38	281534.37	698575
977	68	93.5	WM	25.5	281534.37	698575
979	150	169.1	FM	19.1	281414.11	698706.31
979	61.5	81.3	WM	19.8	281414.11	698706.31

980	168	173.1	FM	5.1	281564.09	698709.57
980	83	108	WM	25	281564.09	698709.57
981	175	196.2	FM	21.2	281585.9	698822.27
981	101.2	125	WM	23.8	281585.9	698822.27
983	172	181.3	FM	9.3	281695.54	698735.78
983	83	120	WM	37	281695.54	698735.78
984	366.5	381.5	FM	15	277278.7	695363.63
984	87	169	GM	82	277278.7	695363.63
985	168	172	FM	4	281692.62	698892.2
985	79	105.2	WM	26.2	281692.62	698892.2
1011	0	33.1	GM	33.1	279038.58	693872.02
1011	223.1	236.5	WM	13.4	279038.58	693872.02
1012	330	371.05	FM	41.05	280329	694357.87
1012	32.5	56.3	GM	23.8	280329	694357.87
1012	270.2	293.5	WM	23.3	280329	694357.87
1018	270	275	FM	5	280454.28	697936.65
1018	176	200.5	WM	24.5	280454.28	697936.65
1019	287	292	FM	5	280465.41	697805.79
1019	195	220	WM	25	280465.41	697805.79
1021	358	374	FM	16	280279.63	697977.4
1021	258.5	276.5	WM	18	280279.63	697977.4
1031	152	190	FM	38	281337.47	698488.21
1031	71.64	92	WM	20.36	281337.47	698488.21
1034	152	155.25	FM	3.25	281778.99	698930.39
1034	68.71	91.5	WM	22.79	281778.99	698930.39
1042	135	152.28	FM	17.28	281949.03	698785.24

1042	54.21	76	WM	21.79	281949.03	698785.24
1044	110	276	FM	166	281053.09	698288.08
1044	22	52	WM	30	281053.09	698288.08
1051	259.4	270.4	FM	11	280541.4	697200.81
1051	165.5	187.1	WM	21.6	280541.4	697200.81
1056	144	154.75	FM	10.75	281753.5	698670.78
1056	71.41	96.08	WM	24.67	281753.5	698670.78
1057	156.99	167.2	FM	10.21	281832.82	698720.94
1057	78.57	98.5	WM	19.93	281832.82	698720.94
1059	194.1	199.7	FM	5.6	281856.69	698901.85
1059	110	133	WM	23	281856.69	698901.85
1061	130	151.85	FM	21.85	281678.61	698371.32
1061	42	62	WM	20	281678.61	698371.32
1062	195	275.5	GM	80.5	276259.073	694261.3455
1062	311	392.8	GM	81.8	276259.073	694261.3455
1076	0	80	GM	80	279326.21	693604.05
1076	251.85	270.5	WM	18.65	279326.21	693604.05
1079	95	244	GM	149	278905.57	694364.46
1079	357	360.8	WM	3.8	278905.57	694364.46
1089	193.5	300.8	GM	107.3	276717.75	695539.25
1089	432.9	439.3	WM	6.4	276717.75	695539.25
1096	175	180.1	FM	5.1	283423.88	698818.68
1096	82	115	WM	33	283423.88	698818.68
1097	90	106.25	FM	16.25	282919.63	698981.14
1097	38.5	57	WM	18.5	282919.63	698981.14
1098	118	121.7	FM	3.7	283266.66	699019.25

1098	58	77	WM	19	283266.66	699019.25
1099	185	186.75	FM	1.75	283049.11	698812.98
1099	130	147	WM	17	283049.11	698812.98
1113	184.8	277	GM	92.2	276533.23	695685.72
1113	402.7	415.45	WM	12.75	276533.23	695685.72
1184	240	250.3	FM	10.3	282745.59	698773.75
1184	0	32	GM	32	282745.59	698773.75
1184	168	206.2	WM	38.2	282745.59	698773.75
1190	214.4	342.5	GM	128.1	276450.56	695579.63
1190	445	464	WM	19	276450.56	695579.63
1193	184.4	285	GM	100.6	276401.67	695474.07
1193	373.2	377.3	WM	4.1	276401.67	695474.07
1200	211.4	347.3	GM	135.9	276404.01	695473.02
1200	423	428.3	WM	5.3	276404.01	695473.02
1204	160.5	227.6	GM	67.1	276809.06	695715.58
1204	370.6	383.15	WM	12.55	276809.06	695715.58
1206	185.6	317	GM	131.4	276231.2	695299.91
1206	501.5	509	WM	7.5	276231.2	695299.91
1207	275	294.18	FM	19.18	282644.68	697792.79
1207	209	232	WM	23	282644.68	697792.79
1208	195.7	252	FM	56.3	282426.54	697806.99
1208	0	17	WM	17	282426.54	697806.99
1209	292	299.2	FM	7.2	282612.24	697600.98
1209	192.5	212	WM	19.5	282612.24	697600.98
1210	222	226.5	FM	4.5	282744.14	698268.54
1210	136.5	163	WM	26.5	282744.14	698268.54

1211	191.8	310.2	GM	118.4	276113.88	695698.18
1211	380.5	394	WM	13.5	276113.88	695698.18
1212	188	298.1	GM	110.1	276314.77	695892.29
1212	449	462	WM	13	276314.77	695892.29
1214	43	153	GM	110	277099.8	694787.44
1214	347	369	WM	22	277099.8	694787.44
1215	130	235	GM	105	277041.57	695314.94
1215	381	384.5	WM	3.5	277041.57	695314.94
1224	213.4	358.3	GM	144.9	275969.65	695906.79
1224	459.2	475.3	WM	16.1	275969.65	695906.79
1225	201.7	308	GM	106.3	276401.2	696182.96
1225	469	496.7	WM	27.7	276401.2	696182.96
1227	266	357.5	GM	91.5	276011.8	696291.52
1227	441.8	442.6	WM	0.8	276011.8	696291.52
1238	189.8	289.5	GM	99.7	275992.35	695408.21
1238	347	352	WM	5	275992.35	695408.21
1239	175.6	287.8	GM	112.2	276412.53	695708.02
1239	424	439	WM	15	276412.53	695708.02
1240	205	337.6	GM	132.6	276110.19	695702.57
1240	452	465.6	WM	13.6	276110.19	695702.57
1242	218.2	330.8	GM	112.6	276278.8	695431.13
1242	451	466	WM	15	276278.8	695431.13
1243	156.7	304.7	GM	148	276413.05	695711.3
1243	407	421	WM	14	276413.05	695711.3
1246	125	169.4	FM	44.4	283647.84	698643.03
1246	45	81.5	WM	36.5	283647.84	698643.03

1248	118	126.9	FM	8.9	283432.85	698956.94
1248	18.5	60	WM	41.5	283432.85	698956.94
1258	200.2	296.7	GM	96.5	276497.78	696368.13
1258	490	500	WM	10	276497.78	696368.13
1260	226	235	FM	9	281732.94	698107.73
1260	134.8	155.5	WM	20.7	281732.94	698107.73
1261	222.7	238	FM	15.3	281641.92	697985.6
1261	130.4	150.4	WM	20	281641.92	697985.6
1262	142.7	153.5	FM	10.8	281512.13	698076.16
1262	42	62.1	WM	20.1	281512.13	698076.16
1263	200	208.3	FM	8.3	281877.93	697998.94
1263	101.5	124	WM	22.5	281877.93	697998.94
1264	177.5	192.6	FM	15.1	281819.73	697913.29
1264	78.5	100.9	WM	22.4	281819.73	697913.29
1265	262.7	272	FM	9.3	281936.27	698193.71
1265	151.3	172.5	WM	21.2	281936.27	698193.71
1266	180	283	GM	103	275883.53	695043.59
1266	319	323	WM	4	275883.53	695043.59
1269	177.6	263.9	GM	86.3	275993.33	695405.23
1269	347	351	WM	4	275993.33	695405.23
1270	172	305.2	GM	133.2	276246.3	696593.9
1270	419	423.4	WM	4.4	276246.3	696593.9
1273	100.5	206.75	GM	106.25	276996.88	696302.61
1273	380.4	406	WM	25.6	276996.88	696302.61
1278	210.8	219.75	FM	8.95	281657.12	698900.56
1278	93	119.6	WM	26.6	281657.12	698900.56

1283	236.5	337.9	GM	101.4	276291.91	695495.21
1283	425	436.9	WM	11.9	276291.91	695495.21
1301	101	134	FM	33	281452.87	698224.77
1301	15.2	35.2	WM	20	281452.87	698224.77
1302	151.6	171.95	FM	20.35	281602.44	698100.52
1302	65.5	86.5	WM	21	281602.44	698100.52
1304	165	181.2	FM	16.2	281632.42	698171.8
1304	69.8	90.8	WM	21	281632.42	698171.8
1309	191	301.2	GM	110.2	276204.69	696331.93
1309	413.5	426	WM	12.5	276204.69	696331.93
1311	220	250.2	FM	30.2	283026.43	698732.33
1311	149.1	171.8	WM	22.7	283026.43	698732.33
1312	250.6	280	FM	29.4	283322.74	698704.48
1312	173	196.5	WM	23.5	283322.74	698704.48
1313	285	316.95	FM	31.95	282151.498	698165.85
1313	180.5	199	WM	18.5	282151.498	698165.85
1314	180	190.45	FM	10.45	282817.922	698798.903
1314	115	137	WM	22	282817.922	698798.903
1315	210	239.9	FM	29.9	283199.22	698703.34
1315	141	162.5	WM	21.5	283199.22	698703.34
1318	245	271.5	FM	26.5	282294.62	698009.98
1318	90.5	113.5	WM	23	282294.62	698009.98
1319	210	232.6	FM	22.6	282269.83	697955.8
1319	85.8	105.3	WM	19.5	282269.83	697955.8
1321	205	231.2	FM	26.2	282221.83	697884.38
1321	74.5	90.5	WM	16	282221.83	697884.38

1323	104	115.05	FM	11.05	282092.47	699131.51
1323	12	42.5	WM	30.5	282092.47	699131.51
1326	204.2	324.5	GM	120.3	276765.64	696459
1326	518.5	539.08	WM	20.58	276765.64	696459
1328	113.6	242	GM	128.4	276998.35	696301.79
1328	424	438	WM	14	276998.35	696301.79
1330	162.5	191.1	FM	28.6	282217.88	699186.76
1330	68.2	96.8	WM	28.6	282217.88	699186.76
1331	235	245	FM	10	282260.66	698133.44
1331	152.5	163.5	WM	11	282260.66	698133.44
1332	195	205.3	FM	10.3	281980.35	698050.14
1332	97	118.5	WM	21.5	281980.35	698050.14
1333	160	181.2	FM	21.2	281664.97	698173.01
1333	65.3	85.4	WM	20.1	281664.97	698173.01
1334	140	153.9	FM	13.9	282040.54	697900.81
1334	52	72	WM	20	282040.54	697900.81
1335	195.8	304	GM	108.2	276684.67	696681.32
1335	490	497	WM	7	276684.67	696681.32
1337	89.6	223	GM	133.4	277081.6	696476.5
1337	452	485.3	WM	33.3	277081.6	696476.5
1338	74.6	192	GM	117.4	277082.29	696476.58
1338	437	470	WM	33	277082.29	696476.58
1339	150.4	257.4	GM	107	276681.85	696304.94
1339	453	485	WM	32	276681.85	696304.94
1340	145	256.3	GM	111.3	276682.53	696304.78
1340	443	464	WM	21	276682.53	696304.78

1341	153.5	292.2	GM	138.7	276981.28	696096.7
1341	486	500	WM	14	276981.28	696096.7
1342	132.8	244	GM	111.2	276982.27	696096.65
1342	419	442.4	WM	23.4	276982.27	696096.65
1351	221.6	365.5	GM	143.9	276259.44	696005.91
1351	469.8	484.3	WM	14.5	276259.44	696005.91
1369	327	343.7	FM	16.7	282081.65	697668.5
1369	232.2	251	WM	18.8	282081.65	697668.5
1370	197.3	197.4	FM	0.1	283127.85	698891.43
1370	129	147.3	WM	18.3	283127.85	698891.43
1371	135	150.35	FM	15.35	282544.2	699086.36
1371	0	13.5	WM	13.5	282544.2	699086.36
1373	124	139.6	FM	15.6	283514.55	698993.59
1373	68	89	WM	21	283514.55	698993.59
1376	75	84.15	FM	9.15	281482.79	698168.72
1376	0	9	WM	9	281482.79	698168.72
1377	165	178	FM	13	283227.82	698935.5
1377	98.25	122.25	WM	24	283227.82	698935.5
1378	144.6	147.6	FM	3	283039.54	698933.25
1378	78	99.5	WM	21.5	283039.54	698933.25
1380	113	130.3	FM	17.3	283335.39	698948.83
1380	33.4	51.8	WM	18.4	283335.39	698948.83
1381	152	191	FM	39	282677.255	699122.229
1381	63	76.5	WM	13.5	282677.255	699122.229
1383	76	82.1	FM	6.1	283347.86	699056.76
1383	0	13.3	WM	13.3	283347.86	699056.76

1384	90	90.5	FM	0.5	282978.15	699070.52
1384	22.5	50	WM	27.5	282978.15	699070.52
1385	231	260.1	FM	29.1	282719.959	698969.749
1385	86	110	WM	24	282719.959	698969.749
1386	151	188.2	FM	37.2	282861.8	698872.63
1386	92	113	WM	21	282861.8	698872.63
1387	163.5	174.65	FM	11.15	283297.8	698838.39
1387	87.5	110.5	WM	23	283297.8	698838.39
1388	315	329.4	FM	14.4	280632.19	698431.31
1388	208.5	236	WM	27.5	280632.19	698431.31
1389	280	289.6	FM	9.6	280646.35	698236.52
1389	202.5	229.5	WM	27	280646.35	698236.52
1390	400	410.2	FM	10.2	280280.49	698335.94
1390	296.6	318.4	WM	21.8	280280.49	698335.94
1391	225	235.6	FM	10.6	282636.62	699046.65
1391	63	82.5	WM	19.5	282636.62	699046.65
1392	108	121.1	FM	13.1	283101.95	699144.1
1392	49	72.5	WM	23.5	283101.95	699144.1
1394	225	260.5	FM	35.5	283108.76	698785.69
1394	161	180.5	WM	19.5	283108.76	698785.69
1396	133.8	190.4	FM	56.6	283820.03	698673.72
1396	57.5	75.2	WM	17.7	283820.03	698673.72
1398	75	90.8	FM	15.8	282797.06	699109.56
1398	19.5	40.5	WM	21	282797.06	699109.56
1400	181	337.5	FM	156.5	280013.93	699167.73
1400	94.3	115	WM	20.7	280013.93	699167.73

1402	164.8	288.9	GM	124.1	276673.39	696199.91
1402	460.8	489.9	WM	29.1	276673.39	696199.91
1403	58	69.1	FM	11.1	283025.49	699178.9
1403	9	34.5	WM	25.5	283025.49	699178.9
1405	391	403	FM	12	280356.745	698540.249
1405	209.5	228.5	WM	19	280356.745	698540.249
1406	317	332	FM	15	280763.55	698257.92
1406	224.5	264	WM	39.5	280763.55	698257.92
1407	290	293.1	FM	3.1	280784.32	698473.18
1407	190	226	WM	36	280784.32	698473.18
1410	144.5	160.2	FM	15.7	283127.1	699013.58
1410	86.5	107.5	WM	21	283127.1	699013.58
1412	137	145.4	FM	8.4	281984.688	699068.125
1412	23	49	WM	26	281984.688	699068.125
1416	142	164.4	FM	22.4	282765.76	698911.35
1416	93	112.5	WM	19.5	282765.76	698911.35
1417	300	451.45	GM	151.45	282066.51	694848.92
1417	672	700.8	WM	28.8	282066.51	694848.92
1418	130.1	139.3	FM	9.2	283676.22	698716.5
1418	8	23	WM	15	283676.22	698716.5
1419	110.5	130	FM	19.5	283615.64	698575.2
1419	29.1	61	WM	31.9	283615.64	698575.2
1424	75	150	FM	75	283735.54	699398.91
1424	0	16	WM	16	283735.54	699398.91
1427	50	106.3	FM	56.3	283660.64	699324.6
1427	0	1.8	WM	1.8	283660.64	699324.6

1430	300	451.45	GM	151.45	282066.51	694848.92
1430	672	700.8	WM	28.8	282066.51	694848.92
1432	194.4	214.1	FM	19.7	283589.78	698412.57
1432	96.7	141.8	WM	45.1	283589.78	698412.57

Appendix 3.2 Data table of selected drill holes used for isopach modelling

HOLEID	TOP	BOTTOM	STRAT	THICKNESS	EAST	NORTH
92	18.59	45.72	WM	27	281249.26	697766.57
265	329.49	341.68	FM	12	280195.494	695528.947
265	243.84	264.41	WM	21	280195.494	695528.947
318	268.22	398.53	GM	130.31	281676.23	694530.1
342	627.89	648	WM	20	282067.626	694134.769
342	280.87	418.95	GM	138.08	282067.626	694134.769
595	470.23	497.79	WM	28	282825.213	696111.757
595	102.93	223.72	GM	120.79	282825.213	696111.757
600	689.76	718.11	WM	28	281885.99	694946.7
612	0	46.65	GM	46.65	277896.64	697962.4
617	285	427	GM	142.00	282537.92	694517.59
618	354.4	482.5	GM	128.10	282090.56	695351.57
620	784.6	796.1	FM	12	282150.03	692510.06
620	722	756	WM	34	282150.03	692510.06
620	367.5	507.6	GM	140.10	282150.03	692510.06
621	357.2	393.5	WM	36	277001.16	699088.19
625	616.4	639	WM	23	280894.13	692578.54
625	348.2	444.8	GM	96.60	280894.13	692578.54
626	285	302.4	GM	17.40	275000.44	695630.93
635	303	378.8	GM	75.80	277294.78	697002.06
640	324.6	369.2	WM	45	276882.3	701254.8
641	218.17	342.8	GM	124.63	276541.06	697006.88
647	424.3	427.1	WM	3	276119.91	696357.75
649	267.6	325.3	GM	57.70	276339.1	692692.16

649	267.6	325.3	GM	57.70	275469.17	694413.93
656	246.7	253.5	WM	7	279611.06	698455.81
659	229.4	252.7	WM	23	282737.88	697215.37
660	282.6	408	FM	76	283995.66	699255.42
660	0	90.7	GM	90.70	282567.93	698497.24
666	0	146.54	GM	146.54	279689.11	697580.8
690	0	53.5	GM	53.50	279077.82	698548.63
704	191	296.1	GM	105.10	276504.6	695912.5
707	212	329.3	GM	117.30	276768.91	696462.08
708	449.6	475.4	WM	26	277088.88	697402
708	73.6	201.7	GM	128.10	277088.88	697401.99
709	481.65	499.4	WM	18	276228.51	697537.45
709	226.4	309.1	GM	82.70	276228.51	697537.45
710	487	493.4	WM	6	276457.63	698435.56
710	185	258.8	GM	73.80	276457.63	698435.56
727	294.2	436.7	GM	142.50	282290.49	694833.3
730	671.85	699.65	WM	28	282781.55	694009.53
730	281.4	423.15	GM	141.75	282781.55	694009.53
732	583.55	591.55	FM	8	281609.83	694219.79
732	526.2	552.65	WM	26	281609.83	694219.79
733	186.2	264.1	GM	77.90	277714.55	697183.95
734	761.2	771.1	FM	10	282859.3	694784.22
734	684	708.25	WM	24	282859.3	694784.22
736	421.85	433.65	FM	12	282020.69	695978.73
736	358.9	383.05	WM	24	282020.69	695978.73
759	367.75	374	FM	6	280984.61	698460.55

774	401.9	437.3	GM	35.40	275851.71	694172.49
774	244.49	316.45	GM	71.96	275851.71	694172.49
789	476.42	481.7	FM	5	277252.07	695717.18
835	75.79	195.45	GM	119.66	277100.5	694455
836	409.74	416.05	FM	6	277408.2	694632.14
839	39	145.75	GM	106.75	277042.04	694695.11
876	273.55	294.05	WM	21	283182.57	698428.46
878	151	257.4	GM	106.40	277910.73	695841.25
894	0	75	GM	75.00	279850.92	698381.46
905	31	65.1	WM	34	284072.96	696947.03
925	485	494.74	FM	10	279975.62	696166.53
926	424.5	434.26	FM	10	280248.46	697258.36
926	0	129.5	GM	129.50	280248.46	697258.36
933	290.8	304.3	WM	14	278736.6	693898.37
933	16	137.5	GM	121.50	278736.6	693898.37
979	61.5	81.3	WM	20	281414.11	698706.31
1012	270.2	293.5	WM	23	280329	694357.87
1018	270	275	FM	5	280454.28	697936.65
1019	195	220	WM	25	280465.41	697805.79
1031	71.64	92	WM	20	281337.47	698488.21
1042	54.21	76	WM	22	281949.03	698785.24
1044	22	52	WM	30	281053.09	698288.08
1051	259.4	270.4	FM	11	280541.4	697200.81
1051	165.5	187.1	WM	22	280541.4	697200.81
1056	144	154.75	FM	11	281753.5	698670.78
1061	130	151.85	FM	22	281678.61	698371.32

1062	195	275.5	GM	80.50	276259.073	694261.346
1062	311	392.8	GM	81.80	276259.073	694261.346
1076	251.85	270.5	WM	19	279326.21	693604.05
1076	0	80	GM	80.00	279326.21	693604.05
1079	357	360.8	WM	4	278905.57	694364.46
1079	95	244	GM	149.00	278905.57	694364.46
1089	193.5	300.8	GM	107.30	276717.75	695539.25
1113	402.7	415.45	WM	13	276533.23	695685.72
1190	214.4	342.5	GM	128.10	276450.56	695579.63
1204	370.6	383.15	WM	13	276809.06	695715.58
1207	275	294.18	FM	19	282644.68	697792.79
1208	0	17	WM	17	282426.54	697806.99
1209	192.5	212	WM	20	282612.24	697600.98
1210	136.5	163	WM	27	282744.14	698268.54
1212	449	462	WM	13	276314.77	695892.29
1215	381	384.5	WM	4	277041.57	695314.94
1215	130	235	GM	105.00	277041.57	695314.94
1225	469	496.7	WM	28	276401.2	696182.96
1227	266	357.5	GM	91.50	276011.8	696291.52
1240	205	337.6	GM	132.60	276110.19	695702.57
1245	54	100.2	FM	46	283580.02	698902.17
1261	222.7	238	FM	15	281641.92	697985.6
1266	319	323	WM	4	275883.53	695043.59
1266	180	283	GM	103.00	275883.53	695043.59
1269	347	351	WM	4	275993.33	695405.23
1270	419	423.4	WM	4	276246.3	696593.9

1270	172	305.2	GM	133.20	276246.3	696593.9
1273	100.5	206.75	GM	106.25	276996.88	696302.61
1278	210.8	219.75	FM	9	281657.12	698900.56
1283	425	436.9	WM	12	276291.91	695495.21
1302	65.5	86.5	WM	21	281602.44	698100.52
1313	285	316.95	FM	32	282151.498	698165.85
1314	115	137	WM	22	282817.922	698798.903
1315	210	239.9	FM	30	283199.22	698703.34
1315	141	162.5	WM	22	283199.22	698703.34
1321	205	231.2	FM	26	282221.83	697884.38
1321	74.5	90.5	WM	16	282221.83	697884.38
1323	104	115.05	FM	11	282092.47	699131.51
1326	518.5	539.08	WM	21	276765.64	696459
1330	68.2	96.8	WM	29	282217.88	699186.76
1335	490	497	WM	7	276684.67	696681.32
1337	452	485.3	WM	33	277081.6	696476.5
1340	145	256.3	GM	111.30	276682.53	696304.78
1342	419	442.4	WM	23	276982.27	696096.65
1342	132.8	244	GM	111.20	276982.27	696096.65
1351	221.6	365.5	GM	143.90	276259.44	696005.91
1369	327	343.7	FM	17	282081.65	697668.5
1369	232.2	251	WM	19	282081.65	697668.5
1376	75	84.15	FM	9	281482.79	698168.72
1380	33.4	51.8	WM	18	283335.39	698948.83
1389	202.5	229.5	WM	27	280646.35	698236.52
1391	225	235.6	FM	11	282636.62	699046.65

1391	63	82.5	WM	20	282636.62	699046.65
1400	94.3	115	WM	21	280013.93	699167.73
1402	460.8	489.9	WM	29	276673.39	696199.91
1403	58	69.1	FM	11	283025.49	699178.9
1403	9	34.5	WM	26	283025.49	699178.9
1405	391	403	FM	12	280356.745	698540.249
1406	317	332	FM	15	280763.55	698257.92
1407	190	226	WM	36	280784.32	698473.18
1410	86.5	107.5	WM	21	283127.1	699013.58
1412	23	49	WM	26	281984.688	699068.125
1416	142	164.4	FM	22	282765.76	698911.35
1427	0	1.8	WM	2	283660.64	699324.6
1430	300	451.45	GM	151.45	282066.51	694848.92
1432	194.4	214.1	FM	20	283589.78	698412.57

Appendix 3.3 Drill hole location map for all selected drill holes

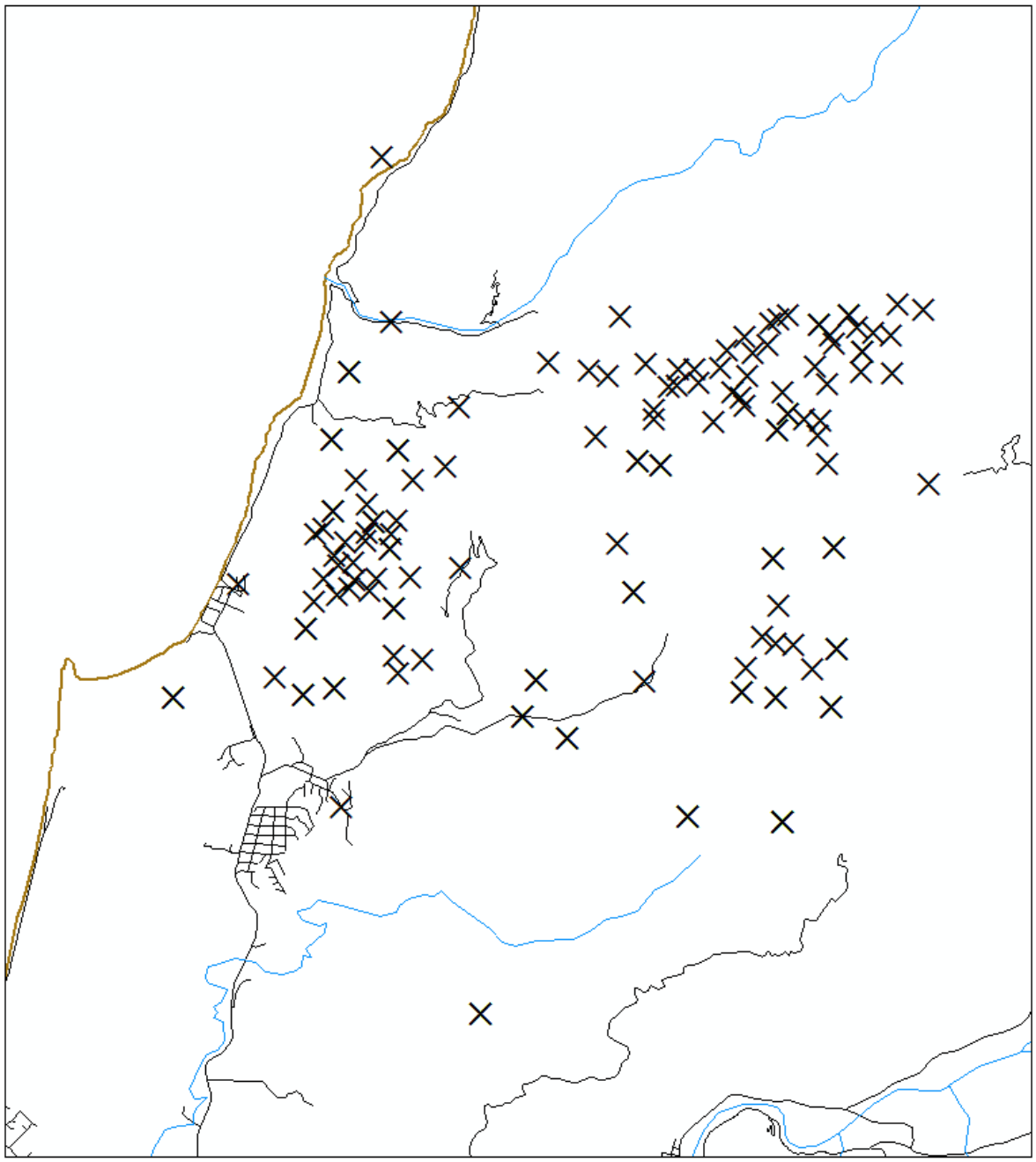

Key

Drill hole location

River

Road

Beach